Sorption of Phenols from Aqueous Solution by Silica Molecular Sieves

by

Gillian Scott

Thesis presented for the degree of

Doctor of Philosophy

University of Edinburgh

1987

ACKNOWLEDGEMENTS

I would like to thank Barrie Lowe for his help and encouragement throughout this work. I am also grateful to John Stageman, John Melling, Geoff Leaver and to members of the zeolite group past and present, for many helpful discussions. A special thanks to Kevin Franklin for his computer software.

The provision of facilities by the University of Edinburgh, ICI Agricultural Division and Warren Spring Laboratory are gratefully acknowledged. Finally, I would like to thank the Science and Engineering Research Council, ICI plc and Warren Spring Laboratory for funding this research.

Declaration

This thesis is of my own composition and is an accurate account of research carried out by myself at the University of Edinburgh between October 1983 and October 1986.

ABSTRACT

An investigation into the sorption of phenols from aqueous solution by silicalite-1 has been carried out. Langmuir sorption isotherms were obtained at 25°C for the uptake of phenol, mono- and di-substituted methyl phenols and p-nitrophenol. A comparison of the behaviour of silicalite-1 samples with different degrees of hydrophilicity has been made, as well as a study of the sorption behaviour of samples of ZSM-5 and silicalite-2 in similar systems.

The effect of the presence of inorganic salt on sorption behaviour was determined for the uptake of phenol from lithium chloride solutions. This produced a "salting out" effect of the phenol from the solution phase. Isotherms for the uptake of p-cresol from methanol water mixtures were also obtained. A reduction in the uptake of p-cresol by the sieve was observed as the amount of methanol in the solution phase increased. Isotherms for the sorption of p-cresol from low molecular weight alcohols illustrated the behaviour of silicalite-1 in non-aqueous systems and suggested a possible method for the recovery of sorbed material.

Finally, the suitability of silicalite-1 for use in a continuous separation process was investigated. This involved its repeated regeneration and use, in a column mode. Efficient breakthrough curves and subsequent desorption curves were obtained for the uptake of p-cresol from dilute aqueous solution.

TABLE OF CONTENTS

CHAPTER 1
INTRODUCTION

1.1 A GENERAL INTRODUCTION TO ZEOLITE MOLECULAR SIEVES

Zeolite is the generic term for a large family of aluminosilicate minerals. The first discovery of a zeolite was made in 1756 when the Swedish mineralogist Cronstedt (1) discovered stilbite. The name "zeolite" given to this new class of minerals came from the Greek *zeein* (to boil) and *lithos* (a rock), and can be explained by their characteristic water loss when heated. This discovery was followed by a succession of recorded findings of other individual members of the group (2).

Zeolite minerals are formed mainly by the metamorphosis of silicate minerals of volcanic origin (2). Hydrothermal crystallisation in basaltic inclusions leads to the formation of large single crystals. Zeolites formed in this way tend to be dispersed in occurrence and are therefore not suitable for commercial use. More massive deposits occur as tiny crystals in sedimentary rocks where they are formed in hot alkaline solutions from volcanic ashes, tuffs and pumices. These give the industrially valuable zeolite minerals which include chabazite, erionite, clinoptilolite and mordenite.

The unique properties of zeolite minerals were already being observed by the early 1900's but it was not until the late 1940's that the first definitive research into their synthesis and properties began. Barrer reported the separation of mixtures using the dehydrated zeolite mineral chabazite in 1945 (3). In 1948, the first industrial research efforts by Milton and colleagues at the Union Carbide Corporation in the U.S.A produced synthetic zeolite molecular sieves A and X. The former does not exist as a mineral, whilst the latter occurs

as the rare mineral faujasite (4,5). This controlled synthesis was a key research achievement and led to the large scale commercial application of zeolites A and X as selective sorbents and catalysts. Since that time *ca* 150 new synthetic species have been discovered. By the end of the 1950's, zeolites were employed as sorbents in large scale separations and they have been used by the petroleum industry as cracking catalysts.

Much of the commercial success of molecular sieve zeolites has been due to their versatility. Zeolite synthesis has evolved over the last 40 years in order to produce materials to tackle new technological problems in the field of separation, ion-exchange and catalysis.

Today zeolites are of ever increasing commercial importance. The work reported in this thesis is concerned with the possible application of zeolite molecular sieves and their silica molecular sieve analogues, in the new and expanding field of biotechnology.

1.1.1 Zeolite Structures

Zeolite frameworks are made up of tetrahedrally coordinated aluminium or silicon atoms linked through oxygen to four others. Thus, there are no unshared oxygen atoms in the framework,and, as in all tectosilicates (zeolites, feldspars and feldspathoids), the ratio of aluminium plus silicon to oxygen atoms is 1:2. Unlike the feldspars or feldspathoids whose structures are relatively dense, the zeolites have open framework structures of small channels and larger cavities. This openness imparts characteristic zeolite properties. The dimensions of these channels are such as to accept molecules of certain size and reject others. These materials have therefore become known as molecular sieves.

For every Si^{4+} ion which is replaced in the framework by Al^{3+}, a negative charge is created which is balanced by an electrochemical equivalent of cations. These cations are mobile and can be exchanged, to varying degrees, by other cations. The strong electric fields set up by the presence of aluminium also causes the zeolite cavities to be polar and contain water molecules. Intracrystalline "zeolitic" water in many zeolites is removed continuously and reversibly.

Zeolites can therefore be represented by the empirical formula -

$$M_{2/n}O.Al_2O_3.xSiO_2.yH_2O$$

where M is the cation with valency n, x is greater than or equal to 2 (assuming that Al-O-Al linkages are disallowed) and y is the relative number of moles of water (which is a function of the porosity and composition of the framework).

There are 36 known zeolite structures, defined by crystallographic techniques, which can be sub-divided into groups by means of their framework topology. The zeolites within each group share a common structural sub-unit which is a particular array of (Al,Si) tetrahedra. These sub-units have been called secondary building units (SBU) by Meier (6) and are shown in Figure 1.1. It is possible to construct every known zeolite framework using one or more of these SBU's. Classification by SBU leads to the classes outlined in Table 1.1. The topologies of all 36 structures have been recorded by Mortier together with details of cation and water (unit cell) sites and source references (7).

It is more appropriate to visualise certain zeolite structures in terms of polyhedral building blocks. These are cage like units designated by greek letters α,β,γ etc. In the structure of synthetic zeolite A for example, units of single four and six membered rings are joined together (8). This gives rise to a polyhedron called the truncated octahedron (Figure 1.2a). The truncated

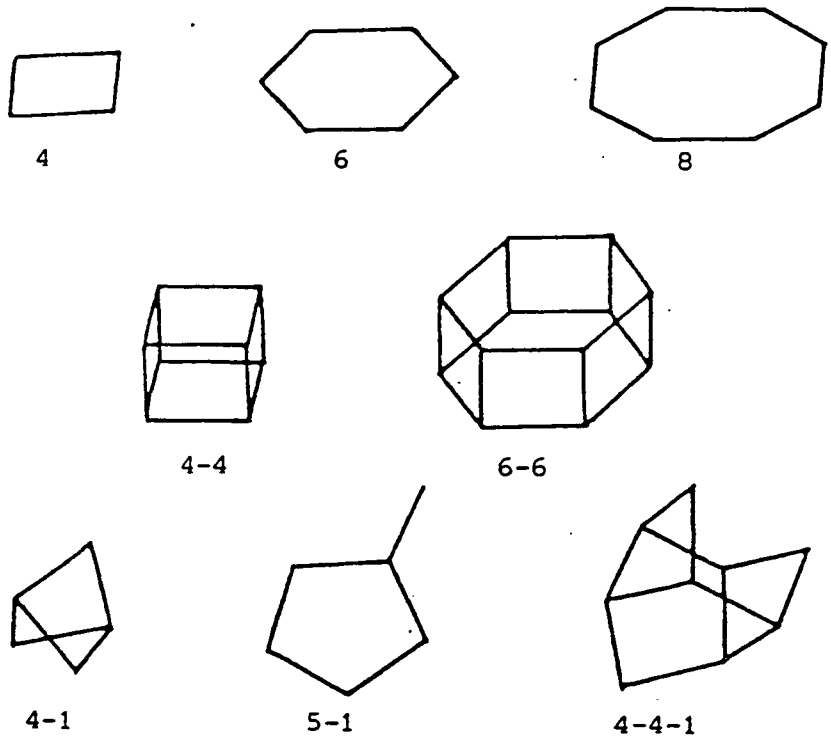

Figure 1.1 Secondary Building Units Identified in Zeolite Structures (6)

Table 1.1

Zeolite Classification[a]

	Idealised unit cell composition	Common structural element
Analcime Group		
Analcime	$Na_{16}[Al_{16}Si_{32}O_{96}]16H_2O$	S6R,S4R
Wairakite	$Ca_8[Al_{16}Si_{32}O_{96}]16H_20$	
Natrolite group		
Natrolite	$Na_{16}[Al_{16}Si_{24}O_{80}]16H_2O$	4-1
Thomsonite	$Na_4Ca_8[Al_{20}Si_{20}O_{80}]24H_2O$	
Heulandite group		
Heulandite	$Ca_4[Al_8Si_{28}O_{72}]24H_2O$	4-4-1
Clinoptilolite	$Na_6[Al_6Si_{30}O_{72}]24H_2O$	
Phillipsite group		
Phillipsite	$(K,Na)_5[Al_5Si_{11}O_{32}]10H_2O$	S4R
Zeolite Na-P	$Na_8[Al_8Si_8O_{32}]16H_2O$	S8R
Mordenite group		
Mordenite	$Na_8[Al_8Si_{40}O_{96}]24H_2O$	5-1
Ferrierite	$Na_{1.5}Mg_2[Al_{5.5}Si_{30.5}O_{72}]18H_2O$	
Chabazite group		
Chabazite	$Ca_2[Al_4Si_8O_{24}]13H_2O$	
Erionite	$(Ca,Mg,Na_{21},K_2)_{4.5}[Al_{4.5}Si_{27}O_{72}]$ $27H_2O)$	D6R, S8R
Zeolite L	$K_6Na_3[Al_9Si_{27}O_{72}]21H_2O$	
Pentasil group		
Zeolite ZSM-5	$Na_n[Al_nSi_{(96-n)}O_{192}]16H_2O$	5-1
Zeolite ZSM-11	(n = *ca* 3)	
Laumontite group		
Laumontite	$Ca_4[Al_8Si_{16}O_{48}]16H_2O$	S4R, S6R S8R
Faujasite group		
Faujasite (and isostructural zeolites X and Y	$Na_{12}Ca_{12}Mg_{11}[Al_{59}Si_{133}O_{384}]$ $260H_2O$	S4R, S6R S8R, D6R
Zeolite A	$Na_{12}[Al_{12}Si_{12}O_{48}]27H_2O$	D4R, S4R S8R

[a]after Barrer (14)

octahedron is known as a β-cage or sodalite unit and the manner in which these cages are stacked to form the structure of zeolite A is shown in Figure 1.2b. The octahedral cages are linked through double four membered rings (D4R) with bridging oxygen atoms following a cubic symmetry. This arrangement gives a central cage of diameter 1.15 nm accessible through six eight membered rings with a free diameter of 0.42 nm. The sodalite unit itself has a cage diameter of 0.65 nm accessible through six membered rings of oxygen atoms with a free diameter of 0.22 nm (9).

The zeolite mineral faujasite which is isostructural with synthetic zeolites X and Y can also be constructed from sodalite units (Figure 1.2c). In this structure however, the sodalite units are joined through four of their eight six ring faces in a tetrahedral array. This arrangement of polyhedra gives faujasite a more open structure than zeolite A. It has a central cage (α-cage) with four twelve oxygen atom windows which have apertures of 0.8 nm. The cage itself has a diameter of 1.25 nm.

The examples above illustrate the manner in which zeolite frameworks can be built up from smaller units. It must be stressed, however, that SBU's are merely crystallographic tools and do not tell us anything about the way in which zeolite crystallisation and growth takes place. It is true that certain polymeric species analogous to SBU's can be found in the media from which zeolite growth takes place, but they cannot yet be linked with certainty to the mechanism of zeolite crystallisation.

An increasingly important group of synthetic zeolites are those of the "Pentasil Group" (Table 1.1; group 7). These zeolites have structures which may be generated by the appropriate stacking of layers of the type shown in Figure 1.3a. In ZSM-5 (10) neighbouring layers are related by an inversion and in

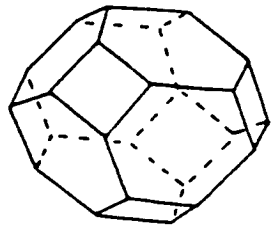

(a) truncated octahedron or Sodalite Cage.

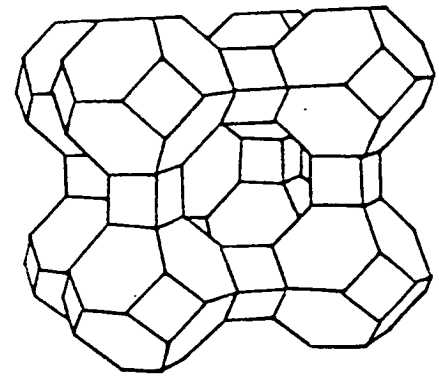

(b) Zeolite A

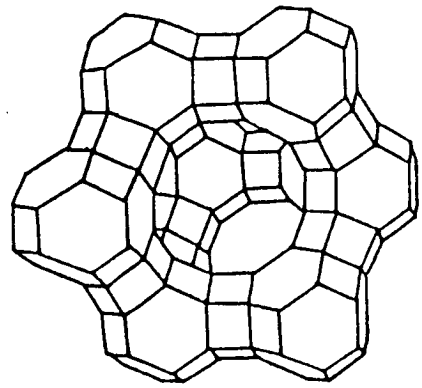

(c) Faujasite

Figure 1.2Structures Based on the Sodalite Cage.

ZSM-11 (11) by a reflection. These two zeolites are therefore structurally very similar, in fact, it is not uncommon to find intermediate structures or intergrowths of ZSM-5 and ZSM-11 (12).The channel systems which emerge from the appropriate stacking of these layers for ZSM-5 (10) and ZSM-11 (11) are shown in Figures 1.3b and 1.3c respectively. Both zeolites have a 3-dimensional channel system defined by 10 oxygen atom rings. The resulting pore window is around 0.6 nm, intermediate in size between synthetic zeolite A and faujasite.

ZSM-5 comprises two types of pore system where zig-zag channels, which are circular in shape, intersect straight elliptical channels. The intersections between the two types of channel afford more free space than the channels themselves. ZSM-11 has only one type of channel where two sets of straight elliptical shaped channels intersect to make up a 3-dimensional array. This network gives two types of intersection, one having free space similar to that in ZSM-5 and the other larger by about 30% (13). Although the differences in structure are small, as we will see later, they can have a profound effect on sorption properties.

The properties of a zeolite are determined both by structure and composition. Structure related properties are more fundamental to a given zeolite. It is often possible to synthesise one zeolite with a range of compositions by varying the Si/Al ratio, or by framework substitution of metals (eg Fe,B) or by cation exchange. However, one cannot modify the basic framework topology of the sieve to any great extent.

The sizes of the windows in a zeolite control the molecular sieving properties of that zeolite. Table 1.2 lists some n-membered ring windows (n = no. of oxygen atoms) together with their free dimensions (14).

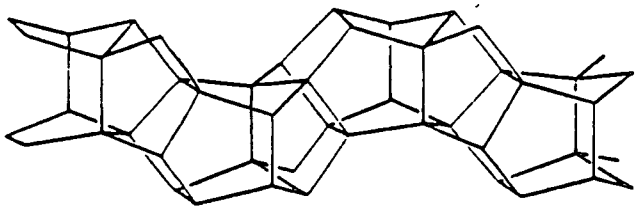

Figure 1.3 (a) Pentasil Layer

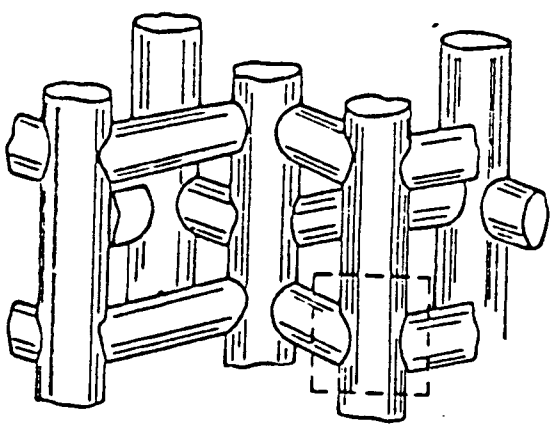

Figure 1.3 (b) ZSM-5 Channel System

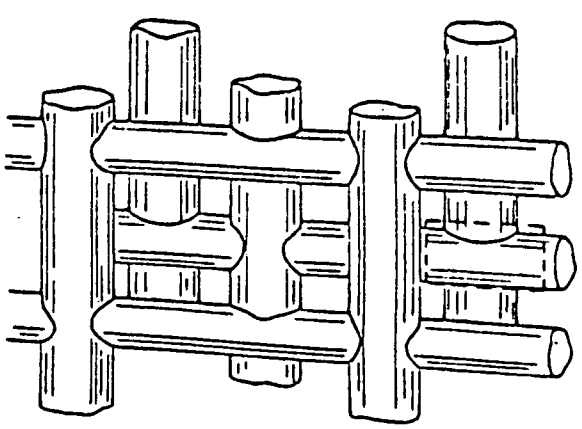

Figure 1.3 (c) ZSM-11 Channel System

Table 1.2

n	Free Dimension (nm)
4	0.115
5	0.196
6	0.28
8	0.45
10	0.63
12	0.80

The pattern of channels and voids in a zeolite determines the ease of diffusion of a sorbate molecule within the intracrystalline free volume. Channels may be one dimensional (1D), for example in mordenite, where all pathways are through non-interconnecting channels; two dimensional (2D), for example in ferrierite, where the sorbate molecule may only migrate within one particular plane; or three dimensional (3D), for example in ZSM-5, where the sorbate molecule has free movement in any direction through the crystal.

Exchange cations, because they are smaller than most sorbate molecules, can migrate more freely within zeolite crystals. Moreover, differences in molecular dimensions of sorbate molecules may be such that for the same zeolite, diffusion of large sorbate species is 1D while for a smaller molecule it could be 2D or 3D.

1.1.2 Evolution of Zeolite Synthesis

Until the early 1940's attempts to synthesise zeolites were confined mainly to the efforts of mineralogists interested in the stability relationships of zeolites with each other and with other minerals. The reaction conditions used were chosen in order to mimic the environment in which zeolites are formed in nature. Therefore, autoclaved reactions under hydrothermal conditions at high temperatures and pressures were carried out. Such reactions were reported to yield mineral type compounds (15).

A new approach to zeolite synthesis was initiated by R.M. Milton and colleagues at Union Carbide Corporation in the late 1940's. The methodology was based on starting with highly reactive alkaline aluminosilicate gels in closed systems and using low temperatures more typical of the synthesis of organic compounds than of mineral formation. This novel approach led to the discovery of *ca* 20 new synthetic zeolites in a short space of time (16).

An important factor in zeolite synthesis is the Si/Al ratio of the reaction mixture. Early synthetic work involved highly aluminous gels which gave products nearly saturated in aluminium (Si/Al = 1). The use of more siliceous gels produced zeolites of intermediate Si/Al ratio ($2 \leq Si/Al < 5$), such as zeolite L (17).

Early zeolites were all produced using very similar chemistry and only two metal cations, sodium and potassium, or mixtures thereof. The next step in the synthetic evolution was the discovery that the cation played an important role in directing the formation of specific structures (18). A major advance in the synthesis of new zeolite materials came from the addition of alkylammonium cations to the synthesis gels. Barrer and co-workers (19) reported the synthesis of N-A, a siliceous analogue of zeolite A, by the addition of tetramethylammonium (TMA) cations to sodium aluminosilicate gels and noted that the effect of the alkylammonium cation was to increase the framework Si/Al ratio. Nitrogenous analogues of zeolites B, X and Y were also synthesised (20).

The immediate effect of this innovation in zeolite synthesis was to produce more siliceous analogues of previously known structures. This was a positive step in terms of zeolite synthesis, because of the high acid and thermal stability of the more siliceous materials. The use of alkylammonium cations

soon led to the discovery of intermediate silica zeolites with novel structures, such as zeolite omega (21).

Work carried out in the laboratories of Union Carbide and Mobil Oil in the early 1970's led to the discovery of a wide range of novel high silica materials (Si/Al>10). These were crystallised from highly siliceous gels (10 < Si/Al < 100) in the presence of organic cations such as tetramethylammonium, tetrapropylammonium and tetrabutylammonium. This new and important class of synthetic zeolites opened up a whole new range of properties and applications, exemplified by the commercially important catalyst ZSM-5 (22).

Since the 1940's there have been over 100 new synthetic zeolites discovered with Si/Al ratios ranging from 1 to >1,000 using a host of inorganic and organic cations.

1.1.3 Effect of Si/Al Ratio on Zeolite Properties

The evolution of zeolite synthesis was discussed in section 1.1.2 and the trend towards the production of more siliceous materials was described. The reasons why researchers have striven to make siliceous zeolites can be explained by the effect of Si/Al ratio on their properties.

In general terms as the Si/Al ratio of a zeolite increases; its thermal stability, acid stability and hydrophobicity all increase and its ion exchange capacity decreases. Table 1.3 shows the change in properties across the series from low to high silica zeolites together with examples from each group.

Table 1.3

ZEOLITE TYPE	PROPERTIES AND APPLICATIONS
"Low Silica Zeolites" $1 < Si/Al < 1.5$ examples; Zeolites A, X	1. High cation exchange capacities. – builders in detergents (23) 2. High selectivity for water, polar and polarisable molecules. – drying agents and purification agents (24). 3. Large pore volumes (0.5 cm^3cm^{-3}) 4. Wide spectrum of pore size available through ion exchange, Cs-A(0.2 nm) -> Na-X(0.8 nm) – application in sugar separation (25) 5. High surface heterogeneity. – early cracking catalysts (26) 6. Low thermal stability 7. Low acid stability
"Intermediate Silica Zeolites" $2 < Si/Al < 5$ examples; Zeolites Y, O	1. Improved acid and thermal stability. 2. Heterogeneous surface – zeolite Y is currently the most important catalyst in hydrocarbon conversion, cracking and isomerisation (26,27). 3. High selectivity for water and other polar molecules. 4. Selective ion-exchange properties clinoptilolite used for; -radioisotope recovery (Cs^+, Sr^{++}) -NH_3 recovery (NH_4^+)
"High Silica Zeolites" $10 < Si/Al < 1000$ examples; ZSM-5, ZSM-11	1. High thermal stability (>1000°C) 2. Good acid stability 3. Little ion exchange capacity 4.Surface approaching homogeneity – hydrophobic / organophilic sorbents – ZSM-5 is an powerful shape selective acid catalyst (28) for the isomerisation of C_8 aromatics, catalytic dewaxing and methanol conversion to gasoline.
Silica Molecular Sieves $Si/Al > 1000$ example; Silicalite-1	1. Homogeneous Surface 2. Essentially hydrophobic - preferentially sorbs organic molecules from water (29)

The diversity in structure, cation content and composition of synthetic zeolites, makes it difficult to access differences due only to a variation in the Si/Al ratio of the framework. This problem was first addressed by Chen (30) who studied the hydrophobic properties of zeolites using samples of mordenite with a range of Si/Al ratios from 5 to 50. This was achieved by post-synthesis modification of the zeolite which entailed acid extraction of aluminium from the framework. A linear relationship was observed between water sorption capacity and aluminium content. The amount of water sorbed was found to be stoichiometrically related to the number of tetrahedrally coordinated alumina sites in the framework; each site was associated with 4 water molecules. It was therefore concluded that the tetrahedrally coordinated silicon atoms within the framework were essentially hydrophobic.

Although ZSM-5 is a high silica zeolite, it can be synthesised with a large range of Si/Al ratios. The aluminium content of the material can be varied over several orders of magnitude. ZSM-5 therefore constitutes a substitutional series, whose physical, chemical and catalytic properties can be studied in order to find direct relationships between aluminium content and properties. Such a study was conducted by Olson and co-workers (31). They reported that composition dependent properties, such as ion-exchange capacity, catalytic activity and hydrophobicity, vary linearly with composition. The effect of aluminium content on water sorption by H-ZSM-5 zeolites is shown in Figure 1.4. It was also noted that these relationships could be extrapolated smoothly to apply to the end member of this substitutional series, a pure silica form of ZSM-5 with a Si/Al ratio of infinity. Such a material exists and is known as silicalite-1 (32,33). Silicalite-1 is an example of an important class of materials called silica molecular sieves (Table 1.3). The structure, composition and properties of silicalite-1 and other silica molecular sieves will now be

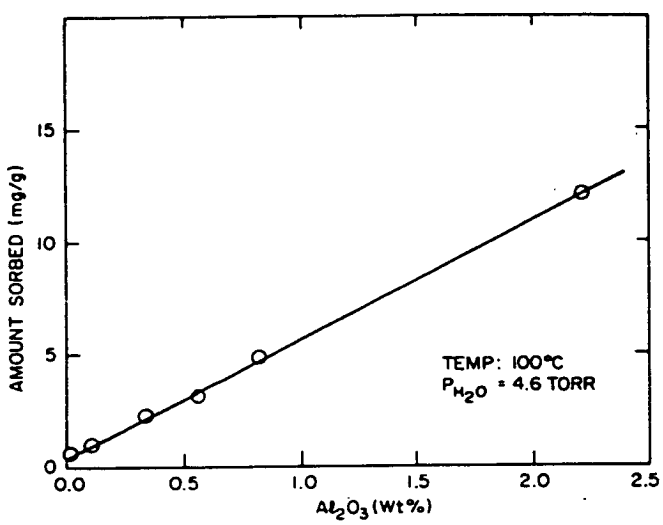

Figure 1.4 Effect of Aluminium Content on Water Sorption of H-ZSM-5 Zeolites at P/P_o = 0.006 (31).

discussed.

1.2 A GENERAL INTRODUCTION TO SILICA MOLECULAR SIEVES

Silica molecular sieves are crystalline silicates with framework topologies analogous to zeolites, but essentially free of aluminium. The first pure silica molecular sieve, silicalite-1 (32,33), was synthesised in the laboratories of Union Carbide Corporation in 1978. Since silicalite-1 contains no strong field gradients normally caused by framework aluminium or hydrophilic sites caused by exchangeable cations, it exhibits a high degree of hydrophobic and organophilic character.

Silicalite-1 has been shown to have a framework topology identical with that of the synthetic zeolite ZSM-5. It has therefore been argued, because there are always traces of aluminium present as impurities in the framework (34), that silicalite-1 is essentially identical to ZSM-5 in an ultra-high silica form. However, because silicalite-1 and other silica molecular sieves exhibit unique properties, they will be considered here as a separate class of materials.

1.2.1 Structure and Composition of Silica Molecular Sieves

Silica molecular sieves are pure silica polymorphs with open framework structures of linked, tetrahedrally coordinated silicon and oxygen atoms. Ideally, there are no unshared oxygen atoms in the framework. The channels are therefore lined with unbroken Si-O-Si bonds and are essentially hydrophobic.

Silica molecular sieves constitute the only known hydrophobic form of porous silica. They are unknown in nature but there are a growing number of synthetic members of this class of materials. These are listed in Table 1.4

together with the zeolites with which they share their framework topology (zeolite isostructures). It can be seen from Table 1.4 that, other than silica-sodalite (a small pore material), silicalite-1 and silicalite-2 are the only two known silica molecular sieves with three dimensional channel structures Their channel systems are shown in detail in Figures 1.3b and 1.3c respectively.

The remaining crystalline silica sieves have unidimensional channel structures and are therefore unlikely candidates as industrial sorbents. In structures with unidimensional channel networks, sorption and diffusion are sensitive to the presence of entrained impurities in the channels. ZSM-39 (41) and EU-4 (37) will not sorb water at room temperature which suggests very small pore structures and rules out their use as sorbents. There has been little reported on the sorption properties of the remaining 1D materials. KZ-1 and KZ-2 were reported (43) to sorb ethanol and n-butanol from aqueous solution. Although these are positive results the two sieves have no advantage over silicalite-1 and silicalite-2 which have the same size of window with the advantage of a three dimensional network. A similar argument can be applied to EU-11 which has been reported to sorb hexane-1,6-diol (37) from aqueous solution. It is therefore unlikely that KZ-1, KZ-2 or EU-11 will gain any commercial significance as sorbents in the 0.6 nm size range.

TEA-silicate, although unidimensional, has a possible advantage over silicalite-1 and silicalite-2. It is defined by a 12-membered ring channel system and therefore has a slightly larger window (*ca* 0.57 x 0.61 nm) (39). TEA-silicate has not yet been synthesised in a form which is free of inorganic cations. It is therefore more aptly described as a *metal organosilicate*. The sorption properties of this novel material have not yet been published. If a synthetic route was established in the absence of inorganic cations, this material could prove to be a very useful sorbent. A hydrophobic molecular

Table 1.4

The Structures of Silica Molecular Sieves

SILICA MOLECULAR SIEVE	ZEOLITE "ISOSTRUCTURE"	CHANNEL STRUCTURE
silicalite-1 (33) F-silicalite (35)	ZSM-5 (10) ZSM-5	3D - defined by 10 membered rings (33)
silicalite-2 (36)	ZSM-11 (11)	3D - defined by 10 membered rings (36)
ZSM-48 (38)	ZSM-48 (38) EU-11 (37)	1D - defined by 10 membered rings (38)
TEA-silicate (39)	ZSM-12 (40) Nu-13	1D defined by 12 membered rings (40)
ZSM-39 (41)	ZSM-39[a] (42)	very small pore (42)
KZ-1 (43)	KZ-1 ZSM-23 (44)	1D - defined by 10 membered rings (44)
KZ-2 (43)	KZ-2 ZSM-22 (45), Nu-10 Theta-1, EU-5	1D - defined by 10 membered rings (45)
EU-4 (37)	EU-4 (46)	structure unknown (sorption data suggests small pore material)
silica - sodalite (47)	sodalite (48)	3D - defined by 4 & 6 membered rings (48) (small pore material)

[a]It has been reported (41) that only up to 0.2% Al can be incorporated into the framework.

sieve defined by pores greater than 0.6 nm would provide a good candidate to tackle several current separation problems.

Silicalite-1 and silicalite-2 are therefore the most interesting and important silica molecular sieves synthesised to date. The synthesis and properties of these two materials will now be discussed.

1.2.2 Synthesis of Silicalite-1 and Silicalite-2

1.2.2.1 Silicalite-1

Silicalite-1 is prepared by hydrothermal crystallisation from reaction mixtures containing tetrapropylammonium cations, hydroxyl ions and a reactive form of silica. The crystallisation mechanism is thought to involve silica clathration of the hydrophobic organic cation in a similar way to the formation of crystalline water clathrates of alkylammonium salts (49). Thus, the silica tetrahedra surround the organic guest molecule in a regular manner which helps to direct crystal growth (50).

The silicalite precursor, formed in the presence of TPA^+ cations, is found to contain 4 TPAOH per unit cell of 96 SiO_2 (51). The silicalite precursor has to be activated (400-500°C) to remove the TPA^+ ions from the channel structure, before it can be used as a sorbent.

The first preparation of the silicalite-1 precursor was described by Dwyer and Jenkins (52), who referred to the calcined product as a metal organosilicate. In early preparations of silicalite-1, where the tetrapropylammonium ions were added as a salt, the hydroxide ions were supplied by the addition of an alkali metal hydroxide (31,52). These alkali metal cations were incorporated into the lattice and had to be removed by ion

exchange with a dilute acid after calcination (31). Alkali metal cations in the lattice reduce the organophilicity of the sieve, as do the hydroxyl groups formed when the ions are exchanged. Figure 1.5 illustrates how sodium ions incorporated into the framework can attack the lattice and even after ion-exchange can leave hydrophilic sites which may not heal on subsequent dehydration.

In order to optimise the hydrophobic properties of silicalite it was necessary to find a synthetic route free of alkali metal cations. The next reported route to silicalite-1 involved the use of TPAOH to provide both the mineraliser (OH^-) and the template (TPA^+) (32,33,53-55) using the system TPA_2O-SiO_2-H_2O.

The problem with this synthetic route to silicalite was that a large excess of TPAOH had to be used to achieve an adequate base content. TPAOH tends to be expensive and the commercial product can contain alkali metal impurities (56). The use of TPAOH as a source of both base and template in the system meant that separate control of alkalinity and concentration of template was not possible. This is a key point, since it has been shown that pH can have a profound effect on the morphology of the crystals obtained (51,57). Figure 1.6 shows the average length of silicalite-1 crystals obtained from a xNa_2O-2TPABr-$20SiO_2$-$1000H_2O$ system as a function of reaction mixture alkalinity (x) (51). It is important for materials to be used as sorbents to use a preparation which yields large crystals with a narrow size distribution.

The systems $(NH_4)_2O$-TPA_2O-SiO_2-H_2O and $(NH_4)_2O$-TPABr-SiO_2-H_2O have also been used to produce alkali metal free silicalite (54,56,58). However a similar problem to that encountered in the presence of alkali metal cations can arise with this synthetic route. Ammonium cations can be incorporated into the

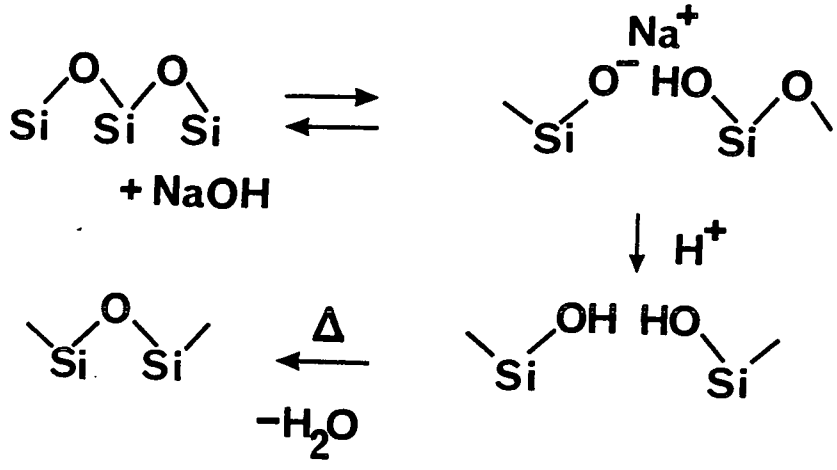

Figure 1.5 Effect of the Presence of NaOH on the Silicalite-1 Lattice.

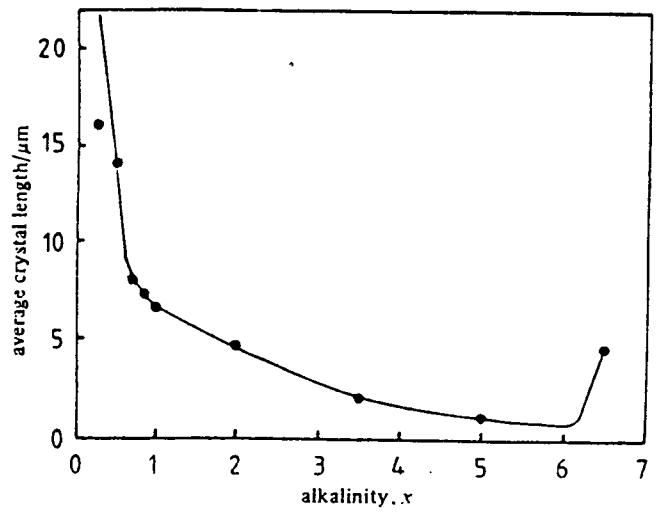

Figure 1.6 Effect of Alkalinity of Reaction Mixture on the Average Length of Silicalite-1 Crystals Obtained (51).

framework (59) during synthesis. Although they can be removed by calcination of the product, hydrophilic defects may remain.

The use of an amine–TPABr–SiO_2–H_2O system described by Fegan and Lowe (60), provides a route by which the pH of the reaction mixture can be controlled by the buffering capacity of the amine. It is important to have strict control over pH throughout the reaction if homogeneous products are to be obtained. The degree of incorporation of the amine into the silicalite precursor is minimised by the use of the cyclic amine, piperazine (PIPZ). Systems using (5–20)PIPZ 2TPABr $20SiO_2$ $1000H_2O$ in stirred reactors at 100°C produced fully crystalline materials with twinned single crystals of *ca* 8 µm x 4 µm x 2 µm.

The above technique was modified by Franklin (59) who used a similar reaction composition , 10PIPZ 2TPABr $20SiO_2$ $1000H_2O$, in a stirred reactor but increased the crystallisation temperature from 100°C to 150°C. This method gave large, single, untwinned crystals (40 µm x 10 µm x 5 µm) with a small particle size range. Silicalite–1 produced by this method is highly hydrophobic in character. At 25°C and a water activity of 0.753, the calcined product sorbs 0.015 cm^3g^{-1}. By comparison, the product obtained by Fegan and Lowe (60) at 100°C, will sorb 0.035 cm^3g^{-1} water under the same conditions. A saturation capacity of 0.047 cm^3g^{-1} (RT) was quoted by Flanigen and co–workers (33), for an early form of silicalite made from a $(TPA)_2O$–SiO_2–H_2O system (100–200°C).

A material called F–silicalite (fluoride–silicalite) was patented in 1978 (35) by Flanigen and co–workers at Union Carbide Corporation. F–silicalite is a silica polymorph with similar structure and properties to silicalite–1. The precursor of F–silicalite is crystallised from a hydrothermal system containing silica, TPA^+ and F^- ions. This material , completely free of hydroxyl ions, exhibits a large degree of hydrophobicity. It has been reported to sorb under 0.01 cm^3g^{-1} water

at 25°C and a vapour pressure of 20 torr (35).

The past developments in silicalite-1 synthesis have been aimed at obtaining a perfect hydrophobic lattice with a crystal morphology defined by large, regular crystals.

1.2.2.2 Silicalite-2

There has been very little reported on the synthesis of silicalite-2. Silicalite-2 was introduced by Bibby and co-workers (36) in 1979 as a silica analogue of the aluminosilicate zeolite ZSM-11. It was prepared by the hydrothermal crystallisation at 170°C of a reaction mixture containing silicic acid, tetrabutylammonium hydroxide and ammonium hydroxide. This preparation is analogous to the silicalite-1 preparation reported by Bibby (58) but using TBA^+ ions rather than TPA^+ as a template. The key to the preferential crystallisation of silicalite-2 is therefore the TBA^+ ion. Indeed, the importance of the TBA^+ ion in the formation of the ZSM-11 structure was made clear in the original ZSM-11 patent (63) filed in 1973.

Since that time ZSM-11 has been successfully crystallised using benzyltriphenyl phosphonium chloride (11) and alkanediamines, $NH_2-(CH_2)_n-NH_2$ (n = 7-12) (64), which suggests that there is some flexibility in the choice of template which will crystallise this structure.

A second method of silicalite-2 synthesis was reported by Rubin and co-workers at Mobil (65). This involved the use of sodium silicate, TBABr and water. However, as already mentioned with regard to silicalite-1 synthesis, it is not advisable to include inorganic cations in the preparation if a highly hydrophobic product is required.

The original method of preparation proposed by Bibby (36) used NH_4^+ ions

which are also unfavourable because of their incorporation into the framework during crystallisation. Moreover, the crystals obtained by this method are small (2-3 μm x 1.5 μm) (36).

A successful crystallisation of silicalite-2 was achieved by Fegan (60) using an analogous system to the PIPZ-TPABr-SiO_2-H_2O mixture for silicalite-1 but with the substitution of TBABr for TPABr. However, no details were given about the morphology or hydrophobicity of this material.

In recent work by Franklin (66) silicalite-2 was synthesised from a reaction mixture of the following composition; 10PIPZ 3TPeABr 20SiO_2 1000H_2O (TPeABr = tetrapentylammonium bromide). It was crystallised under static conditions at 150°C. The product obtained was highly hydrophobic in character (0.010 cm^3g^{-1} water uptake (a_w = 0.753, 25°C)) with a large average crystal size of *ca* 50 μm x 5 μm x 5 μm.

The criteria for the successful synthesis of silicalite-1 and silicalite-2 with optimum size and hydrophobicity are similar. It is necessary to work at a low pH, in a well buffered system and in the absence of inorganic cations.

1.2.2.3 Theoretical aspects of the Hydrothermal Crystallisation of Silica Molecular Sieves

In 1.2.2.1 and 1.2.2.2 the evolution of silica molecular sieve synthesis was shown to be driven by the desired goal of a perfect silica polymorph which would optimise the hydrophobic properties of the material. The importance of alkalinity in the system was brought to light and it was stated that pH control during the reaction was necessary in order to produce a homogeneous product. It is therefore appropriate to discuss the equilibrium processes at work during silicalite synthesis which lead to changes in pH.

A detailed equilibrium model for the crystallisation of silica molecular sieves has been postulated by Lowe (67) and extended by Fegan (68). However the following description is restricted to a summary of the equilibrium processes involved for the two systems from which silicalite was prepared for the purposes of this work.

During the crystallisation of amorphous silica to form a crystalline solid the following stages occur;

1. Induction period - an equilibrium is set up between the solution phase and the gel.
2. Crystal growth at the expense of the gel - the solubility of the crystalline phase is much smaller than that of the gel.
3. Solubility transfer - the amount of silica in solution is now controlled by the crystalline product.
4. Final equilibrium - an equilibrium is set up between the crystalline product and the solution phase.

(a) The xNa_2O 2TPABr $20SiO_2$ $1000H_2O$ system

1. *Induction period.* The amount of silica in solution is controlled by the alkalinity of the mixture. As the pH increases the amount of silica in the solution phase increases.
2. *Crystal growth at the expense of amorphous solid.* During this stage the pH of the reaction will fall due to the incorporation of base molecules into the silicalite;

$$4TPABr+96SiO_2+4NaOH \rightarrow (TPAOH)_4(SiO_2)_{96}+4NaBr$$

The change in pH incurred increases as the alkalinity of the reaction mixture decreases. Reactions of low alkalinity are unbuffered (low concentration of silicate ions) and a large percentage of the total base content is removed

from solution.

3. *Solubility transfer and crystal growth from clear solution.* As the alkalinity of the system increases the amount of silicalite crystallised from clear solution increases. A pH rise is incurred during this period due to a release of base on solubility transfer. δpH_3 (stages as defined on previous page) increases as base content of the reaction mixture decreases, again due to lack of buffering of the system (δpH_3 = change in pH during stage three).
4. *Comparison with experiment* : Both the experimental (68) and the predicted pH curves obtained for the system - $3.5Na_2O$ 2TPABr $20SiO_2$ $1000H_2O$ are shown in Figure 1.7. The changes in pH during stage 1 do not agree well with prediced values. This was thought to be due to the rapid crystallisation of the system. Therefore the dissolution of amorphous solid is the rate limiting step during this time and δpH_1 is under poor thermodynamic control.

(b) The xPIPZ 2TPABr $20SiO_2$ $1000H_2O$ system

In this system pH changes are governed by two factors;

- buffering due to silicate ions (as the number of moles of amine (x) in the system increases the pH and therefore the number of silicate ions increases).
- buffering due to the amine (the buffer capacity of the amine is greatest when the pH = pKa of the amine)

1. *Induction period.* The amount of silica in the system increases as the pH of the system increases.
2. *Crystal growth at the expense of the amorphous solid.* Incorporation of TPAOH causes a decrease in pH. pH changes during this transition are reduced by both amine and silicate buffering. As x increases, the relative amount of silicate buffering decreases since the buffering due to the amine reaches a maximum (RNH_3^+ / NH_2 -> 1). The net result is that as the

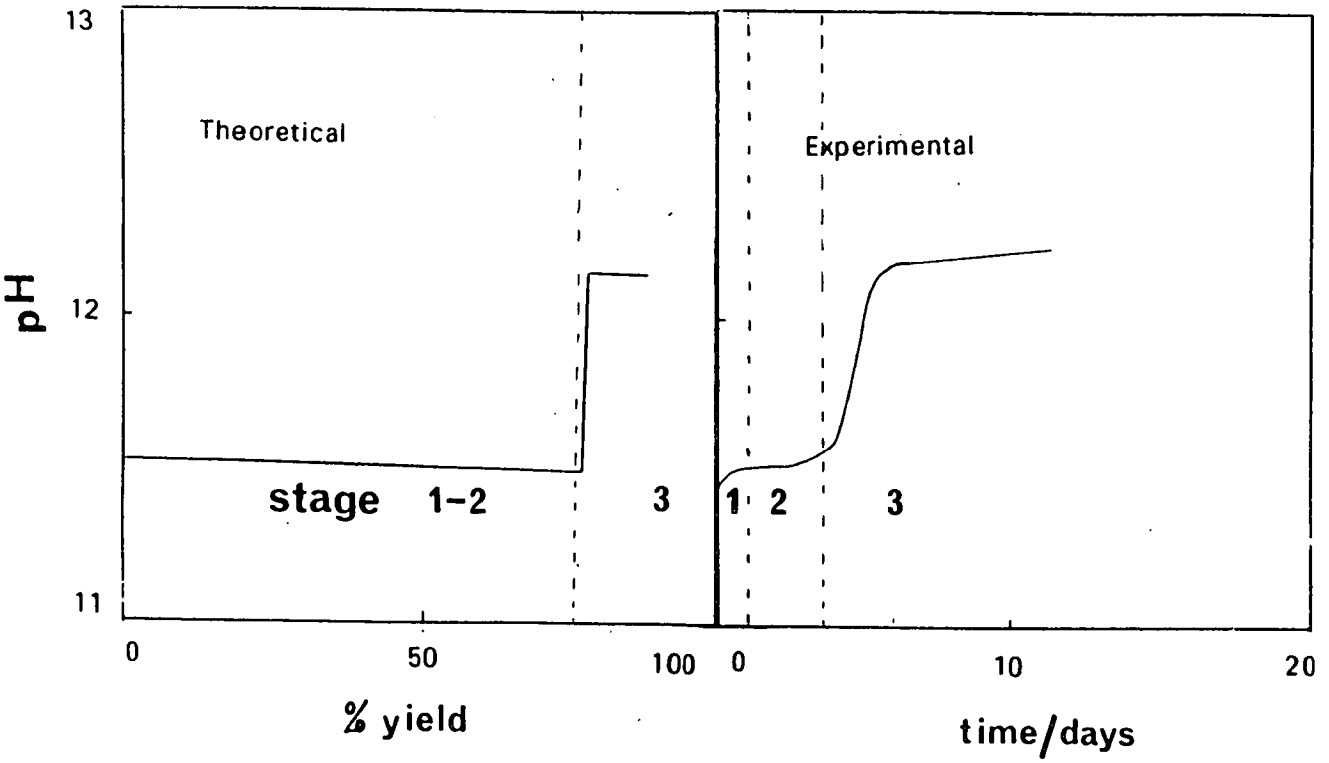

Figure 1.7 Comparison of the Theoretically Calculated and Experimentally Determined pH Profiles for Silicalite Crystallisation in the $3.5Na_2O$ 2TPABr $20SiO_2$ $1000H_2O$ System.

amount of amine in the system increases δpH_2 decreases.

3. *Solubility transfer and crystal growth from clear solution* : A pH rise occurs during this period because of *in situ* generation of base on solubility transfer. As x increases δpH_3 increases. In order to explain this, one must consider the absolute amount of base released into solution and the relative amounts of buffering supplied by the amine and the silicate ions. At x=1 for example, the system is poorly buffered by amine but the pH is so low that the effective base released into solution on solubility transfer is very small. The system can therefore buffer the effect and δpH is low. At larger values of x the base addition to the system increases and since this is a dominant effect δpH_3 does likewise.
4. *Comparison with experiment* As can be seen from Figure 1.8 the experimental results for this system (10PIPZ 2TPABr 20 SiO_2 1000H_2O) are in close agreement with the predicted values. Although no solubility transfer point was seen during the reaction, predicted rises were small, so it may have been missed due to the rate of crystallisation.

In conclusion, the importance of strict pH control during crystallisation can be summarised by the following points;

- changes in pH produces changes in the crystallisation environment and intergrowths can develop where another phase begins.
- limiting the size of pH changes may lead to a more uniform uptake of growth species and reduce microheterogeneity.
- changes in pH cause changes in the growing surface.
- rate of growth changes with pH.
- secondary nucleation induced by change in pH can lead to a large particle size distribution in the product.
- a low pH gives a high yield of crystalline product.

1.2.3 Properties of Silicalite-1

The structure and composition of silica molecular sieves was discussed in section 1.2.1. They are framework silica polymorphs which are hydrophobic in

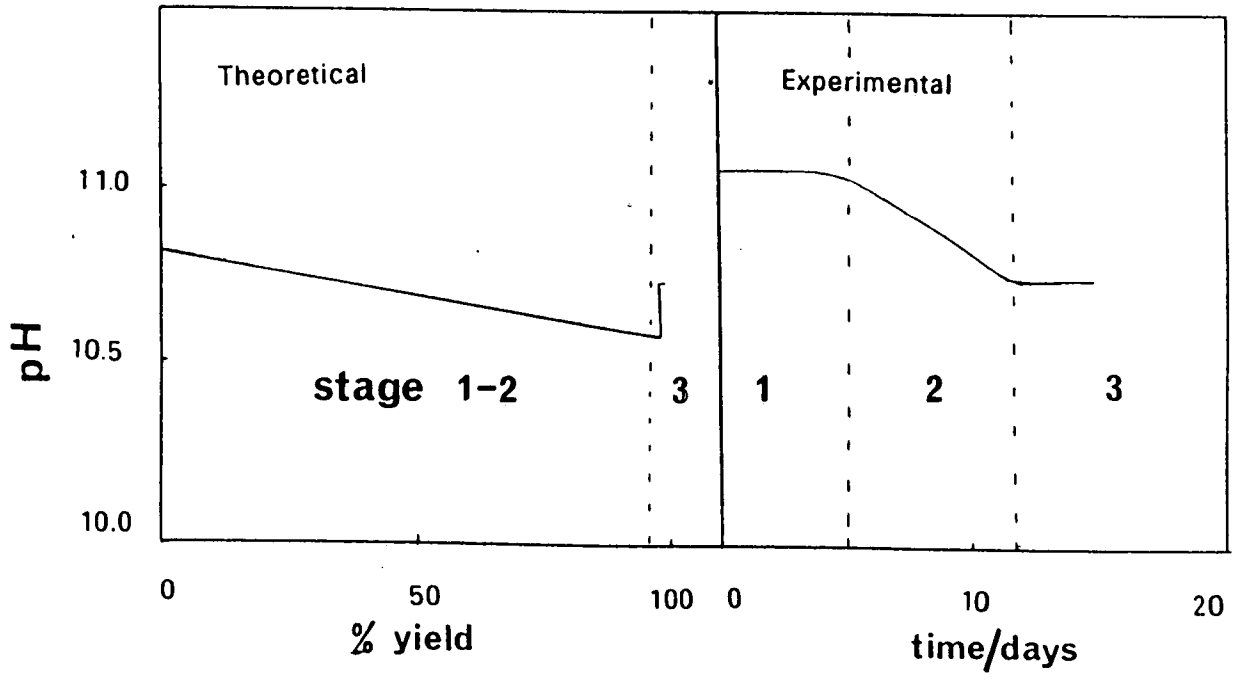

Figure 1.8 Comparison of the Theoretically Calculated and the Experimentally Determined pH Profiles for Silicalite Crystallisation in the 10PIPZ 2TPABr $20SiO_2$ $1000H_2O$ System.

character. The following discussion will deal with silicalite-1, the only member of this family of materials whose properties have been well documented.

Silicalite-1 has a framework topology similar to that of the shape selective acid catalyst ZSM-5 (10). A comparison of the structure related properties of silicalite-1 with those of ZSM-5 is given in Table 1.5. It shows that in terms of structure related properties, silicalite-1 is essentially identical to ZSM-5.

The lack of acid sites in silicalite-1 gives it high stability (33). It is stable in air to over 1100°C and only slowly converts to an amorphous glass at 1300°C. It is resistant to attack by most mineral acids but like quartz it reacts with HF. X-ray emission measurements of the Si kβ band show that the mean Si-O bond energy of silicalite is equal to that of cristobalite and exceeds that of quartz by 0.1eV. Silicalite-1 is used exclusively as a hydrophobic sorbent. It will sorb gases, vapours, liquids and indeed solids up to a limiting size range of *ca* 0.6 nm. For example it will sorb benzene (kinetic diameter 0.59 nm) but rejects molecules larger than 0.6 nm such as neopentane (kinetic diameter = 0.62 nm). Although this pore size effect can be utilised in molecular sieving, the most remarkable property of silicalite-1 is the large degree of surface selectivity it exhibits. Aluminosilicates selectively sorb water and other polar molecules, whereas silicalite-1 is hydrophobic. It exhibits a high degree of selectivity for non-polar molecules smaller than the limiting pore size of the sieve.

Gas phase sorption on silicalite-1 occurs by the filling of micropores as in zeolites and other porous sorbents. A recent study into gas phase aromatic hydrocarbon sorption on silicalite-1 was carried out by Wu and colleagues (70). A summary of the results they obtained is given in Table 1.6. The figures show that for equal surface coverage, the isosteric heats of sorption of benzene,

Table 1.5

Structure Related Properties of ZSM-5 and Silicalite-1

		ZSM-5 (10,69)	Silicalite-1(33)
Refractive Index (as synthesised)		1.48	1.48
X-Ray Diffraction Pattern		Identical	
Crystal Void Fraction		33%	33%
Channel Dimensions/Å			
straight (010)		5.4x5.6	5.7-5.8x5.1-5.2
sinusoidal (100)		5.1x5.5	5.4 ± 0.2
Density/g cm^{-3}		1.77	1.76
Framework Density T atoms/1000Å ^{3}		17.9	18.1
Micropore Volume/cm^3g^{-1}		0.18	0.199
Sorption Volume /cm^3g^{-1} (25°C)	(n-hexane)	0.18	0.199
	(benzene)	0.13	0.134

Table 1.6

Sorption Data for Various Hydrocarbons on Silicalite-1 at 20°C (70)

Sorbent	Kinetic Diameter	Sorption Capacity		q_{st}[a]
		mol/unit cell	cm^3g^{-1}	kJ mol^{-1}
n-hexane	4.3	8.2	0.185	87
benzene	5.9	8.2	0.126	80
o-xylene	6.8	2.9	0.062	48
m-xylene	6.8	4.0	0.085	-
p-xylene	5.9	6.1	0.130	41
ethylbenzene	5.9	6.0	0.140	44
cyclohexane	6.0	-	-	86[b]

[a] measured at θ (fraction of surface covered) = 0.4 for isotherms at 20°C, 100°C and 200°C.

[b] no adsorption at 20°C; estimated from isotherms at 100°C and 200°C.

cyclohexane and hexane are almost twice that of the C_8 hydrocarbons p-xylene, o-xylene and ethylbenzene. This is most likely because the larger C_8 compounds are constrained into a rigid formation by the limiting size of the channels. They will therefore not be free to optimise their interaction with the channel walls. The relatively high heats of sorption obtained for these molecules resulted in near rectilinear shaped isotherms at low temperature (20°C) with maximum sorption capacity reached at low relative pressure. The only exception was cyclohexane where at 20°C, the sorption rate was so slow that it was not possible to determine an isotherm. Cyclohexane has a similar kinetic diameter to the limiting pore size of silicalite-1 but at low temperatures has a rigid configuration which slows the sorption process. At elevated temperatures an appreciable amount of cyclohexane sorption is obtained (70).

The maximum capacities obtained for each sorbate shown in Table 1.6 reveal that the hydrocarbons studied can be divided into four groups: (1) benzene and n-hexane, (2) p-xylene and ethylbenzene, (3) o-xylene and m-xylene and (4) cyclohexane. The differences in capacities between these groups can be explained by steric effects. n-Hexane fills the pores of silicalite-1 most completely due to its small diameter and elastic configuration. Benzene has a higher density of packing than its alkyl substitutes due to a smaller size (71). p-Xylene and ethylbenzene with their alkyl groups on the same axis, fill approximately the same volume as benzene but with fewer molecules due to their increased length. Molecules with diameters larger than the size of the channels but with elastic methyl groups (o- and m- xylene) can be sorbed into silicalite-1, but appear to be restricted to channel intersections which afford more space. Finally, cyclohexane, which can not adopt the flat conformation favourable for sorption, has negligible uptake at room temperature.

A comparison of the sorption properties of silicalite-1 and ZSM-5 (72) revealed that for a series of C_6 - C_8 hydrocarbons the sorptive behaviour of the two sieves was very similar. The extent of hydrocarbon uptake and the relative rates of diffusion were found to be comparable. This implies an equivalent pore size and pore volume for hydrogen exchanged zeolite (H-ZSM-5; 3%(w/w) Al) and silicalite-1. However, the sorptive behaviour of Na-ZSM-5 (2%(w/w) Na, 3%(w/w) Al) was markedly different. Diffusion of larger molecules eg. p-xylene and 3-methylpentane was found to be very slow compared with the other sorbates. It was concluded that:

> "as a result of the presence of sodium ions, the pores of Na-ZSM-5 are appreciably more constricted than in H-ZSM-5 or silicalite-1."

This "constriction" was insufficient to affect the sorption of n-hexane. The steric effect of the Na^+ cation is such that it can influence the free channel size in a manner which is superimposed on a constant skeletal channel geometry. This effect is well known for aluminium rich zeolites such as synthetic zeolite A (23).

Although the sorption capacities of silicalite-1 and ZSM-5 are normally found to be similar, the thermodynamic quantities associated with the sorption are often quite different. A study by Pope (71) compared results obtained on silicalite-1 for the sorption of benzene, toluene and p-xylene to those previously found for ZSM-5 (73). The most striking difference was found in the results for benzene. The heat of sorption (ΔH_m) decreased steadily with surface coverage (80 to 50 $kJmol^{-1}$) for ZSM-5. For silicalite-1, ΔH_m results were independent of surface coverage up to a loading of 3 molecules per unit cell (*ca* 50 $kJmol^{-1}$) This observation is consistent with sorption onto a homogeneous surface on which the sorbed molecules do not interact with each other. However, once the pore volume was half filled, benzene - benzene

interactions began to dominate and a rapid increase in $-\Delta H_m$ and a rapid decrease in entropy (ΔS_m) was observed. The net result was that for silicalite-1, the free energy of sorption (ΔG_m) changed very little with loading.

The sorption of p-xylene was found to be energetically similar on silicalite-1 and ZSM-5. The most important difference was the initial decrease of ΔH_m with coverage observed on ZSM-5 associated with the use of stronger sorption sites which arise from the aluminium and hydrogen content of the zeolite. On silicalite-1, ΔH_m was virtually constant over the whole sorption range. ΔS_m also changed very little as maximum capacity was approached indicating that the environment of the sorbed molecules remained nearly constant. Consequently, ΔG_m was almost invariant from about 5 to 6.5 molecules per unit cell. This could account for the sorption hysteresis which has been observed in p-xylene isotherm experiments (69). For reasons already described the free energy of sorption for benzene also changes only very slowly as saturation is approached. Indeed, Lohse and Fahlke (74) have reported hysteresis in the benzene silicalite-1 system.

In the same publication, Lohse and Fahlke reported step shaped isotherms for the sorption of p-xylene, benzene and n-hexane with a plateau located at half the maximum sorption capacity. The unusual shape of these isotherms can be explained by similar arguments used to explain the thermodynamics above. Entropy measurements made by Pope (71) as a function of surface coverage implied a molecular rearrangement for benzene at *ca* 4 molecules per unit cell. Such a rearrangement could explain the plateau observed at half capacity in the sorption isotherm. Other authors (33, 70) have observed rectilinear isotherms for these sorbates on silicalite-1. It is possible that the fine structure of the isotherms in the latter two examples was missed due to lack of experimental data at low relative pressure.

There are also anomalies in the published data concerned with the thermodynamics of silicalite-1 sorption. As already described, Pope (71) found that heats of sorption of aromatic hydrocarbons were independent of surface coverage up to four molecules per unit cell. This behaviour is as expected for a homogeneous sorbent where there is no interaction between sorbate molecules. However other authors (74 - 76) have found complex variation of $\Delta H_{ads.}$ with coverage, for the same sorbate-sorbent systems, even at low fractional uptake.

These anomalies are probably best explained by differences between the silicalite-1 samples. The relationships between the conditions of synthesis and the nature of the silicalite sample obtained were discussed in section 1.2.2. One can see that deviations from the conceptual composition of silicalite-1 as a completely homogeneous sorbent are bound to occur. The properties of a particular sample of silicalite-1 will depend very much on the size of this deviation from ideality.

The study of the sorption of one gas is a convenient method with which to characterise silicalite-1 but can only give an indication of surface selectivity. The practical applications of silicalite depend very much on the degree of surface selectivity it exhibits. There has been much reported on both gas and liquid phase separations by silicalite-1. Only gas phase separation will be dealt with at this point. Sorption from the liquid phase, which is the main topic of this thesis, is dealt with in sections 1.3 and 1.4.

Silicalite-1 is best suited to problems which involve the separation of non-polar molecules from a polar environment. There are many examples of current separation problems which fall into this category (eg. waste water clean up) and most of these involve sorption from the liquid phase. However,

although fewer in number, there are gas phase separations which utilise the unique properties of silicalite-1.

The potential application of silicalite-1 in scrubbing stack gas to remove sulphur dioxide has been suggested by Chriswell and co-workers (77). The distribution coefficients obtained for various gases present in stack emissions indicated that silicalite-1 would sorb sulphur containing compounds such as SO_2, CS_2 and SMe_2 (distribution coefficients with respect to He all > 1000) in preference to the other components (CO_2, N_2O, CH_4, CO and H_2O; distribution coefficients all < 100). It was found during trials with columns of pelleted (alumina-silicate clay binder) silicalite that SO_2 was quantitatively sorbed until the capacity of the sieve was reached. The other major components did not interfere with the accumulation of SO_2.

An interesting study has been made of the effect of binders on the sorption properties of silicalite-1 (78). In processes such as the one described above it is necessary to use silicalite in a pelleted form. The distribution coefficients for a series of low molecular weight organic compounds on bonded (pelleted with an alumina-clay binder) and non-bonded silicalite-1 at 250°C were determined. It was shown that the more polar compounds (eg. ethanol) had a greater affinity for the bonded silicalite-1. This was explained by the fact that the binder used was polar. Conversely, non-polar hydrocarbons had larger distribution coefficients for the non-bonded material. It would therefore be necessary in any commercial separation to optimise the performance of the sieve by careful choice of binder.

The surface selectivity of F-silicalite-1 (35) (analogue of silicalite-1 crystallised from a mixture containing TPA^+ and F^- ions) has been demonstrated by its successful use as a column packing in gas and liquid

chromatography (79). Separations of low molecular weight alcohols from water were accomplished both in the gas and liquid phase. It was reported at that time that silicalite-1 did not provide an adequate separation of these alcohols under the same conditions. However, the use of silicalite-1 as a column packing for steam chromatography has since been reported (80). The use of steam as a carrier gas in this work was to allow the injection of large volumes of aqueous samples onto the column without serious perturbation of the chromatography. This would be a major advantage in the analysis of organic contaminants in water.

Silicalite-1 proved to be an excellent column packing for this system since it is stable in super-heated steam and has a high affinity for organic molecules, including some relatively polar compounds. In order to obtain a particle size suitable for use in gas chromatography, chromatographic grade silica gel was converted directly into silicalite-1 without a change in overall particle morphology. This represents a possible alternative to the use of binders for obtaining large particle size samples of silicalite-1. With this material, successful separations were made of low molecular weight organic compounds from water.

1.3 LIQUID PHASE SEPARATION BY ZEOLITES

The first separation of gas and liquid mixtures using crystalline zeolites was achieved by Barrer in 1945 (3). It was shown that Ca-chabazite, a zeolite mineral, could separate n-paraffins from branched chain paraffins, aromatic hydrocarbons and cycloparaffins. The most exciting aspect of the separations was their quantitative nature; they could be virtually complete in a single step. Zeolites, because of their regular, well defined structures, could add a new

order of selectivity to mixture separations by sorption.

The possibilities thus revealed began to register with industry some years after the first disclosure. An important boost came with the synthesis of zeolite A in the laboratories of Linde Air Products (4). Other major successes were the syntheses of variants of faujasite, an aluminous form called zeolite X and later the more siliceous zeolite Y. Much of the present commercial success in zeolite technology rests with synthetic zeolites A, X and Y.

In the pioneering work on separation (3) it was shown that the molecular sieving properties of a zeolite could be profoundly modified by ion exchange. For example there are clear differences between the K, Na, and Ca forms of zeolite A (4), respectively termed, sieves 3A, 4A and 5A. The numbers indicate the approximate van der Waals radii which must not be exceeded by a molecule if it is to be successfully imbibed by the sieve.

The exchanged cations occupy the same channels and cavities as the guest molecules and often occupy sites adjacent to the windows or aperture leading from one void to the next. Cations, so located can bar the passage of certain molecules while allowing others through. The effect of the cations on the molecular sieving properties of a sieve is therefore sensitive to the size of the cations and also to the number of cations at or near window sites (2). Ion exchange is now established as a standard method of tailoring zeolites to meet the requirements of a particular separation.

1.3.1 Hydrocarbon Separation

The first commercially significant hydrocarbon separation process to use a zeolite sorbent was introduced in 1964 by Universal Oil Products (UOP). It involved the separation of normal paraffins from branched chain hydrocarbons

by Ca-exchanged zeolite A (sieve 5A) (81). The selectivity in this process is based solely on the molecular sieving effect of the bulky branched hydrocarbons.

World production of n-paraffins (1.6 million tonnes / annum (1975), (82)) is now largely obtained by the use of molecular sieve sorbents. The "Molex" process (UOP) accounted for 500,000 tonnes in 1975 with *ca* 96% recovery of n-paraffins of more than 98% purity (82). n-Paraffins are used to make biodegradable detergents, chlorinated plasticisers and single cell protein, all of which are rapidly expanding commodities. Other companies which operate similar n-paraffin separation processes are British Petroleum, Shell and Union Carbide (IsoSiv).

Equilibrium sorption data (83) for the liquid phase sorption of normal paraffins by molecular sieve 5A has shown that for binary mixtures of n-paraffins, 5A will preferentially sorb the lower molecular weight component. A small degree of selective sorption is therefore also involved in an n-paraffin process.

The next major development in hydrocarbon separation on zeolites made more use of surface selectivity. The separation of p-xylene from other C_8 aromatics by Ba-exchanged zeolite Y was patented by UOP in 1972 (84). Para-xylene is used in the manufacture of terephthalic acid, a precursor of many synthetic fibres. UOP have named their process "Parex" and boast a p-xylene recovery of 99.7% of 99.3% purity from a feed containing o-, m-, p-xylene, ethylbenzene, toluene and other non-aromatic materials. Table 1.7 shows the separation results claimed by UOP for the "Parex" process (85).

Table 1.7

Results Obtained in a Pilot Scale Parex System (85)

Feed	%	Sorbate%	Raffinate%
non-aromatics	0.29	0	0.29
toluene	0.45	1.54	0.28
ethylbenzene	12.38	0.34	14.1
p-xylene	11.76	97.94	0.53
m-xylene	62.96	0.09	70.93
o-xylene	12.16	0.09	13.87

The results show that the chosen molecular sieve is very selective for p-xylene. Although toluene is also strongly sorbed by the sieve this is not crucial since it is only present in minute quantities in the feed.

A sorptive separation scheme for the separation of m-xylene from a similar feed to the one described above using Na-Y has also been patented by UOP (85). The sodium form of zeolite Y was used which changed the selectivity. The patent claims a 98% yield of m-xylene of over 99.5% purity. A process which allows the separation of ethylbenzene (Ebex) using Ca-Y has been reported to give equally impressive results (86).

Another example of a hydrocarbon separation which utilises the "Sorbex Process" is "Olex" which deals with the separation of straight chain olefins from a broad range of paraffins and olefins. Molecular sieve separation is the only efficient way to effect the above separation.

Every UOP process described above makes use of the same basic separation scheme known as the "Sorbex Process" (87). This collective term is used for all their commercial scale bulk separations which utilise molecular sieves. An ideal way to optimally separate a mixture of components by sorption - desorption is to establish a steady state operation where the solid sorbent is moved continuously countercurrent to the liquid feed and desorbent

stream. However the upward movement of a sorbent as a uniform, homogeneous packed bed is virtually impossible to achieve on a large scale. Besides attrition of the sorbent particles, uniform flow of both phases is difficult to obtain. The "Sorbex Process" therefore involves a simulated moving bed, rather than a moving bed with fixed positions for inlet and outlet streams. That is, a stationary bed and periodical movement of the positions where the liquid is introduced and withdrawn. Shifting these liquid inlets and outlets in the direction of the net liquid flow, simulates the countercurrent movement of solid. The "Sorbex Process" is always run as a continuous system. The sieve is regenerated after the sorption stage by the use of a suitable desorbent such as a low molecular weight alcohol (eg. pentan-1-ol or butan-1-ol).

This process has also been applied to the sorption of non-hydrocarbons. The separation of cresols has been successfully carried out with Na-Y (88) and the separation of cresol from a feed mixture containing xylenol has also been patented (89). The most successful sorbent for this process was found to be K-Ba-X.

Soon after the synthesis and characterisation of ZSM-5 and ZSM-11, the medium pore high silica zeolites discovered by Mobil, a comprehensive study of their sorption properties was made (90). A patent was filed (91) which covered hydrocarbon separations involving aromatic and non-aromatic compounds using any high silica zeolite (SiO_2/Al_2O_3 > 12). Most of the examples given involved H-ZSM-5, but others used H-ZSM-12, NH_4-ZSM-12, Cs-ZSM-5 and dealuminated H-Zeolon (mordenite). The most successful examples were those which depended only on molecular sieving to effect the desired separation. The separation of o-xylene from p-xylene and cyclic from normal paraffins were two such examples. Other more specific patents filed by Mobil describe the use of ZSM-5 to selectively sorb lubricant components of

high viscosity index from hydrocarbon base stocks (92) and the use of ZSM-11 to selectively sorb linear from branched aliphatics (93). Whether or not there is any advantage in these high silica zeolites over the more traditional A, X and Y zeolites for hydrocarbon separation is not yet clear. It is probable that each material will be most aptly suited to a different type of separation.

Molecular sieve technology has a firm hold on the market in terms of the separation of hydrocarbons of similar boiling points. The foregoing discussion was not an exhaustive review of liquid phase separation by zeolites. It concentrated on processes patented by UOP but there are numerous patents with different assignees which use similar zeolites but contain specific embodiments. It was not thought appropriate to include all of these.

A recent publication (94) compared the efficiency of sorption separation processes similar to those described above in the liquid and vapour phase. Xylene separation on zeolite molecular sieves was the chosen system. It was concluded that operation in the vapour phase (150°C - 170°C) improved separation efficiency due to an increased mass transfer rate, decreased axial dispersion and a much lower hold up. These effects overcame the large drop in selectivity due to temperature increase (57 - 150°C). It was found that although energy intensive, gas phase separation was highly competitive with the present "Sorbex Process" operating in the liquid phase. It was suggested that moves should be made to improve the efficiency of the present liquid phase processes. Several possibilities such as an increase in temperature to increase mass transfer rates or technological improvements to reduce axial dispersion in industrial units were mentioned. It was concluded that because of energy considerations, future developments should aim to increase the efficiency of present liquid phase processes rather than looking at gas phase alternatives.

1.3.2 Aqueous Phase Separation

The hydrophilic nature of zeolite molecular sieves make them unlikely candidates for aqueous phase separation processes. However, it is possible to make use of their other properties such as large pore diameters and ion exchange capability and to modify them for use in specific aqueous phase processes. Hydrophobic silica molecular sieves are more suitable sorbents for aqueous phase processes, but have the disadvantage of a limiting pore size of 0.6 nm. They are of little use in the separation of larger molecules such as sugars.

Fructose is the sweetest of all sugars present in nature and is known to be useful dietetically as the most ideal sugar. High purity fructose can only be obtained by separation from other monosaccharides. Traditional separation methods include the conversion of fructose into an insoluble lime-fructose complex with calcium chloride and various anion and cation exchange resins. The former method is batchwise in nature and involves too many steps to render it economically viable for large scale production. The latter, ion exchange methods, require a large amount of resin and encounter the serious problem of resin deterioration. In 1976 the first patent (95) which involved sugar separation on zeolites was filed by Toray Industries Incorporated of Japan. This claimed the efficient separation of glucose and fructose by a range of synthetic zeolites (A,X,L,Y) with a range of exchanged cations.

Their most successful separations occurred on Ba-Y and Ca-Y from a 50:50 mixture of glucose and fructose. The separation depends on the ability of fructose to complex with the Ca^{++} or Ba^{++} ions in the zeolite. Fructose is therefore the extract and glucose the raffinate. No attempt to recover the sorbed fructose was described in this patent.

Since the original patent there have been several others filed by UOP (96 - 98). The details contained in these patents together with their specific embodiments are described in Table 1.8.

UOP have a sugar separation process in operation called the "Sarex Process" which concentrates on the separation of fructose from corn syrup with Ca-Y.. Table 1.8 shows that UOP have also filed patents concerning selective sugar sorption on K-X (97,98).

There have been several patents filed by UOP which describe techniques to reduce the solubility of a zeolite molecular sieve in water. One of the suggested methods was to coat the zeolite with a cellulose based binder (99) and another involved impregnation of the zeolite with aluminium cations (100). These patents point to a definite drawback incurred with the use of aluminous zeolites in an aqueous system. At pH 6 - 8, where most of these separations are carried out, the solubility of the zeolite in water is sufficient to present serious problems in long term use.

A patent which describes sugar separation by zeolites X and Y has also been filed by Union Carbide (101). It claims the selective sorption of mannose from glucose by Ba, Sr, Na and Ca forms of zeolite Y and Ba-X. Mannose is a convenient source of mannitol, a commercially significant but expensive material. The epimerisation of glucose, a major source of mannose yields a mixture of the two sugars. The best resolution between mannose and glucose was found with Ba-X.

The use of zeolites in the separation of sugar alcohols has also been patented by Union Carbide (102). The successful separation of mannitol and galactol using Ba-X and Ba-Y and of mannitol and sorbitol using Ba-X was claimed.

Table 1.8

UOP Patents on Sugar Separation

Abstract	Claimed Process	Claimed Zeolites	Ref.
Separation of a Ketose from a feed mixture containing a ketose and an aldose by selective adsorption of ketose with subsequent recovery of ketose.	"Sorbex Process" as described in sec. 1.3.1 40% soln. containing a 50:50 mixture of glucose and fructose. Desorbent: water.	NH_3-, Na-, Ca- K-, Sr-, Ba- exchanged Y Ba-, Na-, Sr-, Ba/K-,Ba/Sr- exchanged X	96
Separation of glucose from fructose by selective adsorption of glucose with subsequent recovery of glucose.	"Sorbex Process" - separation from a feed such as invert sugar or corn syrup. Desorbent: water.	K-exchanged X	97
Isomerisation of glucose into fructose with recovery and recycling of unreacted glucose to isomerisation stage.	Isomerisation with glucose isomerase followed by separation using "Sorbex Process". Desorbent: water.	K-exchanged X	98

An aqueous phase separation process of great current interest which involves the separation of caffeine from aqueous solutions, such as coffee and tea, by contact with a dealuminated form of zeolite Y has been patented by Union Carbide (103). The zeolite called "Ultrahydrophobic Zeolite Y" (UHP-Y) (104) has a SiO_2/Al_2O_3 molar ratio of 4.5 to 35 and is produced by vigorous steam treatment of a low sodium form of zeolite Y. The size of the caffeine molecule dictates the use of a large pore zeolite such as X or Y. The hydrophobic nature of these sieves meant that they had a higher affinity for the molecules in the beverage extracts which were more polar than caffeine. It was found however that the modified, more hydrophobic form of zeolite Y, UHP-Y exhibited a unique selectivity towards caffeine. The overall patented process involved the selective sorption of caffeine from dilute aqueous solution (> 1% w/w) by UHP-Y followed by desorption of at least a portion of the caffeine by ethanol at a temperature of at least 20°C.

The preceding examples show that although zeolites are not intrinsically suited to selective sorption from the aqueous phase, they can be modified by either ion exchange or dealumination, so as to make them suitable for specific separation problems.

The recent advent of high silica zeolites has meant that materials of a more hydrophobic nature are available. An aqueous separation process which uses high silica zeolites (SiO_2/Al_2O_3 > 12) exemplified by ZSM-5 has been patented by Mobil (105). The process involves the recovery of precious metals such as platinum and palladium, via their soluble amine complexes, by selective sorption from aqueous solution. It was shown, for example, that Na-ZSM-5 could quantitatively sorb a tetraaminepalladium II ion from a $5x10^{-3}$M aqueous solution of tetraaminepalladium II chloride. A process of this kind is of great interest since it could lead to the recovery of deactivated precious metals from

spent catalysts. The regeneration of such an expensive commodity is commercially attractive.

Silica molecular sieves, the pure silica analogues of certain high silica zeolites are the obvious choice of sorbents for aqueous phase separations which require shape and surface selectivity. The growth of interest in these materials for this type of separation will be discussed in section 1.4.

1.3.3 Liquid Phase Drying Applications of Zeolites

All zeolites have a high affinity for water and other polar molecules and can in general be used for the removal of water from gases and liquids and for general drying. Co-sorption of the material to be dried must be avoided.

The most important zeolites in terms of drying applications are the different forms of synthetic zeolite A; 3A, 4A and 5A. The sieve 3A is excellent for drying unsaturated hydrocarbon streams such as cracked gas since it excludes all hydrocarbons including ethylene which would undergo polymerisation reactions if co-sorbed. By the same token, 3A is used in the liquid phase for n-paraffinic hydrocarbons and polar liquids such as methanol and ethanol.

Although most liquid phase drying studies have concentrated on small port zeolites to prevent co-sorption , Kiovsky and Koradia (106) have proposed a scheme to dry chlorinated hydrocarbons with mordenite and have found commercially acceptable sorption capacities.

In industrial processes, which include polymerisation or catalytic conversion, even trace amounts of water (<50 ppm) can cause problems and the only practical solution is dehydration by an appropriate molecular sieve. For example, Stannet and co-workers (107) have reported on the use of zeolites to

dehydrate liquid vinyl monomers prior to radiation-induced, ionic polymerisation.

The best choice of zeolite for a particular drying process can be difficult. Many preliminary investigations must be made and the following factors taken into account:

- the effect of possible contaminants in the system on the chosen zeolite
- separation factors
- competitive co-sorption
- environmental stability
- regeneration techniques
- irreversible zeolite contamination

The prodedure for zeolite selection was demonstrated (108) for two commercially important liquids, benzene (80 ppm water and trace HCl) and 1,4 butanediol (1200 ppm water). They used samples of H-mordenite for their studies. General liquid phase drying applications of zeolites were discussed in a review published in 1979 (108).

1.4 LIQUID PHASE SEPARATION BY SILICA MOLECULAR SIEVES

1.4.1 Hydrocarbon Separation

Although the most unique quality of silicalite-1 is surface selectivity, the framework topology of the material with a fixed pore size of *ca* 0.6 nm means that it can find application in separations where it acts simply as a molecular sieve. There have been several patents filed on this topic, all assigned to UOP.

The first patent, filed in 1982 (109), claimed a process for the separation of an ester of a fatty acid from that of a rosin acid by selective sorption of the fatty acid on silicalite-1. Zeolites X and Y were unsuitable for this separation since they allowed the sorption of both the fatty acid and the more bulky rosin acid. Zeolite 5A, another traditional material used in separation, has a pore size which is unable to accommodate either of the esters.

The efficiency of the process was illustrated by an example of the use of silicalite-1 in a column mode. At 160°C and a flow rate of 1.2 cm^3min^{-1} an excellent separation of the two types of ester was observed. The feed stream contained 20% distilled tall oil, 40% methyl-8-reagent (to form methyl esters of fatty and rosin acids) and 40% cyclohexane. Cyclohexane was used as a desorbent to recover the sorbed fatty ester. The overall scheme was analogous to the "Sorbex Process" already described, which was patented by UOP in connection with hydrocarbon separations on zeolites.

Production of fatty esters is the most important process in the industrial chemistry of fatty acids. These esters find the greatest application in the solvent and plasticiser fields. Saturated fatty esters are used in compounding lubricating oil and unsaturated esters are used as drying agents.

A process for the separation of straight chain from branched or cyclic

hydrocarbons has also been patented for silicalite-1 (110). This patent claim s that silicalite-1 is particularly suitable for this process, and that water contamination of the product was eliminated by the use of a hydrophobic sieve. The traditionally used zeolite 5A, on the other hand, requires a relatively high water content (2%,w/w). They also claimed that unlike zeolite 5A which has been shown to discriminate between n-paraffins, selectively sorbing the low molecular weight materials (83), silicalite-1 would sorb them as a class of materials showing no selectivity with number of carbon atoms. The overall scheme claimed, was again analagous to the "Sorbex Process".

The third UOP patent involved the separation of cis and trans olefins by the selective sorption of the smaller trans olefin (111). The use of zeolites for olefin separation is difficult because of the catalysis of olefin reactions by the aluminosilicate. Silicalite-1 can effect the separation with complete elimination of the undesired side effects of dimerisation and polymerisation. The scheme claimed by UOP was again their own "Sorbex Process" with its simulated moving bed operation. The process was exemplified by the use of clay bound silicalite-1 to separate cis and trans but-2-ene. A selectivity factor of two was obtained with selective sorption of the trans species. A 50:50 mixture of pent-1-ene and isopentene was used as a desorbent to complete the cyclic process.

The sorption isotherms of hept-1-ene, benzene, cyclohexane and n-octane on silicalite-1 at 30°C with n-hexane as a solvent have been obtained by Ma and Lin (112). The results were discussed in terms of the shape selectivity of the silicalite-1 and the size and electronic effects of the sorbates. The isotherms were measured at solute concentrations less than 1 mmol cm^{-3}. The sorption capacity of the sorbates was found to decrease in the order benzene > cyclohexane > n-octane which agrees with the vapour phase results

reported by Wu et al (70) and is also consistent with the size differences of these molecules (Kinetic diameter/ Å; 5.23, 6.09, 7.54 respectively). It was found that n-hexene and cyclohexene produced the steepest isotherms and were therefore the most strongly sorbed of the molecules studied. The increased affinity of silicalite-1 towards these molecules was said to be due to the presence of a π-bond. However the relative strength of interaction of the sorbate with the solvent n-hexane must also be taken into account in the analysis of these isotherms.

The sorption of binary solutes, benzene + cyclohexane and cyclohexane + cyclohexene in n-hexane, were also measured. These systems showed that both benzene and cyclohexene were sorbed in preference to cyclohexane with selectivity factors greater than unity. Most of this selectivity can be attributed to the increased size and non-planar configuration of cyclohexane.

No theoretical treatment of the isotherms was attempted. This would have been difficult due to the complexity of the systems involved. The composite isotherms were S-shaped which suggests that competitive sorption of n-hexane was an important factor.

1.4.2 Aqueous Phase Separation

Silicalite-1 is uniquely suited to aqueous phase sorption processes since water is virtually excluded from the pores of this material (33). Before the potential applications in this field are discussed, a short explanation of the hydrophobic nature of the sorbent is deemed appropriate.

The nature of a hydrophobic sorbent surface is very different to that of an ionic surface. For the sorption of water, specific interactions are especially important. In the absence of surface sites which are hydrophilic or of sites for

hydrogen bonding, polar or acid base interactions, the surface becomes homogeneous and hydrophobic. Silicalite-1 fits the above criteria with a continuous framework of Si-O-Si bonds.

In water, each molecule is hydrogen bonded to its neighbours in an approximately tetrahedral configuration, but in silicalite-1 the narrow channels only allow interaction with two or three molecules. There is no strong interaction between the electrically neutral silicalite-1 and the water, thus the steric factor will prevent the sorption of water into the sieve.

The small amount of water which is sorbed by silicalite-1 varies with the method of synthesis used and is probably due to faults in the lattice. These faults can occur during crystallisation through attack on the framework by hydroxyl ions incorporated with the TPA^+ template. Hydroxyl groups which persist after removal of the organic ion from the precursor are also a source of hydrophilic sites. The effect of these sites on the sorption properties of silicalite-1 will be discussed in Chapter 4.

The initial isosteric heat of sorption of water on silicalite-1 is estimated to be 20 $kJmol^{-1}$ (33), substantially below the heat of liquefaction of water. This requires high entropy, low energy sorption and indicates high mobility of the sorbed water molecules.

1.4.2.1 Recovery of Ethanol from Fermentation Broths

Industrialised nations face a critical problem in replacing the sources of liquid fuels that have traditionally been supplied by petroleum. One solution which has stimulated much interest is the use of ethanol produced by fermentation of renewable biomass as a source of liquid fuel.

In a conventional ethanol fermentation process, yeast and other microorganisms convert sugars to ethanol and carbon dioxide. The maximum concentration of ethanol which can be achieved by fermentation is limited by the tolerance of the microorganisms to ethanol. At ethanol concentrations above 2% by weight of the fermentation medium, the rate of fermentation begins to decline. At concentrations of about 20% fermentation ceases. This level represents an inherent limitation on the productivity of ethanol.

Distillation which is the traditional method for the separation of ethanol from fermentation media is expensive, and calls into question the economic viability of the process. There are many investigations currently underway to find alternative, less energy intensive techniques for water - ethanol separation.

In an article by Hartline entitled *Lowering the Cost of Alcohol* published in 1979 (113) the technology available at that time to help lower the cost of ethanol recovery was reviewed. The following energy saving schemes were mentioned:

- absorption of "some of the water" by dry plant materials.
- vapour phase separation using yarn fibres to absorb water. (Comment: energy requirements are bound to be high)
- extraction of ethanol with critical CO_2 (80atms). Estimated cost using this process is 40-60% of ethanol fuel value.
- solvent extraction eg. dibutyl phthalate. Problems caused by emulsion formation in beer. (Comment: A more recent publication concerned with solvent extraction (114) discussed the feasibility of several solvents. Alkanes provided the most encouraging distribution coefficients and were found to cause no growth inhibition in yeast. This was an important factor since water recycling was considered central to the economics of the process.)
- membrane separation; water permeable membranes would require too much pressure to be practical. Ethanol permeable membranes were still in the development stage and it was mentioned that an "ethanol carrier" would most likely have to be used.
- the use of zeolites in the final purification stage to remove residual water (eg. clinoptilolite).
- several energy saving adaptations of original distillation method.

It is clear from the above suggestions that no satisfactory energy saving scheme had yet been devised. The use of hydrophobic sorbents to remove the

ethanol was not mentioned in this review, but has since received much attention.

The announcement in 1978 of the discovery of silicalite-1 (33), proclaimed it as:

> *"a new hydrophobic molecular sieve capable of removing organic molecules from water streams"*

It was in 1980 that the possible application of silicalite-1 in water - ethanol separation was first mooted. Two reports (115,116) published at Oak Ridge Laboratory in the United States outlined the use of silicalite-1 to sorb ethanol from dilute aqueous solutions. In the first they compared the use of silicalite-1 with a styrene - divinylbenzene copolymer. They found from isotherm data that silicalite-1 was the more efficient at ethanol removal from dilute solution. It reached a sorption capacity of 0.08 g EtOH g^{-1} silicalite-1 at an ethanol concentration of 5%(w/w).

The second paper described the use of silicalite-1 in a column mode. A 10%(w/w) aqueous feed solution was pumped through a short (25 cm x 1.9 cm) column packed with sorbent at 1 cm^3min^{-1}. The column was loaded to maximum capacity, then the ethanol desorbed using warm nitrogen (35°C). A sharp breakthrough curve was obtained which indicated an efficient process.

However a low average ethanol concentration for the desorbed vapour (12%,w/w) led to the overall conclusion that silicalite-1 would not make a suitable sorbent for this process. These results were perhaps caused more by a bad choice of desorption conditions than to the lack of suitability of the sieve.

A more optimistic report (117), coupled with the first patent (118) concerned with this process were published by workers at Iowa State

University in 1981. The report described the effect of constituents normally found in fermentation beer on the sorption properties of the sieve. They found that the presence of inorganic salts increased the capacity of silicalite-1 for ethanol and also concluded that the presence of other low molecular weight compounds in the beer would not be detrimental to the process. These by-products would most likely be sorbed by the sieve. If they were then removed with ethanol during the stripping stage, they would result in an increase in the combustible fuel content of the product. If, on the other hand, these trace organics were strongly held by the silicalite-1, periodic stripping under more severe conditions would regenerate the sieve. Either way, in a continuously operating fermenter, an undesirable build up of these by-products in the beer would be avoided. They suggested that addition of surfactant would facilitate the removal (draining) of beer from the void spaces of the column before the ethanol stripping step. Experiments showed an improved sorption of ethanol by silicalite-1 in the presence of Zonyl FSP surfactant which was presumed to be due to an improved interaction of the aqueous ethanol with the sorbent.

Several desorption methods were discussed in this report, such as microwave stripping, stripping gas and displacement gas methods. The conclusions made were that stripping gases such as O_2, CO_2 and N_2 had to be used at very high temperatures (85-95°C) to achieve adequate stripping. Displacement gases (SO_2, NH_3) provided encouraging results. Lower stripping temperatures were possible and regeneration of the column was easier because of the high solubility of these gases in water. However the corrosive nature and high ethanol solubilities of these gases presented a problem.

The patent (118) which was filed by the same establishment, described the concentration of ethanol from dilute solutions using a fixed bed of sorbent. The

overall process claimed included a regenerative step where the ethanol was stripped by CO_2 (*ca* 70°C) followed by a water wash (35-40°C).

Similar patents to the one described above have been filed by Mobil to cover the use of the high silica zeolites, exemplified by H-ZSM-5, for ethanol separation (119,120). The first patent described the use of the CO_2, produced as a byproduct during fermentation, as a stripping gas and the second encompassed the use of the sieve *in situ* to remove ethanol during fermentation.

The hydrophobic nature of high silica zeolites has been known for over a decade (121), but it was not until the recent renewed interest in ethanol production by fermentation that their use in this type of process was proposed. It is unlikely however that they will prove as efficient as silicalite-1 for this purpose because although their affinity for the relatively polar ethanol may be enhanced over silicalite-1, water sorption by these materials would almost certainly be a problem. The British Petroleum Company have filed a European Patent (124) which covers ethanol separation on all zeolites with $SiO_2/Al_2O_3 >$ 12.

Vapour phase studies on ethanol sorption have been carried out by Klein and co-workers (124,125). They suggested that the reason for the substantial amount of water found in desorbed ethanol, reported by workers in the liquid phase (117), could be due to the trapping of water in the interstices between the particles of sorbent. This was minimised by measuring sorption from the vapour phase. They found that the sorption of ethanol by silicalite-1 could be represented by a simple Langmuir mixture model (see Chapter 2) and that the selectivity for ethanol by silicalite-1 was essentially the same in the liquid and vapour phase. It was also inferred that the sorbed phase, although highly

concentrated, was not anhydrous ethanol; in practice 98%(w/w) EtOH was obtained from a 10% beer 25°C.

The most recent patent concerned with ethanol separation from fermentation broths was filed by Union Carbide Corporation (125). This invention was directed at a vapour phase process. In agreement with the previously mentioned publication (117), it claimed poor efficiency of the liquid phase process due to entrapment of the dilute fermentation beer between the particles of sorbent. They proposed a low energy vapour phase scheme using a non-sorbable stripping gas, enriched with ethanol and water, for the sorption step. A comparison of the energy requirements for a liquid and gas phase process was not given. A vapour phase separation process is unlikely to be able to compete with an efficiently run liquid phase process, provided the problem of dilution by residual feed during the desorption stage has been overcome.

The proceedings of the 1983 European Brewery Convention on ethanol recovery (126) included liquid phase sorption isotherms and diffusivity measurements for ethanol on silicalite-1. Column experiments showed steep breakthrough curves for sorption from a 6%(w/w) ethanol solution. However, the average desorbed concentration (in N_2 at *ca* 80°C) of ethanol was only 35%(w/w) compared to the expected value of 91%(w/w). The discrepancy was reported to be as a direct consequence of the structure of the silicalite-1 pellets. The volume of the macropores of the pellets were measured by mercury porosimetry and found to be 0.28 cm^3g^{-1}. It was assumed that the macropores were completely filled with bulk solution and the micropores (0.16 cm^3g^{-1} of pellets) were at equilibrium before desorption. A simple calculation gave a value of 28%(w/w) EtOH for the desorbed product. It was claimed that a substantial improvement could therefore be made by adjusting the ratio of

macropore to micropore volume within the pellet.

In a report for Union Carbide Corporation (127), Pitt and co-workers described the energy considerations for a liquid phase process where the residual feed was flushed out of the interstices in the sorbent bed using gas at room temperature. They found that 90%(w/w) ethanol sorbed from a 10%(w/w) solution could be recovered in a 60%(w/w) fraction by this method. The overall process, which included a second stage ethanol enrichment from 66 to 99%(w/w) and subsequent condensation from the inert stripping gas, was costed. They reported that the present separation method by distillation requires *ca* 30-60% of the product energy. Although some new distillation methods require as little as 20%, the sorption method at 16% of the product energy is certainly competitive with more traditional methods.

Although fermentation itself is an ancient art, fermentation technology in terms of large scale efficiency is a relatively new field. Until recently, most processes have been carried out at low enzyme density with different unit operations (production and separation) separated in time and space. The feasibility of continuous, extractive bioconversion which would solve the problem of product inhibition is currently being studied.

It has for example been proposed to operate ethanol fermentation at elevated temperature under vacuum (128) with continuous removal of ethanol from the fermentor. It was reported that the economic use of a vacuum could provide a condensate of > 30% ethanol from a fermentation broth containing 3-4% ethanol. This would greatly reduce distillation costs. However, vacuum fermentation equipment is expensive to fabricate, use and maintain so this may prove to be impractical. The build up of other inhibitory compounds is also a danger in such a process.

The use of aqueous two phase systems (129) has also been suggested as a means of continuous extractive fermentation. For example, a mixture of two polymers; polyethylene glycol and dextran in water will form two phases. The basis of the process is that the enzyme will be in one of the phases. In a favourable situation, the substrate is partitioned to that same phase and ethanol to the opposite. Early experiments on this system suggested that the productivity of the reactor was improved by a factor of three over traditional methods.

In situ ethanol extraction has also been studied with a view to using sorption technology. Lencki and co-workers (130) looked at the effect of removing ethanol during fermentation on the batch kinetics of glucose utilisation by the yeast *Saccharomyces cerevisiae*. Silicalite-1 and two polymeric sorbents (XAD-4 and XAD-7) were used in the experiments. The addition of the two polymeric sorbents to the fermentation greatly inhibited cell growth. This was due to nutrient and cell sorption by the resins. Silicalite-1 did not cause any inhibition and greatly reduced the concentration of ethanol in the fermentor. This reduction did not increase glucose utilisation to the extent predicted by product inhibition kinetic models. The reasons for this were unclear. It was suggested that ethanol may accumulate inside yeast cells during batch growth and that exterior ethanol concentrations are only of secondary importance in the inhibitory process. It was therefore felt that an in depth knowledge of ethanol inhibition mechanisms must be developed before productivity increases could be optimised. They concluded on a pessimistic note that current extraction processes, including vacuum fermentation, solvent extraction and sorbent methods appeared to be too costly and complex to be practical.

A recent paper by Bui and co-workers (131) compared the use of activated

carbon, silicalite-1 and ZSM-5 in an *in situ* ethanol sorption process. Glucose was found to sorb appreciably on activated carbon and in a competitive manner to ethanol. Ethanol sorption on ZSM-5 was found to be 30% less than that on silicalite-1. This difference could be attributed to either of two factors: water molecules compete with ethanol molecules for the same sites in ZSM-5, or the amount of water sorbed by the sieve was appreciable. This observation confirms a prediction made earlier that ZSM-5 is not as good a candidate for this type of sorption process as silicalite-1. Dynamic experiments showed that out of the three sorbents, sorption and desorption was fastest (almost instantaneous) on silicalite-1. On the basis of the results obtained they concluded that silicalite-1 was the most suitable sorbent for the *in situ* sorption of ethanol from fermentation broths.

Other hydrophobic sorbents which have been studied for ethanol sorption from water have included activated carbon (132) and esterified silica (133). However, the macropores of these materials are extremely detrimental in terms of selectivity. For example, the former patent (132) described a separation experiment using activated carbon in a column mode at room temperature. From a feed solution containing 15%(w/w) ethanol, there was a 50:50 %(w/w) mixture of ethanol and water retained on the sorbent.

From all the available literature, it appears that silicalite-1, whether it is used as an *in situ* sorbent or as part of a more conventional separation process will make an invaluable contribution to energy saving in ethanol recovery from fermentation beers.

1.4.2.2 Sorption of Organic Compounds other than Ethanol from Aqueous Solution

Biotechnology is an ever growing area of modern technology with a wide range of substances now produced by microorganisms. Many of the current

processes involve the production of peptide-based compounds such as proteins, nucleic acids and other polypeptides. These are best recovered by ion exchange chromatography or other specialist chromatographic techniques (134).

However, a number of fermentation processes are carried out in more traditional areas of the chemical industry. Petrochemical modification into specific isomers for use in plastics and polymer synthesis is an area where fermentation technology has already been utilised. ICI, for example, has replaced the conventional synthesis of polyphenylene with a route which employs bacteria to synthesise the 5,6-di-hydroxycyclohexa-1,3-diene precursor (135).

A recent patent (136) disclosed a process for the production of C_2 - C_5 hydrocarbons by the fermentation of biomass. Industrial waste was suggested as a potential nutrient source. The separation procedure proposed in the patent involved vacuum distillation. Silicalite-1 would no doubt be applicable to this system.

An article by Busche (137) published in 1983 reviewed the current state of the art in terms of separation technology applied to aqueous solutions of both low and high boiling organic compounds. For low boiling products, such as ethanol, the conclusions made were similar to those discussed in the previous section (1.4.2.1) of this work. Busche summarised the current separation technology as confined to distillation techniques and solvent extraction, but predicted that future developments lay in the fields of molecular sieve sorption and membrane separation.

For high boiling products, Busche recognised the problem of increased energy requirements. He described current solutions such as vacuum distillation, solvent extraction, fractional crystallisation and acid extraction as

inadequate. Future development was said to rest with membrane technology if the durability and efficiency of the membranes could be maximised.

The potential of molecular sieve technology for the separation of high boiling fermentation products from aqueous media was not recognised in this review. However, as will be described, silicalite-1 could provide a cost effective answer to many separations of this kind.

The applicability of silicalite-1 in the removal of n-butanol from fermentation broths has already been realised (138). Silicalite-1 has a greater affinity for butanol than for the shorter chain alcohol, ethanol.

Detailed studies of the sorption of low molecular weight alcohols by silicalite-1 have been made by Milestone and Bibby (139) who compared equilibrium sorption isotherms for the sorption of various C_1 - C_5 alcohols. It was found that the alcohol concentration at which saturation occurred, decreased as the chain length of the alcohol increased The relative sorption capacities also increased with alcohol chain length. No obvious saturation point was reached from methanol solutions. Only 50 mg g^{-1} was sorbed from the most concentrated solution used (5%,w/v).

These observations are in contrast to alcohol sorption onto aluminous zeolites, where water and the lower alcohols are most strongly sorbed and ethanol is sorbed in preference to butanol (140).

The effect of aluminium and cation content on the sorption of alcohols from aqueous solution by ZSM-5 has also been reported by Milestone and Bibby (141). For ethanol and methanol, the amount of alcohol sorbed increased with Al_2O_3 content of the sieve whereas for n-butanol the opposite was true. Sorption was also found to be dependent on the counter ion present. The

amount of sorbed alcohol decreased as the ionic size of the exchangeable cation increased.

Alcohol desorption experiments showed that the zeolite retained a portion of the alcohol to temperatures sufficiently high (*ca* 250°C) that catalytic breakdown occurred. This observation is another example of the inapplicability of ZSM-5 to commercial alcohol concentration.

The most recently published study of alcohol sorption on silicalite-1 was made by Haegh (142) in 1985, which gave a comparison of the sorption of low molecular weight alcohols (C_1 - C_3) from water by silicalite-1, silicalite-2, F-silicalite (35), ZSM-5 and $AlPO_4$ molecular sieves (143). Haegh showed that alcohols were more efficiently removed by the silicalites than by ZSM-5 or the $AlPO_4$ materials. Of the silicalites studied, silicalite-1 was shown to have the largest capacity. The decrease in capacity exhibited by F-silicalite was said to be due to small amounts of fluorine in the channel system. The smaller capacity observed for silicalite-2 over silicalite-1 (40% less for n-PrOH) is rather surprising given their similar framework topology. The isotherms obtained for the sorption of MeOH, EtOH and PrOH from water on silicalite-1 and F-silicalite were described as Langmuir type isotherms. However, no analysis of the curves to give sorption coefficients was attempted.

Another example of alcohol separation by silicalite-1 was provided by Dessau (91) who reported that n-butanol was selectively sorbed from an aqueous solution containing isobutyl alcohol and tertbutyl alcohol. The amount of each component sorbed was 90.7%, 17.3% and 0% respectively.

An evaluation of the sorption properties of silicalite-1 for potential application to the isolation of low molecular weight organics from drinking water was made by Chriswell and co-workers in 1983 (144). It was found that

compounds as diverse as phenol *170*, acetic acid *72*, ethylacetate *4970*, chloroform *1230* and low molecular weight normal aldehydes; C_2 *100*, C_5 *2800* and C_7 *440* could be recovered from aqueous solution. Distribution coefficients between silicalite-1 and water were established and are shown in italics after each compound mentioned above. These were determined at a single analyte concentration (10 ppm). Although no detailed sorption isotherms were established, the distribution coefficients give a guide to the relative ease of accumulation of each compound on silicalite-1.

Note the peak in the distribution coefficients for the straight chain aldehydes at a carbon chain length of C_5. Lower molecular weight species have an increased affinity for water over silicalite-1 whereas the larger aldehydes must assume a linear, strained conformation to enter the pore structure. The large distribution coefficient of the less polar ester ethyl acetate is also of interest. The accumulated analytes were recovered by gradient elution with methanol water mixtures. An involved study of dichloroacetonitrile sorption and desorption gave quantitative results with over 95% recovery of the analyte. This report successfully illustrated that silicalite-1 could be used for the isolation of a wide variety of organic metabolites from drinking water.

The separation of aromatic compounds from water is a common problem about which there has been little reported. Aromatic compounds are used in many industrial processes and therefore accumulate in waste streams. Phenol derivatives are also common metabolic products and can be specialised enough to warrent their production by a fermentation route (135).

There has only been one reported study into the sorption of aromatic compounds from aqueous solution (145). It dealt with the sorption of phenol, o-cresol, m-cresol, p-cresol and benzyl alcohol from aqueous solution.

Sorption isotherms were obtained at 25°C. The data was fitted to the Freundlich isotherm in the following form:

$$\log(X/M) = {}^{1}/_{n}(\log C) + \log K$$

in which X/M = uptake / mg g^{-1}, C = concentration / mol dm^{-3} and n and K are constants. A solution to the above equation does not take into account a maximum sorption capacity. Silicalite-1 has a limited sorption volume therefore as expected, the sorption data obtained gave a poor fit to this isotherm model. The sorption coefficients obtained were therefore unreliable. A further problem with this work was the poor quality of the silicalite-1. The X-ray diffraction pattern suggested that there was amorphous material in the product. Sodium cations, from the inorganic mineraliser, could have caused a reduction in the hydrophobicity of the crystalline product.

1.4.3 This Work

This work is concerned with the potential application of ultrahigh silica zeolites to the downstream separation of materials produced by biochemical processes. Microbial cultures can produce many organic materials and as already described, the separation of specific products from dilute solutions of such a complex nature is an immense problem. The aim of this work is to assess the applicability of silicalite-1 to such systems.

For this purpose, a study of the properties of silicalite-1 with respect to the sorption of selected phenol derivatives from aqueous solution is described. Sorption isotherms are reported for the different sorbates to allow the selectivity of the sieve for different materials to be quantified.

The retrieval of the sorbed product and subsequent regeneration of the sieve would be of prime importance in any industrial application. For this reason, the potential of several low molecular weight alcohols with respect to their use as desorbents is assessed. The capacity, selectivity and capability for repeated regeneration and use of silicalite-1 in a continuous separation process is also evaluated.

CHAPTER 2
THEORY

2.1 INTRODUCTION

Theoretical aspects of sorption at the solid - liquid interface will be discussed in this chapter. Particular attention will be paid to the sorption of small molecules from dilute solution. On the basis of the sorption phenomena discussed, a simple equilibrium model for sorption from solution by silica molecular sieves will be put forward.

In the theory of sorption, a logical division is made according to whether or not the sorbate is present in dilute solution. For dilute solutions the treatment is very similar to that for gas phase sorption, whereas for more concentrated solutions the theoretical description is inevitably more complicated. The following discussion is therefore restricted to sorption from dilute solution.

2.2 SORPTION OF SOLIDS FROM SOLUTION

The sorption of non-electrolytes at the solid - solution interface may be viewed in terms of two different physical pictures. The first assumes that sorption is confined to a monolayer next to the surface, with the implication that succeeding layers are virtually normal bulk solution. This picture is similar to that given for the chemisorption of gases (146) and similarly carries with it the implication that solid - solute interactions decay rapidly with distance.

Unlike the chemisorption of gases, however, the heat of sorption from solution is usually small and more comparable with heats of solution than with chemical bond energies.

The second picture is one of an interfacial layer or region, multimolecular in depth (up to 10 nm deep) over which the interaction potential with the solid

slowly decays. This situation is more akin to the sorption of vapours (146), which become multilayer near saturation point. Sorption from solution from this point of view corresponds to a partition between a bulk and an interfacial phase.

Although both models have found some degree of experimental support, the monolayer model is more amenable to simple analysis. Moreover, sorption on to a molecular sieve with limited pore dimensions will almost certainly follow more closely to the monolayer model.

Due to the restricted range of concentration involved, the terms *solute* and *solvent* will be used for the two component systems to be discussed. In studies concerned with the solid - liquid interface the following sorption phenomena are of greatest interest;

1. the shape of the sorption isotherm
2. the significance of the plateau found in most isotherms
3. the extent to which the solvent is sorbed
4. the existence of monolayer or multilayer sorption
5. the orientation of the sorbed molecules
6. the existence of specific interactions eg. hydrogen bonding

2.2.1 The Sorption Isotherm

The number of moles of solute species sorbed per gram of sorbent is given experimentally by $\Delta c V_{sol}/m$ where Δc is the change in concentration of the solute during sorption, V_{sol} is the total volume of solution and m is the weight of sorbent. The experimental results obtained in the present investigation were treated in this way to give the uptake U expressed as grams of sorbate per gram of sorbent, $U = M\Delta c V_{sol}/m$ where M is the molecular weight of the

sorbate. The values reported are given as percentage uptakes, i.e. 10^2U.

Given that mole numbers and other extensive quantities are on a *per gram of sorbent* basis, n_o (moles of solute sorbed per gram) is given by,

$$n_o = V\Delta c = n_s\Delta N \qquad (2.1)$$

where V is the volume of solution per gram of sorbent, n_s is the total number of moles of solution per gram of sorbent and ΔN is the change in mole fraction of solute during sorption. In these equations the subscript o denotes (organic) sorbate.

The quantity n_o, is a function of c (the equilibrium solute concentration) and temperature, for a given system. At constant temperature $n_o = f_T(c)$ and this is called the *sorption isotherm function*. The usual experimental approach is to determine this function by the measurement of sorption as a function of concentration at a given temperature.

Various functional forms of *f* have been proposed either of an empirical nature or as a result of specific models. The *Langmuir* sorption equation is a particularly important member of the latter. The Langmuir equation was originally derived to apply to gas phase sorption (147). It assumes the surface to consist of specific sorption sites of area σ^o, and that all sorbed species interact only with a site and not with each other. Sorption is therefore limited to a monolayer.

In terms of sorption from solution it is more plausible to think of an alternative view of the model. Sorption is still limited to a monolayer, but this layer is now regarded as an ideal two dimensional solution of equal size solvent and solute molecules of area σ^o. Therefore lateral interactions, absent in the site picture, cancel out in the ideal solution layer picture, since they are independent of composition. Thus whereas in the original model σ^o is a

property of the solid lattice, in the solution model it is a function of the sorbed species.

For the two dimensional solution picture, if one expresses surface concentrations in terms of mole fractions, the sorption process can be written as

$$O(\text{solute in solution, } N_o^s) + S(\text{sorbed solvent, } N_s) = O(\text{sorbed solute, } N_o) + S(\text{solvent in solution, } N_s^s)$$

The equilibrium constant for this process is given by

$$K = (N_o/N_s)(S)/(O_s) \tag{2.2}$$

where (S) and (O_s) are the solvent and solute activities in solution, and, by virtue of the model, the activities in the sorbed layer are the mole fractions N_s and N_o respectively. Since the treatment is restricted to dilute solutions, (S) is constant and we can write $K_L = K/(S)$; also, $N_o + N_s = 1$ so that equation 2.2 becomes

$$N_o = K_L(O_s)/1 + K_L(O_s) \tag{2.3}$$

Since $N_o = n_o/n_{o,max}$ where $n_{o,max}$ is the number of moles of sorption sites per gram, equation 2.3 can also be written

$$n_o = n_{o,max}K_L(O_s)/(1 + K_L(O_s)) \tag{2.4}$$

$$\text{or } \theta = K_L(O_s)/(1 + K_L(O_s))$$

where $\theta = n_o/n_{o,max}$ or fraction of the surface covered.

In sufficiently dilute solution, activity coefficient effects will be unimportant so that in equation 2.4, (O_s) may be replaced by $[O_s]$ where [ ] denotes concentration.

The equilibrium constant K can be written,

$$K = e^{\Delta S/R}.e^{-\Delta H^\circ/RT} \tag{2.5}$$

where ΔH^o is the net enthalpy of sorption, often denoted $-Q$, where Q is the heat of sorption. Thus the constant K_L can be written

$$K_L = K_L' e^{Q/RT} \tag{2.6}$$

$$\text{where } K_L' = e^{\Delta S/R} \tag{2.7}$$

In equation 2.4 with (O_s) replaced by $[O_s]$, at low concentrations n_o will be proportional to $[O_s]$ with a slope of $n_{o,max}K_L$. At sufficiently high concentrations, n_o approaches the limiting value of $n_{o,max}$. Therefore $n_{o,max}$ is a measure of the capacity of the sorbent and K_L, of the intensity of sorption.

In terms of the ideal model, $n_{o,max}$ should not depend on temperature, while K_L should show anexponential dependence as given by equation 2.6. These two constants can be evaluated by curve fitting a set of experimental data to the Langmuir equation (equation 2.4).

The Langmuir treatment assumes a homogeneous surface. Most surfaces however are heterogeneous, which leads to a variation of K_L with θ. If this variation in K_L is attributed solely to the variation in heat of sorption then the solution to the sorption isotherm gives

$$\theta = n_o/n_{o,max} = a[O_s]^{1/n} \tag{2.8}$$

where $a = \alpha RTnK_L'$ and K_L' is defined in equation 2.7 and α and n are constants. Equation 2.8 is known as the *Freundlich* sorption isotherm (148).

Unlike the Langmuir equation, the Freundlich isotherm does not become linear at low concentrations but remains concave to the concentration axis; nor does it show a saturation or limiting value.

2.2.2 Effect of Temperature

In general, the uptake of sorbate at a given concentration will decrease with an increase in temperature. The effect is greatest at low concentration and the isotherm may reach the same limiting value at high concentrations. The attractive forces between the solute and the sorbate become weaker with an increase in temperature. This phenomenon, coupled with an increase of the solubility of the solute in the solvent, leads to the described effect. Therefore if the solute can be regarded as distributed between the sorbed layer and the solution in a partition equilibrium, the position of the equilibrium is shifted in favour of the solution as the temperature rises, i.e. K_L decreases as required by equation 2.6.

2.2.3 Competitive sorption

On sorption from binary mixtures, preferential or selective sorption occurs. This can be thought of as competitive sorption and can be influenced by several factors. The interaction of each component with the solid surface is important, as is the interaction between the two components in solution. Other factors such as porosity and heterogeneity of the sorbent are also significant.

Although sorption from solution is assumed to involve mainly physical sorption, hydrogen bonding of one component has an effect intermediate between those of physisorption and chemisorption. This in turn would have a profound effect on selectivity. However even relatively small differences in sorptive forces can be responsible for preferential sorption which can be detected experimentally. It is not surprising, therefore, that theoretical treatment of these phenomena is not yet advanced.

The porosity of a sorbent is also an important factor in terms of selectivity. Solid sorbents range from those which are completely non-porous through

those with macro, intermediate and micro pore sizes. Molecular sieves represent the limiting case where preferential sorption of the smaller component of a two component mixture is possible, irrespective of other factors.

A comparison of *chemical* and *steric* effects is shown in sorption from mixtures of benzene and n-hexane by molecular sieves (149). The pores of Linde molecular sieve 5A are too small to admit benzene; n-hexane is therefore preferentially sorbed at all concentrations. The sieves 10X and 13X, however have wider pores which admit both molecules. In this case, competitive sorption depends only on surface selectivity. The interaction between the Π-electron system of benzene and the ionic lattice of the zeolite is so strong that n-hexane is excluded over virtually the whole concentration range.

The orientation of a sorbed molecule can also influence competitive sorption. If a molecule is highly asymmetric, the orientation it adopts may considerably alter the number of molecules which can occupy a unit surface area. Again, this phenomenon is especially important for microporous sorbents where the pores are in the molecular size range.

The effect of temperature on sorption was described in section 2.2.2. As expected from the previous discussion, a rise in temperature leads to a reduction in selectivity.

2.3 A SIMPLE EQUILIBRIUM MODEL FOR SORPTION FROM SOLUTION BY ZEOLITE MOLECULAR SIEVES

2.3.1 Introduction

The sorption of organic sorbates from solution by zeolite molecular sieves is undoubtedly a complicated process. The following treatment is not meant to be definitive or complete; it is offered merely as a simple model to assist in the interpretation of the results obtained in this work.

2.3.2 Derivation of Sorption Isotherm Equation

2.3.2.1 Case in which solvent is not sorbed by sieve.

In this case the sorption may be represented by the equilibrium

$$Z + O_s = ZO \qquad (2.9)$$

where Z represents the *empty* zeolite and O_s represents the organic sorbate dissolved in solvent S. The equilibrium constant K_L is given by

$$K_L = (ZO)/(Z)(O_s) \qquad (2.10)$$

in which ( ) represent activities. As an approximation to the activities of the solid phases we can write

$$(ZO) = (n_o/n_{o,max}) \qquad (2.11)$$

$$(Z) = 1 - (n_o/n_{o,max}) \qquad (2.12)$$

where n_o is the number of moles of sorbate per unit quantity of sieve. Combination of 2.10, 2.11 and 2.12 gives,

$$\theta = (n_o/n_{o,max}) = K_L(O_s)/(1 + K_L(O_s)) \qquad (2.13)$$

and for dilute solutions,

$$\theta = K_L[O_s]/(1 + K_L[O_s]) \qquad (2.14)$$

where [ ] denotes concentrations. One can see that this equation is equivalent to the *Langmuir* equation for sorption derived in section 2.2.1.

2.3.2.2 Case in which solvent is sorbed by sieve.

In this case the sorption equilibrium involves the displacement of sorbed solvent S by the organic sorbate O; sorption may be represented by the equilibrium

$$ZS + O_s = ZO + S \quad (2.15)$$

and the equilibrium constant is given by

$$K_L = (ZO)(S)/(ZS)(O_s) \quad (2.16)$$

where (S) is the activity of the solvent in the bulk solution.

If all the available void space in the sieve is occupied by solvent molecules then,

$$(n_o/n_{o,max}) + (n_s/n_{s,max}) = 1 \quad (2.17)$$

and as an approximation to the solid phase activities we can write,

$$(ZO) = (n_o/n_{o,max}) \quad (2.18)$$

$$(ZS) = (n_s/n_{s,max}) \quad (2.19)$$

Hence the isotherm equation becomes,

$$\theta = (K_L(O_s)/(S)) / (1 + K_L(O_s)/(S)) \quad (2.20)$$

For dilute solutions (S) = 1 and,

$$\theta = K_L[O_s]/(1 + K_L[O_s]) \quad (2.21)$$

2.3.3 Factors which Contribute to K_L

2.3.3.1 Case in which solvent is not sorbed by sieve

As described in section 2.2.3 the Langmuir constant for sorption given here as K_L depends on the affinity of the sorbate for the solvent and the sorbent. The relative magnitudes of separate contributions may be determined by considering the sorption of the organic sorbate O from the gas phase. The relevant equilibria are set out in Figure 2.1. With reference to this figure, K_{zeo} is a measure of the affinity of the sorbate for the molecular sieve,

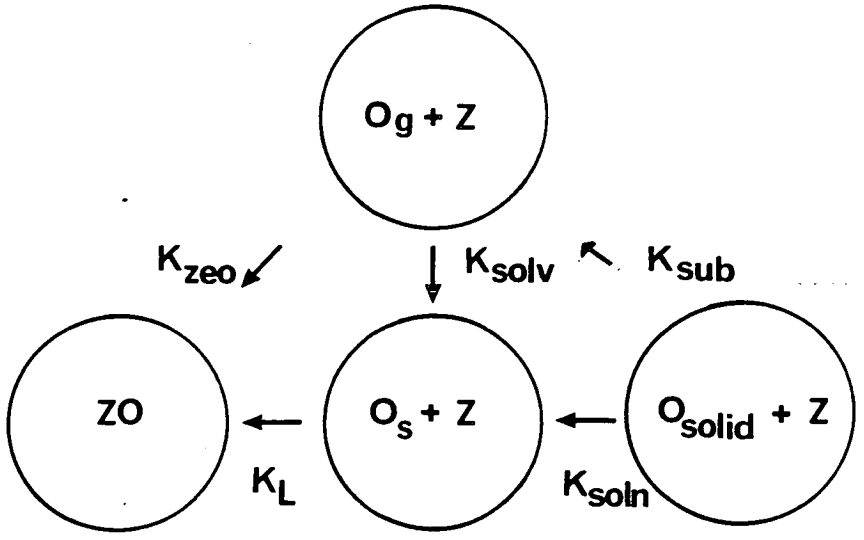

where;

K_{sub} = coefficient for the sublimation of the organic sorbate.

K_{solv} = coefficient for the solvation of the sorbate in solution.

K_{soln} = coefficient for the dissolution of the sobate in the solution phase.

K_{zeo} = coefficient for the sorption of the sorbate from the gas phase.

K_L = coefficient for the sorption of the sorbate from the solution phase.

Figure 2.1 Equilibria Involved in Sorption

$$K_{zeo} = (ZO)/(Z)(O_g) \quad (2.22)$$

and K_{solv} is a measure of the affinity of the sorbate for the solvent,

$$K_{solv} = (O_s)/(O_g) \quad (2.23)$$

It follows that the Langmuir constant K_L is related to K_{zeo} and K_{solv} by,

$$K_L = K_{zeo}/K_{solv} \quad (2.24)$$

This shows that if the affinity of the sorbate for the sieve is large then K_L is large whereas if the affinity of the sorbate for the solvent is large then K_L is small. To separate K_L into its component equilibrium constants it is necessary to determine one experimentally.

K_{zeo} is the Langmuir constant for the sorption of the sorbate from the gas phase and could be measured directly if the sorbate was sufficiently volatile. This is not the case for the materials used in this work.

K_{solv} is related to the equilibrium constants for dissolution, K_{soln}, and sublimation, K_{sub}, of the sorbate. For sparingly soluble sorbates,

$$K_{soln} = (O_s)/(O_{solid}) = \text{solubility of sorbate} = s \quad (2.25)$$

$$K_{sub} = (O_g)/(O_{solid}) = \text{vapour pressure of solid sorbate} = p \quad (2.26)$$

$$K_{solv} = K_{soln}/K_{sub} = s/p \quad (2.27)$$

It is therefore possible to determine K_{solv} from measurable properties of the sorbate. K_{zeo} can therefore be calculated from K_L and K_{solv} ($K_{zeo} = K_L K_{solv}$). For a particular sorbate, once K_{zeo} has been obtained, it is possible to calculate K_L for sorption from any chosen solvent provided the solubility of the sorbate is known since,

$$K_L = K_{zeo}p/s \quad (2.28)$$

2.3.3.2 Case in which solvent is sorbed by sieve.

In this case,

$$K_L = \{(ZO)/(Z)(O_s)\}\{(Z)(S)/(ZS)\} \quad (2.29)$$

$$K_L = \{K_{zeo}/K_{solv}\}\{1/(K_{zeo,s}p_s)\} \quad (2.30)$$

where,

$$K_{zeo,s} = (ZS)/(Z)(S_g) \quad (2.31)$$

and

$$p_s = (S_g)/(S) = \text{vapour pressure of solvent} \quad (2.32)$$

$K_{zeo,s}$ refers to sorption of the solvent from the gas phase, i.e. it is the Langmuir constant for gas phase sorption of the solvent and could be measured experimentally. An alternative route to $K_{zeo,s}$ is by measurement of K_{zeo} using a solvent which is not sorbed by the sieve. $K_{zeo,s}$ for the sorbed solvent can then be obtained from the experimentally observed Langmuir constant by means of the equation

$$K_{zeo,s} = K_{zeo}/p_sK_{solv}K_L = pK_{zeo}/sp_sK_L \quad (2.33)$$

2.3.4 Enrichment Factors

Figure 2.2 shows the shapes of the isotherms which would be expected for sorption of a particular sorbate from both water and from an organic solvent. If the organic solvent was used as a desorbent in a sorption / desorption process the enrichment factor that could be achieved may be defined as the concentration ratio c_s/c_w corresponding to a given fractional uptake θ. If both isotherms are represented by the Langmuir equation then these concentrations are related by,

$$K_{L,w}c_w = K_{L,s}c_s \quad (2.34)$$

The enrichment factor $E_{s/w}$ is given by,

$$E_{s/w} = c_s/c_w = K_{L,w}/K_{L,s} \quad (2.35)$$

and is independent of θ. For the case in which water and the organic solvent

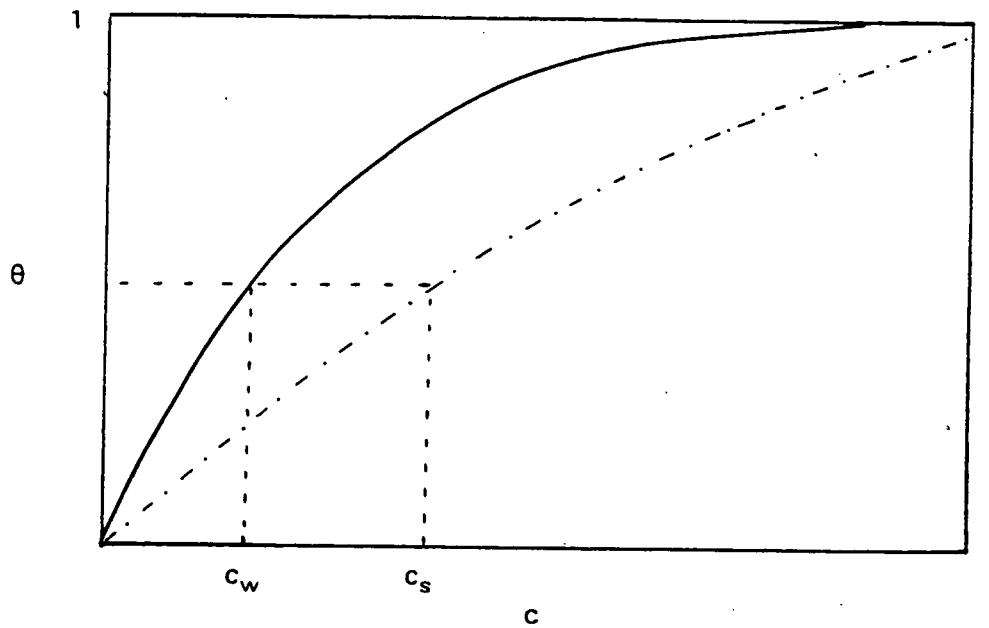

where,

c = concentration of sorbate

c_w = concentration in aqueous solution

c_s = concentration in solvent

Figure 2.2 Nature of Equilibrium Sorption Isotherms Expected for the Uptake of an Organic Sorbate by a Molecular Sieve; (——), uptake from aqueous solution; (-·-·-), uptake from organic solvent.

are sorbed by the sieve,

$$E_{s/w} = (s_s/s_w)(K_{zeo,s}/K_{zeo,w})(p_s/p_w) \quad (2.36)$$

$$E_{s/w} = P_{s/w}(K_{zeo,s}/K_{zeo,w})(p_s/p_w) \quad (2.37)$$

where $P_{s/w}$ is the coefficient for partition between the organic solvent and the water. If there is no significant sorption of water or organic solvent then,

$$E_{s/w} \doteq P_{s/w} \quad (2.38)$$

Thus in this case the enrichment is no better than could be achieved by solvent extraction. However if the solvent is more strongly sorbed than water, then,

$$(K_{zeo,s}p_s/K_{zeo,w}p_w) > 1 \quad (2.39)$$

$$\text{and } E_{s/w} > P_{s/w} \quad (2.40)$$

It follows that there is a distinct advantage in the use of an organic solvent that is strongly sorbed by the sieve. The disadvantage is of course that the solvent must be recovered by desorption before the sieve can be reused.

2.3.5 Practical Enrichment Factors

In practice, enrichment is not carried out at constant fractional uptake. In general the ratio of the initial uptake θ_w to the final coverage θ_s is given by

$$(\theta_w/\theta_s) = (K_{L,w}c_w/K_{L,s}c_s)\{(1 + K_{L,s}c_s)/(1 + K_{L,w}c_w)\} \quad (2.41)$$

which can be simplified for two important cases.

2.3.5.1 Case in which sieve operates at low fractional uptakes in both solvents

In this case,

$$E_{prac,s/w} = (c_s/c_w) = (\theta_s/\theta_w)(K_{L,w}/K_{L,s}) \quad (2.42)$$

and thus the enrichment factor $E_{s/w}$ is reduced by the factor (θ_s/θ_w) and for $E_{prac,s/w}$ to exceed $P_{s/w}$ it is necessary for $(K_{zeo,s}p_s/K_{zeo,w}\,p_w)$ to exceed θ_w/θ_s. If there is no solvent uptake then,

$$E_{prac,s/w} = P_{s/w}(\theta_s/\theta_w) \quad (2.43)$$

and hence the uptake is less than that which can be achieved by partition.

2.3.5.2 Case in which sieve operates near maximum capacity in water and at low coverage in organic solvent

In this case,

$$(1 - \theta_w) = (1/K_{L,w}c_w) \tag{2.44}$$

and

$$\theta_s = K_{L,s}c_s \tag{2.45}$$

Hence,

$$E_{prac,s/w} = (K_{L,w}/K_{L,s})\theta_s(1-\theta_w) \tag{2.46}$$

and the enrichment $E_{s/w}$ is reduced by the factor $\theta_s(1 - \theta_w)$.

2.3.5.3 Consequences

It appears from the foregoing analysis that the optimum enrichment $E_{s/w}$ is only achieved when $\theta_s = \theta_w$ and for all real situations the practical enrichment $E_{prac,s/w}$ is less than the optimum enrichment. For example if $K_{L,w} = 10000$ and $K_{L,s} = 10$ dm^3mol^{-1} then $E_{s/w} = K_{L,w}/K_{L,s} = 1000$, but the practical enrichments for selected values of θ_w and θ_s are as follows:

θ_w	θ_s	$E_{prac,s/w}$
0.9	0.1	12.2
0.8	0.2	62.5
0.7	0.3	186.9
0.6	0.4	440
0.5	0.5	1000

2.3.6 Discussion

The foregoing treatment is very much an oversimplification, but it predicts the general pattern of behaviour to be expected and provides a framework for the interpretation of results obtained in this work.

From a practical point of view the most important conclusions are those associated with the enrichment factor. It is important to recognise that this factor is independent of the affinity of the sorbate for the sieve and of the total uptake. At constant fractional uptake ($\theta_w = \theta_s$) the enrichment factor is always at least as good as could be achieved by solvent extraction ($E_{s/w} = P_{s/w}$) but in practical situations ($\theta_w > \theta_s$) the enrichment $E_{prac,s/w}$ may be significantly less than $P_{s/w}$. However, even in this case, sorption by molecular sieves will have practical advantages over solvent extraction, especially for whole broth separation processes (see Chapter 1 sec. 1.4). To obtain enrichments in excess of those that can be achieved by solvent extraction, it is necessary that the organic solvent is strongly sorbed by the molecular sieve.

2.4 PREVIOUS THEORETICAL TREATMENTS

A review of the liquid phase sorption studies which have been carried out on silicalite-1 to date was included in Chapter 1. Very few of these studies included any theoretical treatment of the sorption data obtained.

Bui and co-workers (131) attempted to fit data for the sorption of ethanol from aqueous solution by silicalite-1 to various sorption isotherms. The Langmuir equation was found to offer the best fit to the data. Values of K (Langmuir constant for sorption) and A_o (maximum capacity of the sieve) were thus obtained at 30, 35 and 60°C. As would be expected (see sec. 2.2.2) K was

found to decrease with temperature whilst the saturation capacity of the sieve remained constant. There was no quantitative assessment given, of the degree of fit of the observed data to the chosen isotherm equation

A paper by Klein and Abraham (124) on vapour phase ethanol and water sorption on silicalite-1, also described the use of the Langmuir sorption isotherm. Vapour phase studies showed that the results were adequately represented by a *Langmuir mixture model* (146). The model was then extended to allow predictions to be made about ethanol sorption from aqueous solution based on vapour phase results. The predicted isotherm provided a reasonable fit to results found by other workers for ethanol sorption in aqueous systems (e.g. Chriswell et al (117) and Milestone and Bibby (139)).

The sorption of solid phenols from aqueous solution is unlike liquid phase ethanol sorption. The relatively hydrophobic phenols accomplish pore filling at a much lower concentration than that achieved for ethanol.

The only theoretical study on sorption results obtained for phenols on silicalite-1 was carried out by Narita and co-workers (145). As described in Chapter 1 (sec. 1.4.2.2) they chose to fit their sorption results to the Freundlich equation. Data for the sorption of phenol, o-, m-, and p- cresol and benzylalcohol from aqueous solution by silicalite-1 was given. The sorption coefficients obtained however had little significance since the degree of fit of the experimental results to the chosen isotherm was not a good one. No quantitative measure of the deviation from the theoretical isotherm was made, but a graphical indication was given by the spread of points around the predicted line.

As described in section 2.2.1, the Freundlich equation does not include a term which takes maximum sorption capacity into account, and it is therefore

unlikely to be useful for solutes which are strongly sorbed by molecular sieves.

The Langmuir equation has been shown to be applicable to the sorption of ethanol from aqueous solution by silicalite-1, and it seems likely that it will apply to the sorption of other solutes by zeolite molecular sieves. However, it has not been tested for systems other than ethanol + silicalite, and indeed there are few, if any, suitable experimental results for such a test.

CHAPTER 3
EXPERIMENTAL

3.1 SYNTHESIS OF MOLECULAR SIEVES

3.1.1 Materials

The materials used for the syntheses were as follows:

- Silica - *CAB-O-SIL M-5 from BDH
- Tetrapropylammonium bromide (TPABr) used as supplied from Aldrich (98%).
- Sodium hydroxide used as suppled from BDH (AnalaR)
- Piperazine hexahydrate used as supplied from Aldrich (98%)
- Glass distilled water was used at all times.

*CAB-O-SIL M-5 is a fumed silica (surface area *ca* 200 m^2g^{-1}) produced by hydrolysis of $SiCl_4$ in a hydrogen and oxygen flame at 1800°C. It has extremely low levels of impurity since it is produced from ultra-pure starting materials.

3.1.2 Synthesis of Silicalite-1 (GS11) from a $3.5Na_2O$ 2TPABr $20SiO_2$ $1000H_2O$ Reaction Mixture at 95°C

3.1.2.1 Equipment

The synthesis was carried out in a 1 litre screw top polypropylene bottle (Figure 3.1). The bottle was fitted with a stainless steel stirring paddle which was positioned *ca* 3 cm from the bottom of the bottle. This ensured efficient mixing and prevented sedimentation of reactants during synthesis. A small hole in the top of the bottle allowed sampling during the reaction. The hole was sealed with a glass stopper to prevent evaporation from the vessel. The bottle was clamped into a 95°C water bath and the stirrer attached to a 150 rpm electric stirring motor.

The water bath was made of copper sheet and a Fimonitor/relay system

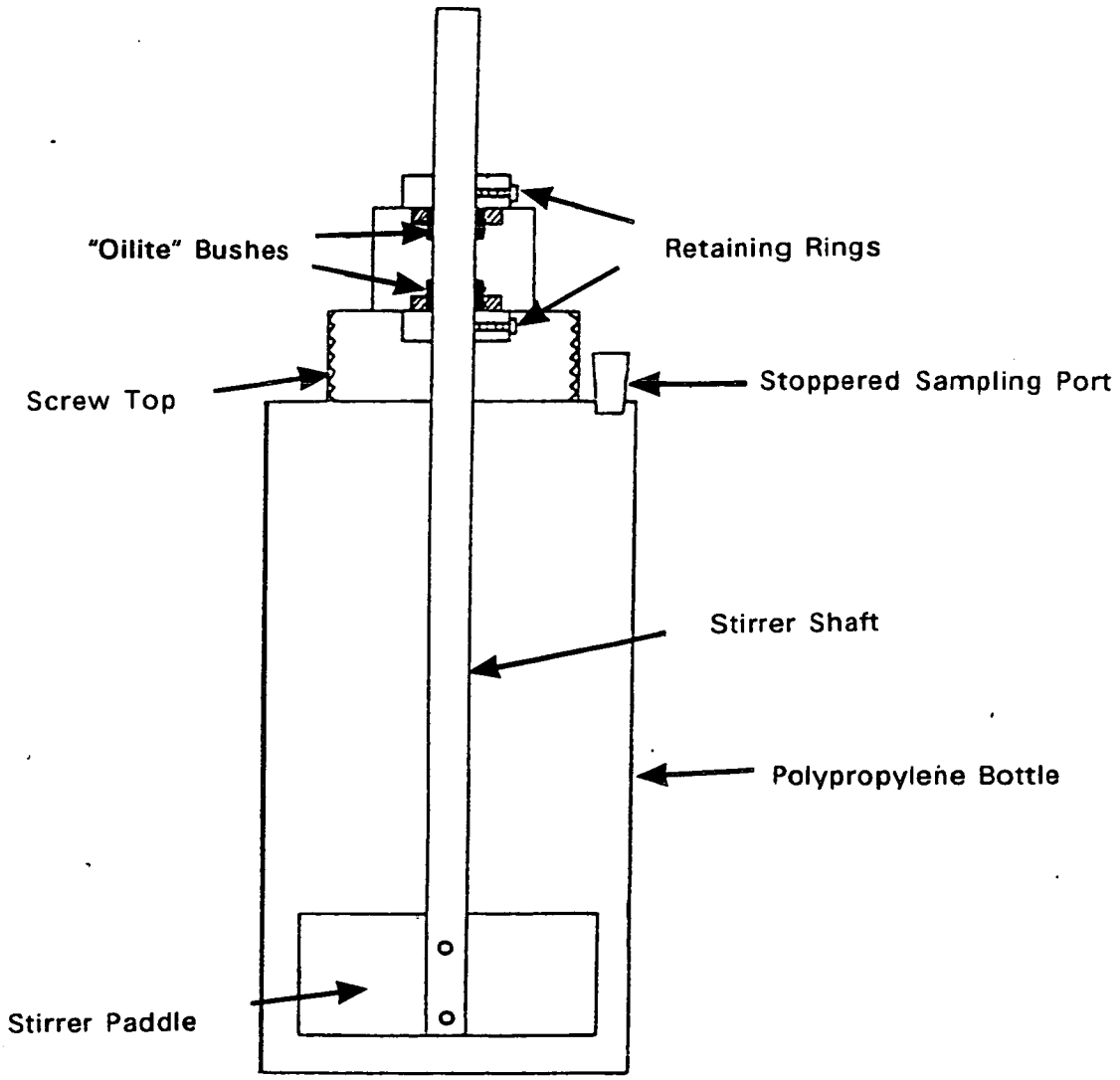

Figure 3.1 Polypropylene Reactor Vessel Used for 95°C Synthesis of Silicalite-1.

maintained the temperature of the bath at 95 $\pm$ 1°C by means of four 1 kW heaters. The water bath was also fitted with a constant head device and covered with polypropylene balls to reduce heat loss and evaporation.

3.1.2.2 Method

Silicalite-1 sample GS11 was prepared using the reaction mixture composition, $3.5Na_2O$ 2TPABr $20SiO_2$ $1000H_2O$. The relative weight of each reactant was chosen to give a total weight of reaction mixture of 500 g. Since the nature of the product obtained is sensitive to the order and manner in which the reactants are mixed, the following procedure was adhered to as far as possible for all syntheses of silicalite-1.

The amorphous silica was weighed into the 1 litre polypropylene bottle to be used for the reaction. A small amount of water was added to the silica and this was blended to a smooth consistency using a Braun Multipractic hand blender. The sodium hydroxide and TPABr were then dissolved in a small amount of water and added to the slurry. The weight of the mixture was then made up to 500 g with water and blended to give a smooth consistency. The reactor vessel containing the mixture was placed immediately in the 95°C thermostat bath and stirred at 150 rpm for the duration of the synthesis.

The conversion of amorphous silica to a crystalline molecular sieve is accompanied by pH changes (51). Samples (*ca* 3 cm^3) were taken from the reaction mixture at regular intervals and the pH measured. Measurements were made with a Philips pH meter (Type 9409). The electrodes were standardised in pH = 9.20 reference buffer solution (BDH tablets) before measurements were made. Samples from reaction mixtures were cooled to room temperature in small pre-rinsed stoppered glass bottles before analysis. Stable pH measurements were obtained after 10 to 15 minutes. The crystallisation was

taken to be complete when the pH readings for samples taken on consecutive days were identical. The completion of the reaction was also confirmed by the gel free nature of samples taken. The crystallisation time for the above preparation was 8 days.

3.1.2.3 Recovery and Post - Synthesis Treatment

When the reaction was complete, the silicalite product was separated from the mother liquor by filtration through a 0.2 µm filter membrane (Gelman). The silicalite was washed several times with water until the washings were near neutral (pH 7-8) and bromide free (silver nitrate test). The product was then dried in an oven at 60°C and calcined in a furnace at 550°C for 24 hours. It was then ion exchanged twice with 1M NH_4Cl solution at 80°C for 16 hours (10 cm^3 soln. / gram solid) and then further calcined (450°C,48 h; 550°C,12 h). The yield based on SiO_2 was 92%.

3.1.3 Synthesis of Silicalite-1 (GS12, GS14) from a 10 piperazine 2TPABr $20SiO_2$ $1000H_2O$ Reaction Mixture at 95°C

3.1.3.1 Equipment

The equipment used for the synthesis of these two silicalite samples was as described in section 3.1.2.1.

3.1.3.2 Method

Silicalite-1 samples GS12 and GS14 were prepared using the following reaction composition, 10 piperazine 2TPABr $20SiO_2$ $1000H_2O$. The total weight of the reaction mixture was 500 g and the following preparation procedure was used. The amorphous silica was weighed into the 1 litre polypropylene bottle to be used for the reaction. A small amount of water was added to the silica and this was blended to give a smooth consistency. The piperazine and TPABr were then dissolved on warming in a small amount of water. This solution was

cooled before adding it to the silica slurry. The weight of the mixture was then made up to 500 g with water and blended well. The reactor vessel containing the mixture was placed immediately in the the 95°C thermostat bath and stirred at 150 rpm for the duration of the synthesis. The criteria for terminating the reaction were as described in section 3.1.2.2 The crystallisation time for this preparation was 6 weeks.

3.1.3.3 Recovery and Post-Synthesis Treatment

When the reaction was complete the silicalite product was separated from the mother liquor by filtration through a 0.2 µm filter membrane. The silicalite was then washed several times with water until the washings were near neutral (pH 7-8) and bromide free (silver nitrate test). The product was dried at 60°C then calcined at 550°C for 24 h followed by 1 h at 800°C. No ion exchange of the product was necessary since there were no inorganic cations present in the reaction mixture. The yield based on SiO_2 was *ca* 89% for both samples (GS12 and GS14).

3.1.4 Synthesis of Silicalite-1 (GS15, GS16, GS17, GS18, GS19, and GS20) from a 10 piperazine 2TPABr $20SiO_2$ $1000H_2O$ Reaction Mixture at 150°C

3.1.4.1 Equipment

The syntheses were carried out in a Baskerville and Lindsay 500 cm^3 stainless steel autoclave (Figure 3.2). The autoclave had a magnetically driven paddle stirrer, a dip tube for sampling purposes, a sample valve and gas outlet/inlet valves. The gas valves were fitted for use during sampling. However at 150°C, the pressure inside the vessel was sufficient to allow sampling without the use of compressed gas. The autoclave had an external heater and the temperature of the reaction was monitored by a thermocouple, and controlled by a Gulton-West temperature controller. The pressure inside the

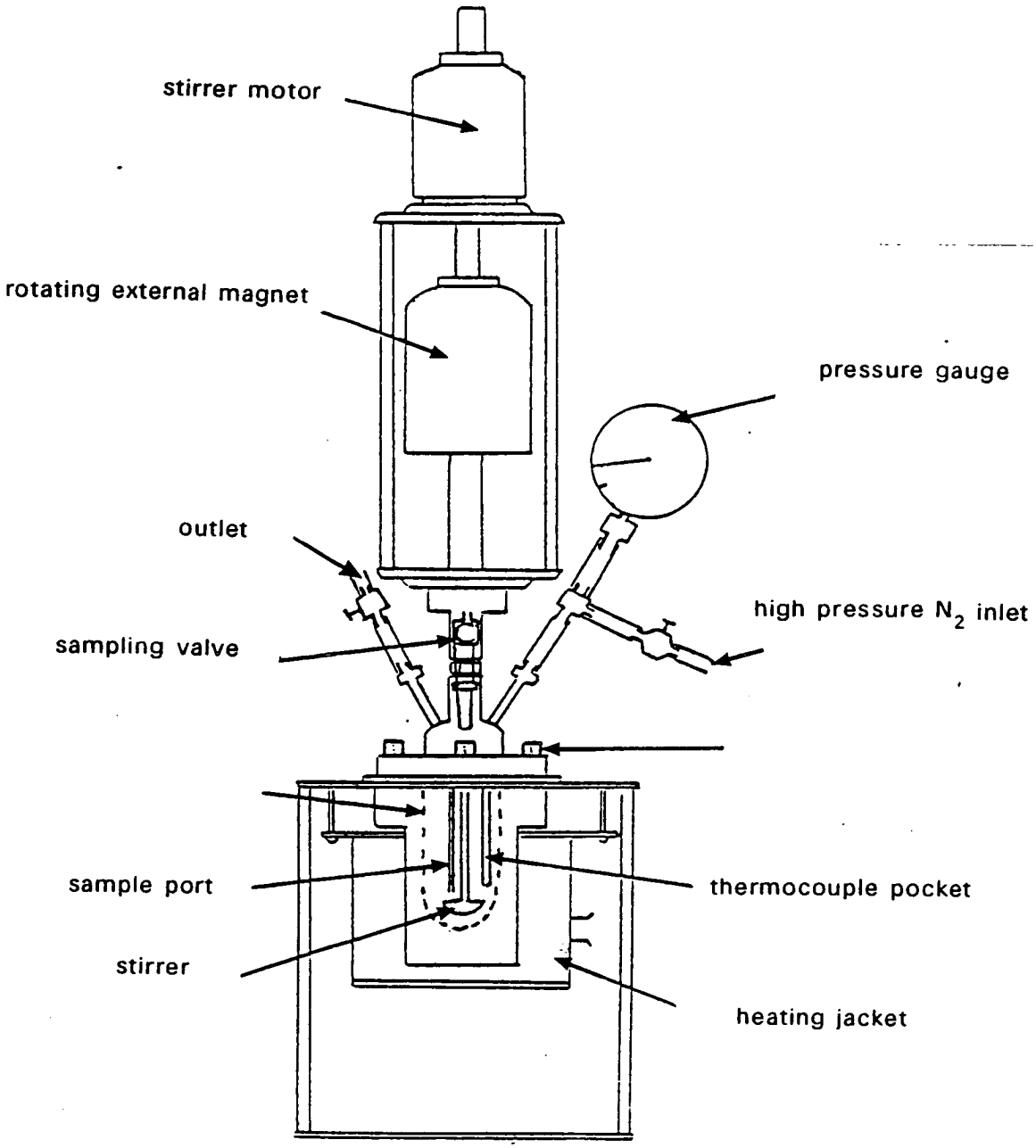

Figure 3.2 Schematic Drawing of 500cm^3 Stainless Steel Autoclave.

autoclave was displayed on a pressure gauge. The autoclave incorporated several safety devices. It was fitted with a temperature cut-out, normally set at *ca* 50°C above the reaction temperature, which came into operation if the primary temperature control circuit failed. The autoclave also had a pressure trip mechanism which switched off the heater if the pressure exceeded a pre-set value, and a bursting disk designed to blow at 45 atm.

3.1.4.2 Method

The reaction mixture was prepared exactly as described in section 3.1.3.2, but the weight of the mixture was made up to 320 g. It was necessary to leave a certain amount of void volume in the autoclave to allow for gas production and for liquid expansion at elevated temperature. The reaction mixture, once prepared was transferred immediately to the 500 cm^3 autoclave reactor vessel. The reaction mixture was then stirred (300 rpm) at 150°C until the synthesis was complete. The criteria for the termination of the reaction were identical to those described in section 3.1.2.2. The crystallisation time for this preparation was 4 days.

3.1.4.3 Recovery and Post-Synthesis Treatment

The recovery and post-synthesis treatment of these samples of silicalite-1 was as described in section 3.1.3.3. The yield based on SiO_2 was *ca* 94% for all samples.

3.1.5 Synthesis of ZSM-5 (GZ1, GZ2, and GZ3) from a 14 piperazine 2TPABr $xAl_2(SO_4)_3$ $20SiO_2$ $1000H_2O$ Reaction Mixture in a Static Bomb at 150°C

3.1.5.1 Equipment

The syntheses were carried out in 30 cm^3 teflon lined, screw top, stainless steel bombs (Figure 3.3). These were constructed in the Chemistry Department workshops. The reactions were carried out under static conditions in a

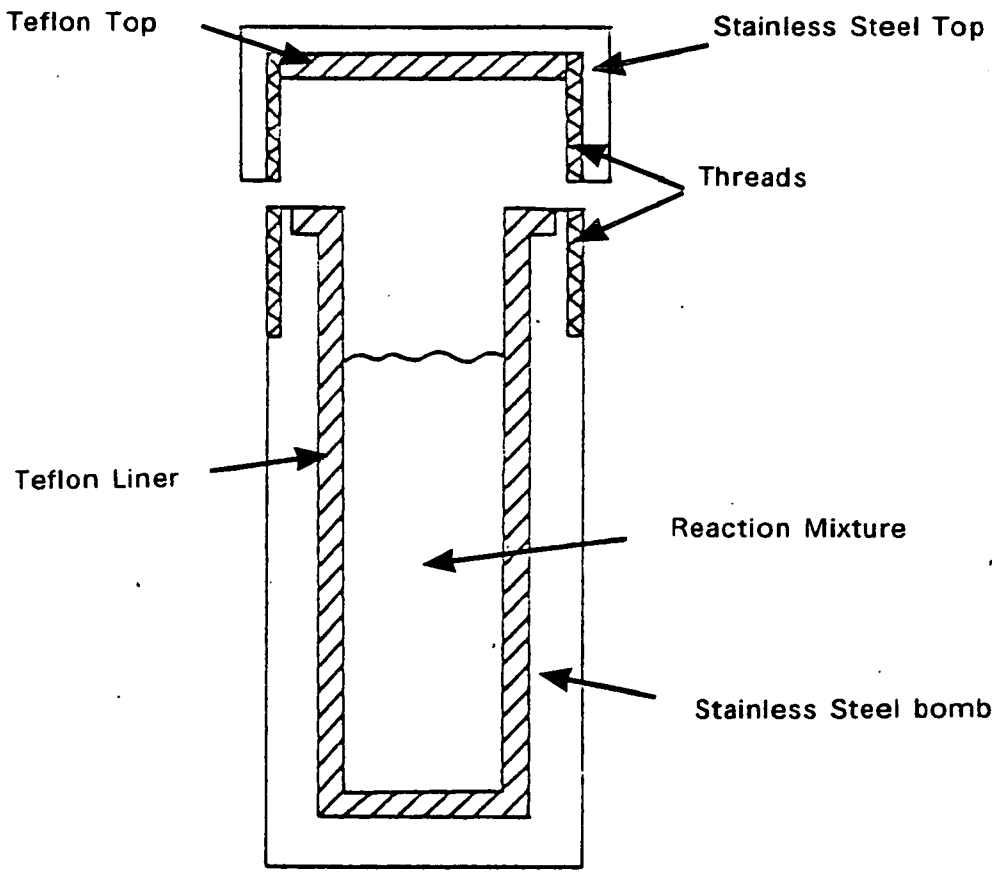

Figure 3.3 Schematic Drawing of a Stainless Steel Screw Top Bomb.

thermostated oven.

3.1.5.2 Method

Samples of ZSM-5, GZ1, GZ2 and GZ3 were prepared using the following reaction composition; 14 piperazine 2TPABr $xAl_2(SO_4)_3$ $20SiO_2$ $1000H_2O$ where x = 0.09, 0.17 and 0.34 respectively. The following preparation procedure was used for each synthesis. The amorphous silica was weighed into a 1 litre polypropylene bottle and blended to a smooth consistency with a little water. The aluminium sulphate was then dissolved in water and added to the silica. This mixture was blended well before adding piperazine and TPABr in the usual way (See section 3.1.3.2). The weight of reactants was then made up to 20 g. It was necessary to leave a void space to allow for the expansion which occurs when the gel is heated to the reaction temperature. The bombs were removed from the oven after 7 days, cooled and a small sample (*ca* 1 cm^3) removed. These samples were examined under the optical microscope. For each sample, after 7 days, no amorphous material could be detected in the crystalline product.

3.1.5.3 Recovery and Post-Synthesis Treatment

The recovery and post-synthesis treatment of the ZSM-5 samples was identical to that described for silicalite-1 in section 3.1.3.3. The yield of product based on SiO_2 was >85% for each synthesis.

3.1.6 Synthesis of ZSM-5 (GZ22) from a 14 piperazine 2TPABr $0.17Al_2(SO_4)_3$ $20SiO_2$ $1000H_2O$ Reaction Mixture in a Stirred Autoclave at 150°C

3.1.6.1 Equipment

The equipment used in the synthesis of this sample of ZSM-5 was identical to that described for the synthesis of silicalite-1 in section 3.1.4.1.

3.1.6.2 Method

The synthesis was carried out using the following reaction composition; 14 piperazine 2TPABr $0.17Al_2(SO_4)_3$ $20SiO_2$ $1000H_2O$. The reaction mixture was prepared as described in section 3.1.5.2 but the weight of reactants was made up to 400 g. The synthesis was carried out in a stirred autoclave (300 rpm) at 150°C. The reaction was sampled after 7days (*ca* 3 cm^3) and examined under an optical microscope. Since no amorphous gel could be detected amongst the crystalline product it was assumed that the crystallisation was complete.

3.1.6.3 Recovery and Post-Synthesis Treatment

The recovery and post synthesis treatment of ZSM-5 sample GZ22, was identical to that described for silicalite-1 in section 3.1.3.3. The yield of product based on SiO_2 was 83%.

3.2 CHARACTERISATION OF MOLECULAR SIEVES

3.2.1 X-Ray Powder Diffraction

3.2.1.1 Instrumentation

Powder patterns were obtained with a Philips X-ray powder diffractometer. The samples were loaded by an automatic sample changer (type PW 1170/02). The goniometer (PW 1050/80) was mounted on an X-ray generator (PW 1730/10) that produced Cu K_α radiation (mean wavelength = 1.5418 Å). Scanning and detection were controlled by motor (PW 1394) and channel (PW 1390) control units respectively. On continuous scanning mode the results were recorded on a chart recorder (PM 8203). A focusing monochromator (AMR 3-202E) was fitted immediately before the detector (PW 1965/60).

3.2.1.2 Conditions

The scans were all carried out on continuous mode from 4 to 50°2θ at a scan rate of $1°2\theta min^{-1}$ and a time constant of 2.

3.2.1.3 Sample Preparation

Since all the samples were in the form of fine powders it was not necessary to grind them before analysis. Each sample was equilibrated with water vapour in a closed system over saturated NaCl solution (a_w= 0.753) at 25°C for 24 h before analysis. Small glass bottles containing *ca* 0.5 g of sample were placed in a dessicator fitted with a stainless steel block for weighting and heat transfer purposes. The dessicator was then evacuated down to the vapour pressure of the water and placed in a thermostat bath (25 ± 1°C). After hydration, the samples were loaded into a sample holder and pressed down firmly and evenly before being placed in the sample changer ready for analysis.

3.2.2 Optical Microscopy

3.2.2.1 Instrumentation

Optical microscopy was carried out with a Vickers model M41 Photoplan optical microscope.

3.2.2.2 Sample Preparation

A small amount of sample was dispersed in water on a microscope slide. This step was not necessary for samples of reaction mixtures where a liquid phase was already present. A cover slip was placed carefully on top before viewing.

3.2.3 Scanning Electron Microscopy

3.2.3.1 Instrumentation

A Cambridge 604 scanning electron microscope fitted with a Practica L2 camera was used. A Polaron SEM coating unit (E5100) was used to coat the samples with a thin gold film.

3.2.3.2 Sample Preparation

Samples were dispersed in *ca* 3 drops of solvent (acetone) on small aluminium studs (1 cm) then coated with gold. This prevents a build up of electrostatic charge on the surface of the sample during analysis.

3.2.4 X-Ray Fluorescence

3.2.4.1 Instrumentation

A Philips spectrophotometer (PW 1450) was used. Instrument calibration and analysis was carried out by the Department of Geology, University of Edinburgh.

3.2.4.2 Sample Preparation

Anhydrous samples were fused with an identical weight of flux (Johnson Matthey Spectroflux 105) and moulded into glass discs before analysis.

3.2.5 Thermal Analysis

3.2.5.1 Instrumentation

A Stanton Redcroft STA-780 Series simultaneous thermal analyser was used and the results were recorded in two ways.

1. Thermal Gravimetric Analysis (TGA), Differential Thermal Gravimetric Analysis (DTG) and Differential Thermal Analysis (DTA) results plotted with temperature directly using a Servogor 460 chart recorder.

2. For all but early samples of silicalite (GS11) the results were collected and stored using a Model B+ BBC micro-computer. After data correction which involved temperature linearisation and DTA and TGA baseline correction, the results were plotted against temperature on a Plotmate A4M plotter.

3.2.5.2 Conditions

The runs were carried out using between 10 and 20 mg of sample in a dry air flow of 0.5 cm^3s^{-1}. The DC amplifier for the DTA signal was set on the 200 µv range for running "as synthesised" samples and the 100 µv range for the calcined samples. The samples were heated from 20 to 900°C at a constant heating rate of 10°C min^{-1}.

3.2.5.3 Sample Preparation

The samples were all equilibrated over water vapour (a_w = 0.753) at 25°C as described in section 3.2.1.3 for at least 24 h before analysis.

3.3 SORPTION OF PHENOLS FROM AQUEOUS SOLUTION BY MOLECULAR SIEVES

3.3.1 Materials

The molecular sieves used for the sorption experiments were as follows:

- Silicalite-1 sample GS11 used as prepared (see section 3.1.2).
- Silicalite-1 samples GS12 and GS14 used as prepared (see section 3.1.3).
- Silicalite-1 samples GS18, GS19, GS20 used as prepared (see section 3.1.4).
- Silicalite-2 samples KF1 and KF2 used as supplied from K.R. Franklin. (See section 1.2.2.2).
- ZSM-5 samples GZ1, GZ2 and GZ3 used as prepared (see section 3.1.5).
- ZSM-5 sample GZ22 used as prepared (see section 3.1.6).

(These molecular sieves were characterised by the techniques given in section 3.2).

The sorbates and reagents were as follows:

- o-Cresol used as supplied from Aldrich (99+%).
- m-Cresol used as supplied from Aldrich (99+%).
- p-Cresol used as supplied from Aldrich (99+%).
- 2,3-Dimethylphenol used as supplied from Fluka (97%).
- 2,5-Dimethylphenol used as supplied from Aldrich (99+%).
- 2,4-Dimethylphenol used as supplied from Aldrich (99%).
- 2,6-Dimethylphenol used as supplied from Aldrich (99.8+%).
- 3,4-Dimethylphenol used as supplied from Aldrich (99+%).
- 3,5-Dimethylphenol used as supplied from Aldrich (99+%).
- p-Nitrophenol used as supplied from Fisons (99%).
- Phenol used as supplied from Fisons (99%).
- Bovine Serum Albumin used as supplied from Sigma (GPR).
- Lysozyme used as supplied from Sigma (GPR).
- $NaH_2PO_4H_2O$ used as supplied from BDH (GPR).
- Na_2HPO_4 used as supplied from BDH (GPR).
- "Pruteen" Supernatant used as supplied by I.C.I Agricultural Division.
- Lithium Chloride used as supplied from BDH (99%).
- Methanol used as supplied from May and Baker (99%).
- Glass distilled water used at all times.

3.3.2 Method

3.3.2.1 Sample Preparation

Before each sorption experiment the molecular sieve to be studied was equilibrated with water vapour (a_w = 0.753) for 18 h at 25°C. Thermal analysis was then carried out on the hydrated material in order that the dry weight used could be calculated.

3.3.2.2 Equilibration of Sample with Aqueous Solution

Samples of hydrated molecular sieve were weighed into 30 cm^3 polypropylene bottles together with a known volume of a dilute aqueous solution of the sorbate. The bottles were then sealed and tumbled in a thermostat bath at 25.0 $\pm$ 0.5°C. The apparatus which was used to provide the tumbling action was designed in order to provide constant mixing without abrasion. Static equilibration is unsatisfactory because of the occurrence of concentration gradients at the solid/solution interface and the possibility of condensation in the free space at the top. Equilibration is therefore too slow to be practical under these conditions. Stirring and shaking can cause particle splintering and are not as satisfactory as the smooth mixing action effected by tumbling. The apparatus which was designed to perform the tumbling action is shown in Figure 3.4. The plastic bottles were fitted into position and tumbled around a central axis at constant speed (*ca* 30 rpm) until equilibration was complete. The appropriate equilibration time for each sorbate was established by carrying out identical sorption experiments over a series of equilibration times. When three consecutive systems gave the same value of uptake, it was presumed that equilibrium had been reached. The length of time necessary varied depending on the size of the sorbate molecule. The chosen times lay between 18 h and 300 h.

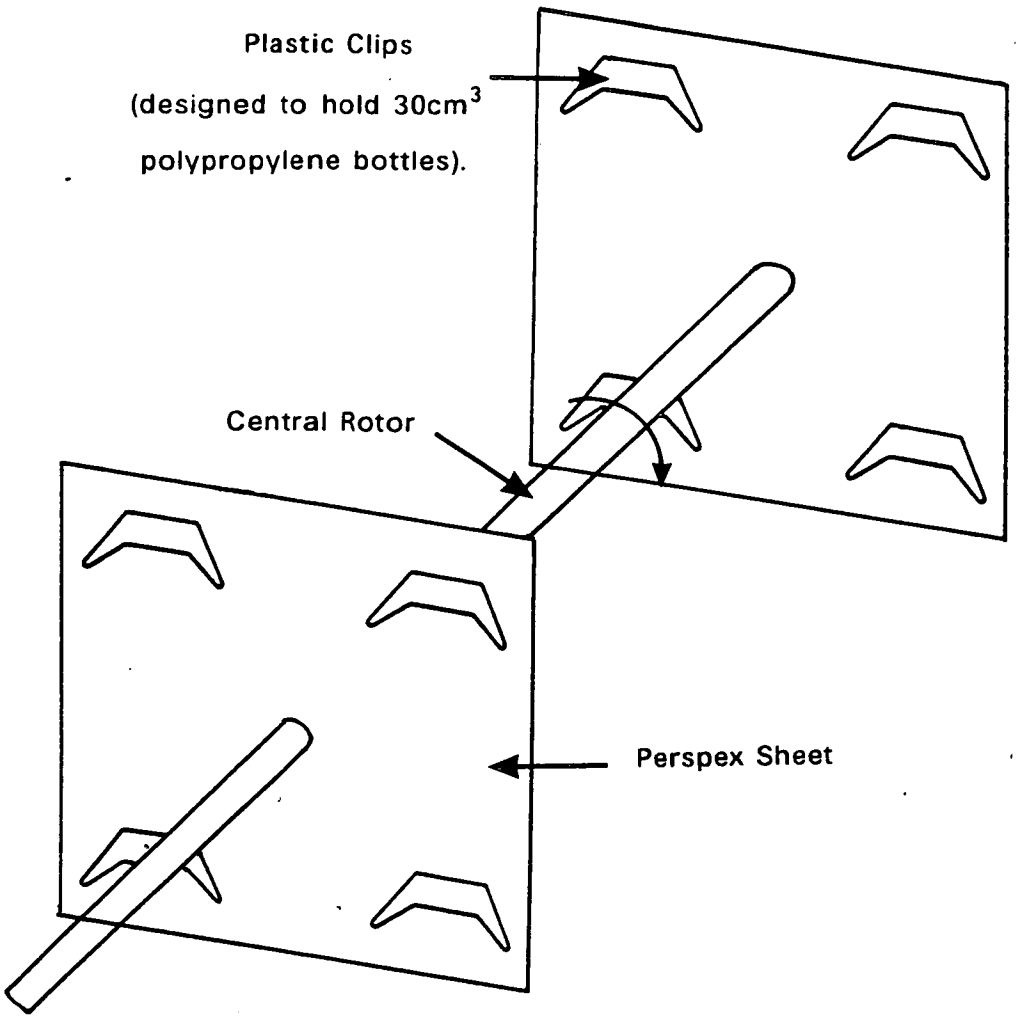

Figure 3.4 Schematic Drawing of Mechanical Tumbling Device Used for Equilibration at 25°C.

The bottles were removed from the water bath and centrifuged (3000 rpm, 15 min) to separate the solution and solid phase. Each solution was analysed by U.V. spectrophotometry. Except in a few cases where direct analysis was possible, an accurate dilution was necessary, to bring the concentration of the phenol within the calibration range of the U.V. spectrophotometer. The chosen wavelength for analysis of each phenol corresponded to an isobestic point in the U.V. spectrum of that phenol in water.

3.3.2.3 Analysis of Phenol by U.V. Spectophotometry

When monochromatic light is absorbed by a solute molecule, the intensities of the incident light I_o and transmitted light I are related by the equation

$$D = \log_{10}(I_o/I) = \varepsilon c x \qquad (3.1)$$

where c is the concentration of the solute, x is the thickness of the absorbing medium and ε is a constant. If c is measured in mol dm^{-3} and x in cm, ε is known as the molar extinction coefficient and is the value of the optical density D for a 1 molar solution when the light path length is 1 cm.

The molar extinction coefficient varies with the wavelength of light and is characteristic of the absorbing species. The above equation is known as the Beer Lambert Law and was used to determine the equilibrium concentrations of the phenols studied. At most wavelengths, the optical density of a solute is dependent on its degree of ionisation in the solvent. A point at which it is independent, is known as an isobestic point. In order to avoid any complications during analysis arising from fluctuations in pH, an isobestic point for each phenol in aqueous solution was established. This wavelength was then chosen for the subsequent calibration. The optical density of each phenol was measured over a range from 240 nm to 300 nm using a Perkin Elmer 402 U.V./Vis scanning spectrophotometer at three different values of pH (4.0, 7, 9.2).

The solutions were prepared using buffer tablets (BDH). The wavelength at which optical density was equal for all values of pH was taken to be an isobestic point in the U.V. absorption spectrum of the phenol concerned. The wavelength chosen for analysis was determined more exactly by using the same procedure but over a much smaller wavelength range on the instrument to be used for the calibration.

When the isobestic point for each phenol had been established, a calibration curve was obtained. Each calibration was made with five standard aqueous solutions of the phenol concerned. The optical density of each solution was measured at the required wavelength and plotted against concentration (mol dm^{-3}). The quartz cells used had a path length of 1cm. According to the Beer Lambert Law each plot should pass through the origin, with a gradient equal to the molar extinction coefficient (ε / $dm^3mol^{-1}cm^{-1}$) of the phenol concerned at the chosen wavelength. The isobestic points, and their corresponding molar extinction coefficients, for each phenol, are given in Table 3.1. The degree of uncertainty in each value was obtained from a least squares analysis of the points on the calibration curve. The final column in Table 3.1 shows that the majority of the calibration curves passed through the origin within experimental error, as dictated by the Beer Lambert Law. For 3,4-dimethylphenol and phenol itself, the calibration curves do not pass through the origin. This was assumed to be due to an instrumental effect and not to the inapplicability of the Beer Lambert Law. The calibration curves obtained in the Chemistry Department were obtained on a Pye-Unicam (PU 8600) U.V. / Vis spectrophotometer. This was a single beam instrument which was fitted with an automatic sample changer. This comprised of a 1 cm quartz cell which was filled through silicon tubing by means of a peristaltic pump. 3 cm^3 of solution was used for each measurement. This ensured that the cell had

Table 3.1

Calibration Curves for U.V. Absorption of Phenols[a]

phenol	medium	λ/nm	extinction coefficient[b] $\varepsilon/dm^3mol^{-1}cm^{-1}$	intercept on optical density axis D
p-cresol	water	281	1428 ± 14	$(6 \pm 6) \times 10^{-3}$
m-cresol	water	260	714 ± 7	$(1 \pm 1) \times 10^{-2}$
o-cresol	water	260	979 ± 9	$(2 \pm 4) \times 10^{-3}$
p-cresol[c]	water	287	1505 ± 13	$(3 \pm 4) \times 10^{-3}$
2,5 dimethylphenol	water	265	1219 ± 10	$(-3 \pm 4) \times 10^{-3}$
3,4 dimethylphenol	water	265	990 ± 4	$(6 \pm 5) \times 10^{-3}$
2,4 dimethylphenol	water	265	948 ± 4	$(3 \pm 3) \times 10^{-3}$
phenol	water	272	1518 ± 26	$(-1.6 \pm 0.8) \times 10^{-2}$
p-nitrophenol[d]	water	347	5490 ± 63	$(1 \pm 1) \times 10^{-2}$
p-nitrophenol[c]	water	347	5521 ± 21	$(1 \pm 2) \times 10^{-3}$
p-cresol	ethanol	281	1929 ± 13	$(2 \pm 2) \times 10^{-2}$
p-cresol[d]	water	270	1274 ± 4	$(3 \pm 4) \times 10^{-3}$
p-cresol[d]	methanol	270	1276 ± 6	$(2 \pm 4) \times 10^{-3}$

[a] Results obtained on a Pye-Unicam PU 8600 U.V./Vis. Spectrophotometer, unless otherwise stated.

[b] Extinction coefficient ε / dm^3 mol^{-1} cm^{-1} equivalent to gradient of calibration curve.

[c] Results obtained on a Perkin Elmer 552 U.V. spectrophotometer.

[d] Results obtained on a Unicam SP500 U.V. spectrophotometer.

been adequately flushed through. The cell was flushed with distilled water between each reading until an optical density of zero (± 0.002) was obtained.

In the subsequent sorption experiment, the optical density of each solution, once equilibrated with silicalite, was measured at the appropriate wavelength for the sorbate concerned. The equilibrium concentration of each phenol could then be determined from the previously established calibration curves.

The spectrophotometers used during visits to ICI Agricultural Division and Warren Spring Laboratory were both double beam instruments (Table 3.1). The procedure for analysis was therefore slightly different. A quartz cell containing water was always present to act as a blank. The cell used for the analyte was therefore removed after each measurement, washed well, and filled to 1 cm from the top with the solution to be measured. Coefficients of the calibration curves obtained by this method are noted in Table 3.1.

3.3.3 Details of Individual Sorption Experiments

The general method used for the aqueous phase sorption experiments was described in the previous section. The specific conditions of each individual set of experiments in terms of the components of the system and the equilibration time, will now be described. Only deviations from the procedure given above will be included.

1. Sorption of phenol, o-cresol, m-cresol, p-cresol, 2,4-dimethylphenol, 3,4-dimethylphenol and 2,5-dimethylphenol from aqueous solution by silicalite-1 (GS18)

The procedure for the preparation, equilibration and subsequent solution phase analysis in these systems was as described in section 3.3.2. Silicalite-1

sample GS18 (0.09 - 0.20 g) was used together with 10 cm^3 of an aqueous solution of the phenol concerned (concentration range; $1x10^{-3}M$ - $1x10^{-2}M$). The cresol systems were equilibrated for *ca* 48 h and the dimethylphenol systems for *ca* 300 h.

2. Sorption of o-cresol, m-cresol and p-cresol from aqueous solution by silicalite-1 (GS14)

The composition of these systems and the procedure used for their preparation, equilibration and subsequent solution phase analysis was as described in 1 above but using silicalite-1 sample GS14. The equilibration time in each case was *ca* 48 h.

3. Sorption of 2,4-dimethylphenol, 3,4-dimethylphenol and 2,5-dimethylphenol by silicalite-1 (GS14)

The procedure for the preparation, equilibration and subsequent solution phase analysis of these systems was as described in section 3.3.2. Silicalite-1 sample GS14 (0.05 g - 0.06 g) was used together with 25 cm^3 of an aqueous solution of sorbate ($7x10^{-5}M$ - $8x10^{-3}M$). The chosen equilibration time in each case was 300 h.

4. Sorption of p-nitrophenol from aqueous solution by silicalite-1 samples GS11(c), GS11(as), GS12(c) and GS12(as)

The procedure for the preparation of these systems was as described in section 3.3.2. Silicalite-1 samples GS11(c), GS11(as), GS12(c) and GS12(as) (0.05 g - 0.06 g) respectively, were used together with 25 cm^3 of an aqueous solution of p-nitrophenol ($1x10^{-4}M$ - $7x10^{-3}M$). They were equilibrated by tumbling at 25°C for *ca* 48 h. They were then removed from the water bath and the solid phase separated by filtration through a 0.2µm filter membrane

(Gelman). Solution phase analysis was carried out on a double beam spectrophotometer (Unicam SP500) without an automatic sampler.

5. Sorption of phenol from aqueous solution by ZSM-5 samples GZ1, GZ2 and GZ3

The procedure for the preparation, equilibration and subsequent analysis of these systems was as described in section 3.3.2. A sample of zeolite (GZ1, GZ2 or GZ3) (0.07 g - 0.12 g) was used together with 10 cm^3 of an aqueous solution of phenol ($2x10^{-3}M$ - $2x10^{-2}M$). They were each equilibrated for *ca* 48 h.

6. Sorption of phenol, p-cresol and m-cresol by silicalite-2

The procedure used for the preparation, equilibration and subsequent solution phase analysis of these systems was as described in section 3.3.2. Silicalite-2 (0.05 g - 0.06 g) was used together with between 5 and 10 cm^3 of an aqueous solution of sorbate ($2x10^{-4}M$ - $1x10^{-2}M$). Each system was equilibrated for *ca* 48 h.

7. Sorption of o-cresol and 2,4-dimethylphenol by silicalite-2

The procedure for the preparation, equilibration and subsequent solution phase analysis of these systems was as described section 3.3.2. Silicalite-2 (0.09 g - 0.11 g) was used together with between 5 and 10 cm^3 of an aqueous solution of sorbate ($2x10^{-4}M$- $1x10^{-2}M$). Each sample was equilibrated for *ca* 48 h.

8. Sorption of phenol from aqueous LiCl solutions (2.5M) by silicalite-1 (GS18).

The procedure for the preparation, equilibration and subsequent solution

phase analysis of these systems was as described in section 3.3.2. Silicalite-1 sample GS18 (0.09 g - 0.11 g) was used together with 10 cm^3 of an aqueous solution of phenol ($1x10^{-3}M$ - $2x10^{-2}M$) in 2.5M LiCl solution. The LiCl solution was prepared in a standard flask before the dissolution of the appropriate amount of phenol. The equilibration time for each system was *ca* 18 h.

9. Sorption of phenol from aqueous LiCl solutions (5M) by silicalite-1 (GS18).

The procedure for the preparation, equilibration and subsequent solution phase analysis of these systems was as described in 8 above using 5M LiCl solution.

10. Sorption of p-cresol from a 10:90 (v/v) mixture of methanol and water by silicalite-1 (GS19).

The procedure for the preparation, equilibration and solution phase analysis of these systems was as described in section 3.3.2. Silicalite-1 sample GS19 (0.09 g - 0.10 g) was used together with 10 cm^3 of a solution of p-cresol ($1x10^{-3}$ - $5x10^{-2}M$) in a mixture containing, by volume, 10 parts methanol and 90 parts water. The methanol water solution was prepared before the dissolution of the appropriate amount of cresol. The equilibration time for each system was *ca* 48 h.

11. Sorption of p-cresol from a 20:80 (v/v) mixture of methanol and water by silicalite-1 (GS19).

The procedure for the preparation, equilibration and subsequent solution phase analysis of these systems was as described in 10 above using a mixture containing, by volume, 20 parts methanol and 80 parts water.

12. Sorption of p-cresol from a 30:70 (v/v) mixture of methanol and water by silicalite-1 (GS19).

The procedure for the preparation, equilibration and subsequent solution phase analysis of these systems was as described in 10 above using a mixture containing, by volume, 30 parts methanol and 70 parts water.

13. Sorption of p-cresol from aqueous salt solution by silicalite-1 (GS14)

The procedure for the preparation of these systems was as described in section 3.3.2. Silicalite-1 sample GS14 (0.05 g - 0.06 g) was used together with 25 cm^3 of an aqueous solution of p-cresol ($1x10^{-3}M$ - $2.5x10^{-3}M$) containing inorganic salt (0 - 0.25M). Salt solutions were prepared from a 50:50 mixture of $Na_2HPO_4.H_2O$ and NaH_2PO_4 in water. The bottles were then sealed and shaken in a water bath (New Brunswick Aquatherm shaking bath) at 25 $\pm$ 1° C for 18 h. These experiments were carried out at ICI Agricultural Division where a tumbling device with which to carry out the equilibrations was not available. After equilibration the bottles were removed from the bath and the solution phase separated by filtration through a 0.2 µm filter membrane (Gelman). The solutions were then analysed using a Perkin Elmer 552 U.V. spectrophotometer which was a double beam instrument used with two 1 cm quartz cells.

14. Sorption of p-nitrophenol from aqueous solutions of salt and protein by silicalite-1 (GS14)

The procedure for the preparation, equilibration and solution phase analysis of these systems was as described in 13 above. Silicalite-1 sample GS14 (0.05 g - 0.06 g) was used, together with an aqueous solution of p-nitrophenol ($5x10^{-4}M$ - $3x10^{-3}M$) with an inorganic salt concentration of 0.05M and a known

amount of soluble protein (0 - 0.015 g cm^{-3}). The salt solution was prepared as in 13 above and the soluble protein used was either Bovine Serum Albumin or Lysozyme.

15. Sorption of p-nitrophenol from aqueous solution by silicalite-1 (GS14) previously shaken with a salt solution containing soluble protein

The procedure for the preparation, equilibration and solution phase analysis of these systems was as described in 13 above. Samples of silicalite-1 (GS14, 0.05 g - 0.06 g) were equilibrated with a salt solution (0.05M) containing 1% soluble protein (lysozyme, 18 h, 25°C) before sorption experiments were carried out. The bottles containing the pre-treated sieve were then made up to 25 cm^3 with p-nitrophenol solution to give final concentrations of $5x10^{-4}$M, $1x10^{-3}$M and $3x10^{-3}$M respectively. The bottles were then sealed and shaken in a thermostat bath as before until they had reached equilibrium. The equilibration time for each system was *ca* 18 h.

16. Sorption of p-nitrophenol from aqueous solution by silicalite-1 (GS14) over a series of equilibration times

The procedure for the preparation, equilibration and subsequent solution phase analysis of these systems was as described in 13 above, using 0.05M salt solutions with a p-nitrophenol concentration of $3x10^{-3}$M. The bottles were sealed and shaken in a thermostat bath at 25°C for between 0.25 and 18 h.

17. Sorption of p-nitrophenol from genuine ("Pruteen") fermentation supernatant by silicalite-1 (GS14) over a series of equilibration times

The procedure for the preparation, equilibration and subsequent solution phase analysis of these systems was as described in 13 above. Silicalite-1 sample GS14 (0.05 g - 0.06 g) was used together with p-nitrophenol solutions

($3x10^{-3}M$) in a 70% (w/v) aqueous solution of supernatant from a single cell protein batch fermentation process (the "Pruteen" process). These systems were then sealed and shaken in a thermostat bath at 25°C for between 0.25 and 18 h as in 16 above.

18. Sorption of phenol from aqueous solution by silicalite-1 (GS20) at 15°C

The procedure for the preparation, equilibration and subsequent solution phase analysis of these systems was as described in section 3.3.2. Silicalite-1 sample GS20 (0.07 g - 0.11 g) was used together with 10 cm^3 of an aqueous solution of phenol ($1x10^{-4}M$-$2x10^{-2}M$). Equilibration was then carried out for 18 h at 15°C.

19. Sorption of phenol from aqueous solution by silicalite-1 (GS20) at 40°C

The procedure for the preparation, equilibration and subsequent solution phase analysis of these systems was described in system 3.3.2. Silicalite-1 sample GS20 (0.06 g - 0.14 g) was used together with 10 cm^3 of an aqueous solution of phenol ($1x10^{-4}M$ - $2x10^{-2}M$). Equilibration was then carried out for 18 h at 40°C.

3.3.4 Determination of the Solubilities of Phenols in Water at 25°C

The solubilities of phenol, o-cresol, m-cresol, p-cresol, 2,4-dimethylphenol, 2,5-dimethylphenol and 3,4-dimethylphenol were determined as follows. Two solutions of each phenol in water were prepared. For each phenol, saturation was approached from the side of both undersaturation and supersaturation. They were equilibrated by tumbling in sealed glass bottles (Figure 3.5) at 25°C for several days. A sample of each solution was then analysed for concentration of organic solute by U.V. spectrophotometry. When concordant readings were observed for previously undersaturated and supersaturated

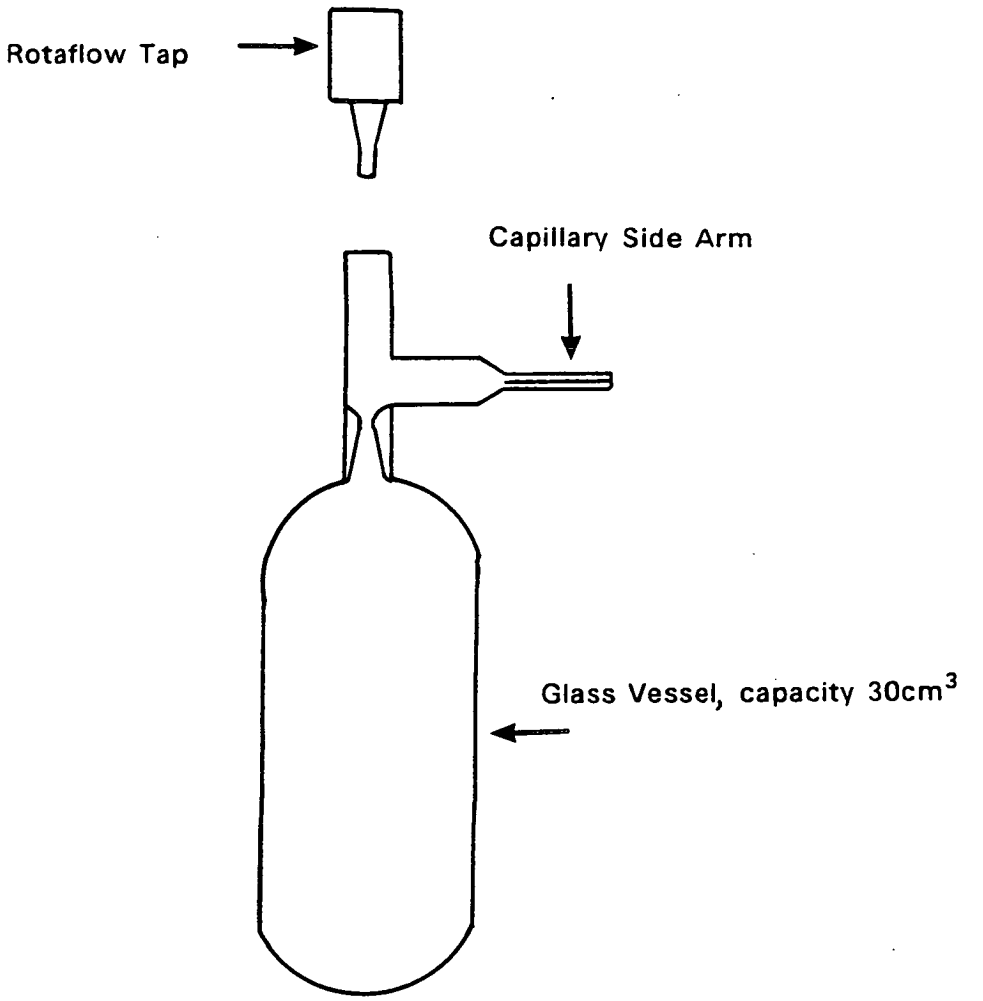

Figure 3.5 Schematic Drawing of Sealed Glass Bottle with Capillary Side Arm.

solutions, it was assumed that equilibrium had been reached.

3.3.5 Determination of the Solubility of Phenol in LiCl Solutions at 25°C

The solubility of phenol in LiCl solutions was determined as described in section 3.3.4 using solutions of phenol in both 2.5M and 5M LiCl.

3.3.6 Determination of the Solubility of p-Cresol in Methanol + Water Mixtures at 25°C

The solubility of p-cresol in mixtures of methanol and water were determined as described in section 3.3.4 using solutions of p-cresol in 10:90 (v/v), 20:80 (v/v), 30:70 (v/v) methanol:water mixtures.

3.4 SORPTION OF P-CRESOL FROM LOW MOLECULAR WEIGHT ALCOHOLS BY SILICALITE-1

3.4.1 Materials

The materials used for the experiments concerned with the sorption of p-cresol from low molecular weight alcohols were as follows:

- Silicalite-1 (GS20) was used as prepared. Details of the preparation of this sample are given in section 3.1.4.
- p-Cresol used as supplied from Aldrich (99+%).
- Methanol solvent from May and Baker (AnalaR grade) was dried over molecular sieve 3A before use. This was necessary in order to exclude water from the systems to be studied.
- Ethanol solvent from BDH (AnalaR grade) was dried over molecular sieve 3A before use.
- Propanol solvent from Fisons (AnalaR grade) was dried over molecular sieve 3A before use.

3.4.2 Method

3.4.2.1 Sample preparation

These sorption experiments required that silicalite samples be completely free from water. This was achieved in the following way. A known amount of previously hydrated (a_w = 0.753, 18 h) silicalite-1 (GS20) was weighed into a specially designed glass bottle (Figure 3.5). The bottle was then placed in a furnace at 450°C for 4 hours. It was removed and cooled over P_2O_5 in an evacuated dessicator. The bottle was taken out when cool and quickly sealed with a "Rotaflow" tap. The capillary side arm of the bottle was attached by means of a rubber tube to an oil pump. The tap was then partially opened and the silicalite-1 was warmed gently on evacuation to remove any residual water. The bottle was then resealed.

3.4.2.2 Equilibration

A 10 cm^3 solution of a known concentration of p-cresol in dry alcohol was then prepared. The capillary side arm of a previously weighed, partially evacuated, glass bottle containing silicalite-1 was placed in the solution. The tap on the bottle was then opened to allow the solution to be drawn in and cover the dry silicalite. When all the solution had been transferred, the bottle was reweighed to give the exact weight of solution in the bottle. Bottles prepared in this way were placed in a thermostat bath (Grant UG3) fitted with a mechanical tumbling device (Figure 3.4) and tumbled at 25°C until equilibration was complete (*ca* 18 h).

3.4.2.3 Analysis

After equilibration the bottles were removed from the thermostat bath and centrifuged in a Centaur 1 MSE centrifuge (3000 rpm, 15 min) to separate the solid and liquid phase. The liquid phase was removed and the silicalite washed with a little cold water to remove any p-cresol adhering to the outside of the

crystals. The sample was recentrifuged and the aqueous phase removed. The remaining sample of silicalite was then dried overnight at room temperature and open to the atmosphere. The dry sample was then analysed by thermal analysis on a Stanton Redcroft STA-780 Series simultaneous thermal analyser (20-900°C), (see section 3.2.5 for details of the conditions used). This provided a value for the total amount of sorbed material (alcohol + p-cresol + water) inside the sieve.

A small amount of the sample (0.009 g - 0.012 g) was then weighed accurately into a small glass vial. A known amount of ethanol was then added to the vial. It was stoppered, shaken and left for at least four hours to allow the p-cresol inside the silicalite to desorb into the solvent. The vial was then centrifuged (3000 rpm, 15 min) and the liquid phase removed. This solution, containing p-cresol and ethanol was analysed for p-cresol by U.V. spectrophotometry (281 nm). The coefficients for the calibration curve obtained for p-cresol solutions in ethanol at 281 nm are given in Table 3.1. All analyses were carried out on a Pye-Unicam PU 8600 U.V. / Vis. spectrophotometer by the method described in section 3.3.2.3.

Three different systems were studied using the above procedure. The uptake of p-cresol from methanol solutions with a concentration range of $4x10^{-3}$M to 0.5M, from ethanol solutions with a concentration range of $1x10^{-3}$ to 0.4M and from propanol solutions with a concentration range of $2x10^{-3}$ to 0.8M were determined.

3.5 COLUMN EXPERIMENTS WITH SILICALITE-1

3.5.1 Materials

The materials used for the column experiments carried out on silicalite-1 were as follows:

- p-Cresol used as supplied from Aldrich (99+%).
- Silicalite-1 samples GS15 and GS17 were used as prepared. Details of the preparation of these samples is given in section 3.1.4.
- Methanol used as supplied from Rathburn Chemicals (HPLC grade).

3.5.2 Method

The apparatus used for the cyclic sorption and desorption of p-cresol by silicalite-1 is shown in Figure 3.6. The glass column used had an internal diameter of 1 cm and was 15 cm long. During the sorption stage, an aqueous feed solution of p-cresol was passed through the column at a known flow rate (1.33 - 1.50 cm^3min^{-1}) by means of a peristaltic pump (Gilson). Samples of eluent were taken at regular intervals by means of a fraction collector (Gilson). These samples were analysed for p-cresol by U.V. spectrophotometry using a Unicam SP500 U.V. spectrophotometer. This was a double beam instrument and was used as described in section 3.3.2.3. The details of the calibration curve obtained for p-cresol on this instrument were given in Table 3.1.

During the stripping stage the feed was changed to 100% methanol which was pumped through the column at a known flow rate (0.6 - 1.5 cm^3min^{-1}). Samples were taken at regular intervals and analysed for p-cresol by U.V. spectrophotometry. The spectrophotometer was calibrated at 270 nm for solutions of p-cresol in both methanol and water. The coefficients of the two calibration curves obtained were identical within experimental error (Table 3.1). Therefore at this wavelength, the concentration of p-cresol in methanol / water mixtures could be determined without errors arising from the variation of the

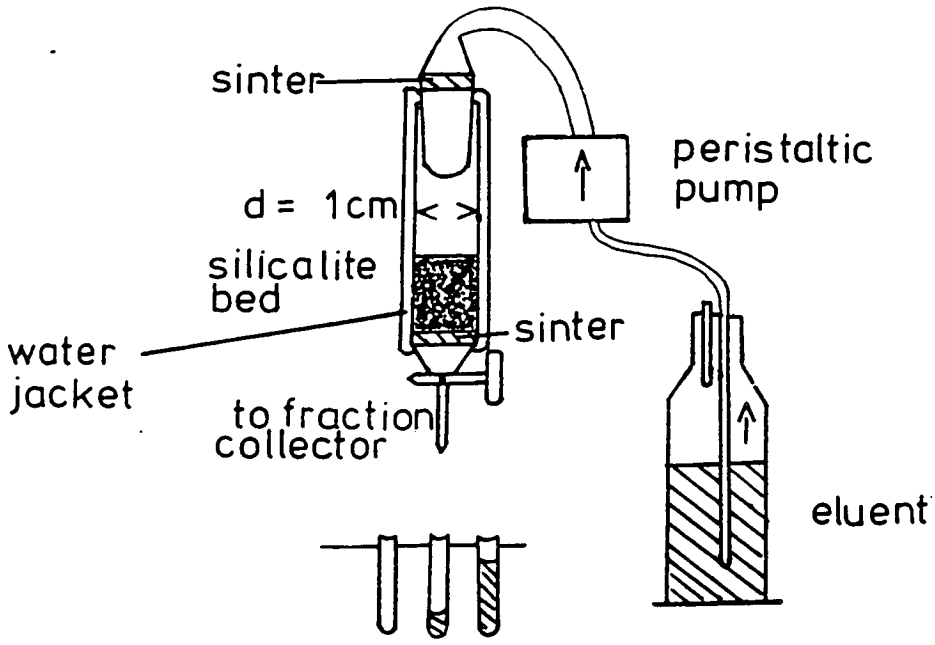

Figure 3.6 Apparatus Used for Column Experiments.

methanol / water ratio in solution.

Two column experiments were carried out using different batches of silicalite-1. Both columns were used in a cyclic mode being loaded with p-cresol and subsequently stripped in a regeneration stage. This was repeated several times. The running conditions of each stage in these column experiments are given below.

1. Column Experiment with sample GS15

This column experiment was carried out with 1.05 g of silicalite-1 sample GS15. The bed height was 2.5 cm and there was a pressure drop of 6 psi across the column throughout the experiment. The concentration of the aqueous feed solution of p-cresol was 5.05 x 10^{-3}M and the stripping solvent was 100% methanol. Both the loading and stripping stages were carried out at room temperature.

The flow rate of both the p-cresol feed solution and the methanol stripping solvent through the column was 1.5 cm^3min^{-1} for the first two cycles (C1a and C1b). On the third cycle (C1c), the flow rate of the feed solution was reduced to 1.33 cm^3min^{-1} and the flow rate of the methanol was reduced to 0.6 cm^3min^{-1}.

2. Column experiment with sample GS17

This column experiment was carried out with 0.99 g of silicalite-1 sample GS17. The bed height was 3.3 cm and there was a pressure drop of 4 psi across the column throughout the experiment. The concentration of the p-cresol feed solution was 5.03 x 10^{-3}M and the stripping solvent was 100% methanol. During the first cycle (C2a), the flow rate of both the feed solution and the stripping solvent was 1.5 cm^3min^{-1} and although the loading stage was

carried out at room temperature, the stripping stage was carried out at 40 - 45°C. The column was heated by pumping warm water through the water jacket attached to the column (see Figure 3.6). On the second cycle (C2b), the flow rate of the stripping solvent was reduced to 1.33 cm^3min^{-1} and the temperature of the column during the stripping stage increased to 55 - 60°C. The column was then loaded for a third time (C2c) with a flow rate of 1.5 cm^3min^{-1} as in the previous stages.

CHAPTER 4
RESULTS AND DISCUSSION

4.1 SYNTHESIS AND CHARACTERISATION OF SILICA MOLECULAR SIEVES

4.1.1 Synthesis of Silicalite-1

Silicalite-1 can be prepared by several synthetic routes. These were described in Chapter 1 (section 1.2.2.1), where the effect of the chosen synthetic route on the product obtained was discussed. Three synthetic routes were used to prepare silicalite samples for this work.

Sample GS11 was synthesised from the reaction mixture $3.5Na_2O$ 2TPABr $1000H_2O$. The details of the synthesis and post - synthesis treatment of the product are given in Chapter 3 (section 3.1.2). After calcination of the silicalite precursor to remove TPA cations from the pores it had to be acid exchanged. This is because sodium ions are incorporated in the molecular sieve along with hydroxide ions or broken siloxane bonds (see Figure 1.6) and must be removed by ion exchange with dilute acid.

Samples GS12 and GS14 were crystallised from the reaction mixture 10 piperazine 2TPABr $20SiO_2$ $1000H_2O$ at 95°C (see Chapter 3 (section 3.1.3). An acid exchange step was not required for these samples where piperazine was used as a mineraliser. However the use of piperazine dictated that the reaction was carried out at a much lower pH (final pH = 10.1) than that for GS11 (final pH = 12.2). This difference in pH had a marked effect on the crystallisation time of the two reactions. The crystallisation of GS11 took only 15 days whereas that of GS12 and GS14 took 6 weeks.

Samples GS15 - GS20 were crystallised from the same reaction

composition than for GS12 and GS14 but with an increase in temperature from 95°C to 150°C (see section 3.1.4). The crystallisation of these samples was complete in 4 days. This reduction in crystallisation time from 6 weeks to four days illustrates the marked effect of temperature on the rate of crystallisation of silicalite-1.

Figure 4.1 (a-c) shows electron micrographs of the typical morphology of the crystals obtained by each method of synthesis. Sample GS11(as) ("as" denotes as synthesised, uncalcined silicalite precursor) made at high pH in the presence of sodium ions is characterised by small, uniform, almost spherical crystals with a diameter of 2 µm. The surface of the crystals has a rather pitted appearance. The silicalite-1 samples prepared from the piperazine mix at 95°C (Figure 4.1 (b)) were made up of lozenge shaped crystals with average dimensions 8-10 µm x 6-8 µm x 2-4 µm. Samples produced in the autoclave at 150°C were of similar character but made up of larger crystals. Sample GS18 (Figure 4.1 (c)) is an example of material produced by this method with an average crystal size of 40 µm x 10 µm x 5 µm.

X-ray powder diffraction is a useful characterisation technique. It produces a "fingerprint" pattern which allows the identification of the structure of the molecular sieve. In addition, the area of the peaks and nature of the baseline gives an indication of the relative crystallinity of the sample. Figure 4.2 shows the X-ray diffraction patterns of GS14 in both the "as synthesised" and calcined form. The pattern obtained revealed that the sample had a ZSM-5 type crystal structure (*MFI* framework) (10) as expected for silicalite-1. Close inspection of the two patterns reveals that there are differences in the relative intensities of some of the peaks, and indeed some peak splitting in moving from the "as synthesised " to the calcined sample. This is caused by a minor perturbation of the framework structure from an orthorhombic to a monoclinic form, on

Figure 4.1 Electron Micrographs of "As Synthesised" Silicalite Samples.

GS11as

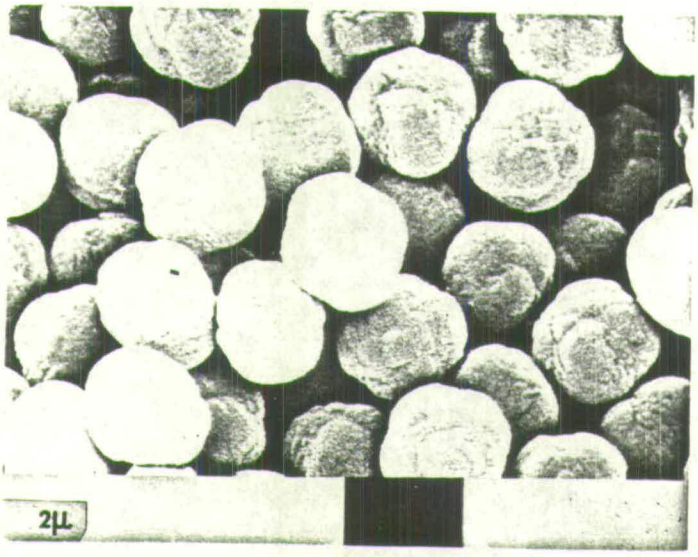

GS14as

GS18as

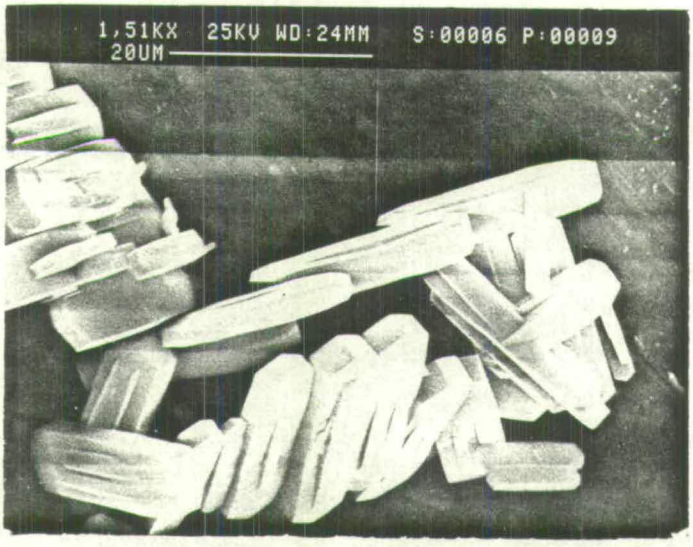

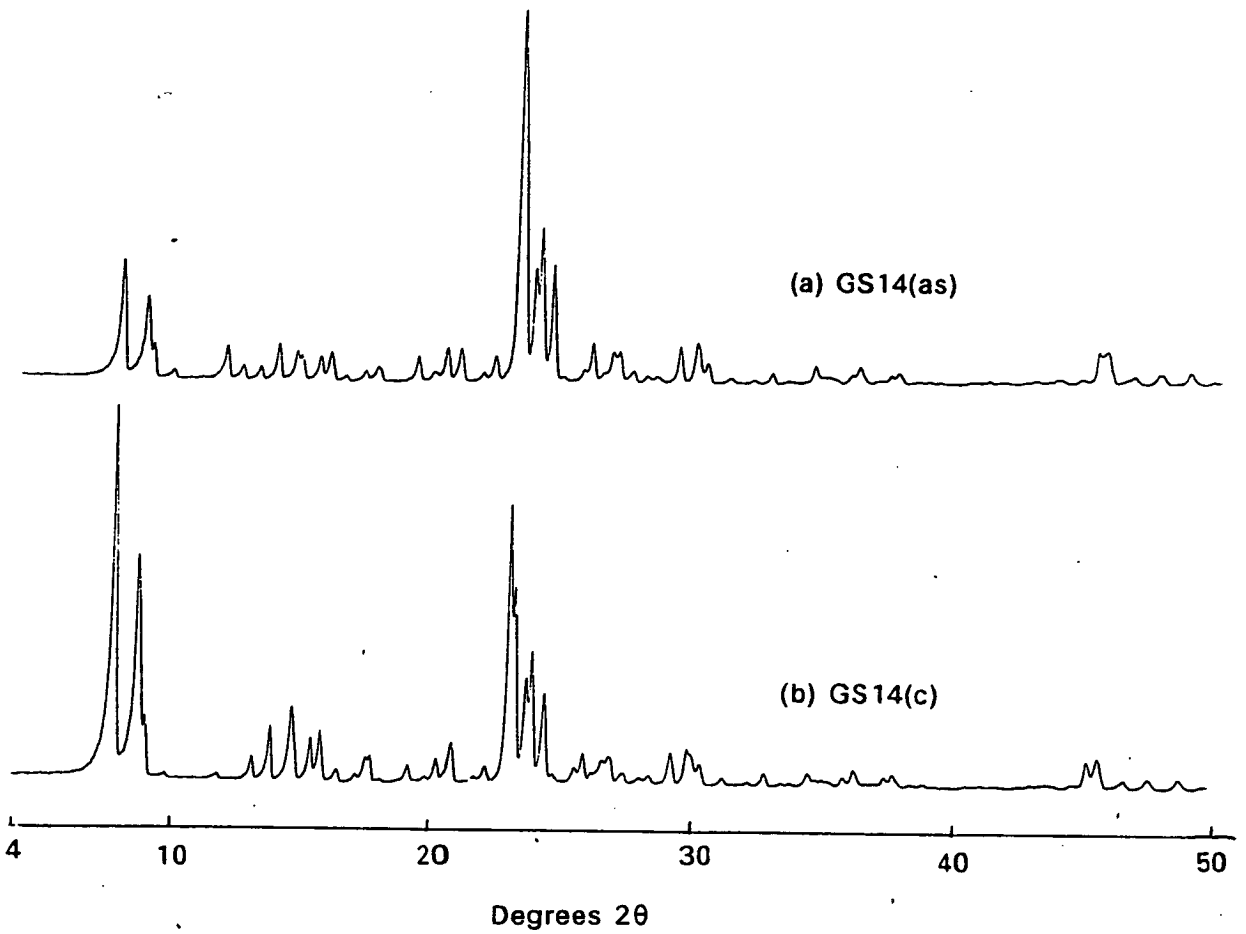

Figure 4.2 Powder X-Ray Diffraction Patterns of Silicalite-1 Sample GS14.

removal of the organic template from the channels. The sharp peaks and flat baseline obtained for these diffraction patterns suggest a highly crystalline sample.

The diffraction pattern obtained for the remaining silicalite samples made, were very similar in nature. They differed only in the relative areas of the peaks obtained. A quantitative measure of their relative degree of crystallinity can be found from a measure of peak areas. A comparison of the height of the largest peak in the diffraction pattern of each calcined sample (at 3.87Å interplanar spacing, d) is given in Table 4.1. A measure of the relative peak heights was considered a good enough indication of the relative degree of crystallinity of each sample. The figures obtained show that all the samples lie within 12% of the average value. It was therefore assumed, given the uncertainty in the determination, that all the samples had a comparable degree of crystallinity.

Figure 4.3 (a-c) shows thermal analysis traces of three "as synthesised" silicalite precursors made by different modes of synthesis. The double peaks in the exotherms obtained in the DTA traces for GS11 (as) and GS18 (as) are artefacts caused by oxygen depletion as the organic material inside the pores decomposes. The size and shape of the DTA peaks obtained depend on the weight of sample used for analysis and the heating rate. The heating rate used in each run was 10°C min^{-1} and the sample size varied between 13 mg and 15 mg as shown in Figure 4.3.

The thermal analysis traces of the three samples show similar characteristics. The pattern of weight loss with temperature by TPA-silicalite can be divided into three stages. Figure 4.4 (a) shows the general form of the trace obtained and the divisions which can be made. Weight loss below 250°C

Table 4.1

Crystallinity of Silicalite-1 Samples

Sample	Peak height of calcined samples/cm (d spacing of 3.86Å)	Crystallinity rel. to average value %
GS11	n.a.	-
GS12	11.7	106
GS14	11.1	100
GS15	9.8	89
GS16	9.9	90
GS17	9.8	89
GS18	11.9	108
GS19	11.8	107
GS20	12.4	112

n.a. = not available

(a) GS11(as)

(sample size = 14.4 mg)

(b) GS14(as)

(sample size = 13.7 mg)

(c) GS18(as)

(sample size = 13.7 mg)

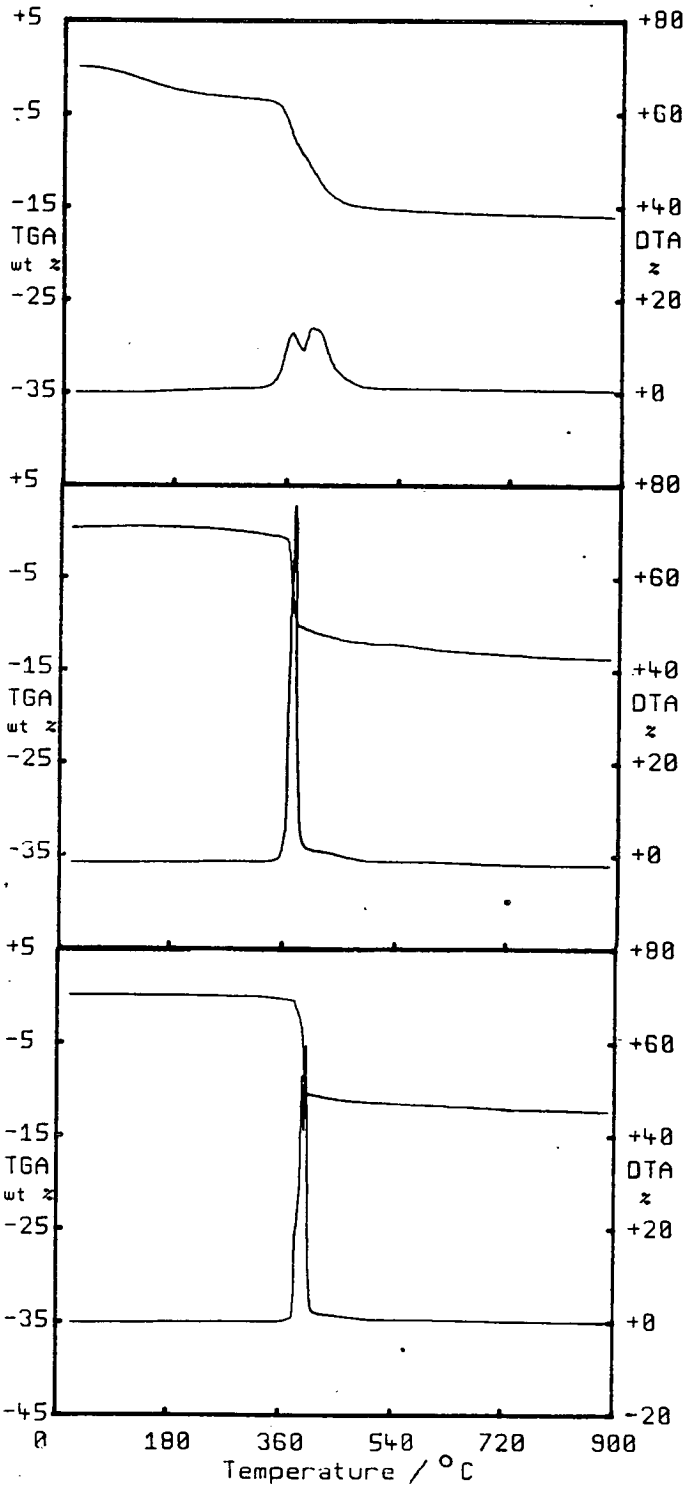

Figure 4.3 Thermal Analysis Traces of "As Synthesised" Silicalite Precursors.

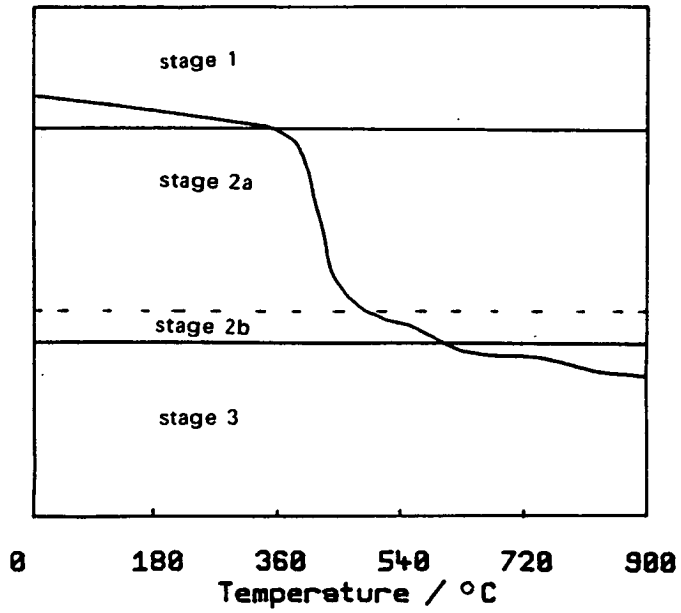

Figure 4.4a Scheme for Thermal Analysis Interpretation.

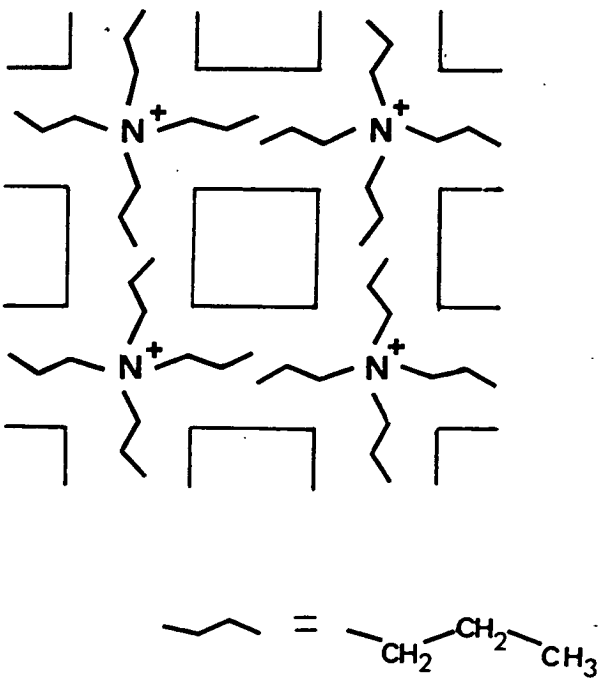

Figure 4.4b Unit Cell of TPA-Silicalite.

(stage 1) corresponds to low temperature water loss from the external surface of the crystals. Above 250°C, the organic template inside the sieve begins to decompose and a large weight loss is observed. This stage can be split into two parts. A weight loss due to the desorption of the decomposed organic template followed by a loss of water from hydroxyl groups previously associated with the quaternary ammonium ion. This can be represented in the following way;

$$[TPA^+]_4\ [Si(O^-)O_{1.5} + Si(OH)O_{1.5}]_4[SiO_2]_{88}$$

2a ↓HEAT

$$\{TPA^+_4 - H_4\} + [Si(OH)O_{1.5} + Si(OH)O_{1.5}]_4[SiO_2]_{88}$$

2b ↓HEAT

$$\{(H_2O)_4\} + [SiO_2 + SiO_2]_4[SiO_2]_{88}$$

A final stage, weight loss above 600°C, corresponds to high temperature dehydroxylation (loss of chemical water).

The % weight loss (w/w) hydrated TPA-silicalite during each stage by the "as synthesised" silicalite precursors are given in Table 4.2. The average weight loss found during stage 2, taken to be due to tetrapropylammonium hydroxide, was 12.1 $\pm$ 0.2%. The total weight loss which would be expected during this stage for an ideal TPA-silicalite composition of $4TPAOH.96SiO_2$ is 11.2% (w/w) in stage 2a + 1.2% (w/w) in stage 2b, which equals 12.4% (w/w). A value of 12.1 $\pm$ 0.2% therefore corresponds to 3.9 $\pm$ 0.1 molecules of TPAOH per unit cell (96 SiO_2).

A schematic representation of the unit cell of silicalite is shown in Figure 4.4 (b). TPA ions have been included in the diagram to illustrate a possible packing arrangement. It is generally accepted that the TPA ions are positioned, one at each intersection with the channel voids filled by out stretched alkyl groups. Samples GS12 and GS14 gave weight losses notably higher than the

Table 4.2

Thermal Gravimetric Analysis of "As Synthesised" Silicalite-1 Precursors

Sample	% Weight Loss (± 0.1) (w/w) hydrated TPA-silicalite Temperature Range		
	0-250°C	250-600°C	0-900°C
GS11	3.1	12.3	16.0
GS12	0.5	13.0	14.8
GS14	0	12.8	13.8
GS15	0	11.8	12.6
GS16	0	11.8	12.8
GS17	0	11.9	12.9
GS18	0.2	12.2	13.4
GS19	0.2	11.7	12.7
GS20	0	11.1	12.3

others between 250°C and 600°C. This is thought to be due to the desorption of excess water during this stage, and not to an excess of organic template.

Any low temperature water loss by "as synthesised" silicalite can only be due to water sorbed on the external surface area of the crystals. Sample GS11 showed a weight loss of *ca* 3.1% (w/w) hydrated TPA-silicalite below 250°C. The electron micrograph of GS11 (Figure 4.1 (a)) shows crystals with a pitted surface which indicates a large external surface area. The other silicalite samples which are made up of larger crystals with relatively smooth surfaces, show little or no weight loss below 100°C, and therefore have little or no external water sorption.

Figure 4.5 (a-c) shows thermal analysis traces of calcined silicalite samples made by different modes of synthesis. These traces show two distinct areas of weight loss with temperature. Below 400°C there occurs a weight loss due to dehydration with a corresponding endotherm on the DTA trace. Between 400°C and 900°C there is a small weight loss incurred due to dehydroxylation of the lattice. The DTA traces above 400°C are featureless, with the exception of sample GS11. A broad, weak exotherm ocurred whose origin is unclear. It may have been produced by the burning out of a little sorbed material which had contaminated the sample prior to analysis.

Table 4.3 shows the uptake of water by each silicalite sample calculated from the low temperature weight losses obtained on thermal analysis. Sample GS11, made in the presence of sodium, is the most hydrophilic material. It was described in Chapter 1 (section 1.2.2.1, Figure 1.6) how sodium ions incorporated into the framework could attack the lattice of the sieve. This produces hydrophilic sites which may not heal even after ion-exchange and calcination. Table 4.3 shows that GS11 sorbed 6.7% water (w/w) dry silicalite.

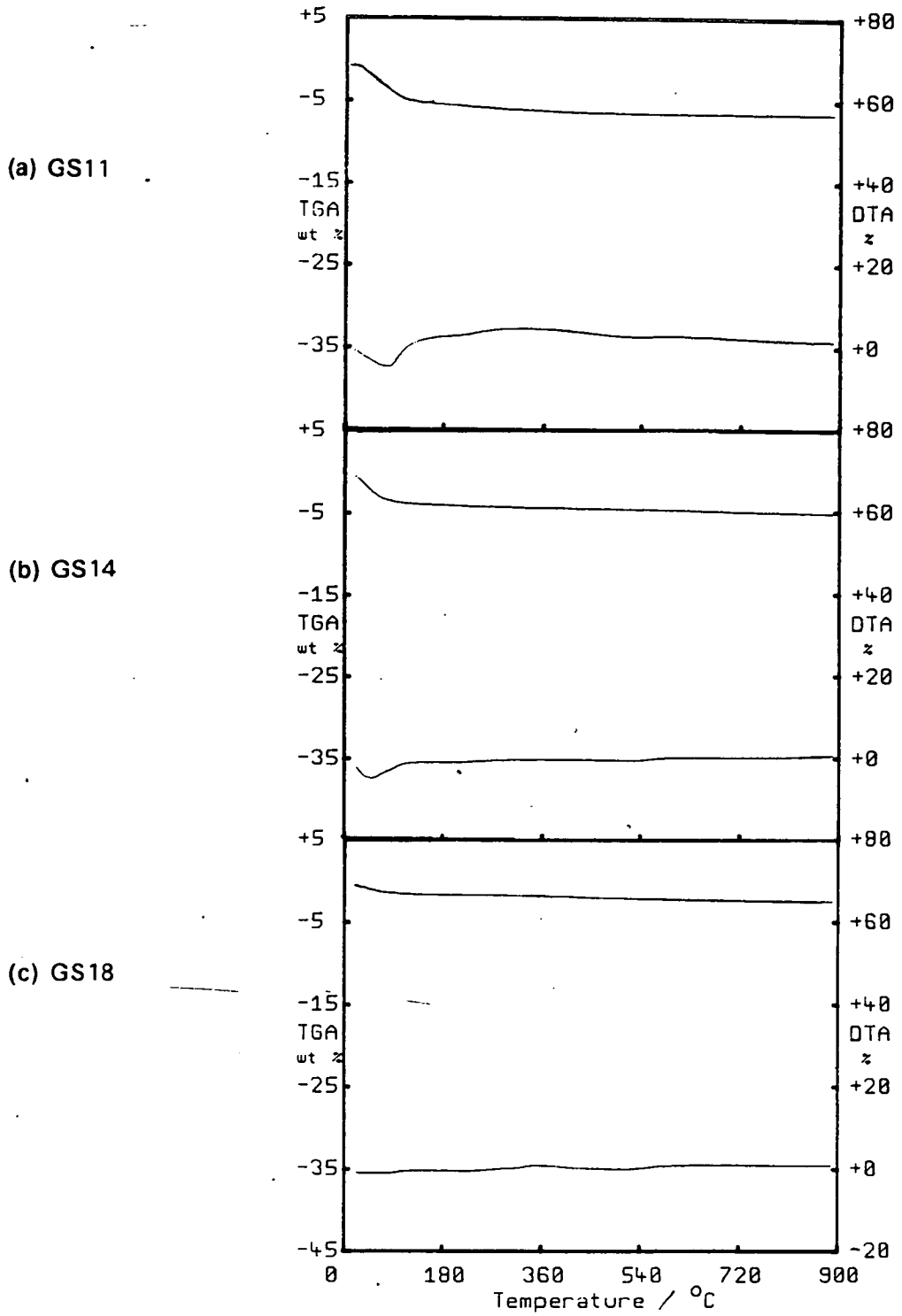

Figure 4.5 Thermal Analysis Traces of Calcined Silicalite-1 Samples.

Table 4.3

Thermal Gravimetric Analysis of Calcined Silicalite Samples

Sample	Weight loss % (w/w) sample. 0–400°C	Weight loss % (w/w) sample 400–900°C	Sorbed water[a] molecules / unit cell (96 SiO_2)
GS11	6.4	0.2	22
GS12	3.5	0.8	12
GS14	3.6	0.9	12
GS15	1.8	0.7	6
GS16	2.0	0.7	6
GS17	2.1	0.9	6
GS18	1.5	0.4	5
GS19	1.9	0.5	6
GS20	2.0	0.5	6

[a]Calculated from weight loss below 400°C.
Weight loss above 400°C is due to dehydroxylation of lattice.

However, much of this sorbed water is presumed to be on the external surface of the sieve. Thermal analysis of "as synthesised" material, as already described, gave a low temperature weight loss of 3.7% (w/w) dry silicalite. The fraction which is sorbed into the pores is likely to be associated with faults in the silicalite lattice. These faults are most probably situated at channel intersections. During synthesis, sodium cations are most likely to be occluded at channel intersections where the quaternary amine group is situated. Weight loss above 400°C is thought to be due to the dehydroxylation of the "hydroxyl nests" which constitute the afore mentioned faults in the lattice.

Sample GS14 is less hydrophilic with a water uptake of 3.7% (w/w) dry silicalite (a_w = 0.753), which corresponds to 12 molecules per unit cell (Table 4.3). The negligible water uptake by the "as synthesised" precursor of this material suggests that the water sorption sites are almost exclusively on the internal surface of the sieve. There are therefore also hydrophilic sites present in this sample of silicalite.

Sample GS18 (Figure 4.5 (c)) and the other samples crystallised at 150°C were the most hydrophobic group of materials produced (Table 4.3). GS18 for example, had a water uptake of 1.5% (w/w) dry silicalite or 5 molecules per unit cell. It is therefore approaching a near perfect hydrophobic lattice. This marked increase in hydrophobicity over the 95°C samples is clearly related to the temperature of crystallisation. At higher temperature the crystallisation is much faster and it appears that the mechanism is more efficient. Fewer unreacted hydroxyl groups are left within the framework during crystallisation. The high temperature weight loss in GS18 is only 0.4% which indicates little dehydroxylation at elevated temperature. This is further evidence of the near perfect lattice which is obtained by this mode of synthesis.

A major element analysis was carried out using X-ray fluorescence on samples GS14 and GS19. The results show that the samples are free from any major impurities (Table 4.4). Small quantities of impurities are present in the starting materials and cannot be avoided. The levels of aluminium are so low that an accurate determination of SiO_2/Al_2O_3 ratio cannot be made by this method. However the results show that the level of impurity in the final product, for both the 95°C and 150°C reaction mixtures, is similar. Therefore the change in hydrophobicity of the material cannot be attributed to a difference in the sodium or aluminium content.

4.1.2 Reproducibility of Silicalite-1 Synthesis

The previous section described the changes observed in the nature of silicalite-1 produced by different synthetic routes. It is also important to compare material made in an identical manner in order to determine the reproducibility of synthesis. A comparison of the properties of GS15, GS16 and GS17, all synthesised at 150°C from a 10 piperazine$_{\wedge}^{2TPABr}$20SiO_2 1000H_2O reaction mixture will now be made. Table 4.5 reveals that in terms of degree of crystallinity, morphology and water uptake, the three samples are virtually indistinguishable. The water uptake values were calculated (w/w) dry silicalite from the low temperature weight losses on calcination of the hydrated samples (Table 4.3). It is important, if one is to consider sets of sorption results on different batches of material, that they all share the same morphology and degree of hydrophilicity.

The particle size distribution patterns obtained for these three batches are shown in Figure 4.6. Samples GS15 and GS17 have normal distributions which peak over the respective ranges; 22-38 µm and 21-54 µm. GS16 shows an asymmetric distribution which rises more slowly in the smaller size bands and

Table 4.4

X-Ray Fluorescence Major Element Analysis Results

Sample	GS14	GS19
Oxide	% W/W	% W/W
SiO_2	98.112	94.825
Al_2O_3	0.088	0.071
Fe_2O_3	0.017	0.014
MgO	0.028	0.029
CaO	0.035	0.038
Na_2O	0.092	0.107
K_2O	0	0
TiO_2	0.019	0.010
MnO	0.002	0.002
P_2O_5	0.003	0.011
Total	98.389	95.103

Table 4.5

A Comparison of the Properties of Silicalite-1

Samples GS15, GS16 and GS17

	GS15	GS16	GS17
% Crystallinity	89%	90%	89%
Morphology	(25μm x 5μm x 5μm)		
Bulk density of precursor/g(cm)$^{-3}$	0.60	0.59	0.38
TPA^+ in precursor molecules/unit cell	3.8	3.8	4.0
Water uptake % W/W dry silicalite (a_w = 0.753, 25°C)	1.8	2.0	2.1

SIZE BAND UPPER	LOWER	CUMULATIVE WT BELOW	WEIGHT IN BAND	CUMULATIVE WT ABOVE	LIGHT ENERGY COMPUTED	MEASURED
188.0	87.2	99.3	0.8	0.0	285	290
87.2	53.5	95.4	3.8	0.8	469	465
53.5	37.6	85.6	9.8	4.6	675	672
37.6	28.1	71.2	14.4	14.4	910	912
28.1	21.5	56.3	14.9	28.8	1186	1188
21.5	16.7	39.9	16.4	43.7	1486	1484
16.7	13.0	28.6	11.3	60.1	1772	1776
13.0	10.1	20.0	8.6	71.4	1955	1929
10.1	7.9	12.9	7.1	80.0	2030	2047
7.9	6.2	9.4	3.5	87.1	2047	2039
6.2	4.8	6.0	3.3	90.6	2034	1992
4.8	3.8	2.1	4.0	94.0	1973	1985
3.8	3.0	0.2	1.8	98.0	1889	1903
3.0	2.4	0.0	0.2	99.8	1784	1749
2.4	1.9	0.0	0.0	100.0	1600	1531

(a) GS15

SIZE BAND UPPER	LOWER	CUMULATIVE WT BELOW	WEIGHT IN BAND	CUMULATIVE WT ABOVE	LIGHT ENERGY COMPUTED	MEASURED
188.0	87.2	98.3	1.7	0.0	526	508
87.2	53.5	85.0	13.3	1.7	795	786
53.5	37.6	63.2	21.8	15.0	1018	1017
37.6	28.1	46.3	16.8	36.8	1189	1185
28.1	21.5	35.2	11.1	53.7	1357	1346
21.5	16.7	25.7	8.5	64.8	1463	1476
16.7	13.0	19.2	6.5	74.3	1631	1636
13.0	10.1	14.4	4.8	80.8	1766	1732
10.1	7.9	10.1	4.3	85.6	1856	1868
7.9	6.2	7.8	2.3	89.9	1945	1940
6.2	4.8	5.6	2.3	92.2	2017	1973
4.8	3.8	2.2	3.4	94.4	2047	2047
3.8	3.0	0.3	1.8	97.8	2028	2046
3.0	2.4	0.0	0.3	99.7	1961	1918
2.4	1.9	0.0	0.0	100.0	1763	1718

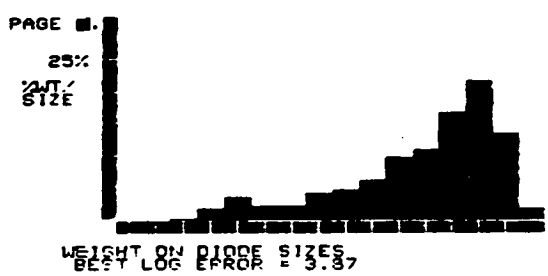

(b) GS16

SIZE BAND UPPER	LOWER	CUMULATIVE WT BELOW	WEIGHT IN BAND	CUMULATIVE WT ABOVE	LIGHT ENERGY COMPUTED	MEASURED
188.0	87.2	98.2	1.6	0.0	254	247
87.2	53.5	90.8	7.4	1.8	400	396
53.5	37.6	77.9	12.9	9.2	551	546
37.6	28.1	63.1	14.8	22.1	707	708
28.1	21.5	50.3	12.8	36.9	893	886
21.5	16.7	39.0	11.3	49.7	1082	1060
16.7	13.0	31.2	7.8	61.0	1291	1295
13.0	10.1	25.0	6.2	68.8	1466	1463
10.1	7.9	18.3	6.7	75.0	1679	1667
7.9	6.2	12.0	6.3	81.7	1883	1880
6.2	4.8	5.9	6.1	88.0	2031	2011
4.8	3.8	1.1	4.8	94.1	2047	2047
3.8	3.0	0.0	1.1	96.9	1891	1903
3.0	2.4	0.0	0.0	100.0	1644	1491
2.4	1.9	0.0	0.0	100.0	1361	1063

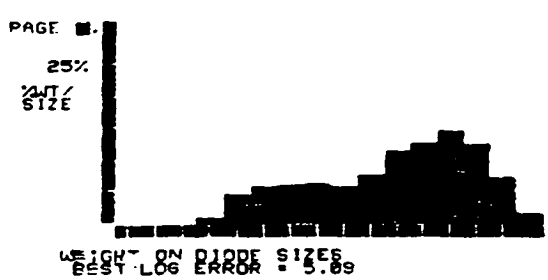

(c) GS17

Figure 4.6 Particle Size Distributions of Silicalite-1 Samples.

has a more pronounced maximum. The reason for this discrepancy is not known since there were no detectable differences in their relative morphology found by microscopy.

The difference in particle size distribution did not effect the bulk density of GS16 which was comparable to that of GS15 (Table 4.5). Sample GS17 had a bulk density which was much smaller than the other two. The reasons for this are not yet known but it is clear that they are more subtle than simply a particle size distribution effect. The effect of this difference on the behaviour of sample GS17 compared to GS15 when used for column sorption experiments will be discussed later (section 4.7). With respect to the morphology, crystallinity and degree of hydrophilicity of the product, silicalite-1 synthesis has been shown to be reproducible. The nature of the crystallisation process however, dictates that there may be subtle differences between samples made by an identical synthetic route. These must be taken into account if a meaningful comparison is to be made of the sorption behaviour of these materials.

4.1.3 Synthesis and Characterisation of ZSM-5

The aim of this synthetic work was to produce samples of the zeolite ZSM-5 with different SiO_2/Al_2O_3 ratios, in order to compare their sorption properties. The end member of the series would naturally be the aluminium free silicalite-1. For this reason, it was necessary to produce the ZSM-5 samples by a similar synthetic route to the silicalite-1 samples with which they would be compared.

ZSM-5 was first prepared by Argauer and Landolt in siliceous systems that contained sodium and tetrapropylammonium ions (TPA) (22). Since that time

there have been many patents and papers described, which claim novel routes to ZSM-5. The production of large crystals has generated great interest and several methods have been reported: For example pH control using salts of organic acids (57) or control of morphology by the addition of nitrogenous bases (other than the nitrogenous organic template) to the reaction mixture (150). However, most published work has involved the use of inorganic cations in the synthesis.

A low sodium synthetic route to ZSM-5 was patented by Mobil Oil Corporation (151). It described the use of primary monoalkylamines in low sodium reaction mixtures. An alkali metal cation free route to ZSM-5 was reported (58). The systems described included [NH_4^+] and TPA ions. The products obtained were calcined to give H-ZSM-5 without the need for preparative ion exchange procedures. This synthetic route was also adopted for silicalite-1 synthesis (see Chapter 1 (section 1.2.2)).

The aim of this work was to make H-ZSM-5 in the absence of inorganic cations and at a relatively low pH. It was hoped that this would give large crystals of the zeolite. The effect of aluminium content on sorption could then be assessed without the added complication of external surface area on sorption, or extra hydrophilic sites due to inorganic cations in the framework.

It was decided to try to produce ZSM-5 by an analogous route to that used for silicalite. This involved the use of TPABr and piperazine. The experimental procedure used for the syntheses are given in Chapter 3 (section 3.1.5). The same basic constituents which were used for the synthesis of silicalite were chosen for the reaction mixture. The main problem was the efficient dispersal of aluminium at the pH (*ca* 10.5) of this mixture. An equal dispersion of aluminium through the reaction mixture is known to be of primary importance

to prevent "aluminium zoning" in the product (152).

To overcome this, the aluminium was added as aluminium sulphate and blended thoroughly into the silica - water slurry before the addition of piperazine and TPABr. In this way, an even dispersion of aluminium was achieved before precipitation occurred. Reaction mixtures with SiO_2/Al_2O_3 ratios of 240, 120 and 60 were prepared as described and crystallised under static conditions at 150°C.

Table 4.6 shows a comparison of some of the properties of the three samples obtained, respectively named GZ1, GZ2 and GZ3. The crystal size of the product decreased as the aluminium content of the reaction mixture increased. This result was as expected, since the presence of aluminium enhances seeding. The crystals also became more squat as the amount of aluminium increased.

An X-ray diffraction pattern of these materials was not obtained due to lack of sample but one can see from the electron micrographs (Figure 4.7) that there is no distinguishable amorphous material present in any of the products.

The values for water uptake showed that all samples of ZSM-5 had increased hydrophilicity over their silicalite-1 counterpart (GS18, 1.5% w/w H_2O). However, water uptake by the product did not increase consistently with the aluminium content of the reaction mixture. The water uptake by GZ2 was slightly greater than that of GZ3 although it was made from a more highly siliceous reaction mixture. The reason for this is unclear, since previous workers have shown (31) that water sorption increases linearly with aluminium content in ZSM-5. Unfortunately a major element analysis of these materials could not be carried out, again because of lack of sample. A measure of their framework aluminium content has therefore not been made.

Table 4.6

A Comparison of the Properties of ZSM-5 Samples

GZ1, GZ2, GZ3 and GZ22

	SAMPLE			
	GZ1	GZ2	GZ3	GZ22
Morphology /μm	16x9x5	13x11x5	5x5x3	9x7x3
Thermal Analysis of Precursor (Weight loss % (w/w) hydrated sieve)				
0-250°C	0.3	0.6	0.7	0.7
250-600°C	11.6	11.6	11.6	11.4
0-900°C	12.9	13.4	13.6	13.3
Water uptake[a] % (w/w) dry sieve	3.5	6.3	5.7	6.1

[a]Calculated from weight loss between 0 and 400°C by samples previously equilibrated with water vapour (a_w = 0.753).

Figure 4.7 Electron Micrographs of ZSM-5 Samples.

GZ1

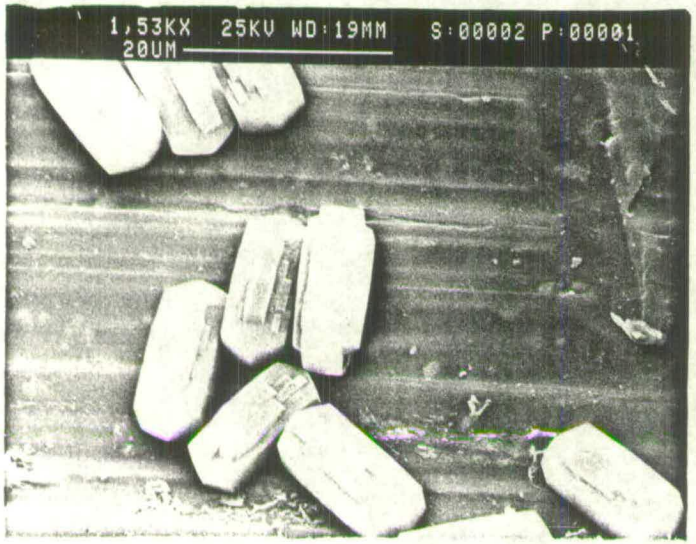

GZ2

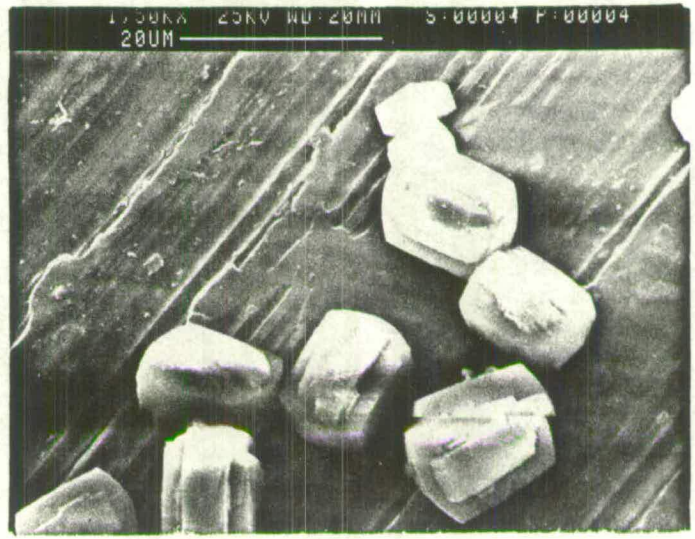

GZ3

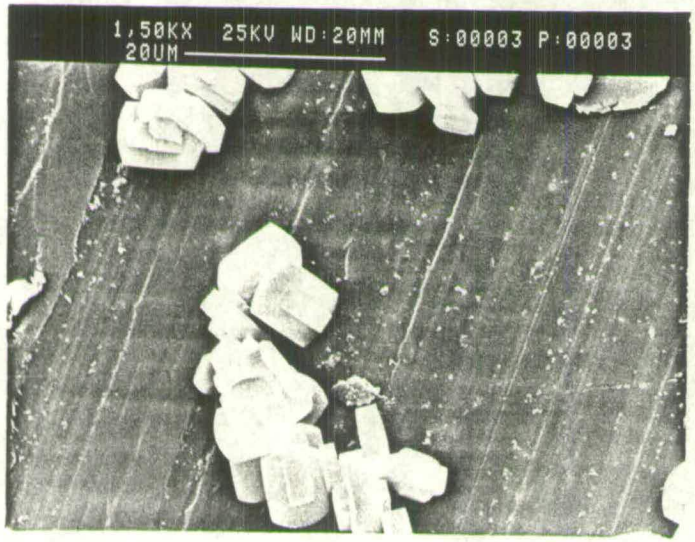

GZ22

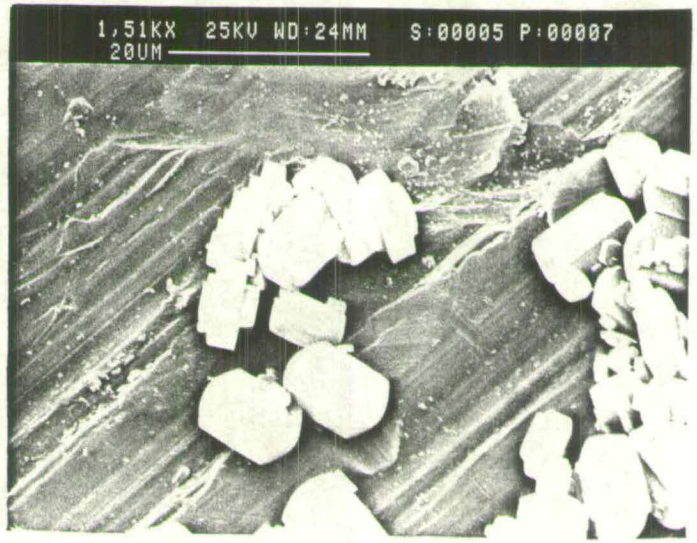

A batch of ZSM-5 was prepared on a larger scale in a stirred autoclave at 150°C using the same reaction mixture as that for GZ2 (SiO_2/Al_2O_3 = 120). The properties of the material obtained (GZ22) are included in Table 4.6. It is interesting that the water uptake by this sample is very close to that of GZ2. An electron micrograph of GZ22 is shown in Figure 4.7. One can see the effect of stirring the reaction mixture on the morphology of the final product. The crystals produced were smaller and more squat than those of GZ2, which was made from the same reaction composition and at the same temperature, but in a static environment.

A major element analysis was carried out on GZ22, the results of which are shown in Table 4.7. This revealed that the SiO_2/Al_2O_3 ratio of the product was 108. From a reaction mixture ratio of 120, this is the expected product ratio. In practice, the product aluminium concentration is not much greater than that of the reaction mixture. This is due to the fact that the reaction goes with high yield.

An X-ray diffraction pattern of GZ22(as) is shown in Figure 4.8. It is characterised by sharp peaks and a flat baseline. This method therefore provides a successful route to a highly crystalline sample of ZSM-5.

The SiO_2/Al_2O_3 ratios of the three materials GZ1, GZ2 and GZ3 have been estimated to be 220, 110 and 55 (all $\pm$ 10) respectively on the basis of the result obtained for GZ22. These are of course merely estimates. However there is some evidence to suggest that they are likely to be correct. For example, GZ2 behaves similarly to GZ22 in terms of water uptake. The change in morphology from GZ1 to GZ3 suggests a systematic increase in aluminium content through the series. Further evidence is provided by a close look at the thermal analysis patterns of the zeolite precursors. These are shown in Figure

Table 4.7

X-Ray Fluorescence Results for GZ22

OXIDE	% W/W in sample
SiO_2	95.0
Al_2O_3	1.51
Fe_2O_3	0.032
MgO	0.007
CaO	0.052
Na_2O	0
K_2O	0
TiO_2	0.006
MnO	0.002
P_2O_5	0.008
Total	96.6

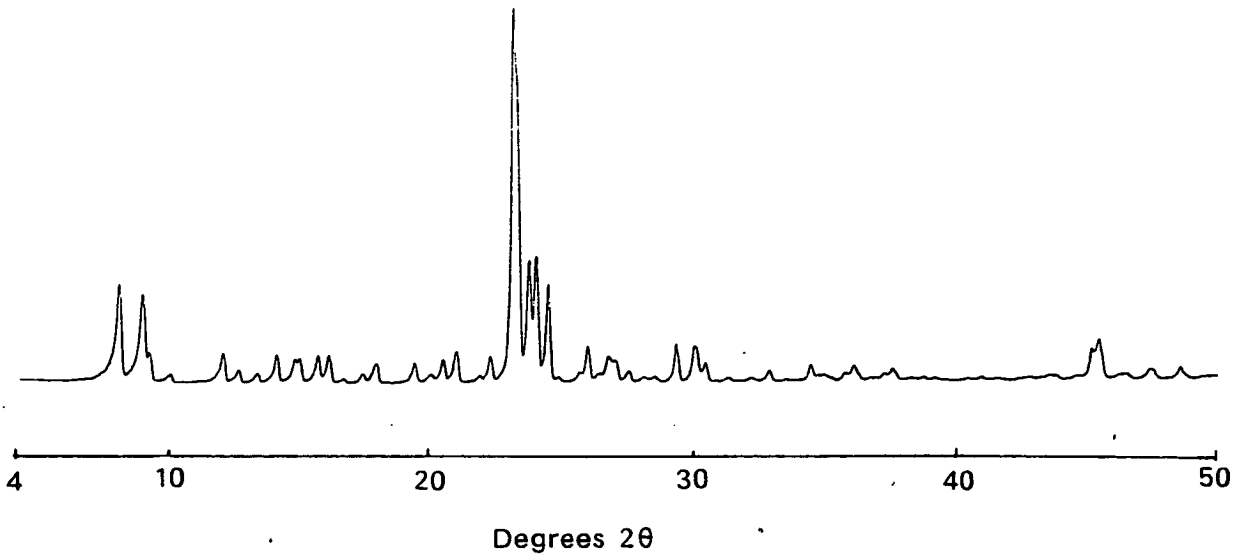

Figure 4.8 Powder X-Ray Diffraction Pattern of "As Synthesised" ZSM-5 (GZ22).

4.9. Comparison of the differential thermal analysis (DTA) traces obtained for each zeolite revealed that the shoulder at *ca* 500°C becomes more pronounced between GZ1 and GZ3. This shoulder is thought to be due to the decomposition, at higher temperature, of TPA ions associated with aluminium sites in the framework. The fact that this peak becomes stronger down the series, suggests a consistent increase in aluminium content (153).

It was not possible to ascertain the position of the aluminium atoms within each framework. The site of the Al atoms is likely to be of prime importance to their sorption properties. This will be discussed more fully in section 4.3.3.

4.1.4 Characterisation of Silicalite-2

Two samples of silicalite-2 were supplied by K.R. Franklin. They had been synthesised by the method described in Chapter 1 (section 1.2.2.2) using tetrapentylammonium bromide (TPeABr) as a structure directing agent, piperazine as a mineraliser, amorphous silica and water. The crystallisation was carried out under static conditions at 150°C. This synthetic route, as already stated, gives a highly hydrophobic product made up of large crystals. Table 4.8 summarises the characterisation of samples KF1 and KF2. Silicalite-2 is a silica molecular sieve, identical in composition to that of silicalite-1 but with a different framework structure. Silicalite-1, as described, has a ZSM-5 type structure, whereas silicalite-2 has a ZSM-11 type structure. The two samples of silicalite-2 are virtually identical in terms of degree of hydrophobicity and morphology. The water uptake values, show that these materials are more hydrophobic than any of the samples of silicalite-1 which have been discussed.

The thermal analysis results of the "as synthesised" materials also shown in

(a) GZ1 (sample size = 16.7 mg)

(b) GZ2 (sample size = 15.4 mg)

(c) GZ3 (sample size = 14.5 mg)

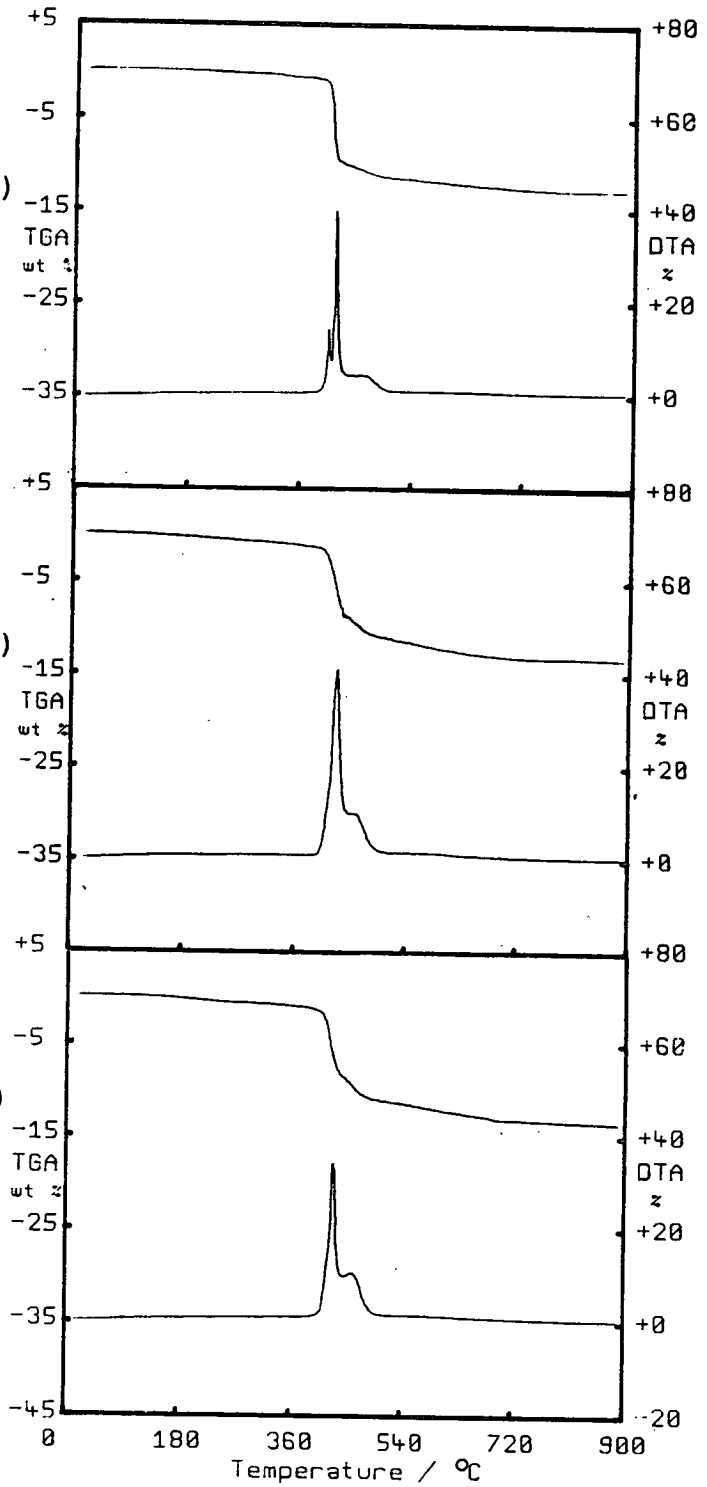

Figure 4.9 Thermal Analysis Traces of "As Synthesised" ZSM-5 Samples.

Table 4.8

A Comparison of the Properties of Silicalite-2 Samples KF1 and KF2

	KF1	KF2
Morphology	50 - 60 µm x 5 µm x 5 µm	
Relative Crystallinity	90%	100%
Thermal Analysis of Precursor (Wt. Loss % (w/w) sample)		
0-250°C	0.3	0.4
250-600°C	11.9	12.0
600-900°C	0.5	0.4
Water uptake[a] % (w/w) sample	1.4	0.9

[a]Calculated from weight loss between 0 and 400°C of samples previously equilibrated with water vapour (a_w = 0.753).

Table 4.8 revealed that an average of 12.0% $TPeA^+$ (w/w) hydrated silicalite-2 was present in each material. This corresponds to 2.6 molecules of quaternary amine per unit cell of $96SiO_2$. It would be expected to be less than 4 since there is not enough room inside the lattice to fit one molecule of $TPeA^+$ at each intersection (*cf* silicalite-1 and TPA^+). The thermal analysis trace of sample KF2 is shown in Figure 4.10. It exhibits a sharp peak for the burning out of the organic template. This suggests a highly crystalline material, free from stacking faults and intergrowths.

The X-ray diffraction patterns of sample KF2 in both the "as synthesised" and calcined form are shown in Figure 4.11. These show that KF2 is predominantly of the ZSM-11 type structure and is highly crystalline. The differences between the "fingerprint" diffraction patterns of silicalite-1 (ZSM-5) and silicalite-2 (ZSM-11) are very subtle. They were described as follows, in a patent (154) by the inventors of the two materials, Mobil Oil Corporation:

> "ZSM-5 contains a doublet at about 10.1, 3.73, 3.00 and 2.01Å interplanar spacing; ZSM-11 shows a singlet at these values."

The appropriate d spacings are marked on Figure 4.11. Comparison with the pattern for silicalite-1 (GS14(as)) in Figure 4.2 shows a doublet in these positions. The only anomalous peak in the pattern for silicalite-2 is that at the smallest d-spacing. It has a slight amount of doublet character. There may therefore be a small amount of silicalite-1 (ZSM-5) present as an intergrowth in the sample of silicalite-2 (ZSM-11). The level of this impurity can not be determined from the available information. The morphology of the samples which both consist of large coffin shaped single crystals (50-60 µm x 5 µm x 5 µm) with a smooth surface and a very low degree of crystal twinning shows no evidence for an intergrowth. The thermal analysis results and XRD patterns also suggest that this sample is predominantly silicalite-2.

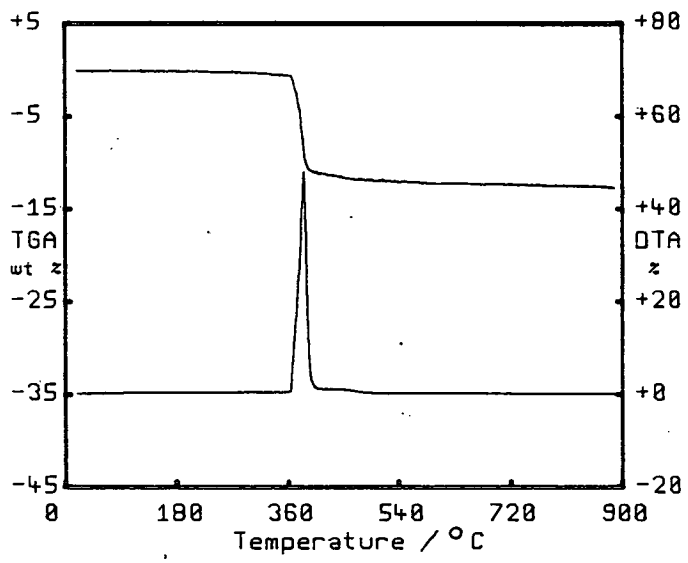

Figure 4.10 Thermal Analysis Trace of "As Synthesised" Sample of Silicalite-2 (KF2).

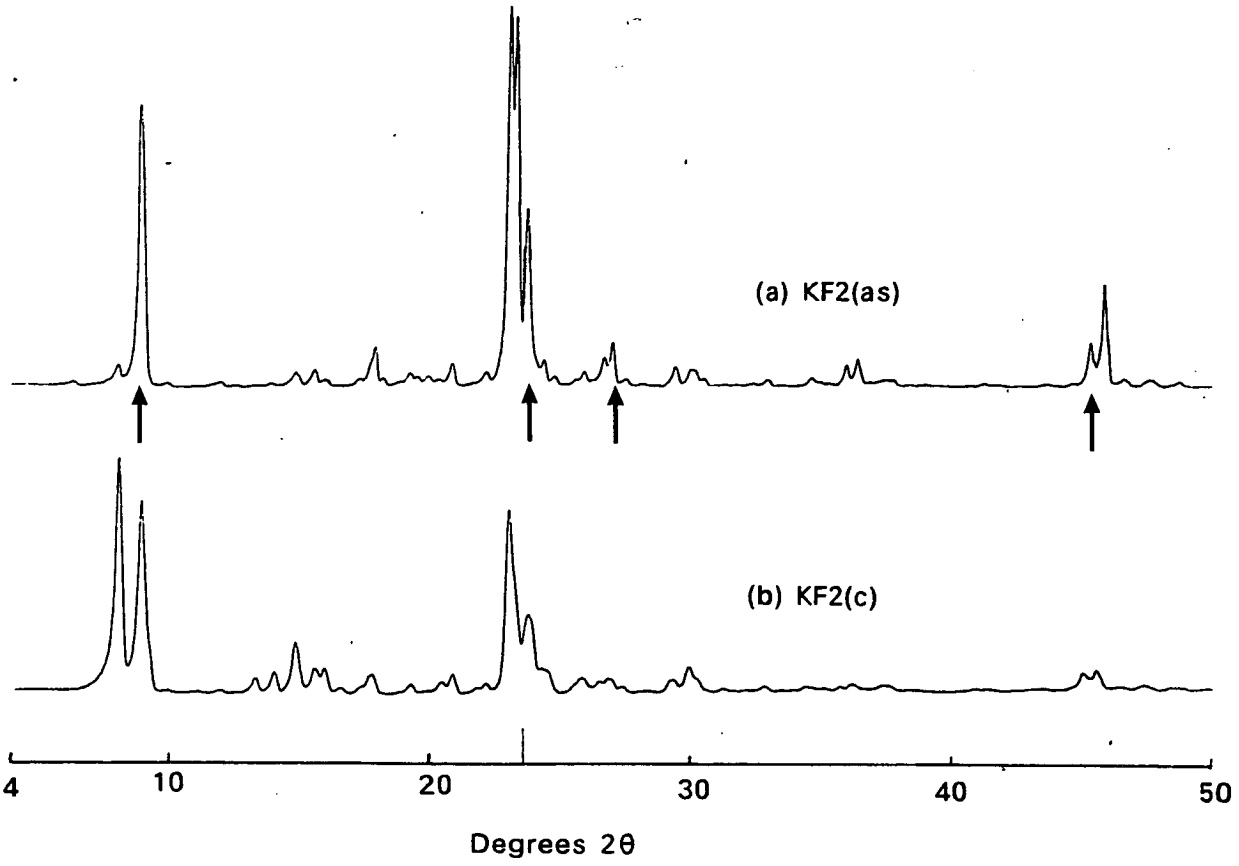

Figure 4.11 Powder X-Ray Diffraction Patterns of Silicalite-2 Sample KF2.

Sorption results described in section 4.3.3 will reveal that the silicalite-2 samples behave differently to those of silicalite-1 under certain conditions.

In this section, the synthesis and characterisation of the molecular sieves which were used for this work, has been described. A critical assessment of their sorption properties can now be made with a full understanding of their individual physical characteristics.

4.2 SORPTION OF PHENOLS FROM AQUEOUS SOLUTION BY MOLECULAR SIEVES

4.2.1 Introduction to Method

The sorption of a series of mono- and di-substituted phenols from aqueous solution by silicalite-1 was studied. The uptake of the sorbate was measured at constant temperature and at various equilibrium concentrations so that sorption isotherms could be constructed.

The extent of sorption i.e. the uptake of the sorbate, in a given experiment was taken to be equal to the change in the bulk concentration of the sorbate during equilibration. The initial concentration of the sorbate was known and the equilibrium concentration found by U.V. spectrophotometry. The U.V. absorption for each sorbate was determined as a function of concentration at the wavelength corresponding to its isobestic point. All measurements were therefore independent of pH. All uptakes, U, were calculated as grams of sorbate per 100 grams of anhydrous sorbent.

It was necessary to carry out preliminary investigations in order to establish the optimum experimental conditions. For example, the optimum ratio of aqueous solution to solid sorbent for each sorption experiment had to be

found. The nature of the equilibrium sorption experiment is such that the result is independent of the solution to sorbate ratio for any given equilibrium concentration. However, in terms of the accuracy of the results obtained, the liquid to solid ratio is of prime importance. Clearly, the greater the change in concentration of the sorbate from its initial to equilibrium value, the smaller the error incurred in the calculation of the uptake of sorbate. A small amount of aqueous solution and a relatively large amount of sorbent would therefore be favourable.

In order to assess all these factors, a computer model of the sorption experiment was set up. It was first necessary to carry out preliminary sorption experiments on all the chosen sorbates to establish the relative order of magnitude of uptake to be expected. For these experiments an arbitrary liquid to solid ratio of 500 was chosen, and approximate isotherms for each sorbate were obtained.

All the possible sources of error in the experiment were then incorporated into a simple computer program. These included; errors in the weight and composition of the sorbate (these were minimised by using silicalite which had been hydrated to a known degree (25°C., a_w = 0.753)); error in the initial volume and concentration of the sorbate and error in the equilibrium concentration of the sorbate. The computer program generated points on a particular isotherm, given the empirical coefficients of the curve. It then calculated, for different solid to liquid ratios, the expected size of the combined error in each point. For these calculations, it was assumed that the isotherm could be represented by the Langmuir Equation.

Figure 4.12 shows the possible spread of points which could be expected on a p-cresol isotherm for different liquid to solid ratios. These are illustrated

by *extreme isotherms* which represent error limits. As a general rule, as the liquid to solid ratio increases, the difference between the two extreme isotherms increases. The points near maximum uptake are more sensitive to experimental error than those on the steep part of the isotherm. Points obtained at relatively low concentrations will therefore be more reliable for use in the calculation of isotherm parameters.

Figure 4.13 shows extreme isotherms predicted for p-cresol at a liquid to solid ratio of 250 but with values of the weight of sorbate and volume of solution which differ from those used for Figure 4.12 (b). Comparison of these figures suggests that the relative amount of each component is more important than the absolute values.

Isotherms similar to those shown in Figure 4.12 were generated for each sorbate to be analysed. The same general pattern was found in each case, although the relative sensitivity of each sorbate isotherm to experimental error, varied according to the predicted shape of that isotherm. For example for 2,4-dimethylphenol, preliminary experiments gave a Langmuir isotherm characterised by a slow increase in uptake with concentration. The projected values of the extreme isotherms for this sorbate are shown in Figure 4.14. These show that the errors are predicted to be substantial even in the initial part of the isotherm.

After careful consideration of the above factors an optimum liquid to solid ratio of 100 was chosen for the sorption experiments. It was felt that a further reduction in the ratio was not justified in terms of increased accuracy when balanced against practical considerations. Separation difficulties emerge when dealing with small volumes of liquid and large quantities of solid. It was decided to use approximately 0.1 g of sorbent to 10 cm^3 of solution for each

Figure 4.12 Effect of Liquid to Solid Ratio on the Predicted Experimental Error in Model Isotherms for p-Cresol Sorption from Aqueous Solution by Silicalite-1.

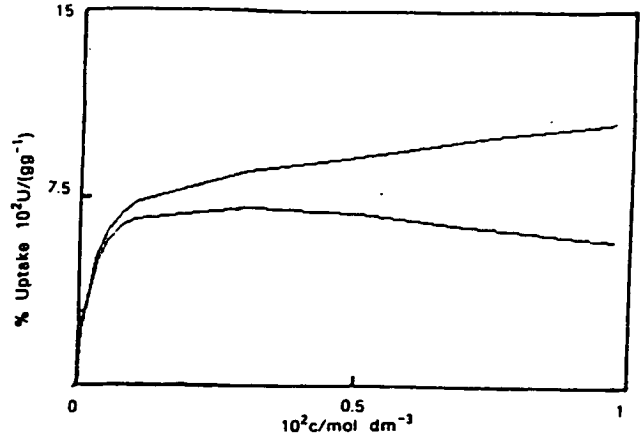

(a) weight of silicalite = 0.03 g
volume of solution = 25 cm^3
liquid/solid ratio = 833 cm^3g^{-1}

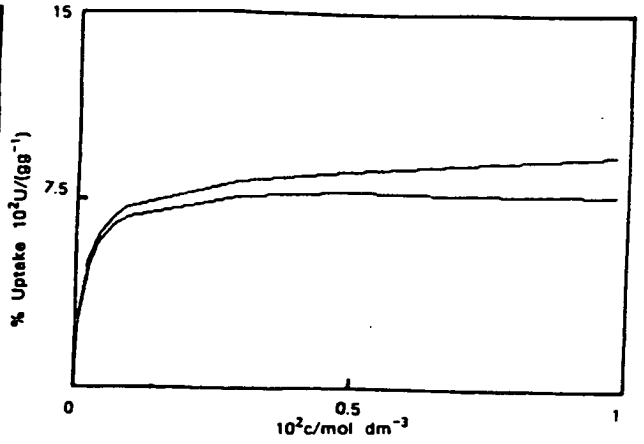

(b) weight of silicalite = 0.1 g
volume of solution = 25 cm^3
liquid/solid ratio = 250 cm^3g^{-1}

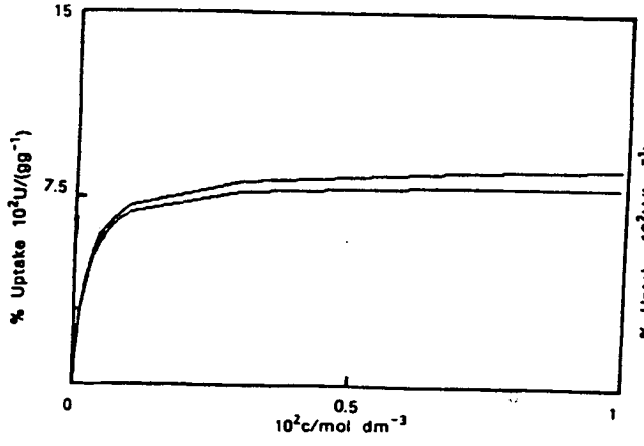

(c) weight of silicalite = 0.1 g
volume of solution = 10 cm^3
liquid/solid ratio = 100 cm^3g^{-1}

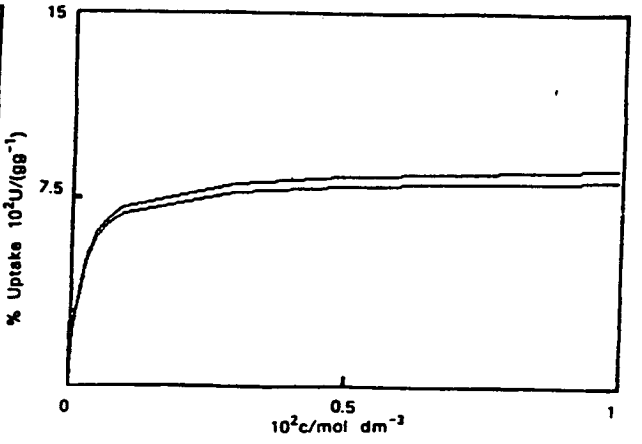

(d) weight of silicalite = 0.2 g
volume of solution = 10 cm^3
liquid/solid ratio = 50 cm^3g^{-1}

Notes:

1. Langmuir equation was used to produce model isotherms for all of the above. Parameters used were as folows;
   p_1 ($100U_{max}/(gg^{-1})$ = 8.4, p_2 ($K_L/dm^3\ mol^{-1}$) = 5100.

2. Sources of error other than those related to changes in the relative amounts of components used were constant for all of the above.

3. Extinction coefficient for sorbate at wavelength of analysis,
   ε = 1428 + 14 $dm^3mol^{-1}cm^{-1}$.

Figure 4.13 Predicted Experimental Error in Model Isotherms for p-Cresol Sorption from Aqueous Solution by Silicalite-1.

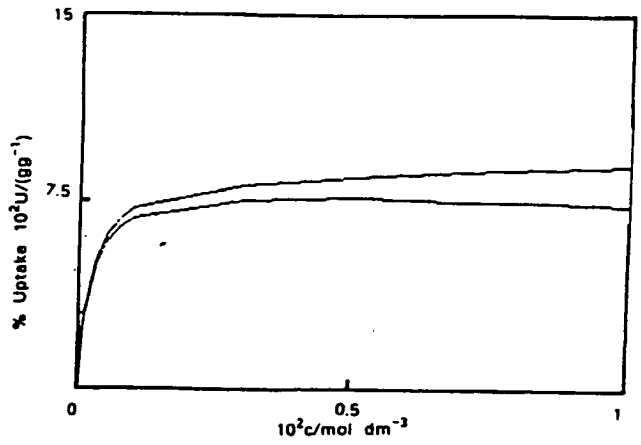

(a) weight of silicalite = 0.06 g
volume of solution = 15 cm^3
liquid/solid ratio = 250 cm^3g^{-1}

Notes:

1. Langmuir equation used to produce model isotherms had parameters; p_1 $(100U_{max}/(gg^{-1})$ = 8.4, p_2 (K_L/dm^3mol^{-1}) = 5100.

2. Extinction coefficient for sorbate at wavelength of analysis, ε = 1428 + 14 $dm^3mol^{-1}cm^{-1}$.

3. These isotherms were generated for identical conditions to those in Figure 4.12b but for a smaller amount of each component in the system.

Figure 4.14 Effect of Liquid to Solid Ratio on Model Isotherms for the Uptake of 2,4-Dimethylphenol from Aqueous Solution by Silicalite-1.

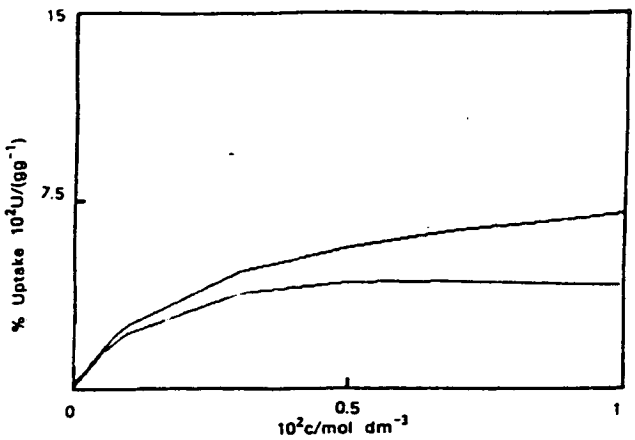

(a) weight of silicalite = 0.06 g
volume of solution = 25 cm^3
liquid/solid ratio = 417 cm^3g^{-1}

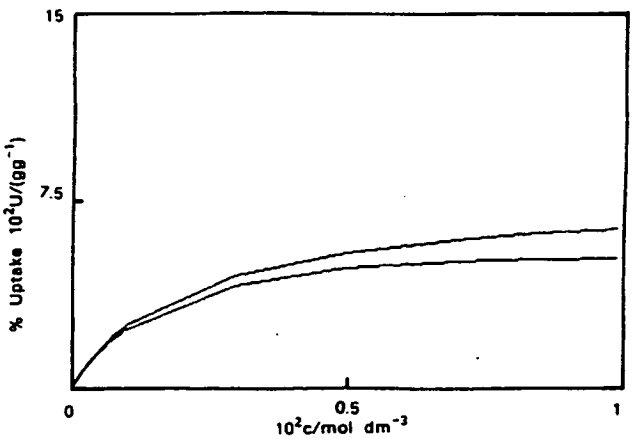

(b) weight of silicalite = 0.06 g
volume of solution = 10 cm^3
liquid/solid ratio = 167 cm^3g^{-1}

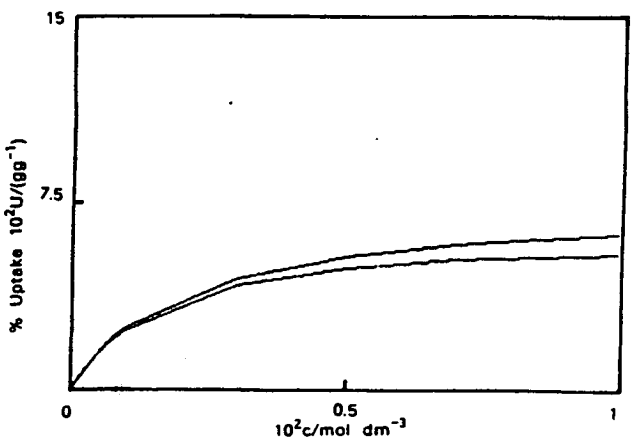

(c) weight of silicalite = 0.1 g
volume of solution = 10 cm^3
liquid/solid ratio = 100 cm^3g^{-1}

Notes:

1. Langmuir equation used to produce model isotherms had the following parameters; p_1 ($100U_{max}/gg^{-1}$) = 7.2, p_2 (K_L/dm^3mol^{-1}) = 517.
2. Sources of error other than those related to changes in the relative amounts of components used, were taken to be constant for all of the above.
3. Extinction coefficient for sorbate at the wavelength of analysis, ϵ = 948 + 9 $dm^3mol^{-1}cm^{-1}$.

equilibration.

The necessary equilibration time for each sorbate was established by identical simultaneous sorption experiments which were analysed after different lengths of time. Equilibration was taken to be complete when the same result was obtained for several consecutive analyses. The time taken for equilibration varied from 1 hour to 7 days depending on the size of the sorbate molecule.

The equilibration was assisted by continuous tumbling of the solid and liquid slurry. This prevented the formation of concentration gradients at the solid/solution interface. It is preferable to stirring as this can lead to particle splintering.

The largest source of error in this type of experiment is related to the accuracy with which the equilibrium concentration of the sorbate can be measured. Efficient separation of the aqueous solution from the solid sorbent is necessary. It is also important not to upset the equilibrium during the course of the separation. Various standardisation experiments were set up to test the reproducibility of results obtained using different separation techniques. "As synthesised" silicalite precursor, which contains tetrapropylammonium cations, and hence cannot take up sorbate, was used as an inert standard in these experiments.

After testing both filtration (0.2 μm) and centrifuge (3000 rpm) techniques, as well as a combination of the two, the most efficient and reproducible procedure was found to be one which involved repeated centrifuge. This is described in Chapter 3 (section 3.3.2.2).

The determination of the sorbate concentration by U.V. absorption is an important source of error in the final result. Figure 4.15 shows the effect that a

change in the uncertainty of the calibration curve for p-cresol would have on the final result. At constant liquid to solid ratio, the size of the possible spread of points is very sensitive to the error in this calibration. It appears that the uncertainty in the gradient of the best fit line (= extinction coefficient, ε) is especially important. This result underlines the fact that it is imperative in an experiment of this kind, to have an accurate calibration. The calibration curves obtained for each sorbate studied are given in Table 3.1.

This section has described how the optimum experimental conditions for the sorption systems to be studied were determined. For the majority of the experiments, this procedure was rigorously adhered to. Reasons for the few deviations mentioned in Chapter 3 (section 3.3) will be given in the course of the discussion.

4.2.2 Physical Properties of Phenols

In this section , some of the relevant physical properties of the mono- and di-substituted phenols which were used as sorbates will be described. The sorption results obtained will then be discussed in later sections in the light of these properties.

The size and shape of the sorbate molecules has an important effect on the extent to which they are sorbed. Figure 4.16 shows the smallest molecular diameter of each of the phenols studied. Each value was estimated by careful measurement from a scale model of the molecule concerned. 2,6-Dimethylphenol, 2,3-dimethylphenol and 3,5-dimethylphenol were totally excluded from the pores of silicalite as result of their size. However, it will be shown that size can have a profound effect on sorption without a total molecular sieving action.

The systems which were studied involved the sorption of an organic

Figure 4.15 Effect of Degree of Uncertainty in Extinction Coefficient of Sorbate on the Predicted Experimental Error in Model Isotherms.

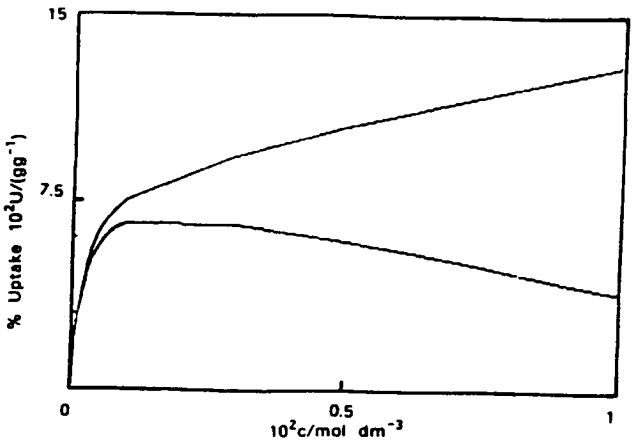

(a) weight of silicalite = 0.06 g
volume of solution = 25 cm^3
liquid/solid ratio = 417 cm^3g^{-1}
extinction coefficient, ε = 1428 + 2%

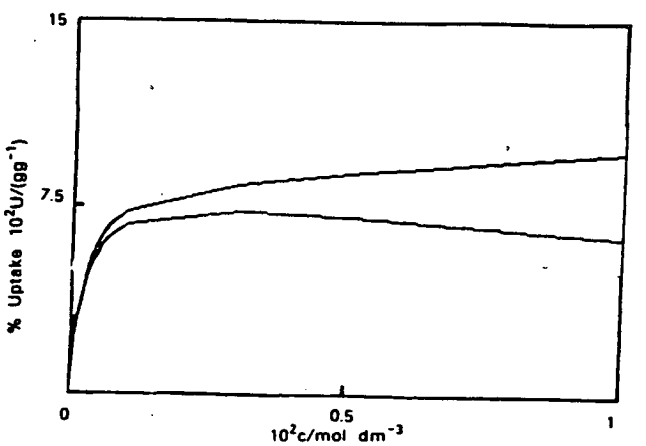

(b) weight of silicalite = 0.06 g
volume of solution = 25 cm^3
liquid/solid ratio = 417 cm^3g^{-1}
extinction coefficient, ε = 1428 + 1%

Notes:

1. Langmuir equation used to produce model isotherms had the following parameters; p_1 ($100U_{max}/(gg^{-1})$ = 8.4, p_2 (K_L/dm^3mol^{-1} = 5100.

2. Sources of error other than those related to the extinction coefficient of the sorbate, taken to be constant.

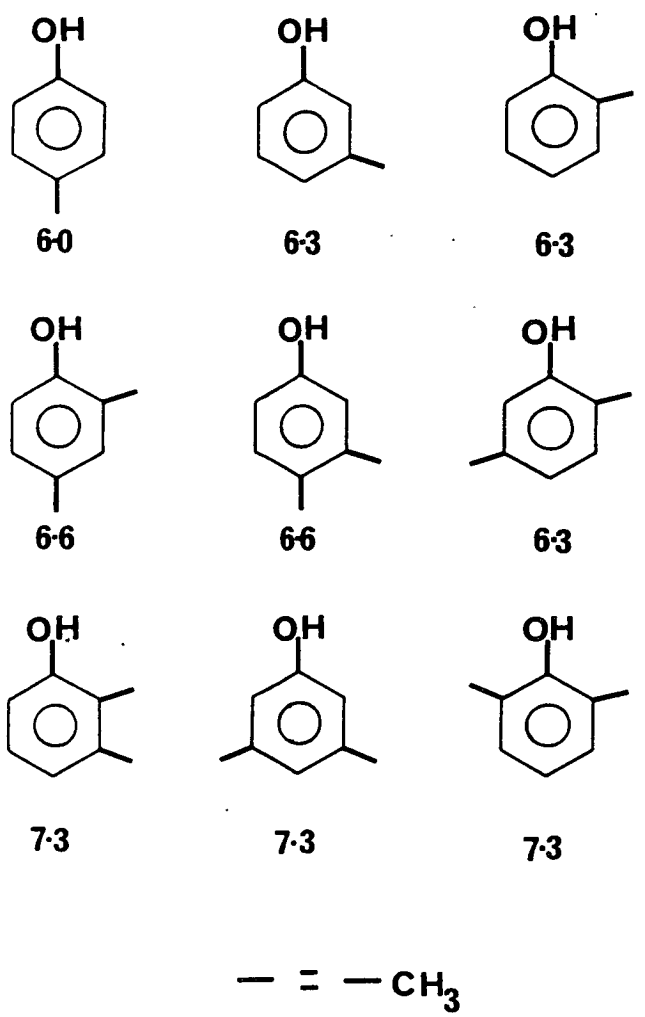

[a] Smallest molecular diameter/Å given below each structure.

Figure 4.16 Structures and Diameters of Phenols Studied [a].

molecule from aqueous solution by a hydrophobic, organophilic molecular sieve. The relative hydrophilicity of the organic molecule was therefore an important factor in determining the position of the sorption equilibrium. In order to assess the hydrophilicity of a material it is first necessary to find its solubility in water. These were determined for all the phenols concerned by the method given in Chapter 3 (section 3.3.4) and are given in Table 4.9. The literature values given below for o-cresol, m-cresol and p-cresol, agree closely with those obtained in this work.

	this work (g/100ml) 25°C	literature (155) (g/100ml) 25°C	20°C
o-cresol	2.8 ± 0.1	-	2.5
m-cresol	2.4 ± 0.1	2.3	2.2
p-cresol	2.2 ± 0.1	-	1.9

Solubility depends not only on hydrophilicity but also on the strength of the intermolecular bonds in the crystal lattice. The stronger these bonds, the lower the vapour pressure of the solid and the smaller its solubility. To find a true measure of the strength of solvation of each organic compound in water one must correct the solubility for the contribution from properties of the material in the solid phase.

The vapour pressure of each phenol was calculated from data given in reference (156). These were converted into a value for p/atm at 25°C by the method given in Appendix 1.

The equilibrium constant for the solvation reaction K_{solv} was obtained from $K_{solv} = s/p$. Values of K_{solv} for each phenol sorbed by silicalite are given in Table 4.9. It is possible to rationalise these values using the following set of rules:

Table 4.9

Properties of Sorbates Used

Sorbate	Molecular Diameter /nm	Solubility in Water /mol dm^{-3}	Vapour Pressure[a] 10^4p/atm	K_{solv}/ mol dm^{-3} atm^{-1}	pKa[b]
o-cresol	0.63	0.262	5.21	503	10.20
m-cresol	0.62	0.218	1.61	1354	10.01
p-cresol	0.60	0.204	1.46	1397	10.17
2,4-dimethylphenol	0.65	0.0638	1.94	383	10.45
2,5-dimethylphenol	0.63	0.0286	1.93	148	10.22
3,4-dimethylphenol	0.66	0.0380	0.71	535	10.32

[a]Measured at 25°C (156).
[b]Measured at 25°C (157)

1. Solvation is strongest when the hydroxyl group is exposed.
2. Solvation is weakest when there is a methyl group ortho to the hydroxyl group due to the steric hindrance of solvation.
3. Extra methyl groups reduce the strength of solvation.

Figure 4.17 shows the phenols in decreasing order in terms of degree of solvation.

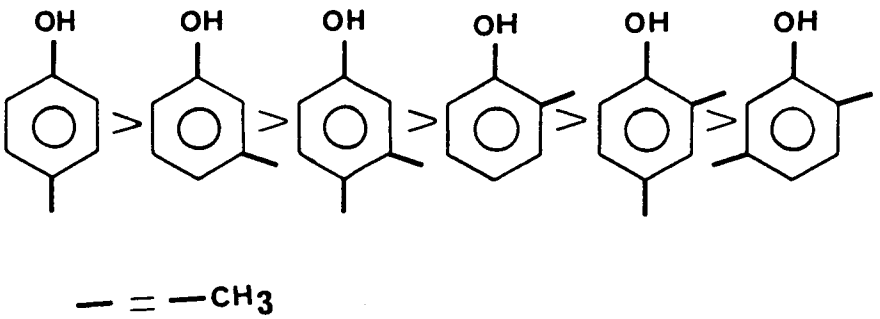

Figure 4.17 Phenols Studied in Decreasing Order of Degree of Solvation.

The relative values of K_{solv} will be of central importance in the explanation of the sorption results obtained.

The vapour pressure of the solid will of course also be important since there may be a direct relationship between the strength of intermolecular binding in a crystal lattice and the strength of binding inside the sieve.

The pKa values (157) of the phenols studied are given in Table 4.9. The monosubstituted phenols are more acidic than the disubstituted phenols but the differences between the individual values are not great. Since in the sorption experiments, the pH of the sorbate solution was normally between 5

and 6, it appears that ionisation of the phenols was negligibly small. Furthermore, it is unlikely that silicalite, which is a non polar sieve, will selectively sorb the ionised form of the phenol. It is therefore assumed, for the subsequent discussion on sorption, that it is the unionised form of the phenol which is taken up.

4.2.3 Sorption of Phenols from Aqueous Solution by Silicalite-1 (GS18) at 25°C

The sorption of 2-methylphenol (o-cresol), 3-methylphenol (m-cresol), 4-methylphenol (p-cresol), 3,4-dimethylphenol (3,4-dmp), 2,5-dmp, 2,4-dmp, 2,6-dmp, 2,3-dmp and 3,5-dmp from aqueous solution by silicalite-1 (GS18) was carried out. The results obtained for the % uptake $10^2U/(gg^{-1})$ of each sorbate relative to dry weight of silicalite-1 (GS18) over the given range of equilibrium concentrations are shown in Appendix 2, Tables (i)-(vi). The method used for these experiments is given in Chapter 3 (section 3.3.2 and 3.3.3(1)).

It was found that 2,6-dmp, 2,3-dmp and 3,5-dmp with molecular diameters of 0.73 nm were excluded from the pores of silicalite-1. This is not a surprising result since the limiting pore size of silicalite-1 is reported to be *ca* 0.6 nm (33). However 3,4-dimethylphenol with a molecular diameter of 0.66 nm was "elastic" enough to be successfully sorbed.

4.2.3.1 Mono-Substituted Phenols

The sorption isotherms obtained for the three isomers o-cresol, m-cresol and p-cresol are shown in Figure 4.18. Each isotherm has a steep initial slope and reaches a plateau at high sorbate concentrations. This shape is indicative of Langmuir behaviour and indeed the lines drawn through the experimental points are best fit lines to the Langmuir equation. In Chapter 2, the theoretical basis for the application of the Langmuir equation to sorption by molecular

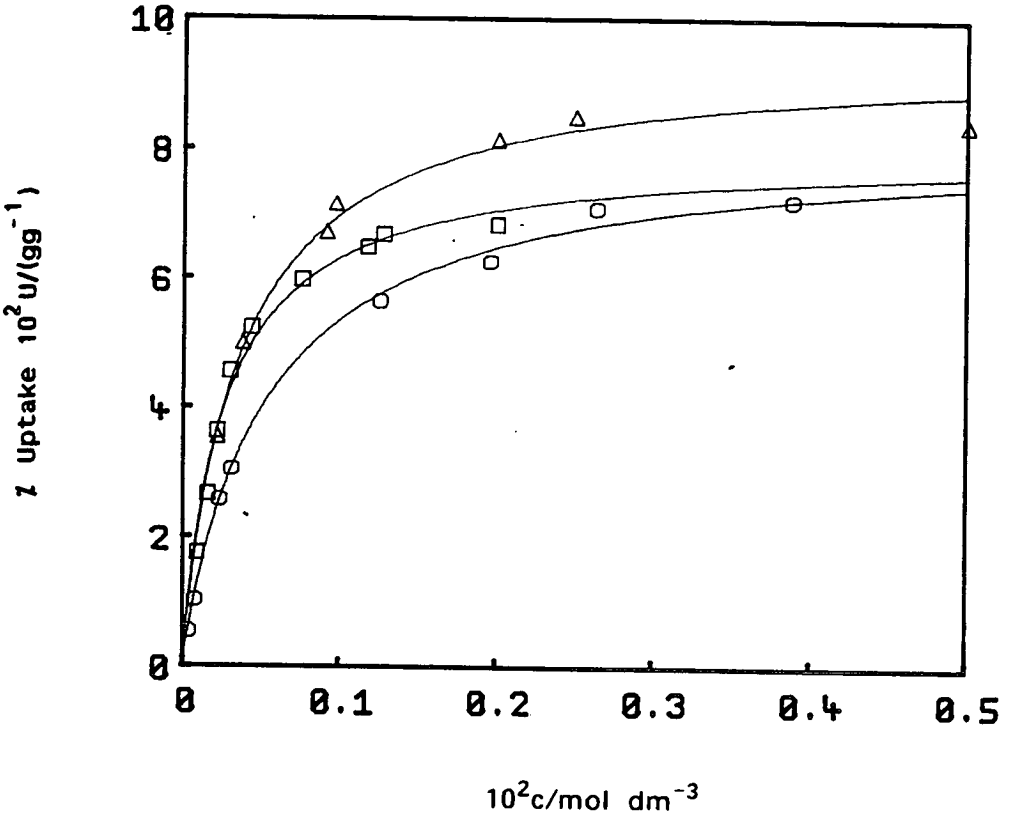

Figure 4.18 Sorption of Cresols From Aqueous Solution by Silicalite-1 (GS18) at 25°C.
O,o-Cresol; △, m-cresol; □, p-cresol.

sieves was discussed.

The parameters found from a general least squares fit of each set of experimental points to the Langmuir equation are shown in Table 4.10. Both o-cresol and p-cresol have maximum uptakes of *ca* 4 molecules per unit cell. There are four channel intersections per unit cell of silicalite as shown in Figure 4.4 (b). It therefore appears for both o-cresol and p-cresol, that at maximum uptake, one molecule at each channel intersection in the lattice is a favourable arrangement. This behaviour can be explained by the fact that channel intersections afford more space than the channels themselves. Any faults in the lattice such as broken siloxane bonds, which may provide specific binding sites for the sorbed species, are also likely to be found at channel intersections, and could perhaps account for the observed effect. A substantially larger maximum uptake was obtained for m-cresol. It is conceivable that this is due to the position of the methyl group on the ring. The geometry of the channel intersection is such that a molecule of m-cresol could sit with one substituent pointing up into a straight channel and the other into a sinusoidal channel. It would then take up less space than a corresponding molecule of o-cresol or p-cresol. This arrangement could allow more than one molecule of m-cresol to sit at certain intersections.

Electronic effects may also be responsible for the preferential packing of m-cresol. Electron donation by a lone pair of the phenolic oxygen onto the ring would lead to electron rich ortho and para positions relative to the meta position (Figure 4.19). This would reduce the electron donation by the methyl substituent in o-cresol and p-cresol and lengthen the $C-CH_3$ bond relative to that in m-cresol.

The Langmuir coefficients K_L for the three cresols are also shown in Table

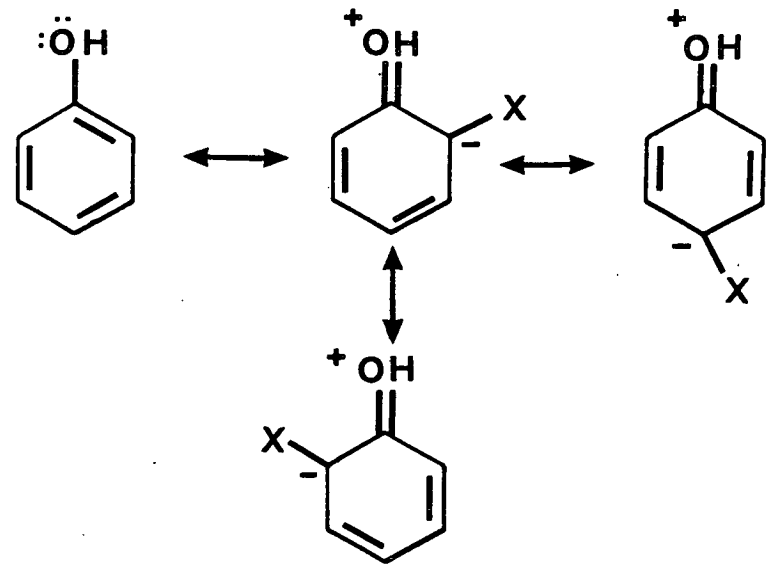

X = H for phenol

Figure 4.19 Electronic Effects in Phenol

4.10. The size of these values which are an approximation to equilibrium constants for sorption, suggest a strong driving force towards sorption. This is as expected for the sorption of relatively hydrophobic organic molecules by an organophilic, hydrophobic molecular sieve.

The Langmuir coefficients K_L for the three cresols decrease in the order p-cresol > m-cresol > o-cresol. The magnitude of the coefficient depends both on the strength of interaction between the sorbate and the sieve and the interaction of the sorbate with the solution phase. In this instance, the degree of sorbate - solution phase interaction corresponds to the hydrophilicity of the sorbate. The factors which contribute to K_L were discussed in Chapter 2 (section 2.3.3). It was shown that the relative size of these separate contributions could be determined by considering the sorption of the organic sorbate from the gas phase. The relevant equilibria were shown in Figure 2.1. It is therefore possible to correct the Langmuir constant (K_L) for the contribution from the hydrophilicity of the sorbate. This is achieved by multiplying K_L by K_{solv} (equations 2.22 - 2.24). Values of K_{solv} for the cresols studied are given in Table 4.9.

The values of K_{zeo} (= K_L x K_{solv}) thus obtained, correspond to Langmuir constants for the sorption of each sorbate from the gas phase. The values for the three cresols are given in Table 4.10. The degree of binding to silicalite therefore decreases in the order p-cresol > m-cresol > o-cresol. This pattern can be explained by the shape of the three isomers. p-Cresol is the most symmetrical of the three and the linear nature of the molecule should mean that dispersive interactions inside the sieve are optimised. The strength of binding of m-cresol is diminished presumably due to the loss of symmetry. o-Cresol shows a substantial decrease in binding strength over the other two. This is probably a result of two factors. The increased molecular size of

Table 4.10

Sorption Parameters for the Uptake of Cresols

from Aqueous Solution by Silicalite-1 (GS18) at 25°C

	o-cresol	m-cresol	p-cresol
$100U_{max}$/ gg^{-1}	8.2 ± 0.4	9.2 ± 0.5	8.0 ± 0.7
U_{max}/ mol/unit cell	4.3 ± 0.2	4.8 ± 0.3	4.2 ± 0.4
$10^{-3}K_L$/ dm^3mol^{-1}	1.9 ± 0.4	3.2 ± 0.8	3.8 ± 1.0
$10^{-5}K_{zeo}$/ atm^{-1}	10 ± 2.0	43 ± 11	53 ± 14
$10^{-2}K_s$/ $dm^6\ mol^{-2}$	5.0 ± 2.0	7.0 ± 1.8	7.8 ± 2.1

o-cresol suggests that there may be some repulsive interaction with the channel walls. In addition, the capacity of the hydroxyl group to take part in hydrogen bonding is severely diminished by the proximity of the adjacent methyl group. Hydrogen bonding could enhance sorption through interaction with polar sites which occur as faults within the lattice or through intermolecular hydrogen bonding of sorbed species.

If the strength of binding of these molecules is directly related to the strength of their intermolecular bonds in the crystalline or liquid phase, the values of K_{zeo} divided by vapour pressure (p/atm) should be constant. The values thus obtained, denoted K_s /dm^{-6} mol^{-2}, are included in Table 4.10. The values of K_s do indeed agree within experimental error, although the underlying trend suggests that the factors which affect binding to silicalite are somewhat different to those which affect intermolecular binding.

Cresol sorption by silicalite-1 has also been studied by Narita and co-workers (145). However, they attempted to fit their data to the Freundlich equation and obtained a less satisfactory agreement than was observed for the Langmuir equation in this work. It is difficult to make a direct comparison between the results in the publication by Narita and those of this work since they did not tabulate their data. However, values of maximum uptake were reported, which are given below,

	maximum uptake/ (molecules/unit cell)	
	Narita (145)	this work
o-cresol	3.47	4.3 $\pm$ 0.2
m-cresol	4.10	4.8 $\pm$ 0.3
p-cresol	3.65	4.2 $\pm$ 0.4

Therefore the trend observed by Narita and co-workers is the same as that observed in this work but the capacity for each sorbate is reduced. This

reduction in capacity could be due to the quality of their silicalite. The x-ray powder pattern of their material implies from the broad peaks, and uneven baseline, that the material was not completely crystalline.

Narita and co-workers collected less data for each isotherm than in this work and as stated above, used a less appropriate model for the subsequent analysis. The results also suggest that their molecular sieve was of low crystallinity.

4.2.3.2 Di-Substituted Phenols

The isotherms obtained for the sorption of 2,4-dimethylphenol, 2,5-dimethylphenol and 3,4-dimethylphenol by silicalite-1 (GS18) are shown on Figure 4.20. The shapes of the isotherms are more diverse than those obtained for the three cresol isomers. 2,5-Dimethylphenol exhibits an extremely steep isotherm and the maximum capacity is not obvious from the graph. 3,4-Dimethylphenol produced an intermediate type isotherm, not unsimilar to those obtained for the cresols. 2,4-Dimethylphenol on the other hand gave a flat isotherm, where uptake by the sieve increased only very slowly with concentration. At an equilibrium concentration of 5×10^{-3}M, the amount of sorption had not yet reached a maximum value.

As for the cresols previously described, the lines drawn through the data points are best fit lines to the Langmuir equation. The parameters for these curves are given in Table 4.11. The errors shown, which are evaluated by a general least squares curve fitting program, are substantially greater than those found for the cresol systems. This is thought to be due to the difficulty involved in obtaining accurate results for these materials which are only slightly soluble in water. Standard solutions which are near saturation concentration have to be used. The problem is especially acute for

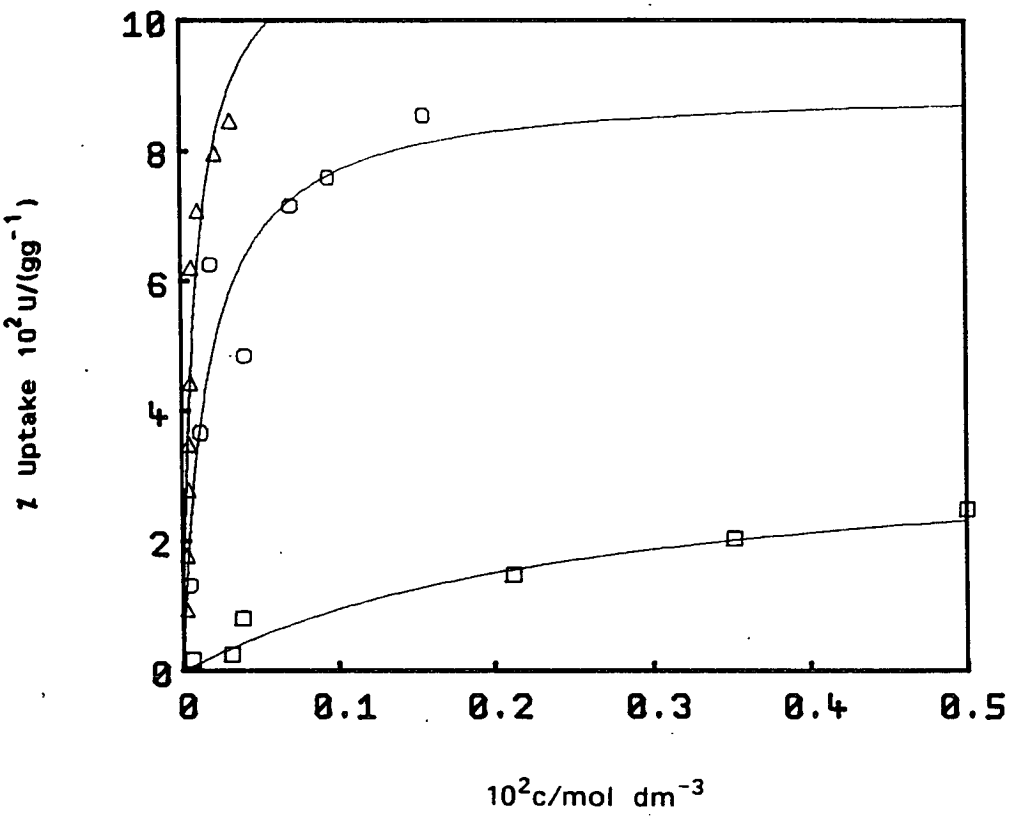

Figure 4.20 Sorption of Dimethylphenols from Aqueous Solution by Silicalite-1 (GS18) at 25°C;
□, 2,4-dimethylphenol; △, 2,5-dimethylphenol; ○, 3,4-dimethylphenol.

Table 4.11

Sorption Parameters for the Uptake of Dimethylphenols

from Aqueous Solution by Silicalite-1 (GS18) at 25°C

	2,4-dmp	2,5-dmp	3,4-dmp
$10^2 U_{max}$/ gg^{-1}	3.6 ± 1.5	12 ± 4	9.0 ± 2.0
U_{max}/ mol/unit cell	1.7 ± 0.6	5.5 ± 1.8	4.1 ± 0.9
$10^{-3} K_L$/ $dm^3 mol^{-1}$	0.4 ± 0.4	11 ± 9	6.0 ± 5.5
$10^{-5} K_{zeo}$/ atm^{-1}	1.4 ±1.4	16 ± 13	32 ± 29

2,4-dimethylphenol where relatively high equilibrium concentrations lead to only small values of uptake.

Although the error in K_L is almost 100% for each dimethylphenol, the values obtained were reproducible to within 5%. This suggests that the size of the uncertainty in K_L is very sensitive to small deviations from the best fit curve. Therefore although the errors quoted are large, it is justifiable to discuss the relative size of the values obtained.

The values of K_L and U_{max} found for these three isomers are more widely spread than those of the cresols. Their solubilities in water, vapour pressures and calculated values of K_{solv} were given in Table 4.9. They are substantially less soluble in water than the cresols by virtue of their extra methyl substituent. The values of K_{solv} decrease in the order 3,4-dmp > 2,4-dmp > 2,5-dmp. 2,4-Dimethylphenol and 2,5-dimethylphenol have smaller values of K_{solv}, and are therefore less hydrophilic than any of the cresols. 3,4-Dimethylphenol on the other hand, with an unhindered hydroxyl group to counter balance the effect of the extra methyl substituent, has a slightly higher values of K_{solv} than o-cresol.

The values of K_L obtained depend on both the degree of solvation and the relative size and shape of the molecule. 2,5-Dimethylphenol is substantially more hydrophobic, but of similar size than o-cresol. The symmetrical positioning of its second methyl group renders it a relatively small, but highly hydrophobic molecule. The effect of this on sorption is illustrated by the Langmuir coefficient K_L obtained, which is greater than for the other sorbates studied. The value of K_{zeo} for this molecule is reduced relative to the other phenols. This reinforces the observation made earlier for o-cresol, that an unhindered hydroxyl group on the sorbate molecule is important in terms of

strength of binding to the sieve. 2,5-Dimethylphenol shows the highest maximum uptake, therefore the size of the molecule and its relatively high hydrophobicity are obviously dominant factors in maximising packing efficiency.

3,4-Dimethylphenol has a similar K_{solv} to o-cresol, but has a Langmuir coefficient for sorption which is greater by a factor of three. This is due to the contribution to K_L made by the strength of binding to the sieve. The ratio of their K_{zeo} values is about 3. This can be attributed both to the free and therefore interactive hydroxyl group in the dimethylphenol and to the extra methyl substituent which can interact with the non-polar channels. Although 3,4-dimethylphenol has a molecular diameter (0.66 nm) which is substantially larger than the limiting pore size of silicalite, it is clearly flexible enough to move through the channels. A predicted maximum uptake of 4.1 molecules per unit cell suggests that at maximum capacity one molecule sits at each intersection.

2,4-Dimethylphenol was the least successful sorbate of this series in terms of degree of uptake by silicalite. The reason for this result is linked to the fact that 2,4-dimethylphenol has the disadvantages of both a large molecular diameter and a sterically hindered hydroxyl group, without the advantage of exceptionally high hydrophobicity. It is a good deal larger and more hydrophilic than its 2,5-dimethylphenol counterpart. Both its methyl substituents are situated at electron rich positions on the ring. As described in the previous section, this is caused by electron donation onto the ring from the phenolic oxygen and could be disadvantageous. The low value of K_L found for this system is coupled with a low value of maximum uptake. With a maximum uptake of less than two molecules per unit cell, the sorption of 2,4-dimethylphenol by silicalite-1 is clearly not energetically favourable.

Figure 4.21 shows the general trends observed in the sorption results found for the substituted phenols studied. One can see that the two separate contributions to K_L have a different degree of influence on the final value. The magnitude of the binding contribution K_{zeo} determines the order of the resulting K_L values with the exception of 2,5- and 3,4-dimethylphenol. They are both relatively hydrophobic molecules and the favourable contribution made to K_L through the poor sorbate - solvent interaction is enough to give these molecules the two largest K_L values.

It is clear from the results presented so far that the value of the Langmuir coefficient for sorption for a particular sorbate would be difficult to predict. It depends on at least two factors, whose relative contributions would be difficult to quantify, without a large amount of data on an extensive range of sorbates.

The specific nature of the sieve is an important variable which would also have to be considered. The next section deals with the variation in K_L values obtained using identical systems to those described above but with slight modifications in the nature of the sieve.

4.3 EFFECT OF MOLECULAR SIEVE PROPERTIES ON SORPTION

4.3.1 Effect of External Surface Area on Sorption

In section 4.1.1, the physical properties of silicalite-1 (GS11) synthesised at 95°C using sodium hydroxide as a mineraliser were discussed. Properties such as morphology (Figure 4.1), crystallinity (Table 4.1) and water sorption (Table 4.2 and 4.3) were dealt with. The material was compared with two samples of silicalite-1 prepared with piperazine as a mineraliser at 95°C (GS12-GS14) and at 150°C (GS15-20).

Figure 4.21

(a)Relative hydrophilicity of phenols[a].

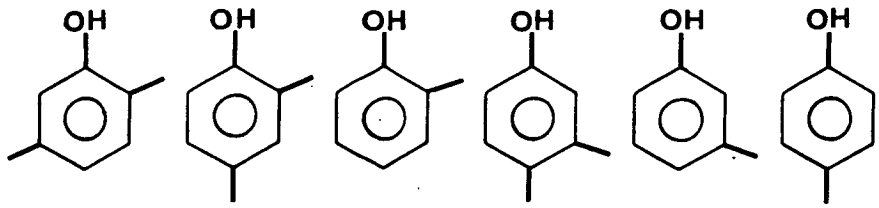

increasing hydrophilicity (K_{solv})

(leads to a decrease in K_L)

(b) Relative binding strength to sieve of phenols.

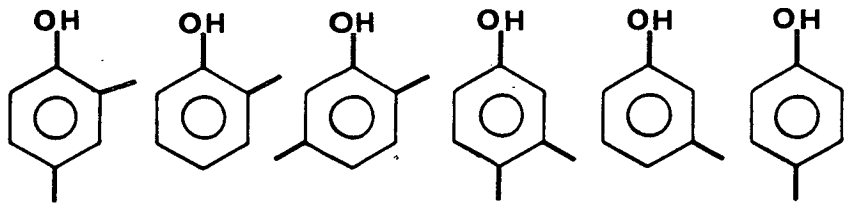

increasing K_{zeo}

(leads to an increase in K_L)

(c) Relative Values of Langmuir Sorption Coefficient (K_L) for Phenols.

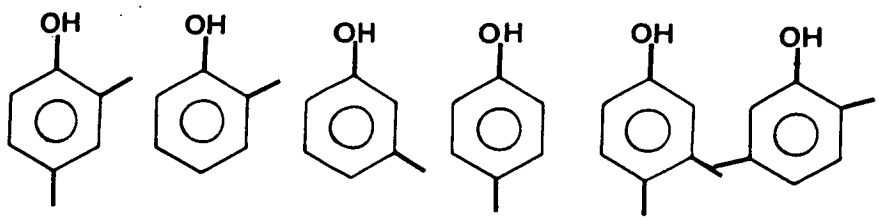

increasing K_L

[a] - = $-CH_3$

This section describes the difference in sorption behaviour of two batches of silicalite-1 prepared at 95°C but in the presence of sodium hydroxide (GS11) and in a cation free system (GS12). The sorbate used in these experiments was p-nitrophenol and they were carried out in a similar manner to those described in section 4.2.2. For experimental details see Chapter 3 (section 3.3.2 and 3.3.3(4)).

The isotherms obtained for the sorption of p-nitrophenol by silicalite-1 samples GS11 and GS12, are given in Figures 4.22 and 4.23 respectively. (For experimental results see Appendix 3). Both curves represent the best fit of the data to the Langmuir equation. It is clear from Figure 4.22 that the uptake of p-nitrophenol by sample GS11 does not follow typical Langmuir behaviour. The degree of uptake rises very steeply with concentration in the early part of the isotherm as one would expect but no maximum capacity is reached at higher concentrations. For a sieve of this nature where there is a limited pore volume, a maximum sorption capacity is expected and is normally observed.

The isotherm obtained for the uptake of p-nitrophenol by GS12 is shown in Figure 4.23. This isotherm approximates much more closely to Langmuir behaviour. It is rectilinear with an extremely steep initial slope and a flat plateau. The Langmuir constants obtained from this curve are given in Table 4.12. The value for K_L is substantially greater than any obtained for the methyl substituted phenols discussed in the previous section. p-Nitrophenol has a molecular diameter of 0.6 nm and a water solubility of 0.12 mol dm^{-3} (155). Unfortunately, due to lack of vapour pressure data, values for K_{solv} and K_{zeo} could not be evaluated. However, there is clearly a strong binding interaction between this molecule and the molecular sieve. The fact that it is taken up more readily than the analogous p-cresol, suggests that there is a favourable interaction between the NO_2 substituent and the internal surface of the sieve.

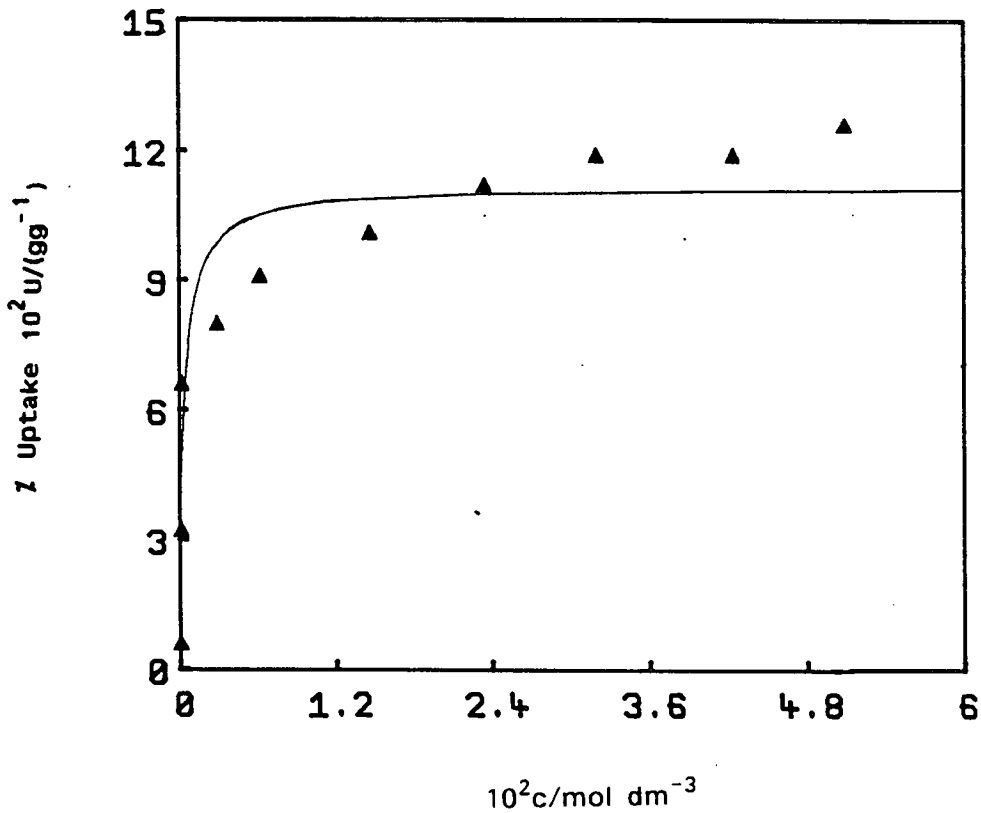

Figure 4.22 Sorption of p-Nitrophenol from Aqueous Solution by Silicalite-1 (GS11) at 25°C. Curve given by Langmuir Equation with 10^2U_{max} = 11 + 2 / (g/g^{-1}) and $10^{-4}K_L$ = 2.4 + 2.9 / dm^3 mol^{-1}.

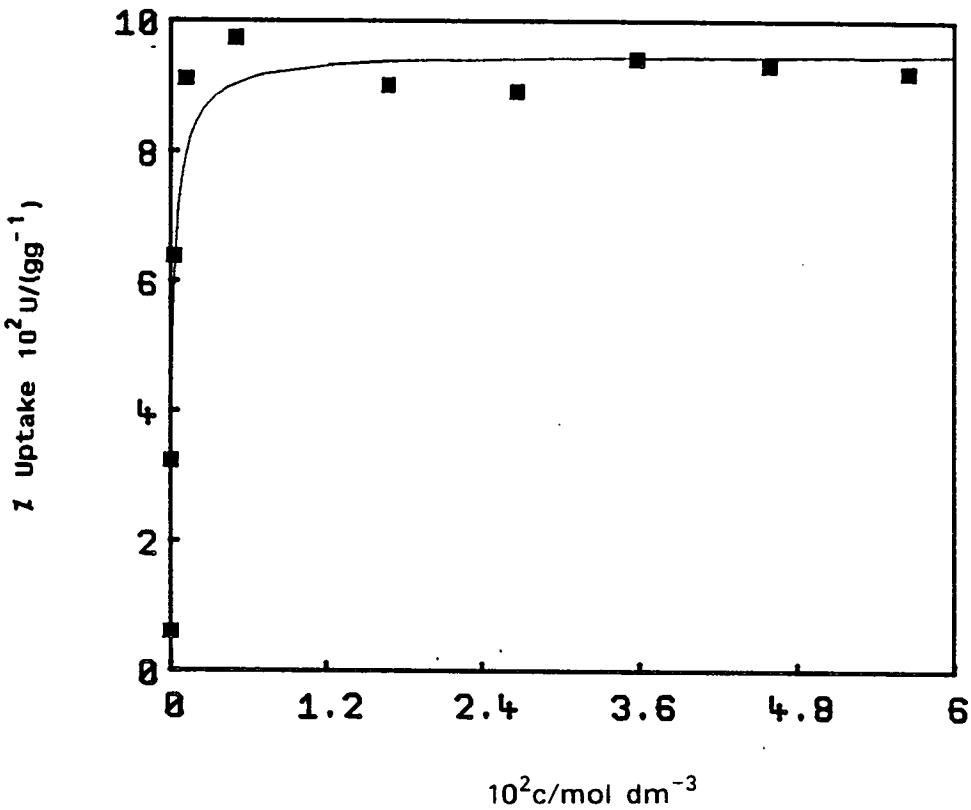

Figure 4.23 Sorption of p-Nitrophenol from Aqueous Solution by Silicalite-1 (GS12) at 25°C.

Table 4.12

Sorption Parameters for the Uptake of p-Nitrophenol

from Aqueous Solution by Silicalite-1 (GS11 & GS12) at 25°C

	GS12	$GS11_{corr}$
$10^2 U_{max}$/ gg^{-1}	9.5 ± 1.2	7.9 ± 1.3
U_{max}/ mol/unit cell	4.2 ± 0.5	3.5 ± 0.5
$10^{-4} K_L$/ $dm^3 mol^{-1}$	3.6 ± 3.4	3.6 ± 4.1

In order to explain the differences in behaviour between GS11 and GS12, it is necessary to compare their physical properties. The electron micrographs of the two samples (Figure 4.1) reveal obvious differences. Sample GS11 is made up of small highly twinned crystals with a pitted surface which are almost spherical in shape. Sample GS12, by comparison, is characterised by much larger, lozenge shaped crystals with a smooth surface. Therefore the difference in morphology may explain the unusual behaviour of GS11.

The degree of external surface sorption in these materials can be measured using "as synthesised" precursors. The pores of the as synthesised materials are filled with tetrapropylammonium cations and as such are devoid of any internal surface sorption capacity.

Sorption experiments with p-nitrophenol were carried out on GS11 as synthesised (as) and GS12(as) in an analogous manner to those on the calcined materials. The results obtained are given in Appendix 3 (tables iii and iv). GS12 showed negligible sorption, outside experimental error, over the whole concentration range, whereas GS11(as) showed substantial sorption. The isotherm obtained is shown in Figure 4.24 together with the isotherm obtained for GS11 (calcined), which we now know is a composite isotherm of both internal and external surface sorption.

It is likely that it was the contribution from external surface sorption which caused the deviation of the GS11 isotherm from Langmuir behaviour. Multi-layer sorption of p-nitrophenol on the external surface of the crystal would lead to the observed absence of a maximum sorption capacity.

It is possible from the results obtained for GS11(as) to correct the original isotherm of the calcined material for the contribution from external surface sorption. Subtraction of GS11(as) from GS11 gives GS11(corr). The resultant

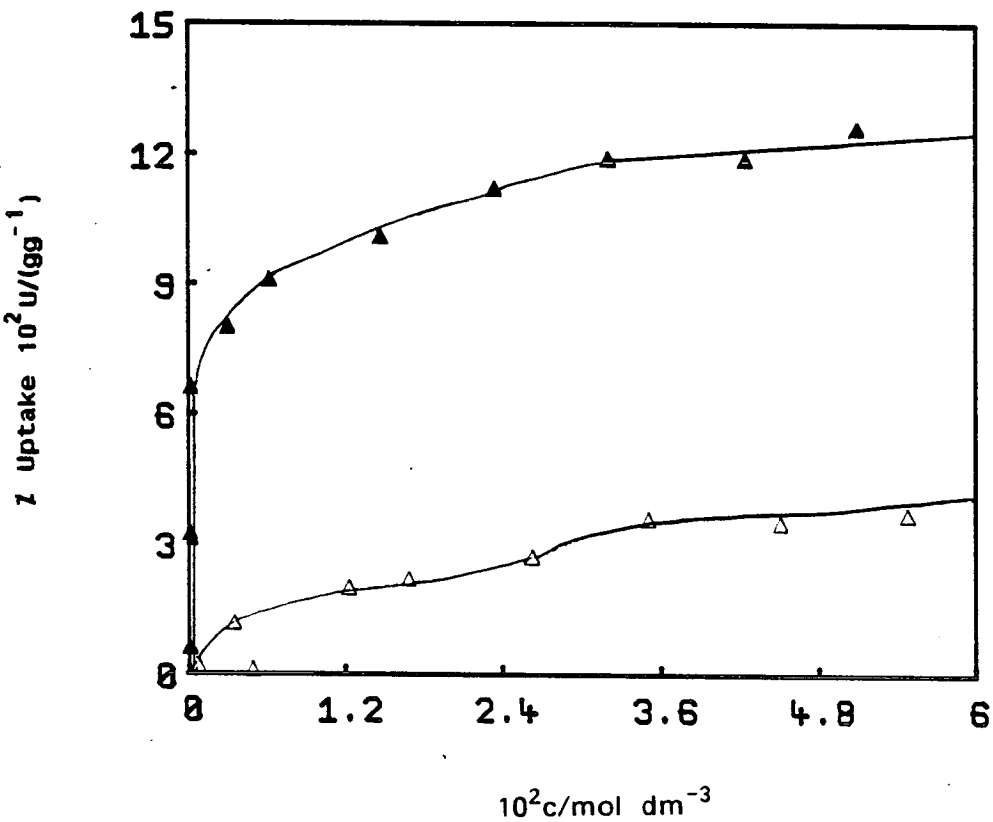

Figure 4.24 Sorption of p-Nitrophenol from Aqueous Solution by Silicalite-1 at 25°C;
△, GS11(as); △, GS11.

isotherm is shown in Figure 4.25 together with the original isotherm obtained for GS12 for comparison. The isotherm of GS11(corr) now reaches a steady plateau which would be expected for such a system. The Langmuir coefficients of this curve are given in Table 4.12.

The values of K_L for the two isotherms are identical. This result implies that although the external morphology of the sieves is very different, the nature of the internal surface of each material is similar. Water sorption results for the two calcined materials are given in Table 4.3. They reveal that there is a substantial difference between the degree of hydrophilicity of the two samples The portion of water sorption which can be attributed to external surface sorption can be found by looking at water uptake by the as synthesised materials (Table 4.2). Any weight loss below 250°C on thermal analysis of the water vapour equilibrated as synthesised samples is due the desorption of water from the external surface. Above that temperature tetrapropylammonium is burnt out of the pores. Table 4.2 shows that, as expected, GS11(as) shows a much higher contribution from external water than GS12(as). The value of water sorption by the calcined materials can therefore be corrected for this. Such a correction reveals that under the same conditions (25°C, a_w=0.753), the two samples sorb a similar amount of water onto their internal surface. It is therefore not surprising that they gave the same sorption coefficients for the internal surface sorption of p-nitrophenol.

The internal sorption capacity of the two sieves for p-nitrophenol (Table 4.12) are identical to within experimental error and average slightly less than four molecules per unit cell (3.9 $\pm$ 0.5).

These results show that it is necessary to use molecular sieves which have a negligible external surface area in order to obtain well defined sorption

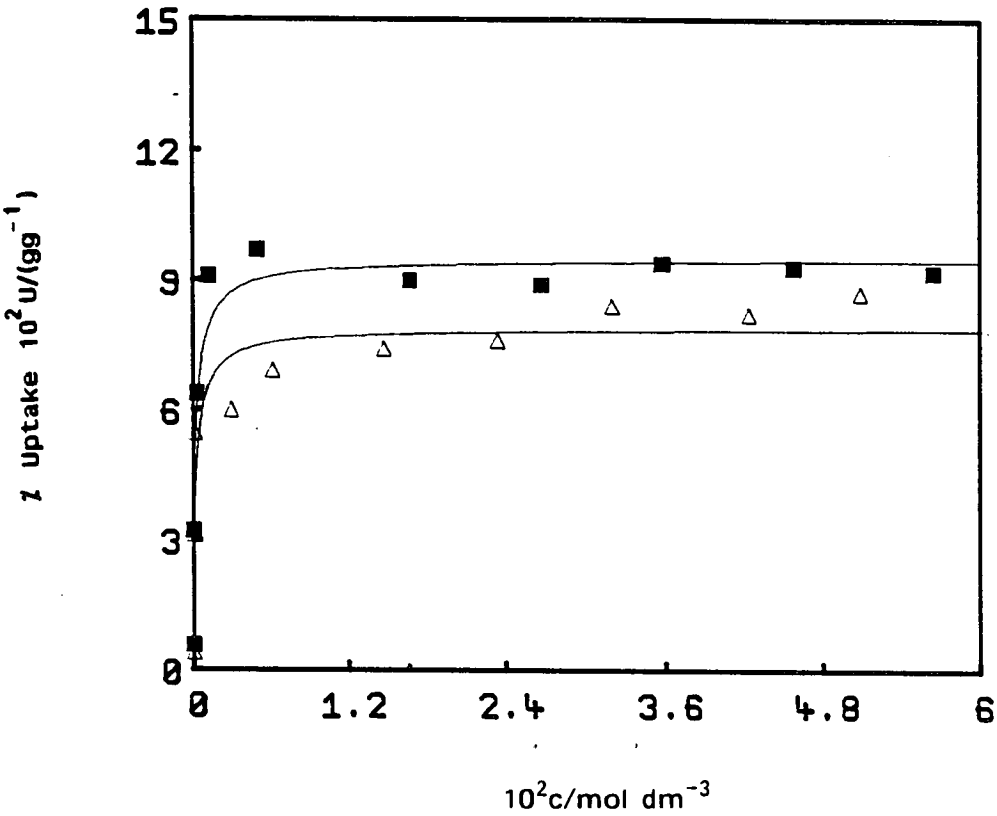

Figure 4.25 Sorption of p-Nitrophenol from Aqueous Solution by Silicalite-1 at 25°C;
□, GS12; △, GS11(corr).

isotherms which exhibit Langmuir behaviour. Crystals with a smooth external surface and with a typical size of 10 µm x 8 µm x 4 µm were found to be satisfactory in this respect. The batch of silicalite-1 made in the presence of sodium cations which consisted of 2 µm crystals with a pitted surface were unsuitable. Undesirable external surface sorption made direct analysis of the results impossible.

4.3.2 Effect of Hydrophilicity on Sorption

The sorption of various substituted methyl phenols from aqueous solution by silicalite-1 sample GS18 was discussed in section 4.2. The synthesis of GS18 was carried out at 150°C under autogenous pressure with piperazine as a mineraliser. Silicalite-1 sample GS14 was prepared at 95°C using the same reaction mixture.

The physical properties of these two samples of silicalite-1 were compared in section 4.1.1 (see Tables 4.1-4.4 and Figures 4.1-4.4). In terms of degree of crystallinity, SiO_2/Al_2O_3 ratio, and degree of purity, the two samples are essentially identical. Differences are found in their morphology and degree of hydrophilicity. From the results discussed in the previous section, it can be assumed that GS14 and GS18 are both outside the size range where external surface effects would be observed. Other than relative external surface areas, general morphology would not be expected to have an effect on equilibrium sorption properties. Differences found in the sorption properties can therefore be linked directly to the differences in the hydrophilicity of the two samples.

Sorption isotherms were obtained for the sample GS14 using the same sorbates as for GS18 and under identical experimental conditions (see Chapter 3 section 3.3.2 and 3.3.3 (parts 2 and 3)) For experimental results see Appendix

The isotherms obtained for o-cresol, m-cresol and p-cresol are shown in Figure 4.26. These isotherms follow the same general pattern as those obtained for GS18 (Figure 4.17). However, a closer comparison of the two groups of isotherms reveals a consistent difference. Figures 4.27-4.29 respectively, give a direct comparison of the sorption of o-cresol, m-cresol and p-cresol by GS14 and GS18. In each case, GS14 produces an isotherm with a steeper initial slope and a diminished maximum sorption capacity, relative to that of GS18.

Table 4.13 shows the Langmuir parameters K_L and U_{max} obtained for the GS14 isotherms. The values given can be compared directly with those in Table 4.10 which apply to the GS18 isotherms. The Langmuir parameters confirm the qualitative observations made above.

The sorbate - solution interactions are of course unchanged from one system to the next. All changes in K_L are therefore due to changes in the relative strength of binding of each sorbate to the given molecular sieve. The values of K_{zeo} obtained for the two materials show that there is a substantial increase in the relative binding strength of GS14 with respect to GS18 for the three cresols studied.

These observations can be explained by the relative capacity for hydrogen bonding of the two sieves. GS14 sorbs 15 molecules per unit cell of water as opposed to 5 molecules per unit cell by GS18 under the same conditions (Table 4.3). As discussed in section 4.1.1, this implies that sample GS14 has more lattice faults than GS18. These faults provide hydrophilic sites for water sorption and this explains the high equilibrium water uptake by GS14.

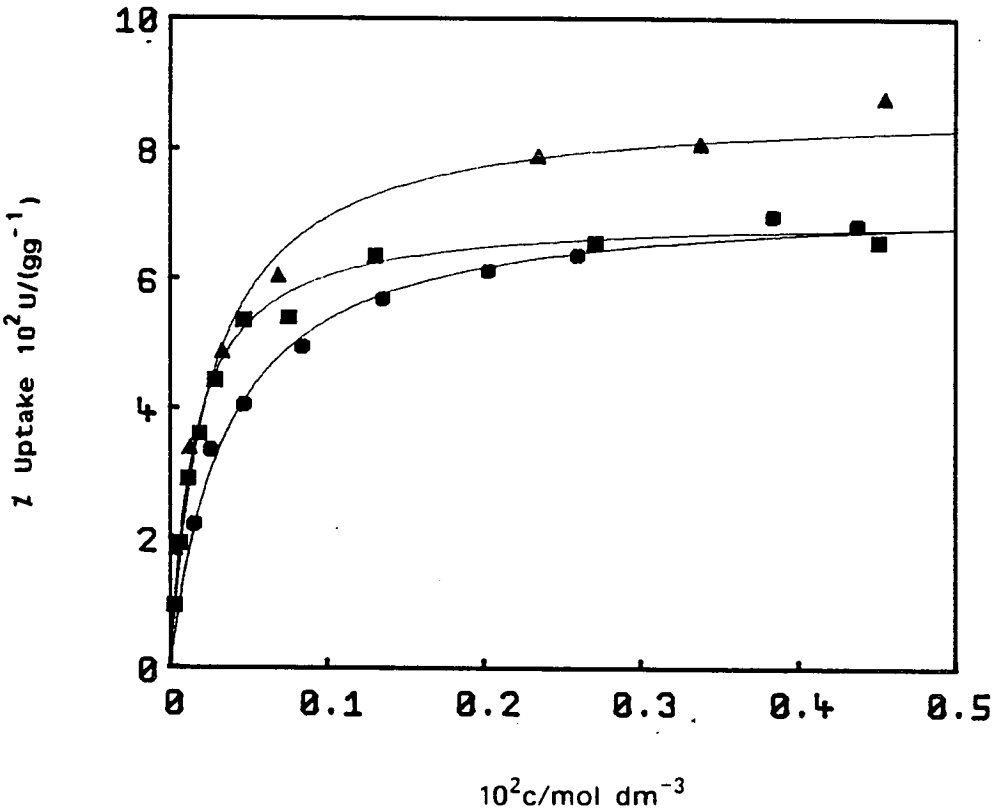

Figure 4.26 Sorption of Cresols from Aqueous Solution by Silicalite-1 (GS14) at 25°C; ●, o-cresol; ▲, m-cresol; ■, p-cresol.

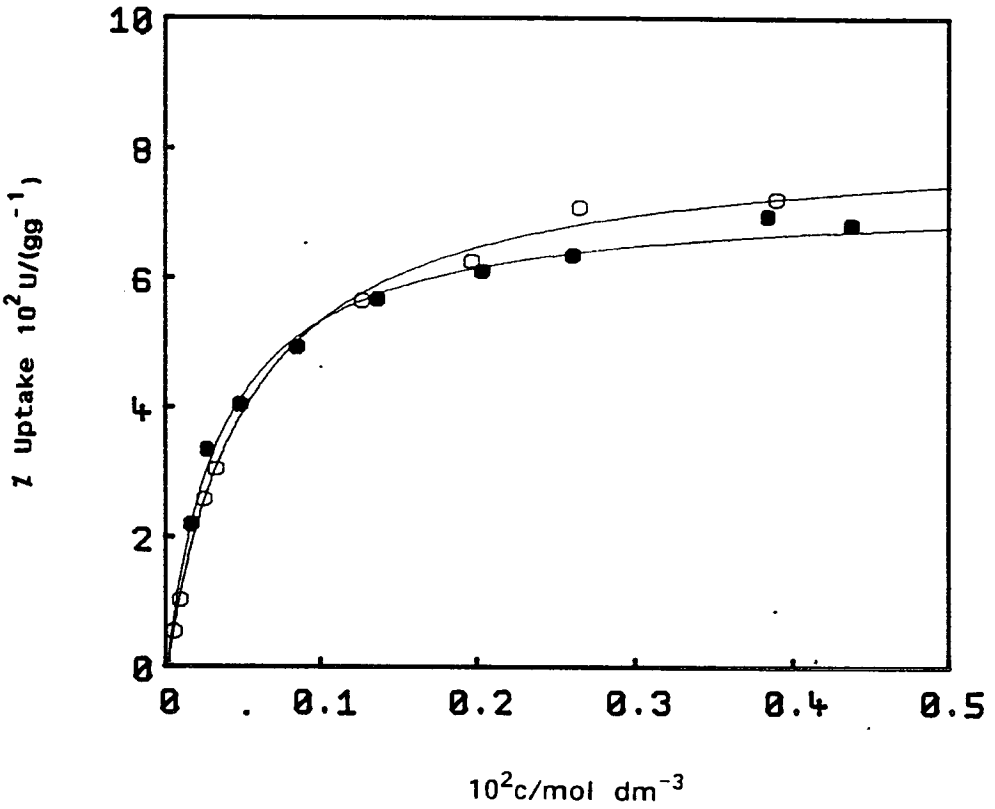

Figure 4.27 Sorption of o-Cresol from Aqueous Solution by Silicalite-1 at 25°C;
○, GS18; ●, GS14.

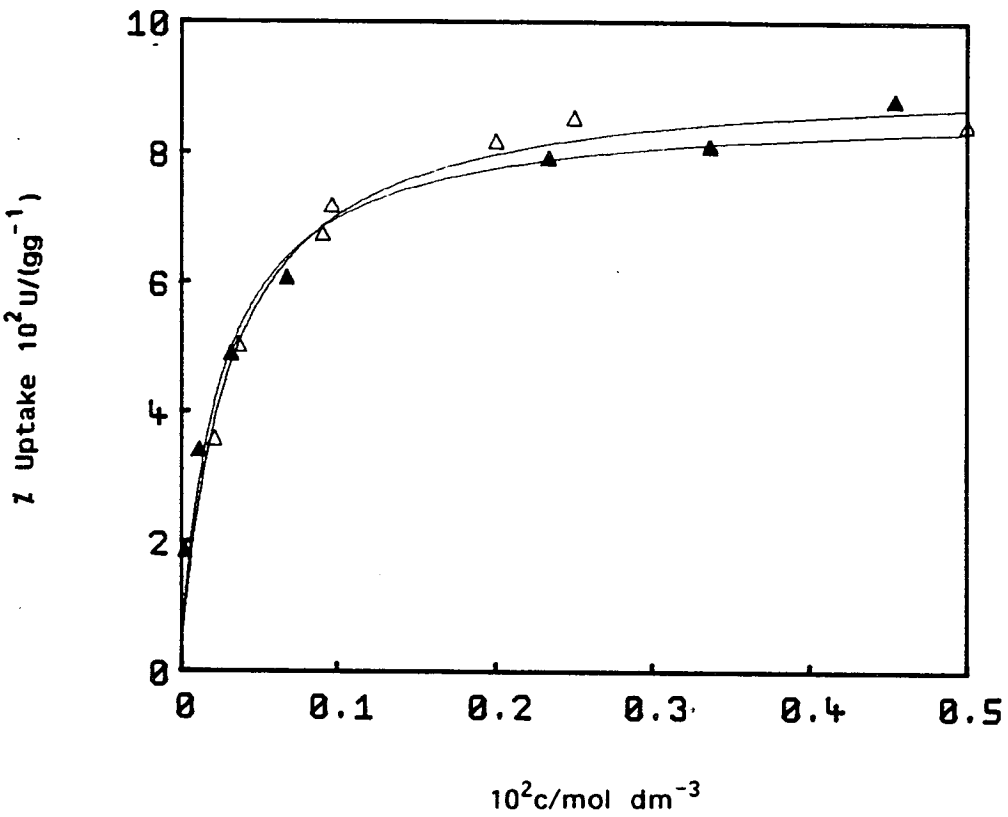

Figure 4.28 Sorption of m-Cresol from Aqueous Solution by Silicalite-1 at 25°C;
△, GS18; ▲, GS14.

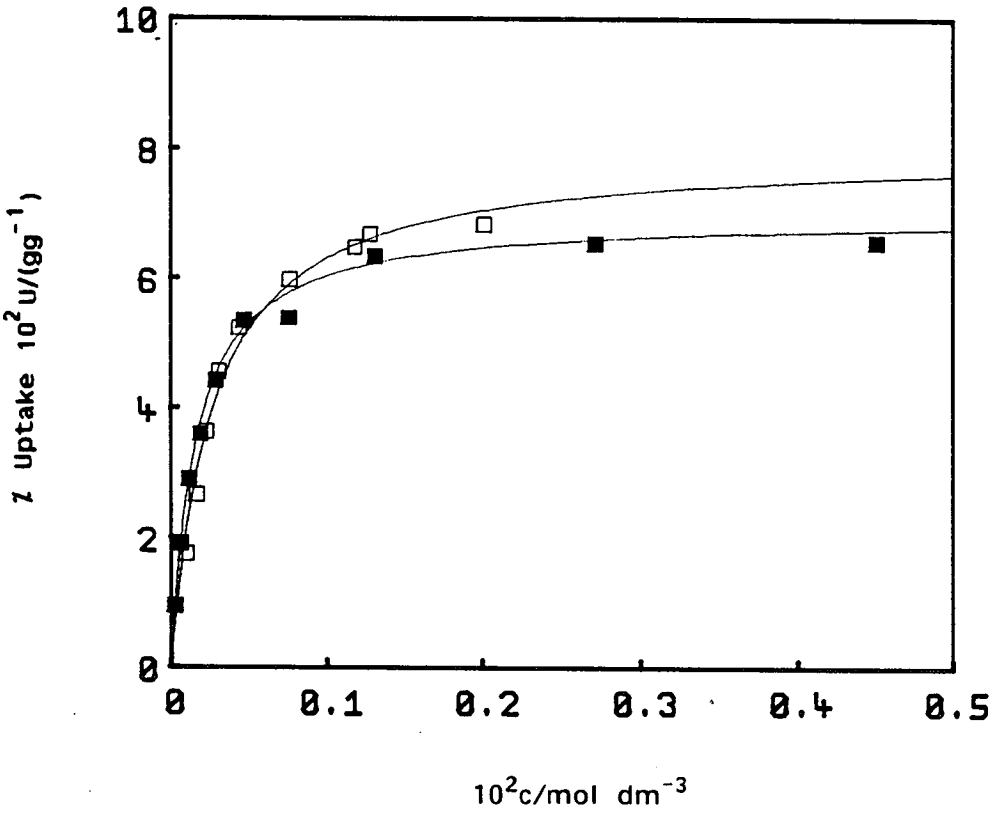

Figure 4.29 Sorption of p-Cresol from Aqueous Solution by Silicalite-1 at 25°C;
□, GS18; ■, GS14.

Table 4.13

Sorption Parameters for the Uptake of Cresols

from Aqueous Solution by Silicalite-1 (GS14) at 25°C

	o-cresol	m-cresol	p-cresol
$10^2 U_{max}$/ gg^{-1}	7.3 ± 0.4	8.7 ± 0.6	7.0 ± 0.3
U_{max}/ mol/unit cell	3.8 ± 0.2	4.6 ± 0.3	3.7 ± 0.1
$10^{-3} K_L$/ $dm^3 mol^{-1}$	2.8 ± 0.6	4.0 ± 0.8	6.4 ± 0.8
$10^{-5} K_{zeo}$/ atm^{-1}	14 ± 3.0	54 ± 11	89 ± 11

The reduction in maximum sorption capacity observed for all the cresols studied can be explained by the increase in water activity inside the sieve. Vapour phase results show that GS14 would sorb at least 15 molecules of water per unit cell from aqueous solution. As already described, the silicalite lattice is made up of four intersections per unit cell. Any lattice faults are likely to be found at channel intersections, so at least 4 molecules of water per intersection would be expected at each intersection in GS14, as opposed to only 1-2 in GS18. It is clear that this difference in water capacity could lead to the observed differences in cresol capacities. However, the cresols show a larger binding coefficient on GS14 than on GS18. This suggests that the more polar environment of GS14 enhances cresol binding.

The sorption of dimethylphenols by GS14 was also studied. Figure 4.30 shows the isotherms obtained for 2,5dmp, 3,4dmp and 2,4dmp. Again, they show the same pattern as that observed for GS18 (Figure 4.20). Although their basic shape is the same, the relative size of the initial slopes and positions of the plateaux are different. Figures 4.31-4.33 allow direct comparison between the isotherms obtained for GS14 and GS18.

The Langmuir sorption coefficients shown in Table 4.14 allow a quantitative comparison with those found for GS18 (Table 4.11). The differences found for these three sorbates are rather less straight forward than those of the cresols. Figures 4.32 and 4.33 reveal that the initial slopes of the isotherms for the different silicalite samples are superimposable for the sorbates 2,5-dimethylphenol and 3,4-dimethylphenol. This suggests that for these two molecules, hydrogen bonding interactions within the sieve are not as important as for the cresols. For 3,4-dimethylphenol, K_{zeo} is identical for the two sieves. Both 3,4-dimethylphenol and 2,5-dimethylphenol show a reduced capacity on GS14 compared to that of GS18. This was also found for the cresols studied

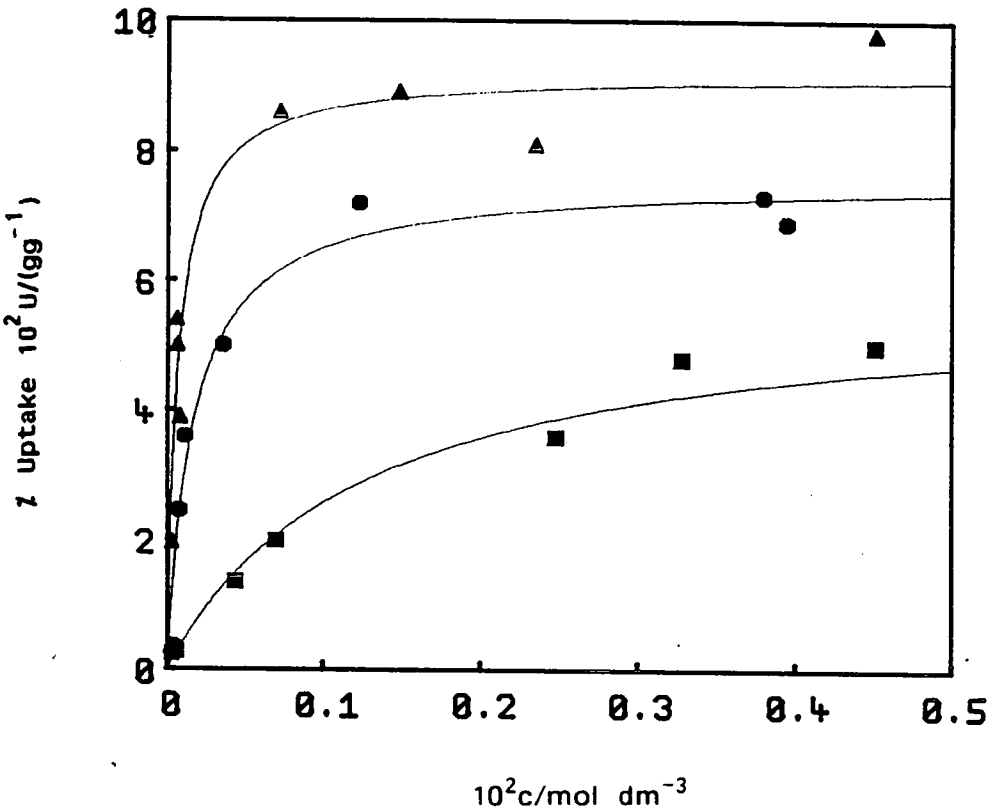

Figure 4.30 Sorption of Dimethylphenols from Aqueous Solution by Silicalite-1 (GS14) at 25°C;
■, 2,4-dimethylphenol; ▲, 2,5-dimethylphenol; ●, 3,4-dimethylphenol.

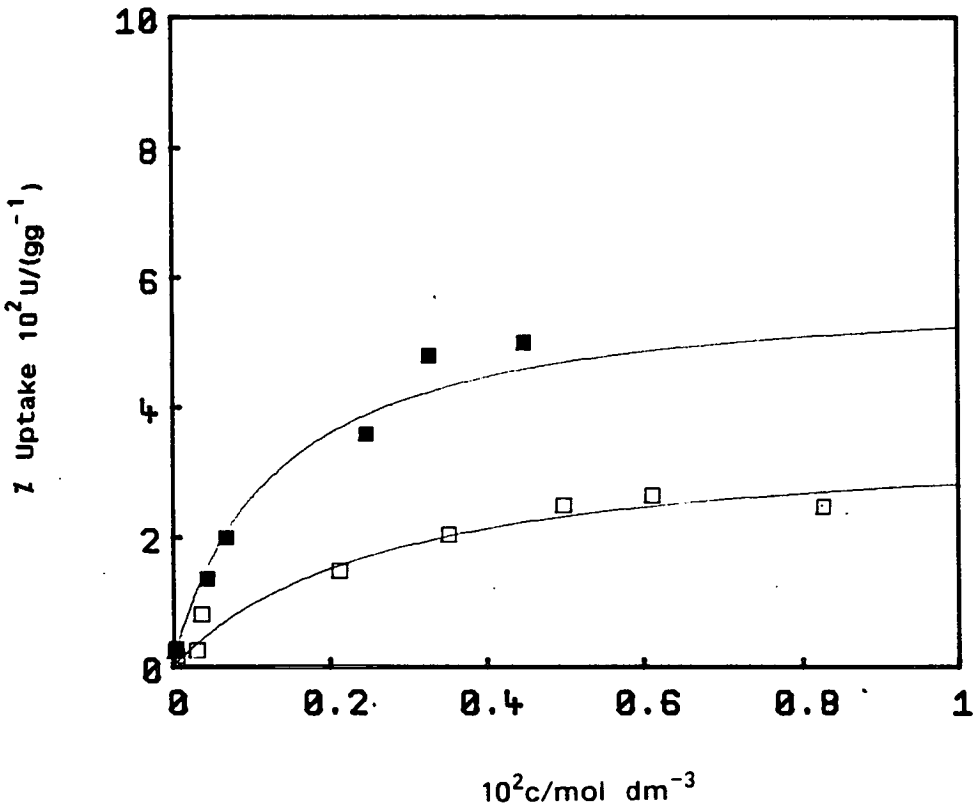

Figure 4.31 Sorption of 2,4-Dimethylphenol from Aqueous Solution by Silicalite-1 at 25°C;
□, GS18; ■, GS14.

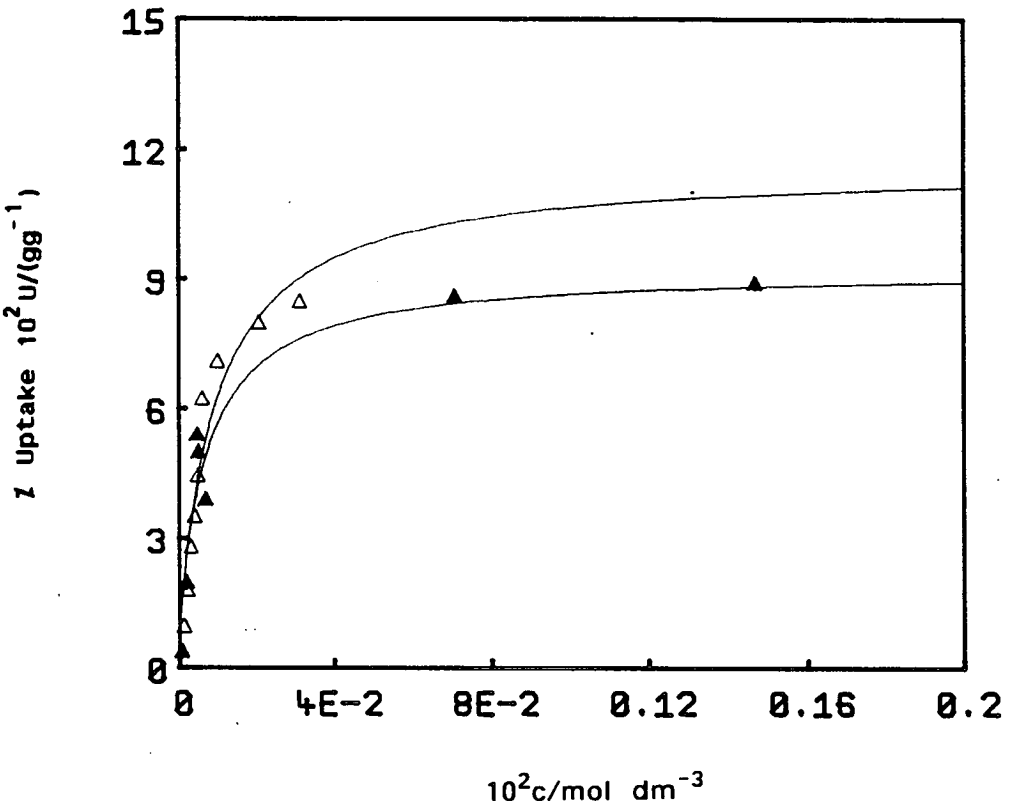

Figure 4.32 Sorption of 2,5-Dimethylphenol from Aqueous Solution by Silicalite-1 at 25°C;
△, GS18; ▲, GS14.

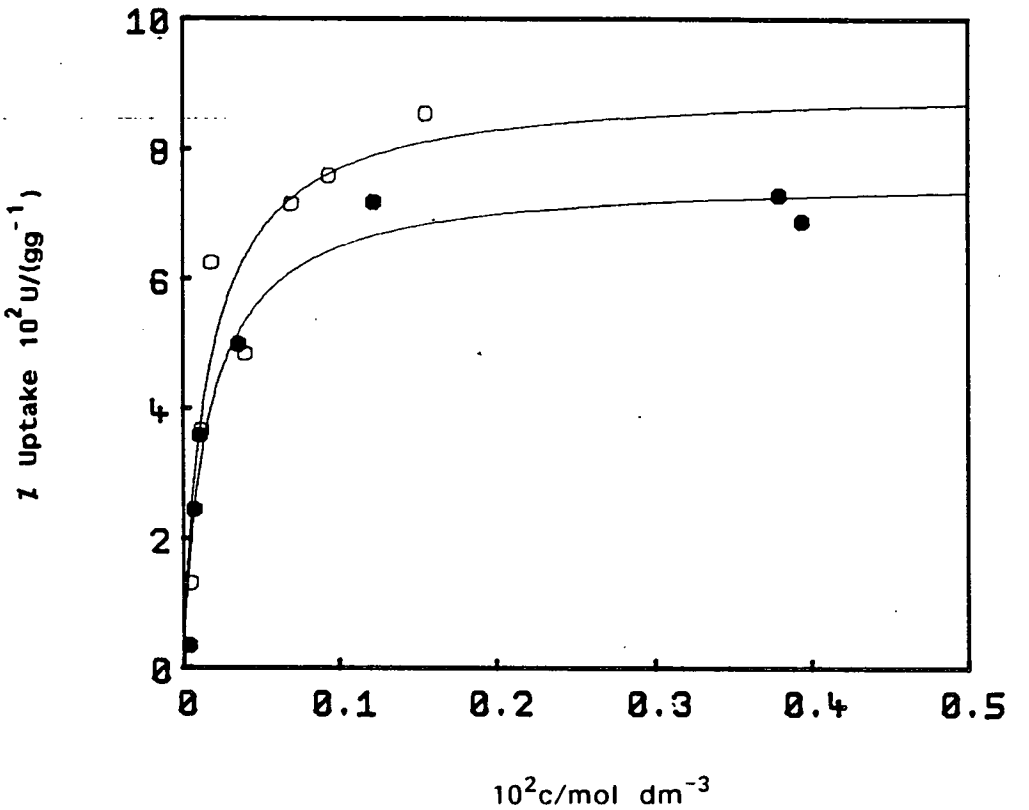

Figure 4.33 Sorption of 3,4-Dimethylphenol from Aqueous Solution by Silicalite-1 at 25°C;
○, GS18; ●, GS14.

Table 4.14

Sorption Parameters for the Uptake of Dimethylphenols

from Aqueous Solution by Silicalite-1 (GS14) at 25°C

	2,4-dmp	2,5dmp	3,4dmp
$10^2 U_{max}$/ gg^{-1}	5.9 ± 1.6	9.2 ± 1.3	7.6 ± 1.3
U_{max}/ mol/unit cell	2.7 ± 0.7	4.2 ± 0.6	3.5 ± 0.6
$10^{-3} K_L$/ $dm^3 mol^{-1}$	0.79 ± 0.71	14 ± 11	6.0 ± 5.5
$10^{-5} K_{zeo}$/ atm^{-1}	3.0 ± 3.0	21 ± 16	32 ± 29

and the same explanation is assumed to apply.

2,4-Dimethylphenol on the other hand presented a different picture. The isotherms in Figure 4.31 show that for this molecule there was a dramatic change in the initial slope in moving from GS18 to GS14. This observation is borne out in the calculated values of K_L and K_{zeo}. It is not certain why 2,4-dimethylphenol is more sensitive than the others to changes in the hydrophilicity of the sieve. It has the highest solubility in water of the three, and has the smallest binding coefficient to both GS18 and GS14. It is possible that on balance, 2,4-dimethylphenol finds the increased number of polar sites within the lattice of GS14 a more favourable environment for sorption. Unlike all the other phenols studied, 2,4-dimethylphenol shows a higher maximum uptake in GS14 than in GS18. This can be explained on energetic grounds. It has a maximum uptake of only 1.7 molecules per unit cell on GS18. This is due to an equilibrium situation which favours the solution phase even at high concentrations and not because of lack of space inside the sieve. Therefore, because the sorption interactions are more favourable inside GS14, an increase in maximum capacity is observed despite the increase in the number of water molecules present.

This series of experiments on silicalite-1, sample GS14, have shown that even small changes in the character of the molecular sieve can lead to observable changes in sorption behaviour. As a general rule, it was found that an increase in the hydrophilicity of the sieve, led to an increase in the binding coefficients of the sorbed aromatic phenols.

A diminished maximum sorption capacity for the phenols was found for the more hydrophilic molecular sieve. This was probably due to increased sorption of water molecules leading to the partial exclusion of the phenolic sorbates.

It is clear that to achieve optimum sorbate-sorbent interactions, when dealing with a sorbate which contains polar groups, that a sorbent with hydrophilic as well as organophilic character is preferable. However when a polar solvent such as water is involved, any increase in the polarity of the sieve leads to an increase in the sorption of that solvent. This ultimately leads to a reduction in the selectivity of the sieve for the organic sorbate. A balance must be found between the hydrophilic and organophilic properties of the sieve if optimum selectivity is to be achieved.

4.3.3 Effect of Aluminium Content on Sorption

The previous section dealt with the effect of hydrophilic sites inside silicalite-1 on its sorption properties. It is now proposed to expand on this theme with the study of a series of molecular sieves containing different amounts of aluminium.

Section 4.1.2 dealt with the synthesis and characterisation of the materials to be discussed. It was estimated that the SiO_2/Al_2O_3 ratios of the ZSM-5 samples; GZ1, GZ2 and GZ3 were approximately 220, 110 and 55 (all $\pm$ 10) respectively. The morphology of the three samples (Figure 4.7) suggested that there would be no complications arising from external surface sorption. Any difference in the sorption behaviour could therefore be linked directly to the increased number of aluminium atoms within the framework.

The substitution of Al^{3+} for Si^{4+} in the framework results in a charge imbalance which must be countered by a cation, in this case a proton. Electrostatic field gradients are also set up by the presence of aluminium. The surface of the sieve becomes polar and both Lewis and Bronsted acid sites are established.

The effect of aluminium content on water sorption was discussed with respect to the three samples of ZSM-5 prepared, in section 4.1.3 (Table 4.6).

Sorption isotherms were obtained for the uptake of phenol from aqueous solution by GZ1, GZ2 and GZ3 and are shown in Figure 4.34 (for experimental details see Chapter 3 (section 3.3.2 and 3.3.3(5)) and Appendix 5). A sorption isotherm obtained by the same method on silicalite-1 (GS18) is also shown. The SiO_2/Al_2O_3 ratio of GS18 was estimated from X-ray fluorescence measurements to be >1000 (Table 4.4).

The ZSM-5 isotherms reveal that there is little difference between the three samples with respect to phenol sorption. They all show a similar initial slope to that of silicalite-1, with a reduced maximum capacity, presumably due to increased water content.

The sorption coefficients obtained are given in Table 4.15. Phenol is highly solvated in aqueous solution, more so than any of the substituted phenols studied. This reflects the fact that it has a free hydroxyl group and no methyl substituents on the ring to hinder solvation. Consequently, phenol has a smaller Langmuir coefficient for sorption onto silicalite-1 (GS18) than any of the substituted phenols studied, with the exception of 2,4-dimethylphenol. The maximum sorption capacity of silicalite-1 is four molecules per unit cell within experimental error. This was also found for several of the other phenols studied, where maximum capacity corresponds to one molecule per channel intersection in the lattice.

Sorption of phenol by GZ1, a sample of ZSM-5 with a SiO_2/Al_2O_3 ratio of 240, which corresponds to approximately one aluminium atom per unit cell, showed a change in behaviour over that of silicalite-1. The maximum sorption capacity was reduced by one molecule per unit cell and the binding coefficient

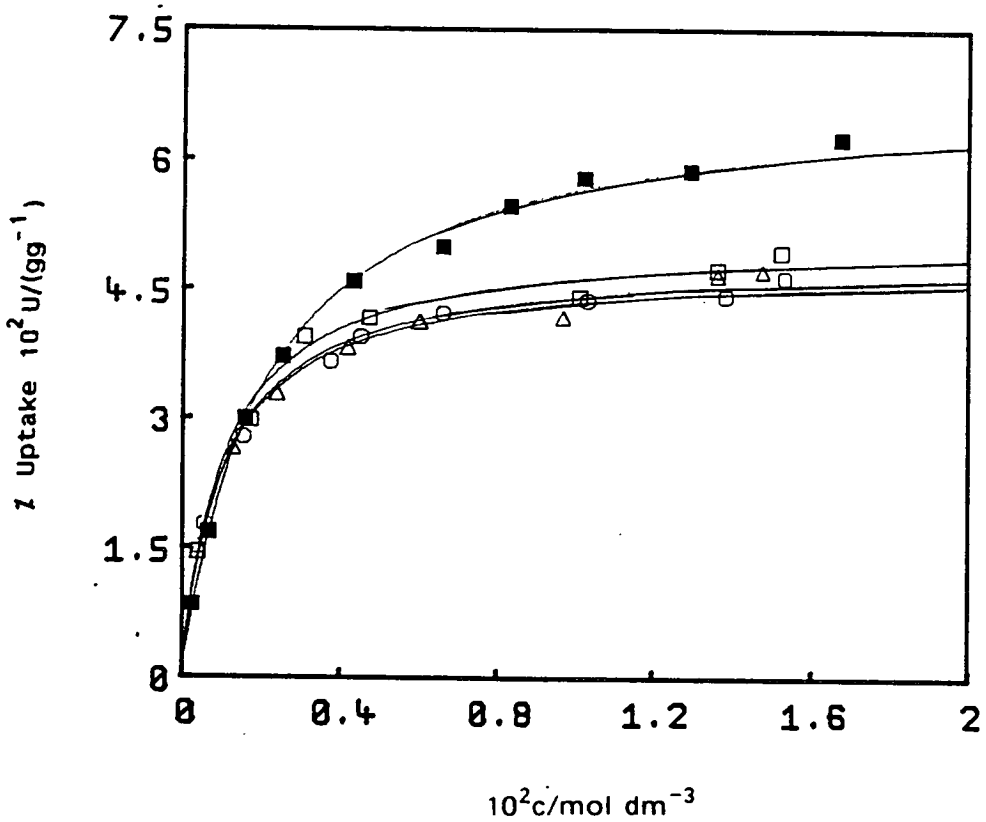

Figure 4.34 Sorption of Phenol from Aqueous Solution by ZSM-5 and Silicalite-1 at 25°C; ■, silicalite-1 (GS18); □, GZ1; ○, GZ2; △, GZ3.

Table 4.15

Sorption Parameters for the Uptake of

Phenol from Aqueous Solution by ZSM-5 at 25°C

	GS18	GZ1	GZ2	GZ3
$10^2 U_{max}$/ gg^{-1}	7.4 ± 0.4	5.1 ± 0.3	4.9 ± 0.3	4.8 ± 0.3
U_{max}/ mol/unit cell	4.3 ± 0.3	3.0 ± 0.2	2.9 ± 0.2	2.8 ± 0.2
$10^{-2} K_L$/ $dm^3 mol^{-1}$	5.45 ± 1.20	9.56 ± 3.10	9.64 ± 2.72	9.74 ± 1.91
$10^{-4} K_{zero}$[a]/ atm^{-1}	11.0 ± 2.4	19.3 ± 5.5	19.4 ± 5.5	19.6 ± 3.8

[a]Based on solubility in water = 0.912 mol dm^{-3} (25°C), $p_o = 4.526 \times 10^{-4}$atm and $K_{solv} = 2015$mol $dm^{-3}atm^{-1}$.

of the phenol almost doubled. The reduction in sorption capacity was almost certainly due to an increase in water sorption by GZ1 (Table 4.6) over GS18 (Table 4.3). The increase in K_{zeo} is due to the increased polarity of the sieve caused by the presence of aluminium.

Through the series of ZSM-5 samples from GZ1 to GZ3, the sorption behaviour changes very little. The binding coefficient K_{zeo} increased and the sorption capacity decreased, through the series, as one would expect for an increase in the aluminium content of the sieve. The size of these changes however were much smaller than expected. The effect of an increase from one to approximately four molecules of aluminium per unit cell in the lattice was minimal in terms of the sorption properties studied. The thermal analysis results and morphological evidence discussed in section 4.1 strongly suggest that there is indeed an increase in framework aluminium in the product. A possible explanation for the result is the distribution of aluminium throughout the lattice. The position of the aluminium atoms within the lattice would be of vital importance in determining any change in sorption properties of the sieve. It is possible, that as the loading of aluminium increases, the sites are positioned in such a way as to only have a long range effect on sorption properties.

These results suggest that an increase in aluminium content of the sieve does not give a well defined change in sorption behaviour. If aluminium distribution is important, then the method of synthesis of the zeolite will determine any change in properties.

4.3.4 Effect of Structure on Sorption

Silicalite-1, which has a structure similar to that of ZSM-5, is not the only

all silica polymorph of a zeolite. A summary of all the known silica molecular sieves was given in Table 1.4. All these materials have the same composition but different framework structures. A study of the sorption properties of one of these materials would give an insight into the relationship between structure and sorption capacity for various sorbates

It was necessary that the chosen material could be made in a highly hydrophobic form and made up of large crystals so that it could be compared to silicalite-1 without complications.

Silicalite-2 has a structure identical to that of the zeolite ZSM-11. It is defined by 10-membered ring channels as is ZSM-5, but they are both straight rather than one straight and one sinusoidal. The channel systems of the two materials are shown in Figure 1.3. The ZSM-11 network, as described in Chapter 1, gives rise to two types of intersection. One has free space similar to that in ZSM-5, and the other is larger by about 30%.

Silicalite-2 can be prepared in the absence of inorganic cations to produce large hydrophobic crystals. It was therefore a good candidate with which to study the effect of a change in structure on sorption properties. Samples of silicalite-2 were provided by K.R. Franklin and their characterisation was described in section 4.1. Although this material will be referred to as silicalite-2, it is probable that it is an intergrowth of silicalite-1 and silicalite-2.

Sorption isotherms were obtained for the sorption of o-cresol, m-cresol, p-cresol, phenol and 2,4-dimethylphenol from aqueous solution on silicalite-2 (KF1 and KF2) at 25°C (for experimental details see Chapter 3 (section 3.3.2 and 3.3.3 (parts 6 and 7)) and Appendix 6). Figure 4.35 shows the isotherms obtained for o-cresol, m-cresol and p-cresol on silicalite-2 (KF1). Their behaviour is different to that previously found for silicalite-1 samples GS14 and

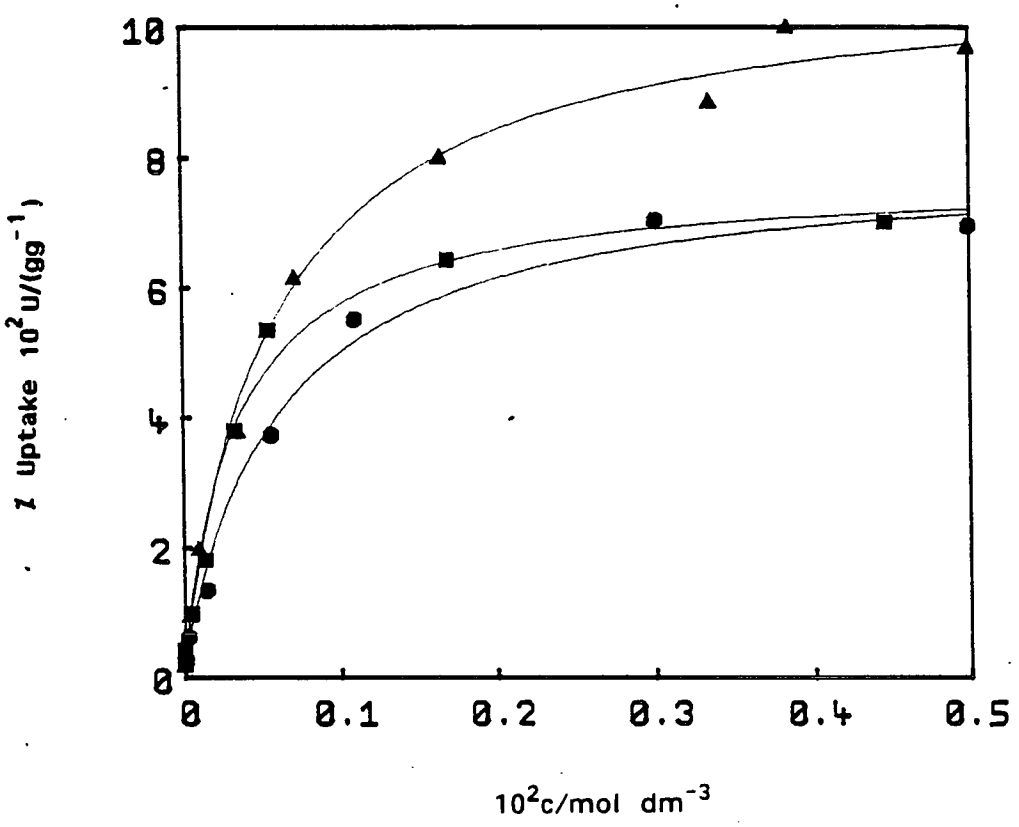

Figure 4.35 Sorption of Cresols from Aqueous Solution by Silicalite-2 (KF2) at 25°C; ●, o-cresol; ▲, m-cresol; ■, p-cresol.

GS18. Their initial slopes are less steep than for the other two sieves and the maximum uptake of m-cresol has increased markedly. In Figures 4.36-4.38 the sorption isotherms obtained for the three cresols are compared directly with those found previously for silicalite-1 (GS18). The isotherms obtained for o-cresol and p-cresol on the two sorbents are very similar. For silicalite-2, they are less steep, but reach a similar plateau to those of silicalite-1. The flatter isotherms are probably as a result of the decreased polarity of silicalite-2 compared to silicalite-1. KF1 was shown to sorb only 0.9% w/w water (25°C, a^w = 0.753) as opposed to 1.5% w/w by GS18 under the same conditions. The isotherms suggest that the maximum capacity of the sieve has not been affected by the change in framework topology.

The sorption parameters obtained for these isotherms are shown in Table 4.16. They reveal that the binding coefficients for all three cresols are larger, although only marginally, than those obtained for GS18 (Table 4.10). The sorption capacities of o-cresol and p-cresol remain at four molecules per unit cell. m-Cresol on the other hand shows a substantial rise in sorption capacity on silicalite-2. It was previously shown that more than one molecule of m-cresol may be sorbed at each channel intersection in silicalite-1 at maximum capacity. The results suggest that this phenomenon is enhanced in silicalite-2. This is probably by virtue of the larger amount of space available at certain of its intersections relative to silicalite-1.

The silicalite-2 isotherms are also compared with those for the more hydrophilic of the two silicalite-1 samples studied (GS14) in Figures 4.39-4.41. These show identical trends, but the differences are more pronounced than those found for GS18. The following series can be constructed for the three materials in terms of degree of hydrophilicity and the size of the binding coefficient to the three cresols;

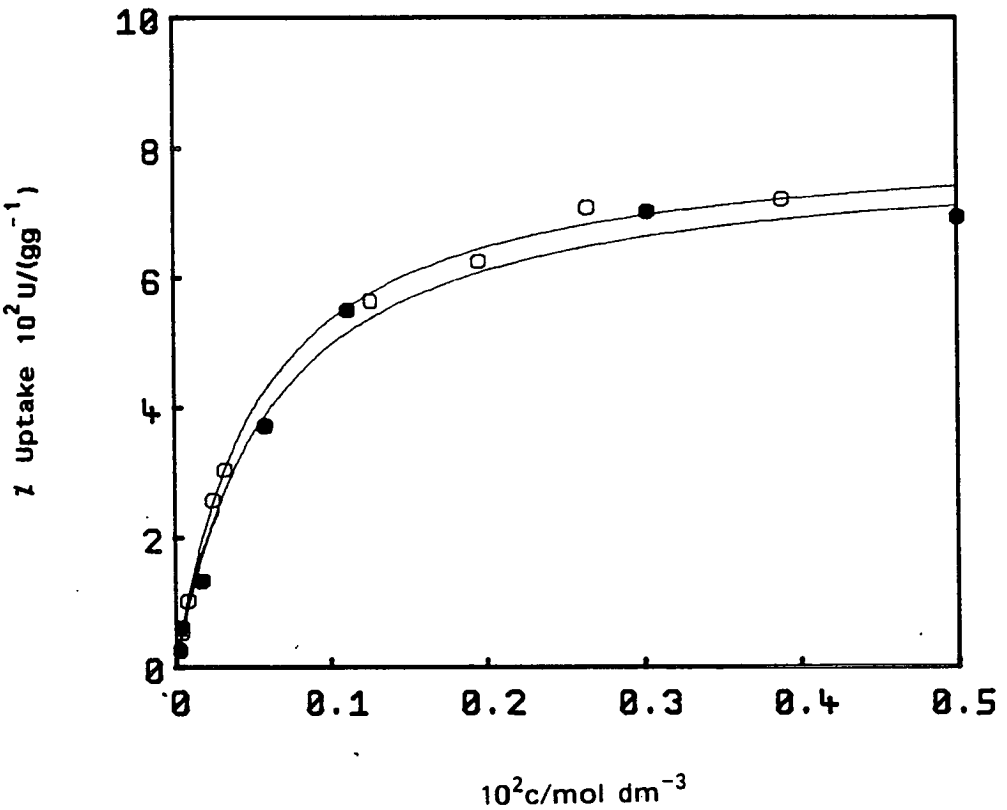

Figure 4.36 Sorption of o-Cresol from Aqueous Solution by a Silica Molecular Sieve at 25°C; ○, silicalite-1 (GS18); ●, silicalite-2 (KF1).

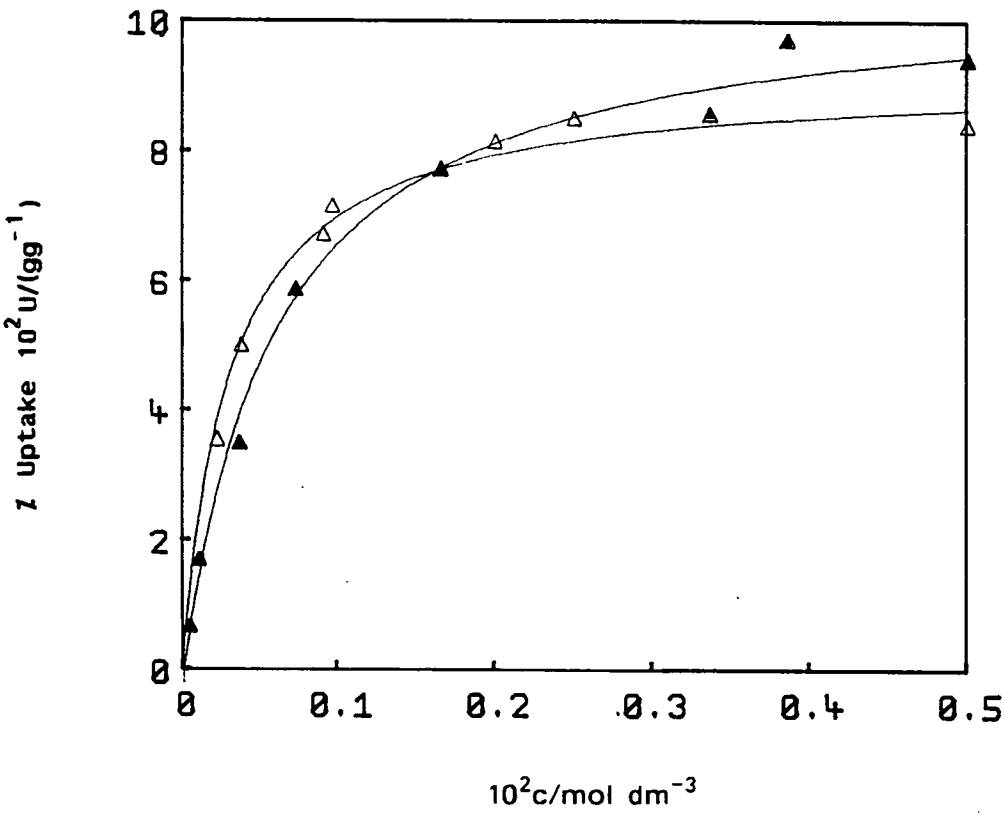

Figure 4.37 Sorption of m-Cresol from Aqueous Solution by a Silica Molecular Sieve at 25°C; △, silicalite-1 (GS18); ▲, silicalite-2 (KF1).

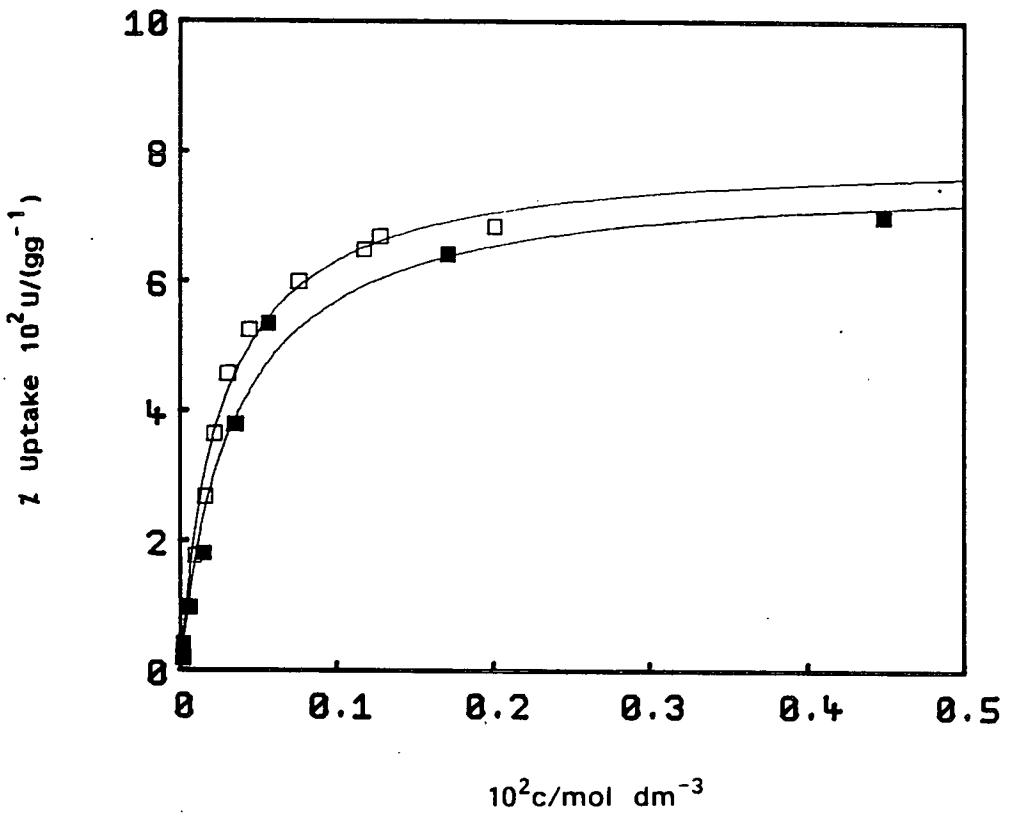

Figure 4.38 Sorption of p-Cresol from Aqueous Solution by a Silica Molecular Sieve at 25°C; □, silicalite-1 (GS18); ■, silicalite-2 (KF1).

Table 4.16

Sorption Parameters for the Uptake of

Phenols from Aqueous Solution by Silicalite-2 at 25°C

	o-cresol	m-cresol	p-cresol
10^2U_{max}/ gg^{-1}	8.0 ± 0.6	10.9 ± 0.9	7.7 ± 0.9
U_{max}/ mol/unit cell	4.2 ± 0.3	5.7 ± 0.5	4.0 ± 0.5
$10^{-3}K_L$/ dm^3mol^{-1}	1.6 ± 0.5	1.7 ± 0.5	2.9 ± 1.1
$10^{-5}K_{zeo}$/ atm^{-1}	8.6 ± 2.5	23 ± 7.0	40 ± 15

Table 4.16 (cont)

Sorption Parameters for the Uptake of

Phenols from Aqueous Solution by Silicalite-2 at 25°C

	phenol	2,4-dmp
10^2U_{max}/ gg^{-1}	9.9 ± 1.3	8.5 ± 6.2
U_{max}/ mol/unit cell	5.8 ± 0.8	4.0 ± 2.9
$10^{-3}K_L$/ dm^3mol^{-1}	0.25 ± 0.09	0.06 ± 0.06
$10^{-5}K_{zeo}$/ atm^{-1}	5.0 ± 1.8	0.21 ± 0.21

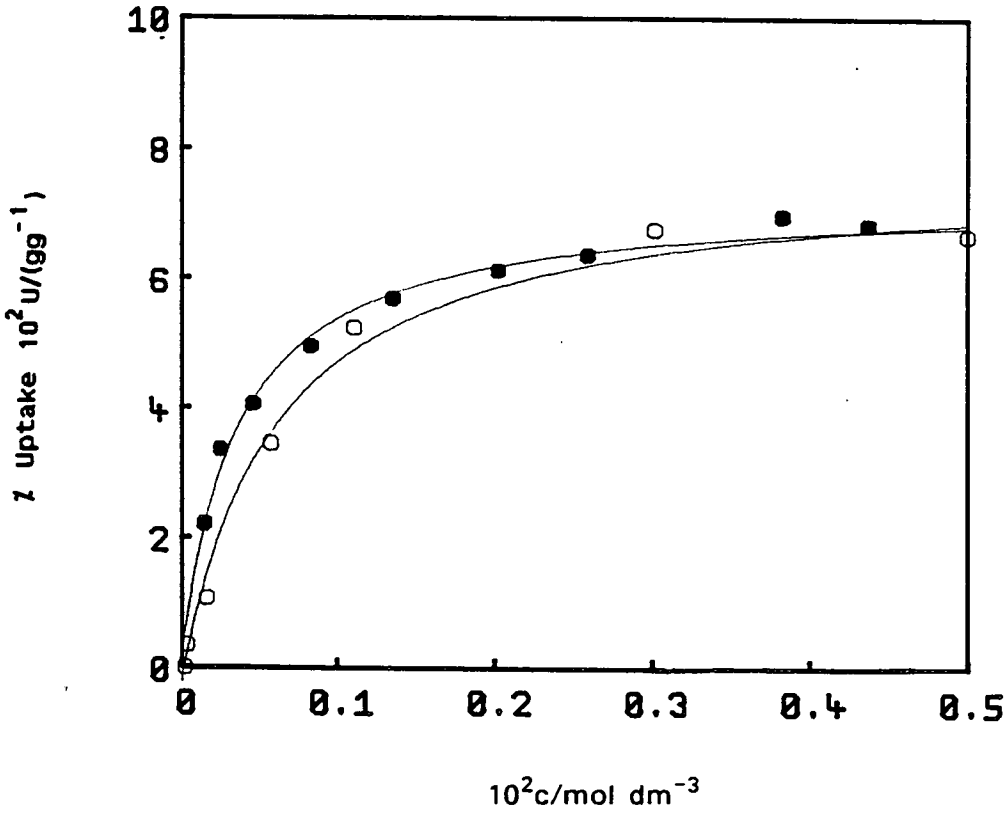

Figure 4.39 Sorption of o-Cresol from Aqueous Solution by a Silica Molecular Sieve at 25°C; ●, silicalite-1 (GS14); ○, Silicalite-2 (KF1).

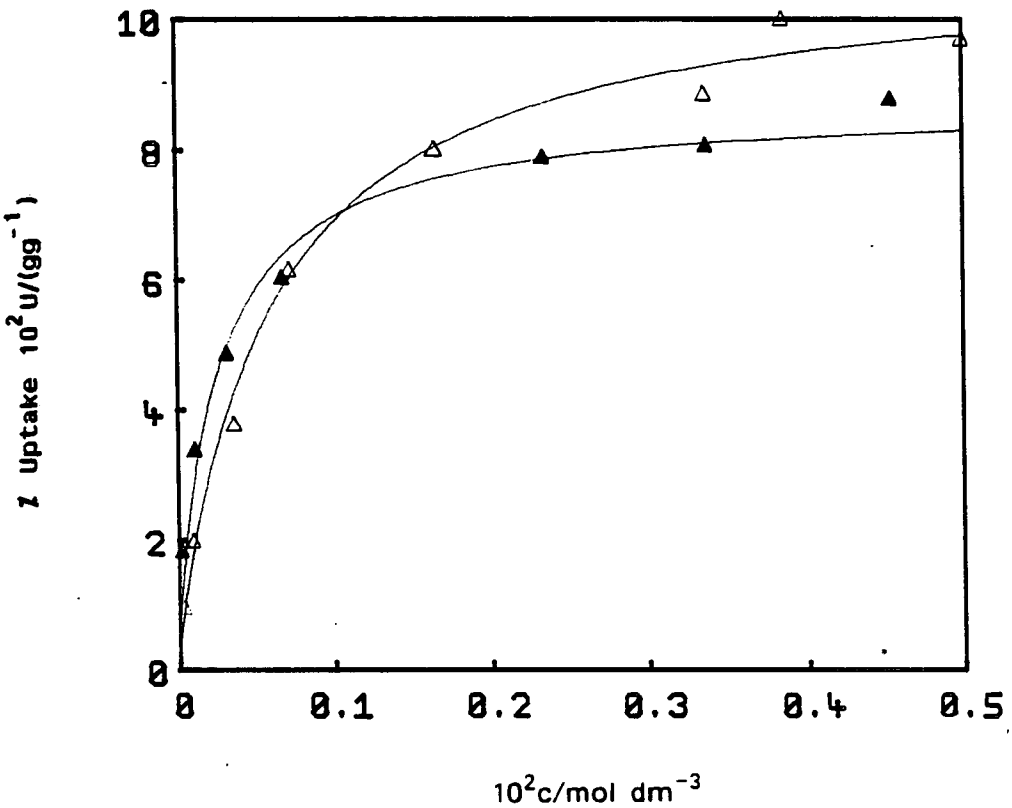

Figure 4.40 Sorption of m-Cresol from Aqueous Solution by a Silica Molecular Sieve at 25°C; ▲, silicalite-1 (GS14); △, silicalite-2 (KF1).

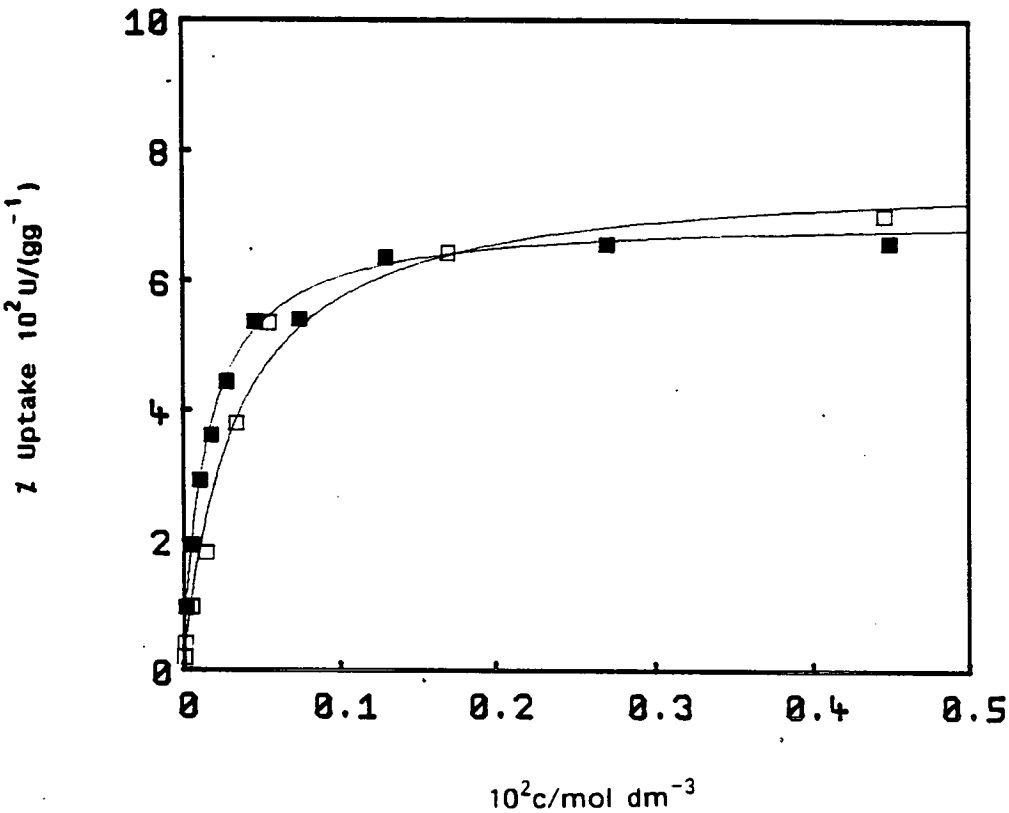

Figure 4.41 Sorption of p-Cresol from Aqueous Solution by a Silica Molecular Sieve at 25°C; ■, silicalite-1 (GS14); □, silicalite-2 (KF1).

silicalite-2(KF1)<silicalite-1(GS18)<silicalite-1(GS14)

The results suggest that the only observed effect due to framework topology was the increase in the capacity of the sieve for m-cresol. In order to try to substantiate the observation made with m-cresol the behaviour of other sorbates were studied. Phenol and 2,4-dimethylphenol, the smallest and largest respectively of the materials previously studied with silicalite-1, were chosen.

The phenol isotherm (Figure 4.42) displays similar changes to those of m-cresol. A slightly flatter isotherm and an enhanced capacity over that obtained for silicalite-1 sample GS18. The binding coefficient is half that obtained for GS18 (Table 4.16) and the maximum sorption capacity is increased by 1.5 molecules per unit cell. The behaviour exhibited for m-cresol has therefore been reproduced by phenol.

Figure 4.43 shows the isotherm obtained for 2,4-dimethylphenol on silicalite-2 (KF2) and includes those previously found for silicalite-1 samples GS14 and GS18. Quite dramatic differences are observed. 2,4-Dimethylphenol was shown, through the studies carried out on silicalite-1, to be particularly sensitive to changes in the internal polarity of the sieve. This may explain the flat isotherm obtained on the extremely non-polar silicalite-2 (KF2). However, it does not explain the change in the basic shape of the isotherm. The curve rises gently with concentration and it appears not to have reached a maximum value within the concentration range of the experiment. It has a maximum capacity of 4 $\pm$ 2.9 molecules per unit cell according to the Langmuir parameters (Table 4.16). The error in this value cannot be reduced since it was very difficult to obtain reliable results at higher aqueous phase concentrations. This was because the small amounts sorbed from solutions of high molarity inherently yielded large errors.

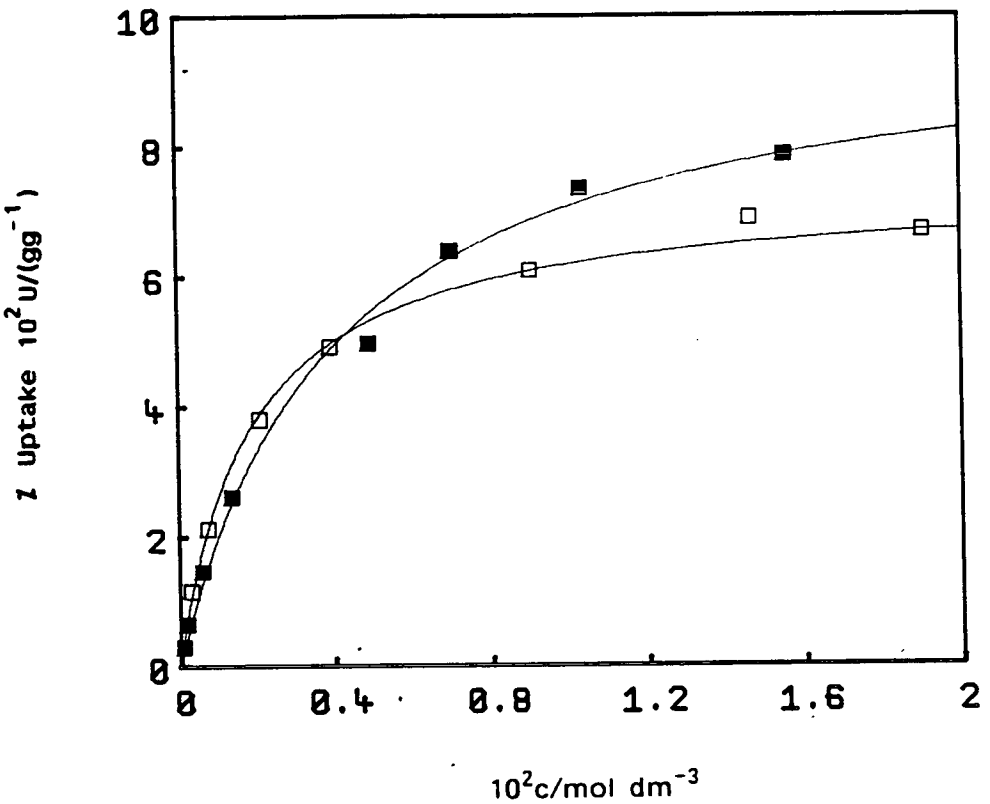

Figure 4.42 Sorption of Phenol from Aqueous Solution by a Silica Molecular Sieve at 25°C; □, silicalite-1 (GS18); ■, silicalite-2 (KF2).

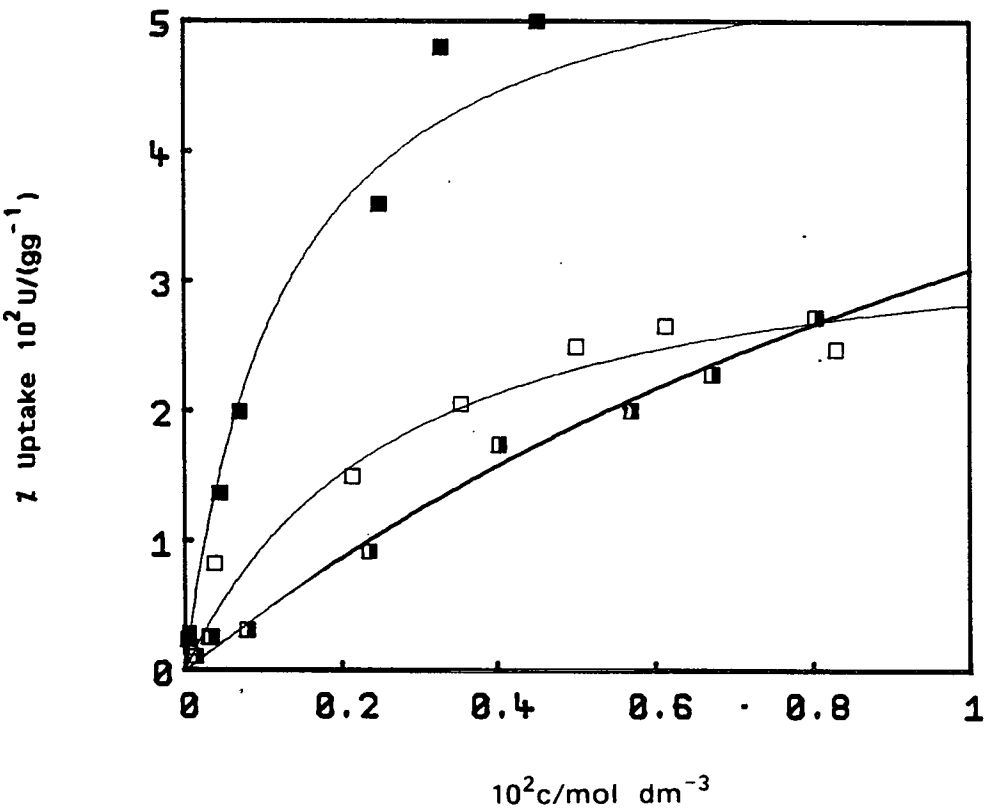

Figure 4.43 Sorption of 2,4-Dimethylphenol from Aqueous Solution by a Silica Molecular Sieve at 25°C; □, silicalite-1 (GS18); ■, silicalite-1 (GS14); ◨, silicalite-2 (KF2).

The results obtained for silicalite-2, have shown that for the systems studied, the equilibrium sorption properties are more dependent on the composition of the sieve than on slight changes in framework topology. It must be stressed, that radical changes in structure, such as substantial changes in the channel diameters, would have caused extreme differences in properties. The effect of small changes, such as that between silicalite-1 and silicalite-2, would perhaps be more pronounced in the diffusion rates rather than the equilibrium sorption properties.

4.4 SORPTION OF PHENOLS FROM MULTI-COMPONENT SYSTEMS BY SILICALITE-1

The effect of changes in the nature of the molecular sieve on sorption properties was discussed in the previous section. This involved changes in the binding coefficient of each sorbate to the molecular sieve while the sorbate - solution interactions remained constant. The effect of changes in the sorbate - solution phase interactions on sorption will now be discussed.

4.4.1 Effect of Inorganic Salt on Sorption

The sorption of phenol from aqueous solutions of lithium chloride on silicalite-1 (GS18) was studied. The dependence of the size of the sorption coefficient on the strength of solvation of phenol in solution was thus determined.

Isotherms for the sorption of phenol from pure water, 2.5 M LiCl and 5.0 M LiCl by GS18 are shown in Figure 4.44 (for experimental details see Chapter 3 (section 3.3.2 and 3.3.3 (parts 8 and 9) and Appendix 7). One can see that the addition of lithium chloride to the system has a substantial effect on the nature

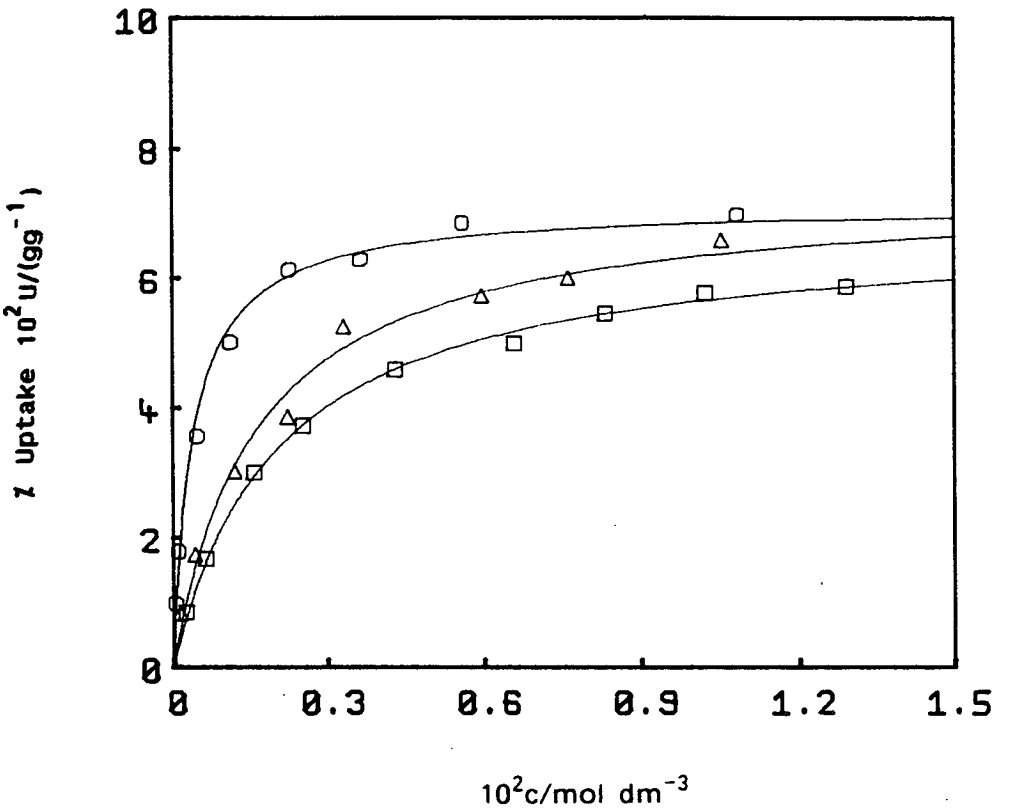

Figure 4.44 Sorption of Phenol from Aqueous Salt Solution by Silicalite-1 (GS18) at 25°C; □, 0M LiCl; △, 2.5M LiCl; ○, 5M LiCl.

of the isotherm obtained. The increase in the initial slope suggests a salting out effect. The phenol is less solvated in solution and therefore the equilibrium is shifted towards a greater amount in the sorbed state for any given equilibrium concentration. Maximum sorption capacity appears not to be affected, since at high concentrations the three isotherms converge.

Table 4.17 shows the Langmuir sorption coefficients K_L for these systems; the values bear out the above observations. The maximum uptakes for each isotherm corresponded within experimental error to four molecules per unit cell. This result is not surprising, since an inorganic salt such as lithium chloride, which is highly solvated in aqueous solution, would not be expected to enter the pores of silicalite. Therefore the maximum sorption capacity for phenol, as was observed, should not be affected.

There is very little in the literature concerning the effect of inorganic salt on sorption by silicalite. However, a report from the U.S. Department of Energy (117), which concerned the use of silicalite in an ethanol fermentation process, looked at the effect of sodium chloride on the system. They found a 3% increase in the capacity (v/v) of silicalite for ethanol on addition of 10% (w/v) salt to the sorbate solution. This is in direct disagreement with this work where LiCl had no effect on sorption capacity. However, because the sodium chloride experiments were carried out in a column mode which may not have been operating at maximum capacity, a shift in the dynamic equilibrium would have produced the observed result, without a change in the maximum capacity of the sieve.

The dependence of K_L on the variation in K_{solv} between 0 and 5.0 M LiCl can be seen from these results. It appears that there is a threshold above which one sees a marked change in behaviour. Although K_{solv} decreases almost

Table 4.17

Sorption Parameters for the Uptake of Phenol

from Aqueous Solutions of LiCl by Silicalite-1 (GS18) at 25°C

	No LiCl	2.5M LiCl	5M LiCl
$10^2 U_{max}$/ gg^{-1}	7.4 ± 0.4	7.4 ± 0.8	7.1 ± 0.5
U_{max}/ mol/unit cell	4.3 ± 0.3	4.3 ± 0.6	4.1 ± 0.3
$10^{-3} K_L$/ $dm^3 mol^{-1}$	0.54 ± 0.12	0.61 ± 0.20	2.5 ± 1.0
$10^{-4} K_{zeo}$/ atm^{-1}	10.9 ± 2.4	4.7 ± 1.6	10.0 ± 4.0
Solubility s/mol dm^{-3}	0.912	0.352	0.185
K_{solv}[a]/ mol $dm^{-3} atm^{-1}$	2015	778	398

[a]Based on vapour pressure, p = 4.526×10^{-4}atm.

linearly with an increase in the concentration of LiCl, K_L shows a more complex variation. The presence of 2.5 M LiCl in solution has little effect on K_L even though K_{solv} is significantly reduced. However, in 5 M LiCl solution, there is a five fold decrease in the solvation coefficient (K_{solv}) of the phenol relative to pure aqueous solution and a corresponding five fold increase in the sorption coefficient K_L. This is of course a complex system where it would be impossible to model accurately the interactive processes which affect the final equilibrium. The results suggest however, that at a certain concentration which is between 2.5 M and 5 M LiCl, the effect of the salt becomes significant. This concentration threshold would change according to the inorganic salt used and the sensitivity of the solvation shell of the sorbate to changes in the structure of the solution.

4.4.2 Effect of Methanol on the Uptake of p-Cresol by Silicalite-1

The effect of an organic solvent as a third component in the aqueous phase sorption process was determined as follows. The study involved the uptake of p-cresol from methanol water mixtures by silicalite-1. Methanol was chosen as the organic component as it was expected to be little sorbed compared with the cresol. Other workers have shown (142) that methanol is not sorbed to any great extent (<0.2g/100g) even at high solution phase concentrations.

Isotherms at methanol levels of 10%, 20% and 30% by volume were established and are shown in Figure 4.45 (for experimental details see Chapter 3 (section 3.3.2 and 3.3.3 (10-12)) and Appendix 8). It is clear from the isotherms obtained that the addition of methanol to the system had a profound effect on sorption. One can see that the concentration scale for equilibrium concentration on the graph has been extended relative to that for previous isotherms to accommodate the increased concentrations required to approach

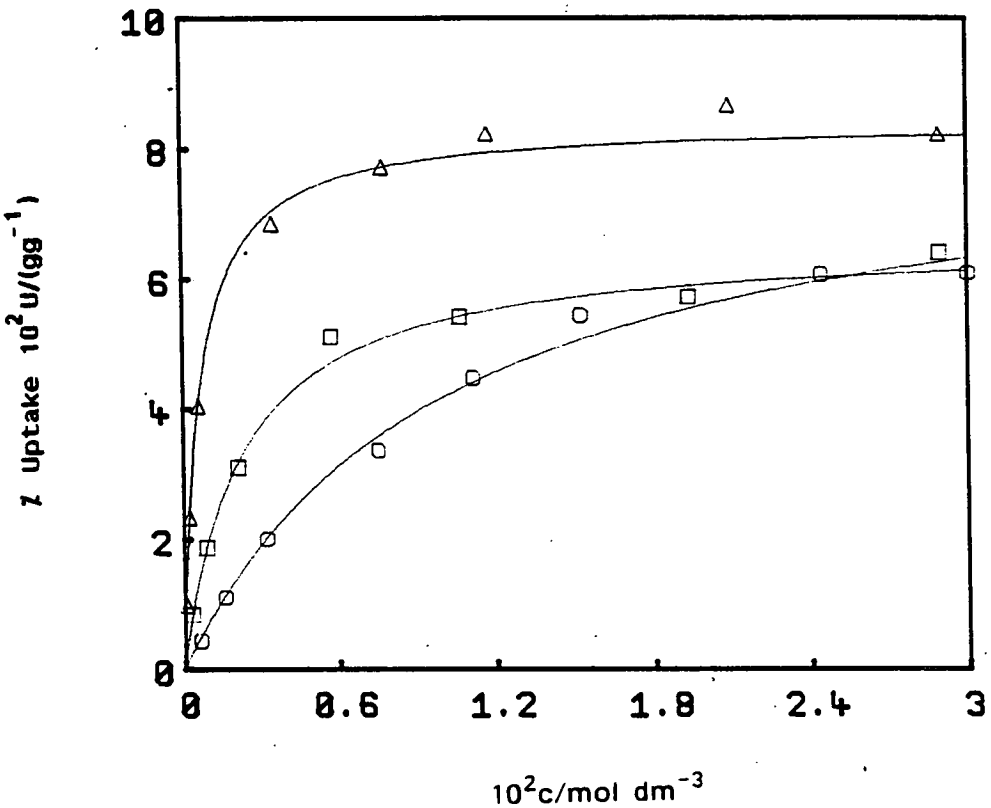

Figure 4.45 Sorption of p-Cresol from Aqueous Methanol Solutions by Silicalite-1 (GS19) at 25°C;
; △, 10 (MeOH):90 (H_2O) (v/v); □, 20:80; ○, 30:70.

maximum sorption capacity.

In general terms, the addition of methanol to the system led to a dramatic decrease in the extent of sorption. The sorption parameters obtained are compared in Table 4.18 with those previously found for the pure water system. The maximum uptake of p-cresol does not appear to be affected on the addition of 10% (v/v) methanol to the solution phase. However, in 20% methanol, a substantial reduction in the capacity of the sieve was observed. It is not clear whether this was an anomaly or whether it was caused by an increase in the competition by methanol for sorption sites within the sieve. The 30% methanol system gave a maximum capacity which was restored to around four molecules per unit cell. However, this predicted capacity was not reached within the concentration range of the experiment. It cannot therefore be stated with certainty whether or not methanol sorption is affecting p-cresol capacity at high volume fractions of methanol. It has been shown (section 4.3.2) that changes in levels of water sorption can have an effect on sorbate capacity on silicalite-1. It therefore seems likely that the larger molecule methanol could have an even greater effect. However, this is not apparent from the values of U_{max} in Table 4.18.

The values of K_{zeo} (= $K_L K_{solv}$) unexpectedly decrease with increasing methanol concentration. This implies a breakdown in the simple theoretical treatment outlined in Chapter 2. The systems are undoubtedly complicated and a full description would require more extensive experimental work and an improved theory.

It is possible to conclude however, that methanol water mixtures behave differently to pure water systems and that an increase in methanol content leads to a decrease in the sorption coefficient K_L for p-cresol.

Table 4.18

Sorption Parameters for the Uptake of

p-Cresol from Aqueous Solutions of Methanol at 25°C

	Methanol % (v/v) in Aqueous Phase			
	0	10	20	30
$10^2 U_{max}$/ gg^{-1}	8.0 ± 0.7	8.4 ± 0.3	6.7 ± 0.4	8.5 ± 1.1
U_{max}/ mol/unit cell	4.2 ± 0.4	4.4 ± 0.2	3.5 ± 0.2	4.2 ± 0.6
$10^{-3} K_L$/ $dm^3 mol^{-1}$	3.8 ± 1.0	1.5 ± 0.3	0.44 ± 0.10	0.10 ± 0.03
$10^{-5} K_{zeo}$/ atm^{-1}	53 ± 14	24 ± 5	8.0 ± 1.9	5.2 ± 0.7
solubility s/mol dm^{-3}	0.204	0.235	0.275	0.768
K_{solv}[a]/ mol $dm^{-3} atm^{-1}$	1397	1609	1883	5259

[a]Based on vapour pressure, p= 1.46 x 10^{-4}atm

4.4.3 Effect of Contaminants Normally Found in Fermentation Broths on Sorption by Silicalite-1

The previous two sections have shown that a third component in the aqueous phase can radically affect the sorption behaviour of the system. The hydrophobic properties of silicalite-1 have led to speculation about its possible use in downstream processing of biochemical products (see Chapter 1 (section 1.4.2)), particularly the extraction of the valuable fermentation product from the broth. A typical industrial fermentation supernatant is a multi-component system containing inorganic salts, carbohydrates, nucleic acids, protein and several low molecular weight organic metabolites. It is therefore necessary to establish the effect of such constituents on the sorption properties of silicalite, as part of the assessment of its potential for use in a biochemical extraction process.

It was mentioned in section 4.4.1 that a report from the U.S. Department of Energy (117) discussed the effect of inorganic salt on ethanol sorption by silicalite. These workers also studied the effect of an added surfactant. The addition of surfactant to the beer would facilitate the removal of broth from the void spaces before an appropriate desorption stage. 0.1% (w/w) Zonyl FSP surfactant was added to the solution of ethanol and resulted in a 3% increase in ethanol uptake. It was proposed that this was due to a better interaction between the aqueous ethanol solution and the sorbent. The effect of other constituents typically found in a fermentation broth has never been ascertained. Proteins, nucleic acids and carbohydrates may indeed affect the silicalite. A typical fermentation broth contains active cells (1-100 g dm^{-3}), nutrient salts (0.5-2 g dm^{-3}), extra cellular protein (1-2 g dm^{-3}), nucleic acids and extra cellular carbohydrate.

An attempt was made to model a fermentation supernatant in order to look at the behaviour of silicalite in a well defined system. The two main constituents of a fermentation supernatant are inorganic salts and soluble protein. A systematic study of the effect of inorganic salt and soluble protein on sorption by silicalite-1 was made. Concentration ranges similar to those found in fermentation broths were used.

Silicalite-1 sample GS14 was chosen for this study. The physical properties of this material are described in section 4.1. The two organic sorbates p-cresol and p-nitrophenol were chosen for the sorption experiments. The sorption of these two phenols from a pure aqueous solution by this or an analogous sample of silicalite-1 had already been studied (section 4.3.1, Figure 4.20 and section 4.3.2, Figure 4.24)

The sorption measurements in the presence of these added substituents were carried out in a similar manner to those in the pure water system (for experimental details see Chapter 3 (section 3.3.2 and 3.3.3 (13-17)).

The first study concerned the effect of a 50:50 mixture of disodium hydrogen phosphate and sodium dihydrogen phosphate on the sorption of p-cresol. The results obtained are shown in Table 4.19. Two initial concentrations of p-cresol were used, to see the effect of salt on two areas of the sorption isotherm. At the higher initial concentration of 2.3×10^{-3}M, p-cresol would be expected to fill the pores of silicalite, but only to partly fill them at a concentration of 1×10^{-3}M. The results show that in both cases, there was no evidence for a change in behaviour of the silicalite up to 0.25 M salt solution. The percentage sorption of p-cresol was within percentage error of the figure obtained for the salt free standard in all cases. Therefore, the presence of sodium phosphate at a concentration twenty times higher than

Table 4.19

Effect of Inorganic Salt on the Uptake of

p-Cresol from Aqueous Solution by Silicalite-1 (GS14) at 25°C

Sample	Conc. of $(Na,H)_3PO_4$ /M	Initial Conc. of Cresol $/10^{-4}$M	Sorption (% w/w) on dry GS14
A_1	0	10.07 + 0.09	3.94 ± 0.06
B_1	0.05	"	4.01 ± 0.06
C_1	0.10	"	3.99 ± 0.06
D_1	0.25	"	3.89 ± 0.06
A_2	0	25.2 + 0.2	7.2 ± 0.2
B_2	0.05	"	7.3 ± 0.2
C_2	0.10	"	7.2 ± 0.2
D_2	0.25	"	7.5 ± 0.2

that normally found in a fermentation broth, had no effect on sorption. This is not a surprising result when one considers the results obtained for lithium chloride solutions discussed in section 4.4.1. A ten fold increase in the salt concentrations described above was needed to produce an effect in that case.

The effect of protein on the uptake of p-nitrophenol from aqueous solution was also determined. The sorption of p-nitrophenol from dilute aqueous salt solutions (0.05 M) at 25°C containing a known amount of soluble protein (0-1.5% (w/w)) was studied. p-Nitrophenol, rather than p-cresol, was used as a reference in this case, because of the presence of protein in the solution to be analysed. The U.V spectrum of p-nitrophenol (λ_{max}; 320 nm, 400 nm; isobestic point; 343.6 nm) is significantly different to that of a typical protein (λ_{max}; 280 nm). This allowed U.V. determination of p-nitrophenol in the final solution without introducing a large error due to variation in the amount of protein in the sample against that in the blank. p-Cresol has a U.V. absorbance spectrum (λ_{max}; 280 nm, 300 nm ; isobestic point; 287 nm) which is similar to that of a protein. An accurate p-cresol determination would therefore be difficult.

The results of the experiment are shown in Table 4.20. Two different proteins were used; BSA (bovine serum albumin) which is a globular protein with a molecular weight around 68,000 and Lysozyme, a globular protein with a molecular weight around 14,600. BSA was used for initial experiments but its water solubility became a limiting factor. Lysozyme was used for the remainder of the experiments.

For all three initial concentrations of p-nitrophenol, the same percentage uptake by weight of dry silicalite was found for solutions containing from 0 to 1.5% soluble protein. The presence of protein in the solution did not have any effect on the sorption properties of the sieve. At high concentrations of protein

Table 4.20

Effect of Protein on the Uptake of p-Nitrophenol

from Aqueous Solution by Silicalite-1 (GS14) at 25°C

Sample	Protein Present/ $g(100ml)^{-1}$	Initial Conc. of p-Nitrophenol $/10^{-4}M$	Sorption (% w/w) on dry GS14
CON1	0	30.0 ± 0.3	9.8 ± 0.3
A_1	0.04	"	9.7 ± 0.3
B_1	0.07	"	9.4 ± 0.3
C_1	0.50	"	9.7 ± 0.3
E_1	1.5	"	9.4 ± 0.3
CON2	0	5.01 ± 0.04	3.07 ± 0.04
A_2	0.04	"	3.07 ± 0.04
B_2	0.07	"	3.07 ± 0.04
D_2	1.0	"	3.06 ± 0.04
E_2	1.5	"	3.05 ± 0.04
CON3	0	10.03 ± 0.09	6.25 ± 0.08
D_3	1.0	"	6.17 ± 0.08
E_3	1.5	"	6.10 ± 0.08

samples A_1, B_1; protein used - BSA; others - Lysozyme

(BSA 0.5%, Lysozyme 1.0%), a precipitate of protein was seen to form around the silicalite during the equilibration period (18 hours). From the above results this did not seem to hinder p-nitrophenol sorption. The precipitate did not form immediately and the layer around the silicalite, once formed, grew thicker. An experiment was therefore carried out to ensure that once the protein covering on the silicalite was complete, the sorption of p-nitrophenol was still unhindered.

Solutions of protein were equilibrated at 25°C with silicalite for 18 hours before adding p-nitrophenol to the bottles and equilibrating for a further 18 hours. The results of these experiments are shown in Table 4.21. Three initial concentrations of p-nitrophenol were used, all containing 1% (w/w) protein. Comparison of these results with those for the controls, shows that the uptake of p-nitrophenol is not affected by a protein covering on silicalite.

The effect of a genuine fermentation supernatant on the uptake of p-nitrophenol from solution was now determined. The supernatant used was from a single cell protein fermentation called the "Pruteen" process. The levels of soluble protein in this broth were especially high. To obtain information about the differences in the rate of uptake as well as the uptake achieved at equilibrium, the following experiment was set up. Four silicalite samples were equilibrated at 25°C for 0.25, 1.25, 4.25 and 18 hours respectively in a 70% (v/v) solution of "Pruteen" supernatant containing a known concentration of p-nitrophenol. A control experiment was carried out using p-nitrophenol in an aqueous salt solution of the sorbate. The results of these two experiments are shown in Table 4.22(i) and (ii).

The results for the control experiments show that within 15 minutes, 90% of the uptake expected at equilibrium is achieved. Equilibrium between the

Table 4.21

Effect of Protein on the Uptake of p-Nitrophenol

from Aqueous Solution by Silicalite-1 (GS14)

Previously Equilibrated in a Solution of Lysozyme (1% (w/w))

Sample	Lysozyme Present/ $g(100ml)^{-1}$	Initial Conc. of p-Nitrophenol $/10^{-4}M$	Sorption % (w/w) on dry GS14
CONTROL 1	0	30.0 ± 0.3	9.8 ± 0.3
D_1	1.0	"	9.3 ± 0.5
CONTROL 2	0	5.01 ± 0.04	3.07 ± 0.04
D_2	1.0	"	2.98 ± 0.04
CONTROL 3	0	10.03 ± 0.09	6.25 ± 0.08
D_3	1.0	"	6.09 ± 0.08

Table 4.22

Effect of Protein on the Uptake of p-Nitrophenol from Aqueous Solution by Silicalite-1 as a Function of Time

Sample	Initial Conc. p-Nitrophenol /10^{-4}M	Equilibration Time/h	Uptake (% w/w) on dry GS14
	(i) from aqueous salt solution (0.05M $(Na,H)_3PO_4$)		
A_1	30.1 ± 0.3	0.25	8.8 ± 0.3
B_1	"	1.25	10.1 ± 0.3
C_1	"	4.25	10.2 ± 0.3
D_1	"	18.0	9.7 ± 0.3
	(ii) from aqueous "Pruteen" solution (70% v/v)		
A_2	30.1 ± 0.3	0.25	5.0 ± 0.3
B_2	"	1.25	8.8 ± 0.3
D_2	"	4.25	7.4 ± 0.3
E_2	"	18.0	8.0 ± 0.3

aqueous phase and the sorbed phase is achieved in between 15 minutes and 1 hour. The sorption of p-nitrophenol from the supernatant after 15 minutes only gives 60% of the uptake obtained at equilibrium. This suggests that the sorption of p-nitrophenol from this supernatant is slightly slower than from a dilute salt solution. The uptake values after 1.25 and 4.25 hours show the same pattern as those of the control, both being close to the equilibrium value (18h). The value of uptake found at equilibrium is only 80% of the corresponding value found for the control. Whether or not this is a real observation, is uncertain, due to the difficulties involved in the analysis. The nature of the supernatant led to difficulties in the U.V. analysis of the final concentrations of p-nitrophenols. A constituent in the supernatant could cause a decrease in p-nitrophenol sorption by the supernatant in several ways. There may be a compound present which is preferentially sorbed by the silicalite or p-nitrophenol may undergo preferential sorption on a constituent. The supernatant as a whole could also alter the affinity of p-nitrophenol for the aqueous phase relative to the hydrophobic sorbent.

It has been shown that the sorption of p-cresol from aqueous solution by silicalite-1 is not perturbed by the presence of inorganic salt at concentration levels typical of a fermentation supernatant. Previous experiments on the sorption of phenol from LiCl solutions have shown that any effect would be advantageous. Larger salt concentrations, such as those used for the phenol experiments, would produce a salting out effect of the metabolite from the solution phase into the sieve. Similar experiments with p-nitrophenol have shown that the process is not significantly perturbed by protein, although there appears to be an 18% reduction in the uptake from "Pruteen" supernatant. It is likely that other substituted phenols, including ones of commercial interest could be sorbed from real fermentation broths by silicalite-1 without any

significant problems.

The long term effect of continuous exposure to a fermentation supernatant on the behaviour of the sieve can not be predicted. Protein lodged on the surface with its inevitable bacterial growth could present a problem. It would however be feasible to regenerate the sieve after long term exposure by either steam or chemical treatment. However, calcination is probably the prefered method, as this would not only remove the organic material but would also "heal" any broken siloxane bonds consequent on prolonged treatment in water.

4.5 EFFECT OF TEMPERATURE ON THE SORPTION PROPERTIES OF SILICALITE-1

A study was made of the effect of temperature on the sorption of phenol from aqueous solution by silicalite-1 (GS20). Isotherms were obtained at 15°C, 25°C and 40°C and are shown in Figure 4.46 (for experimental details see Chapter 3 (section 2 and 3.3.3 (18,19)) and Appendix 9). As the temperature of sorption decreases, the initial slope of the isotherm increases. In terms of sorption capacity, there appears to be a distinct difference in the position of the plateau obtained at 15°C and those at 25°C and 40°C. Table 4.23 contains the sorption parameters for these isotherms which give a more quantitative picture of the results.

The solubilities of phenol in water included in the table, are literature values (155). This data is considered reliable because the value quoted at 25°C agrees closely with the value of 0.912 mol dm^{-3} obtained earlier in this work by the method given in Chapter 3 (section 1.3.5). As the temperature rises, the degree of solvation of the phenol by water in the solution phase decreases. However, a resultant increase in the Langmuir coefficient for sorption, K_L is not observed.

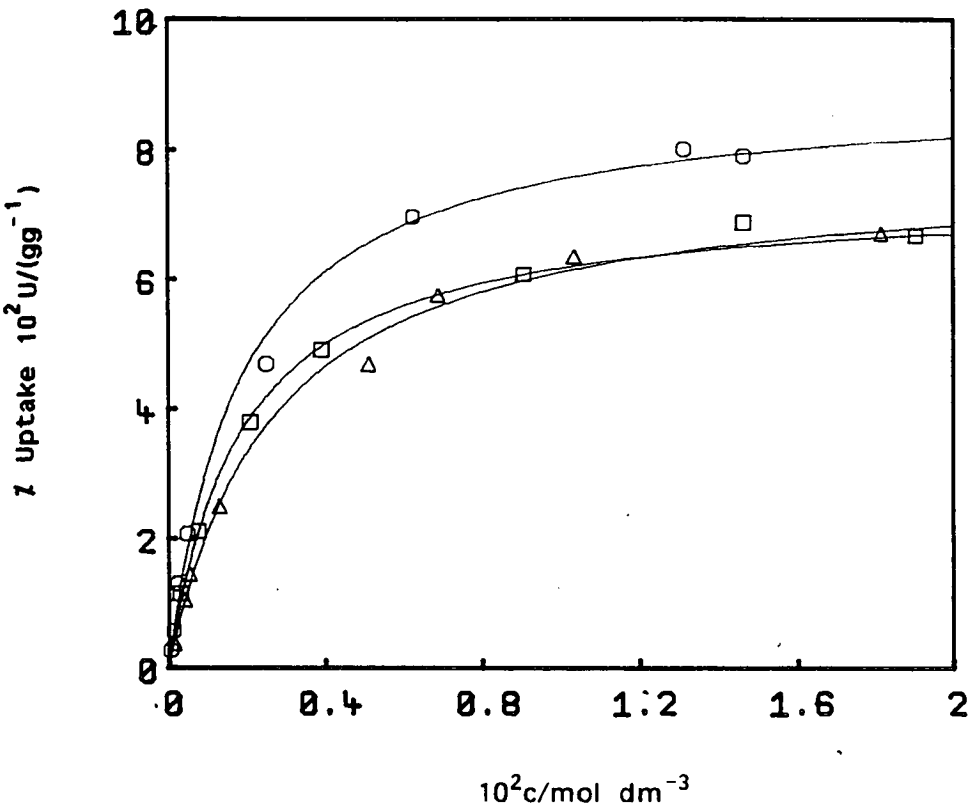

Figure 4.46 Sorption of Phenol from Aqueous Solution by Silicalite-1 (GS20);
○, 15°C; □, 25°C; △, 40°C.

Table 4.23

Sorption Parameters for the Uptake of

Phenol from Aqueous Solution by Silicalite-1 (GS20)

	15°C	25°C	40°C
$10^2 U_{max}$/ gg^{-1}	9.0 ± 0.7	7.4 ± 0.4	7.8 ± 0.7
U_{max}/ mol/unit cell	5.2 ± 0.4	4.3 ± 0.3	4.5 ± 0.4
$10^{-3} K_L$/ $dm^3 mol^{-1}$	0.55 ± 0.17	0.54 ± 0.12	0.38 ± 0.11
solubility s/mol dm^{-3}	0.840	0.915	1.02
10^4p/atm	1.801	4.526	13.25
K_{solv}/ mol $dm^{-3} atm^{-1}$	4659	2022	770
$10^{-4} K_{zeo}$/ atm^{-1}	26 ± 8.0	11 ± 2.4	2.9 ± 0.9

This is due to a simultaneous decrease with temperature in the binding coefficient of the phenol to the sieve. The values of K_L obtained are therefore as a result of a thermodynamic balance between the extent of solvation in the solution phase and the equilibrium coefficient for binding to the sieve. The two balancing factors lead to an overall decrease in K_L with temperature.

The values found for maximum uptake, revealed that at 15°C, there is an increase in the capacity of the sieve for phenol compared to the other two temperatures. The reason for this is unclear, although it is thought that it may be due to a phase change of the phenol inside the sieve at this relatively low temperature. One can visualise a sorbed phase which has more solid than liquid character at reduced temperature. It would be interesting to carry out further experiments at lower temperatures in order to assess whether or not there is a further increase in sorption capacity.

The temperature studies carried out have shown that an elevation in temperature would be a possible method for the desorption of sorbed species from silicalite. A reduction in temperature however, increases the selectivity of the molecular sieve for the organic sorbate. There is also some evidence that an increase in the packing efficiency of the sieve can be achieved at low temperatures.

4.6 SORPTION OF P-CRESOL FROM LOW MOLECULAR WEIGHT ALCOHOLS BY SILICALITE-1

4.6.1 Introduction

The selectivity of silicalite-1, in terms of the uptake of small organic molecules from aqueous solution, has been demonstrated. It has been shown that methylphenols will fill the pores of the sieve up to an average of 4

molecules per unit cell at maximum capacity. However, an efficient method for the removal of the material, once sorbed, has not yet been described.

The recent interest in the application of silicalite in the recovery of bioproducts from fermentation broths was described in Chapter 1 (section 1.4.2). This has promoted a search for cheap and efficient methods for the removal of sorbed material from the sieve.

A report from the U.S Department of energy (117), on ethanol recovery, describes several possibilities for ethanol desorption. Microwave stripping is described since ethanol, but not silicalite absorbs in the microwave region. It has since been reported however (144), that this method is not suitable for the removal of other organics. Gas stripping of ethanol was tried using CO_2, N_2 and O_2. The optimum stripping temperature in each case was found to be 85 - 90°C. In an attempt to lower the stripping temperature the use of SO_2 as a displacer gas was considered. With its high solubility in water it is also easier to subsequently remove from the sorbent. However disadvantages of this gas are its high corrosiveness and high solubility in ethanol.

The isolation of polar organics from drinking water by silicalite-1 has been described (144). Molecules such as acetone and acetonitrile were successfully recovered using solvent elution from 100% water to 100% methanol. Other techniques such as high pressure Soxhlet extraction, and microwave stripping were not as successful and abandoned in favour of the elution technique. Thermal desorption was also attempted but most analytes decomposed at the temperatures required for their removal from silicalite.

A patent (110) on the separation of normal paraffins from cyclic and branched chain paraffins described the use of a displacer molecule in solution as a desorbent. n-Tetradecane was removed from the pores of silicalite by a

16% solution of n-decane in isooctane. The disadvantage of this process is in the separation of the desired product from the high boiling displacer.

Work described in section 4.4.2, on the sorption of p-cresol from methanol / water mixtures, suggested an alcohol such as methanol would be a good candidate for use as a desorbent or as a displacer molecule in this type of system. A study was therefore carried out of the sorption of p-cresol from the low molecular weight alcohols; methanol, ethanol and propanol. It was hoped that the isotherms obtained would give a quantitative picture of the relative effectiveness of each alcohol as a desorbent.

4.6.2 Choice of Experimental Method

The method used to obtain sorption isotherms from aqueous solutions involved equilibration of the sorbate and solution phase in polypropylene bottles, in a water bath, followed by the removal of the solution phase and analysis by U.V spectrophotometry. This approach was inadequate when dealing with organic solutions.

A method had to be devised to ensure that water was totally excluded from the sieve before the experiment. Secondly, a bottle with an adequate sealing mechanism had to be designed. Finally, the previous method of analysis had to be revised. The results obtained with organic solvents gave very small differences between initial and final solution phase concentrations in relatively strong solutions. A simple comparison of concentration before and after equilibration was therefore inadequate.

The experimental method which was chosen is described in Chapter 3 (section 3.4). Figure 3.5 shows the glass vessel which was designed to allow a completely dry sample of silicalite to be obtained and to ensure an adequate

seal during equilibration.

4.6.3 Results and Discussion

The treatment of the results obtained was as follows: The dry weight of silicalite (GS20) used and initial concentration of the cresol were both known. After equilibration a small amount of silicalite (*ca* 0.01g) was removed. The cresol contained in this tiny sample was washed out with excess ethanol. The amount of cresol was determined by UV specrophotometry. From the concentration of cresol found in the ethanol solution, the original weight percent of cresol in the equilibrated sample could be determined. To convert this value into an uptake by dry weight of silicalite, the dry weight of the original equilibrated sample was determined by thermal gravimetric analysis.

Thermal analysis traces provided a value for the total amount of water, alcohol and cresol in the sample. Examples of typical traces obtained are shown in Figure 4.47. These are three traces obtained for the methanol and p-cresol experiments 3, 4 and 6. The large exotherms on the differential thermal analysis (DTA) traces show that p-cresol is indeed present and that a certain amount of it decomposes as it is desorbed from the sieve. However, it is unclear from the TGA (% weight loss with temperature) traces, how much of the weight loss below 180°C is due to p-cresol boiling out of the pores and how much is solvent. For this reason, thermal analysis could not be used as the sole technique for the determination of sorbed cresol.

Isotherms for the sorption of p-cresol from methanol, ethanol and propanol obtained by this method are shown in Figure 4.48. The slope of the isotherms decreases through the series from methanol to propanol. This is due to changes in the solvent - cresol interactions as well as in the interaction

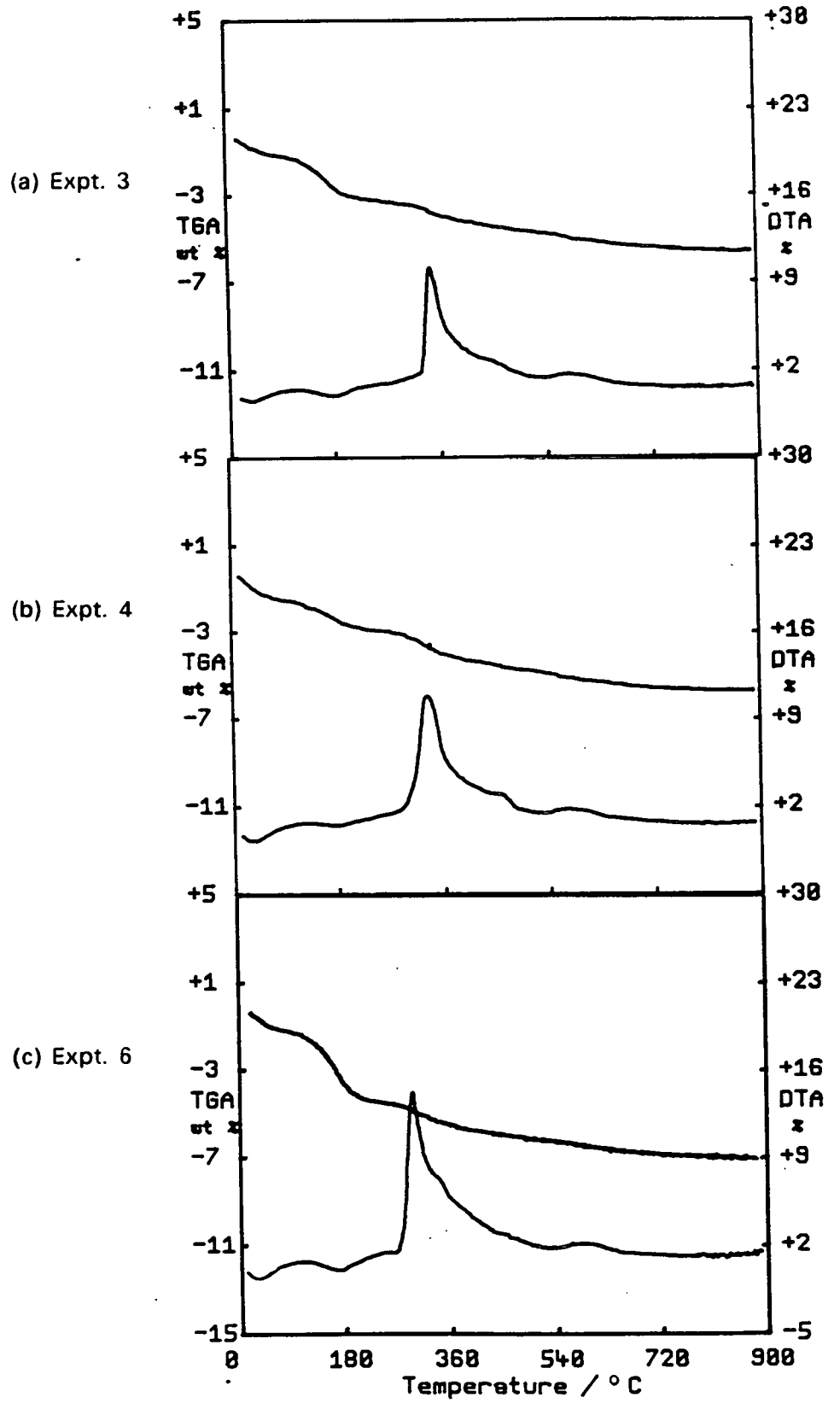

Figure 4.47 Thermal Analysis Traces of Silicalite-1 Samples Equilibrated with p-Cresol Solutions in Methanol at 25°C.

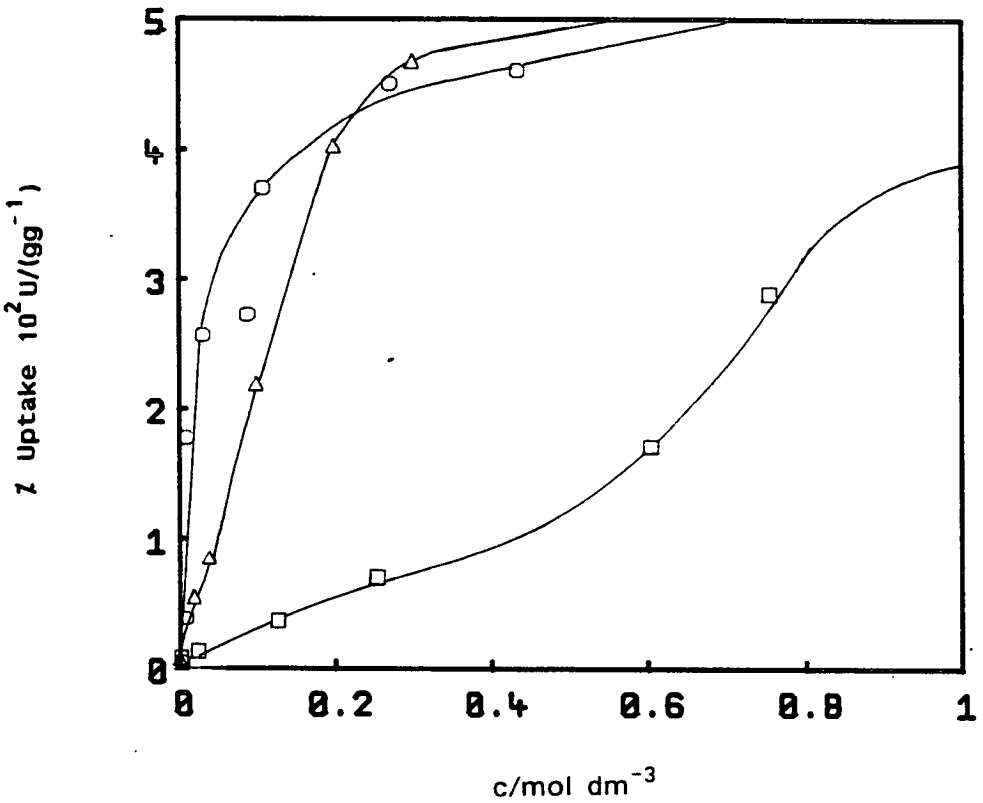

Figure 4.48 Sorption of p-Cresol from Low Molecular Weight Alcohols by Silicalite-1 (GS20) at 25°C; ○, methanol; △, ethanol; □, propanol.

between each solvent and the silicalite.

It has been shown by previous workers (139) that silicalite will sorb propanol in preference to ethanol, and ethanol in preference to methanol from their aqueous solutions. Therefore, both the increase in competitive sorption with alcohol chain length, coupled with the probable preference of p-cresol for the longer chain alcohols, gives rise to the observed isotherms.

It is clear from the amount of cresol required in solution before any significant sorption is obtained that any of the chosen alcohols would make suitable desorbents. The isotherms suggest that the efficiency of removal would increase as the chain length of the alcohol increases from C_1 to C_3.

The isotherms obtained did not follow simple Langmuir behaviour. S-shaped isotherms were observed for ethanol and propanol, becoming more distinct as the chain length of the alcohol increased. This effect was almost certainly due to competitive sorption. At low concentrations of p-cresol, the alcohol is sorbed preferentially. As the concentration of cresol increases, it displaces alcohol from sorption sites within the sieve. This gives rise to S-shaped isotherms. As the chain length of the alcohol increases, a greater concentration of cresol is necessary before it can successfully compete with the alcohol. The result of this phenomenon is that the propanol isotherm is almost concave in shape.

Thermal analysis coupled with solution phase analysis, made it possible to estimate the amount of organic solvent present in the sieve after equilibration. Subtraction of the amount of cresol sorbed from the total weight loss from each equilibrated sample, gave the amount of solvent plus water sorbed by the sieve. These values are given for each system in Tables 4.24 - 4.26, together with cresol uptake values. The water present will have been sorbed during the

Table 4.24

Sorption of p-Cresol and Methanol from Solution by Silicalite-1 (GS20) at 25°C

Sample	Final Conc. of p-Cresol in Methanol 10^2c/M	% Uptake of p-Cresol 10^2U/(gg^{-1})	% Uptake[a] of Methanol 10^2U/(gg^{-1}) (± 10%)
1	0.421 ± 0.005	0.26 ± 0.01	3.1
2	0.85 ± 0.01	0.38 ± 0.01	2.5
3	1.01 ± 0.02	1.77 ± 0.02	3.9
4	3.16 ± 0.05	2.56 ± 0.02	3.0
5	8.9 ± 0.1	2.72 ± 0.03	1.5
6	10.8 ± 0.1	3.7 ± 0.1	3.6
7	27.0 ± 0.4	4.5 ± 0.1	3.2
8	43.4 ± 0.4	4.6 ± 0.1	2.5

[a]Values include a small amount of water.

Table 4.25

Sorption of p-Cresol and Ethanol from Solution by Silicalite-1 (GS20) at 25°C

Sample	Final Conc. of p-Cresol in Ethanol 10^2c/M	% Uptake of p-Cresol 10^2U/(gg^{-1})	% Uptake[a] of Ethanol 10^2U/(gg^{-1}) (± 10%)
1	0.188 ± 0.002	0.040 ± 0.001	2.2
2	1.87 ± 0.02	0.54 ± 0.01	3.1
3	3.95 ± 0.06	0.85 ± 0.02	2.4
4	9.87 ± 0.02	2.19 ± 0.03	3.5
5	19.8 ± 0.3	4.02 ± 0.05	1.5
6	29.8 ± 0.5	4.67 ± 0.05	3.0
7	39.7 ± 0.6	5.34 ± 0.06	2.8

[a]Values include a small amount of water.

Table 4.26

Sorption of p-Cresol and Propanol from Solution by Silicalite-1 (GS20) at 25°C

Sample	Final Conc. of p-Cresol in Propanol 10^2c/M	% Uptake of p-Cresol $10^2(gg^{-1})$	% Uptake[a] of Propanol $10^2(gg^{-1})$ (± 10%)
1	0.247 ± 0.003	0.072 ± 0.005	8.4
3	12.7 ± 0.2	0.36 ± 0.02	7.9
4	25.3 ± 0.3	0.70 ± 0.02	6.4
5	60.5 ± 0.9	1.71 ± 0.04	6.5
6	75.5 ± 0.8	2.89 ± 0.05	5.5

[a]Values include a small amount of water.

washing stage and can be taken to vary little from one experiment to the next. In terms of sorbed solvent, one can see that methanol and ethanol do not appear to be competing successfully with p-cresol since their uptake values are constant over the whole cresol concentration range. Neither methanol nor ethanol exhibit pore filling from solution in silicalite. Therefore, although p-cresol may have to compete with these alcohols for specific sites within the sieve, there is enough free volume for these molecules to be sorbed simultaneously. Propanol shows an appreciable sorption at low p-cresol concentrations, which diminishes as the cresol concentration in solution increases. The latter is therefore an example of a true competitive equilibration. The effect that this has on the isotherm obtained has already been illustrated. Figure 4.49 shows the isotherm for the uptake of p-cresol from propanol together with the curve for propanol sorption over the same range. This clearly illustrates the phenomenon of competitive sorption.

These results have clearly shown that a desorbent would be much more effective if it is sorbed by the sieve to a significant extent. As one would expect, competitive sorption by a "displacer" molecule greatly enhances its capacity to bring about desorption of the desired organic. However one must bear in mind the regeneration of the sieve. In order to assess the best choice of desorbent for an industrial process, a choice would have to be made between the efficiency of the desorption process and the cost of the regeneration of the sieve.

4.7 THE USE OF SILICALITE-1 IN A COLUMN MODE

In order to successfully apply a sorbent to any automated process, it is necessary to assess its behaviour under conditions of continued regeneration and use. Previous sections have described the sorption of phenols from

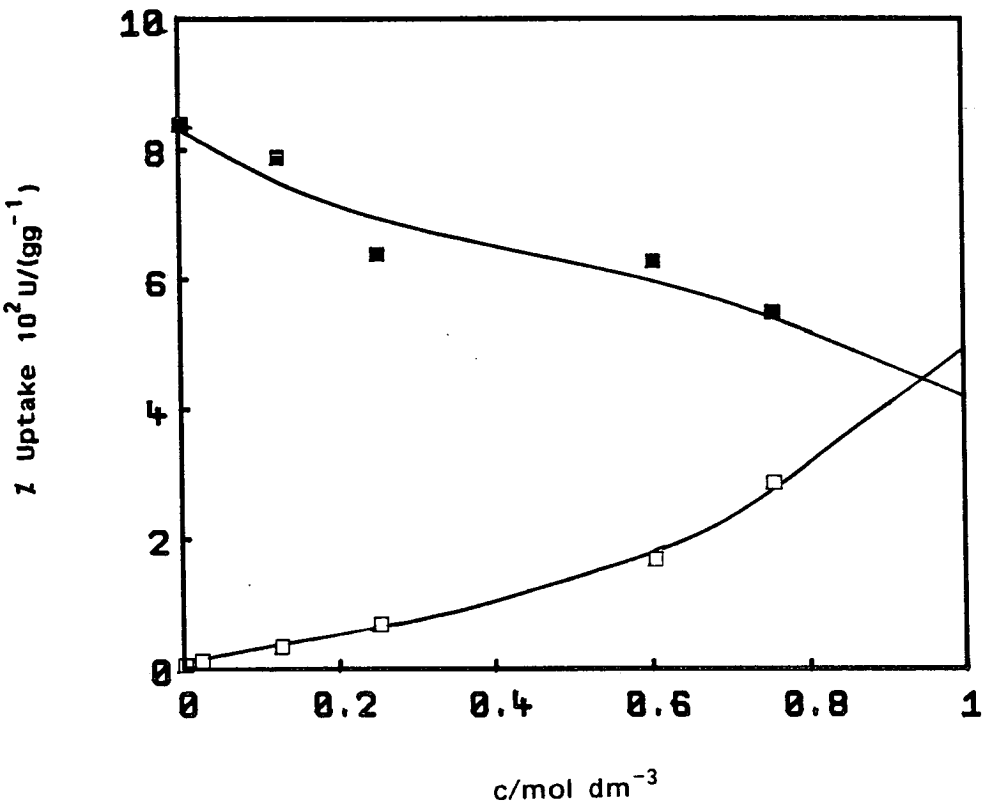

Figure 4.49 Uptake by Silicalite-1 (GS20) from p-Cresol Solution in Propanol at 25°C; ■, propanol; □, p-cresol.

aqueous solution by silicalite-1 under equilibrium conditions. It has been shown that silicalite-1 can successfully sorb small molecules from dilute solutions. Equilibrium experiments have also suggested that desorption of these molecules would occur in low molecular weight alcohols. It is highly probable that any application of silicalite in a large scale separation process would involve its use in a column mode. The cyclic loading then stripping of p-cresol on a silicalite column has therefore been studied.

The two batches of silicalite-1 which were used in this study were GS15 and GS17. A summary of some of the physical properties of these materials was shown in Table 4.5. They were made by an identical route, in the presence of piperazine at 150°C and therefore have similar characteristics. They are both highly hydrophobic and consist of large single crystals. The only detectable difference between the two samples is in terms of their relative bulk densities which are 0.60 g/cm^{-3} and 0.38 g/cm^{-3} respectively. The reasons for this are unclear, but the effect it has on their sorption behaviour will be described.

The apparatus shown in Chapter 3 (Figure 3.6) was used to carry out the experiments. The silicalite sample to be used was packed into a glass column and a feed solution passed through the bed with a regular flow rate using a peristaltic pump. The concentration of the feed solution was 5×10^{-3}M or 0.5 g dm^{-3} and the flow rate was kept between 0.33 and 0.5 cm^3min^{-1}. The cresol was then stripped off the column using 100% methanol at a similar flow rate to complete the cycle.

Samples of eluent were taken at regular intervals and analysed for p-cresol by U.V. spectrophotometry. The wavelength chosen for analysis was 270 nm. The extinction coefficients obtained for solutions of p-cresol in both methanol and in water were the same within experimental error at that wavelength (ε =

1274 ± 4 $dm^3mol^{-1}cm^{-1}$, see Table 3.1). It was therefore possible to analyse solutions of p-cresol that contained unknown quantities of methanol and water without errors arising from solvent effects.

The analysis of samples eluted during the sorption stage led to the construction of breakthrough curves for p-cresol. Similarly, the analysis of samples eluted during the stripping stage produced desorption curves.

4.7.1 Column Experiment 1

Column experiment 1 consisted of three sorption / desorption cycles on Column 1 containing 1.05 g of silicalite-1 sample GS15. The experimental details are given in Chapter 3 (section 3.5). The aim of the experiment was to keep the various running parameters of the column constant for each cycle in order to establish how silicalite behaved in a continuous mode. The variation in the flow rate of feed solution and stripping solvent on different cycles was due to the nature of the peristaltic pump used and was not intended. Although a flow rate of 1.5 cm^3 min^{-1} was sought for each run, it was not always achieved.

The first cycle carried out on Column 1 (C1a) produced a satisfactory breakthrough curve which is shown in Figure 4.50. It is characterised by a steep increase in p-cresol concentration of the eluent stream after an initial breakthrough at 90 cm^3 of feed solution or *ca* 5% by weight sorption on the column. The curve levels off at around 300 cm^3 eluted and mass balance figures (Table 4.27), show that silicalite sorbed 8.5% (w/w) when fully loaded. This figure is slightly higher than the 8.0% (w/w) previously obtained for fully loaded p-cresol at equilibrium (see Table 4.10).

The subsequent stripping stage produced a sharp desorption curve (Figure

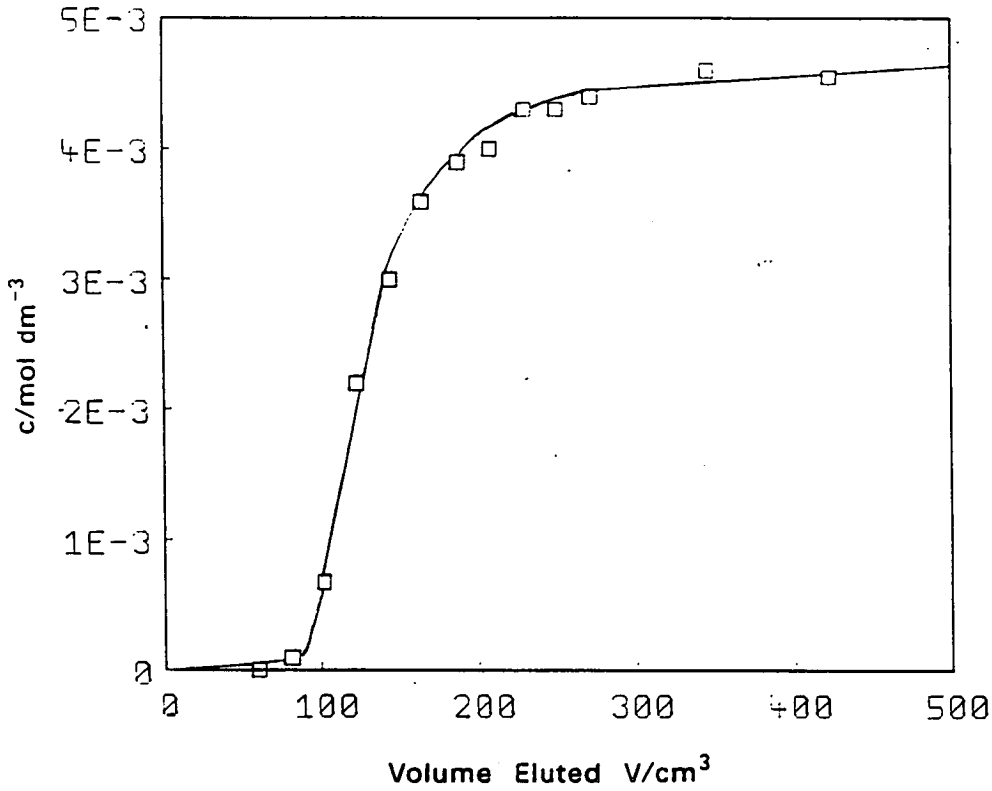

Figure 4.50 C1a Breakthrough Curve.

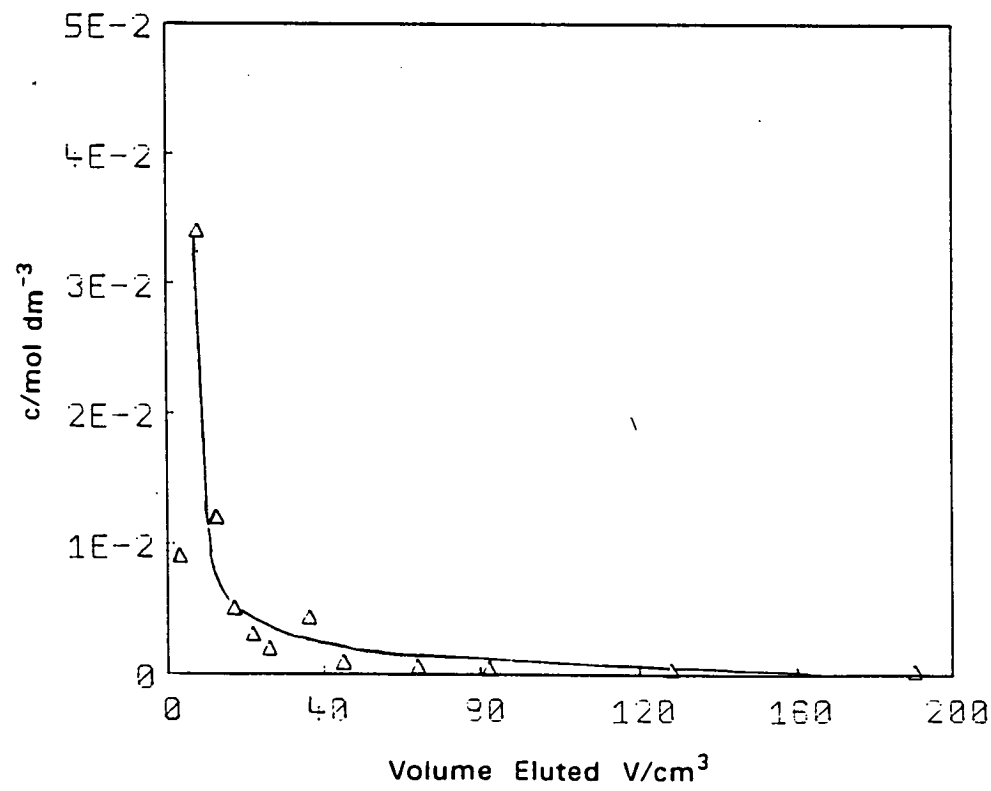

Figure 4.51 C1a Desorption Curve.

Table 4.27

Mass Balance Calculations for Column Experiment 1[a]

Run No.	C1a	C1b	C1c
Wt. of p-Cresol Sorbed from Previous Run / 10^{-2}g	-	4.36	4.46
Wt. of p-Cresol Sorbed During Run / 10^{-2}g	8.94	4.30	6.43
Total Wt. of p-Cresol on Column / 10^{-2}g	8.94	8.66	10.89
Total Wt. of p-Cresol Recovered on Stripping / 10^{-2}g	4.58	4.20	5.69

[a]Weights given refer to 1.05 g of dry silicalite in column.

4.51) in which 80% of the total p-cresol desorbed was removed in the first 45 cm^3 of solvent. However, mass balance figures reveal that only 51% of the cresol sorbed in C1a was successfully removed using methanol.

The breakthrough curve obtained for experiment C1b (Figure 4.52) was therefore affected by the residual p-cresol on the column from the previous run. The breakthrough of p-cresol in the eluent stream came almost immediately, followed by a steep increase up to almost the feed concentration as observed in C1a. Mass balance measurements indicated that 4.30×10^{-2}g of p-cresol was sorbed during this run, bringing the total weight of cresol on the column up to 8.66% (w/w), which is similar to that previously obtained. The stripping of column 1b (Figure 4.53), again only led to the desorption of 49% of the total cresol on the column.

Although experiment C1c led to a slightly larger total loading of the column (10.69% (w/w)), of which a greater percentage was desorbed (52%), the overall pattern observed was the same (Figures 4.54 and 4.55). The slight improvement in the mass balance for C1c was probably due to the slower flow rate used in both stages of the cycle.

The results of this experiment as a whole were encouraging, but it was decided to attempt to improve the fraction of p-cresol removed from the column during the stripping stage. The problem of a decrease in the slope of the breakthrough curve, due to loss of efficiency on continuous cycling, was also noted.

4.7.2 Column Experiment 2

In Column Experiment 2, a further three sorption / desorption experiments were carried out on a column containing 0.99 g of silicalite-1 sample GS17.

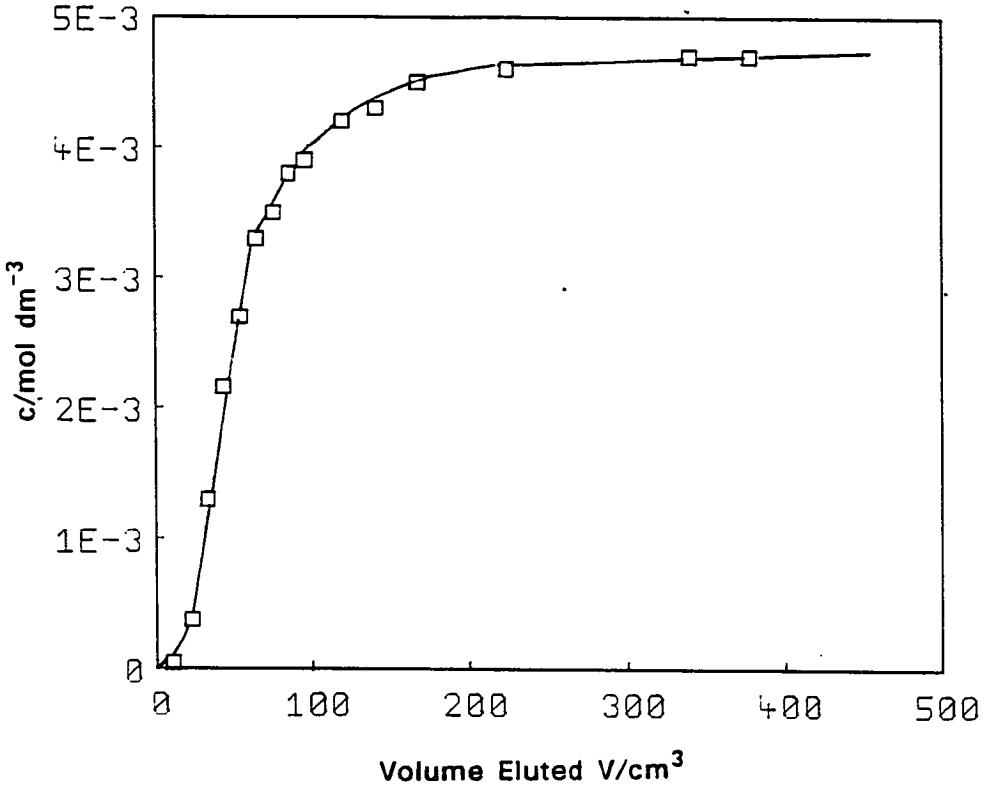

Figure 4.52 C1b Breakthrough Curve.

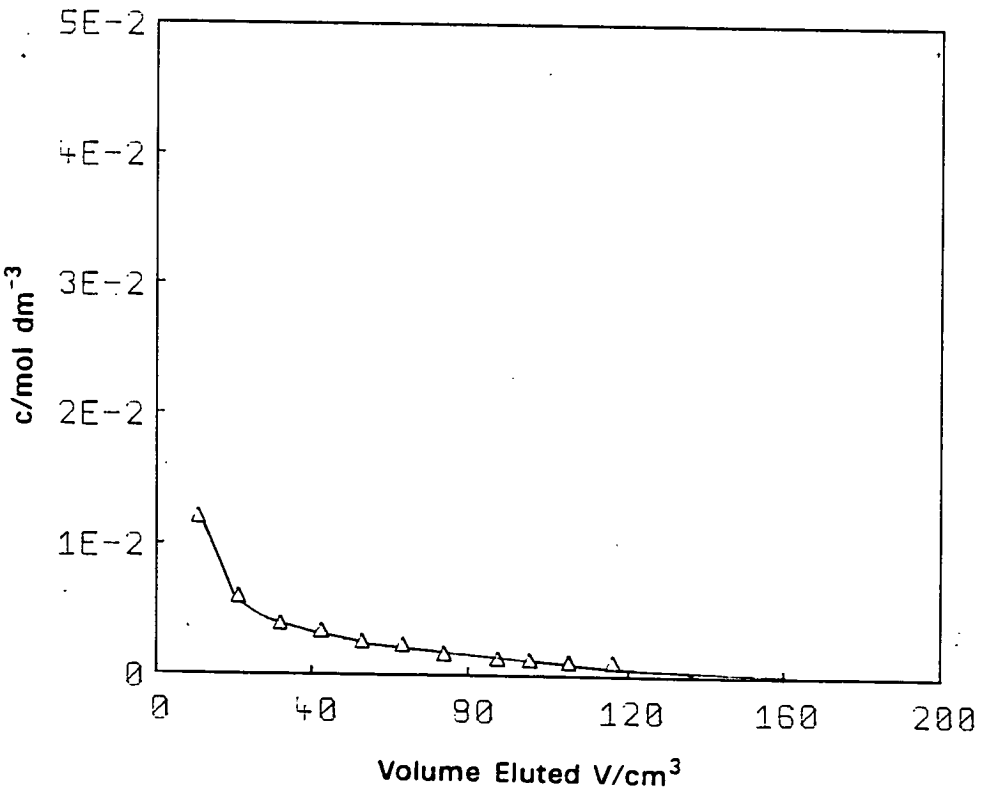

Figure 4.53 C1b Desorption Curve.

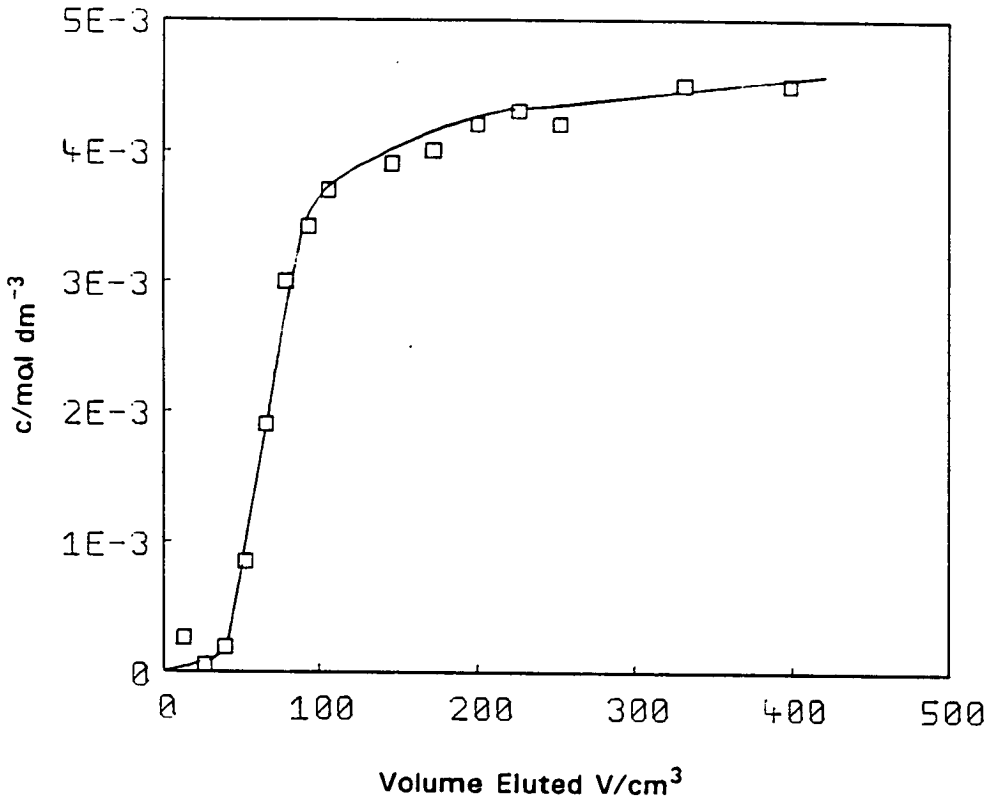

Figure 4.54 C1c Breakthrough Curve.

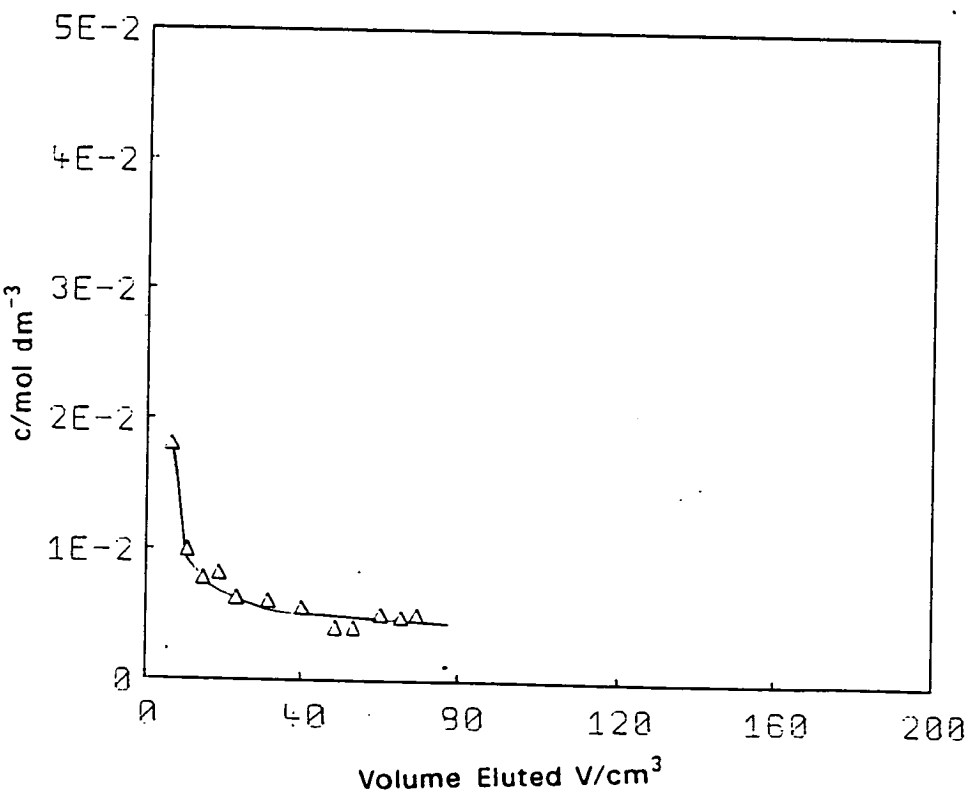

Figure 4.55 C1c Desorption Curve.

The details of the experiment are given in Chapter 3 (section 3.5). The breakthrough curve obtained for run C2a illustrates an extremely efficient process (Figure 4.56). A breakthrough of p-cresol did not occur until *ca* 7% (w/w) had been sorbed on the column. The total amount of cresol sorbed onto the column after a steep rise in eluent concentration and a flattening off of the curve was 9.2 x 10^{-2}g (Table 4.28). The improvement in the efficiency of loading and in the final capacity of the column using GS17 rather than GS15 is due to the difference in nature of the two batches. The particle size distributions of the two batches (Figure 4.6) are similar although GS17 has a slightly larger average crystal size. This, and other unknown factors, contribute to the fact that GS17 has a smaller bulk density than GS15. If a column packing material is to carry out an efficient separation, it is necessary to optimise the contact of the solution phase and the sieve. Optimum values of crystal size and bulk density must be found to achieve this. Increased pressure drop caused by small closely packed crystals must be balanced against loss of efficiency through diffusion limitations in larger crystals. It is clear that GS17 must be closer to the optimum material for this system than GS15.

In order to improve on the desorption figures obtained in Column Experiment 1, it was decided to heat the column to 40 - 45°C using a water jacket during the stripping stage. The desorption curve obtained (Figure 4.57) was steeper than those observed in C1a-c, suggesting greater efficiency of action. Mass balance measurements (Table 4.28) revealed that 75% of the total cresol on the column had been stripped. An increase of the methanol stripping temperature from room temperature to 40 - 45°C halved the amount of cresol left on the column after stripping from 4.4% (w/w) to 2.3% (w/w).

In C2a, 94% of the total cresol removed during the stripping stage was found in the first sample taken (10.5 cm^3). This suggests that "removable"

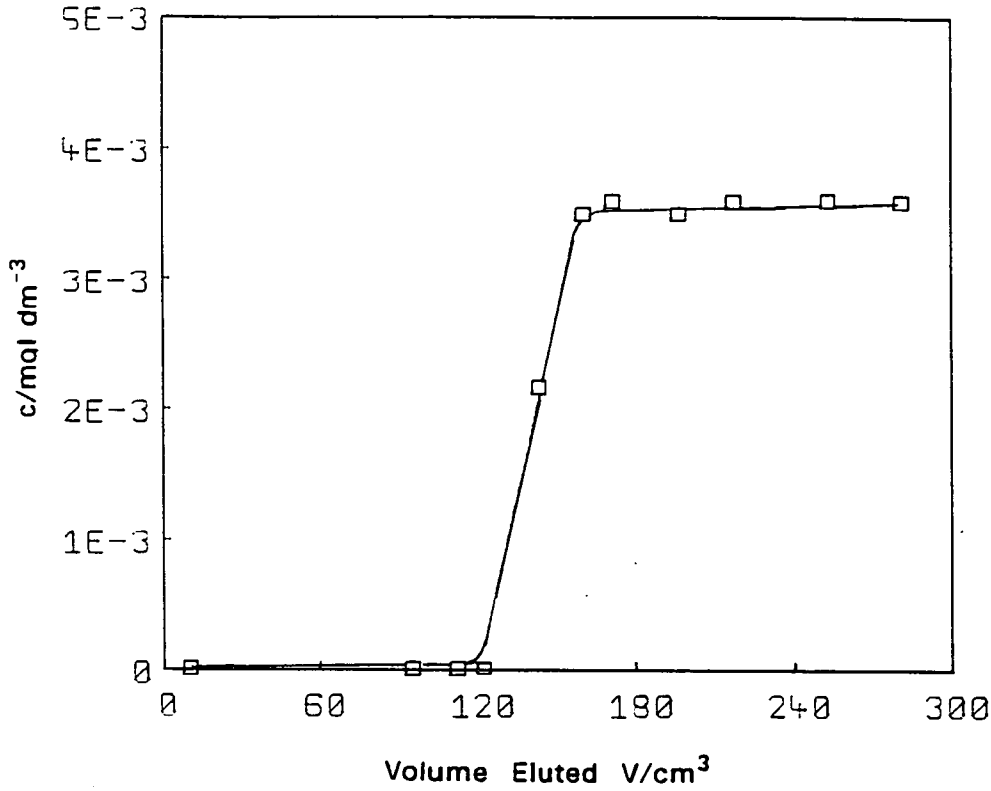

Figure 4.56 C2a Breakthrough Curve.

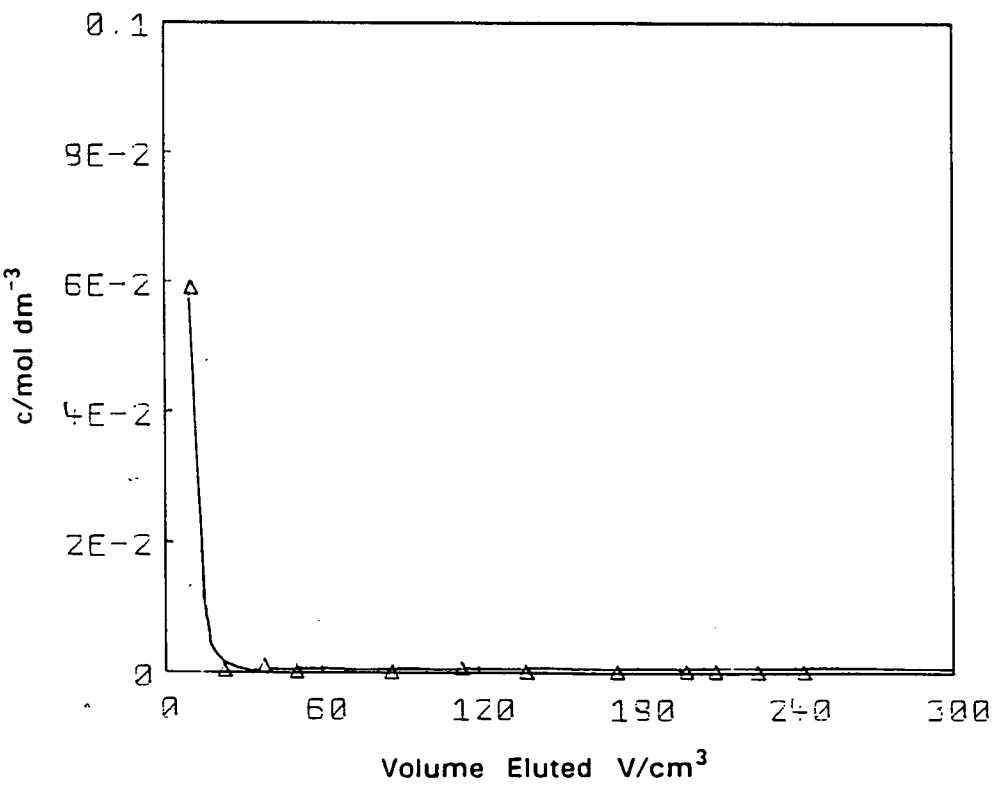

Figure 4.57 C2a Desorption Curve.

Table 4.28

Mass Balance Calculations for Column Experiment 2[a]

Run No.	C2a	C2b	C2c
Wt. of p-Cresol Sorbed from Previous Run / 10^{-2}g	-	2.34	2.33
Wt. of p-Cresol Sorbed During Run / 10^{-2}g	9.50	7.59	7.95
Total Wt. of p-Cresol on Column / 10^{-2}g	9.50	9.93	10.28
Total Wt. of p-Cresol Recovered on Stripping / 10^{-2}g	7.15	7.60	-

[a]Weights given refer to 0.99 g of dry silicalite in column.

p-cresol is very readily desorbed but there remains a fraction of the sorbate which cannot be encouraged to desorb, even on the addition of excess solvent. This observation implies that a type of energy minimum is set up between the p-cresol and the sieve at a certain value of coverage. It is possible that p-cresol is difficult to remove from a limited number of preferential sites within the sieve.

The second cycle in this experiment led to the sorption of 7.58×10^{-2}g bringing the total amount on the column up to 9.93×10^{-2}g, a similar total to the first run. The breakthrough curve obtained gave an earlier detection of p-cresol in the eluent stream (Figure 4.58). This was thought to be due to the residue on the column from the previous run. After breakthrough however, the increase in the p-cresol concentration of the eluent with time was slower than on the previous run. This suggests a decrease in the efficiency of the packing material caused by a closer packing of the crystals from the previous run. It is believed that as the pressure drop across the column increases, some of the eluent finds favourable channels through the packed bed, therefore escaping proper contact with the sieve.

The stripping stage for this run was carried out with the column temperature at 55 - 60°C. The desorption curve obtained (Figure 4.59) shows a higher initial concentration of p-cresol in the eluent with volume of methanol eluted. However, the mass balance results reveal that there is little improvement in the total amount of cresol stripped from the column. The residual p-cresol after run C2b was in fact identical to that left after run C2a. A second increase in stripping temperature of the stripping agent did not succeed in improving its desorption properties.

The column was then reloaded for a final run (C2c) in order to look at the

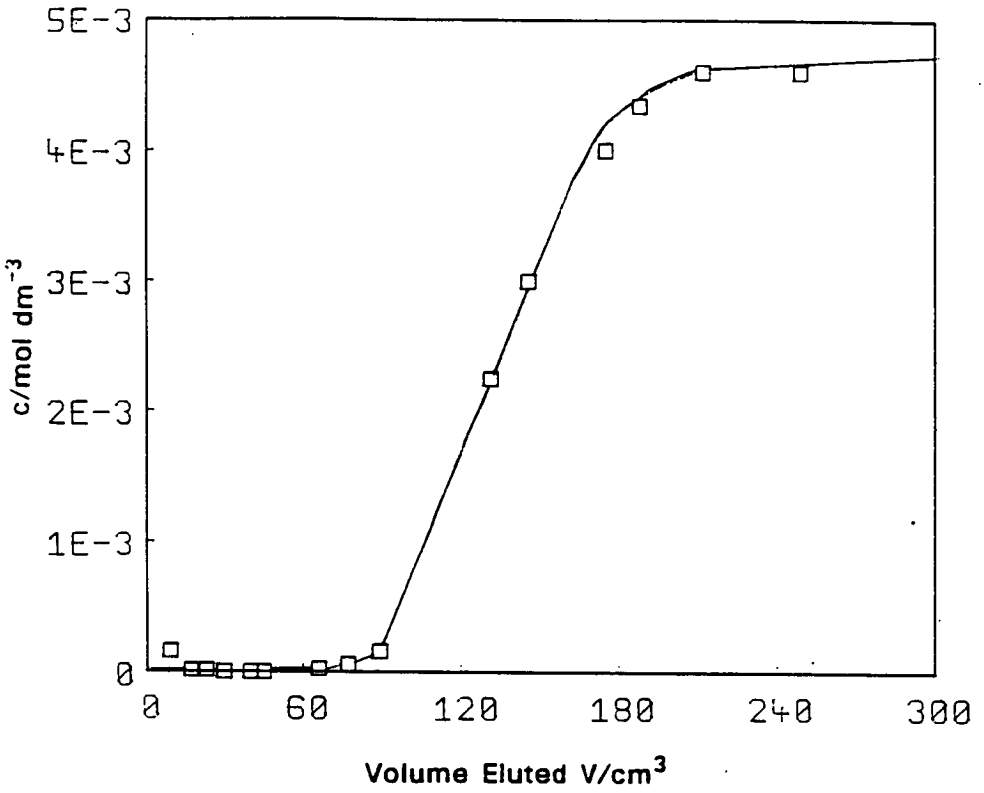

Figure 4.58 C2b Breakthrough Curve.

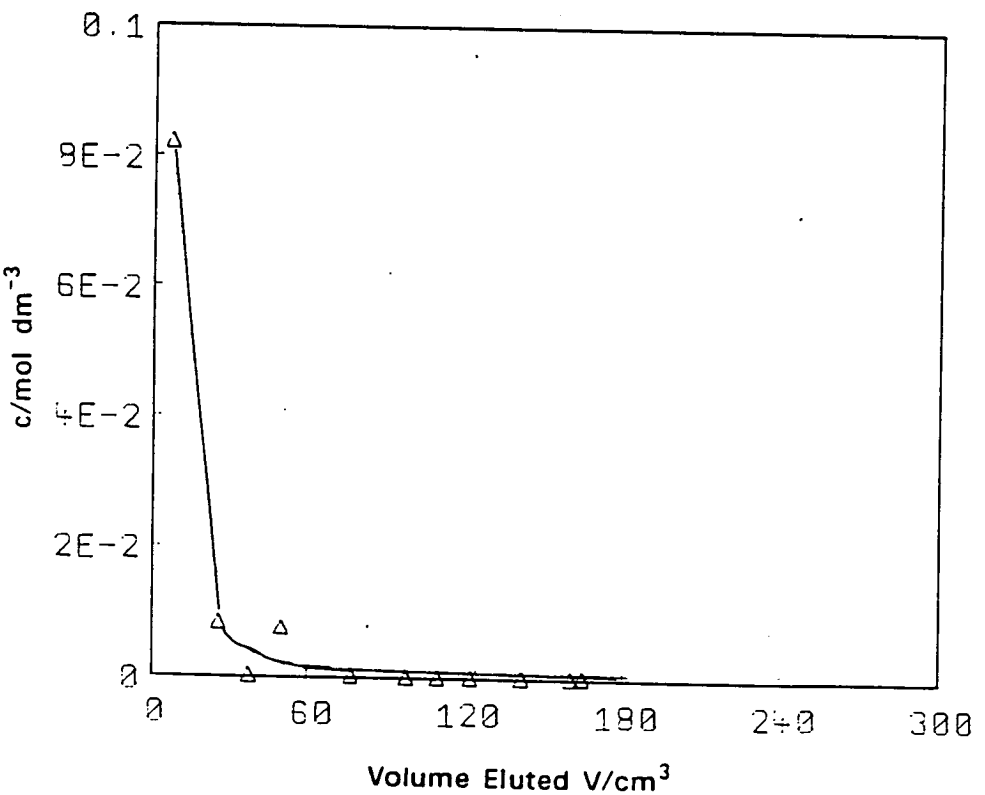

Figure 4.59 C2b Desorption Curve.

continuing trend in the efficiency of the column. The breakthrough curve obtained (Figure 4.60) shows a marked decrease in efficiency over the previous two. Although the mass balance figures show that a total amount of 10.3 x 10^{-2}g of p-cresol was present on the column at the end of this run, there is cause for concern over the changing shape of the breakthrough curves obtained on continuous cycling of a column packed with silicalite-1.

4.7.3 Conclusions

The two column experiments described, illustrated the use of silicalite-1 as a column packing. It was successfully used in a cyclic mode for the sorption of p-cresol from a dilute solution, with subsequent solvent stripping. However, the experiments have also highlighted several inherent problems in such a system.

The problem of residual organic left on the column could be tackled in several ways. It was shown that an increase in the temperature of the stripping solvent increased substantially the amount of organic recovered. The use of different solvents was not investigated, but equilibrium sorption isotherms obtained for the uptake of p-cresol from ethanol and propanol (section 4.7), suggest that they would be more efficient than methanol. However, the increase in the uptake of solvent by the sieve which would occur during the stripping stage for these higher alcohols, may lead to a problem with the regeneration of the column. The only regeneration carried out in the case of methanol was room temperature drying. It is also worth noting that in an industrial process, the cost of removing last traces of sorbed metabolite, would have to be weighed against the possibility of running the column at slightly less than its maximum capacity.

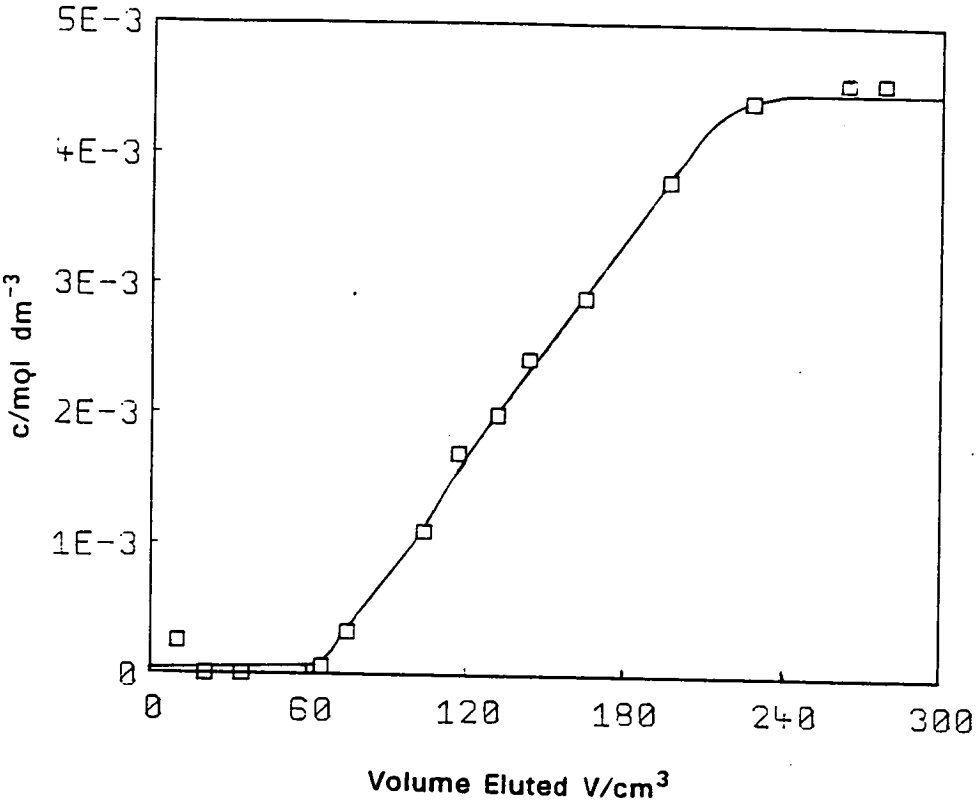

Figure 4.60 C2c Breakthrough Curve.

The second major problem with the system is the loss of efficiency of the column observed on repeated use, presumably caused by the packing down of the crystals. This could be overcome by using the silicalite on a non-porous support material. The problem of increase in pressure drop with column height could also be minimised in this way. On an industrial scale, the packing density of such a material would be a disadvantage. Larger single crystals or pelleted material are an obvious answer to the pressure problem, but the efficiency of the column would suffer under these conditions due to diffusion limitations.

Therefore, although it has been shown that silicalite can be used in cyclic sorption / desorption systems, there are various factors to be considered before the efficiency of such a system could be optimised.

CHAPTER 5
CONCLUSION

The work completed leaves no doubt that silicalite-1 is effective in the removal of certain aromatic phenols from water. The sorption isotherms obtained follow Langmuir behaviour and can be interpreted in terms of a simple theoretical model of the system. The magnitude of the Langmuir sorption coefficient for each phenol is controlled by two factors. A contribution from the binding interaction between the sorbate and the sieve (K_{zeo}) and another from the solvation of the sorbate in solution (K_{solv}).

The theoretical model shows that the Langmuir coefficient for sorption from aqueous solution is related to K_{zeo} and K_{solv} by, $K_L = K_{zeo}/K_{solv}$. Values of K_L and K_{solv}, determined experimentally for each sorbate, give values of K_{zeo}. The relative size of K_{zeo}, which is equivalent to the coefficient for sorption from the gas phase, for each sorbate, reveals the features which lead to strong binding. A phenolic hydroxyl group, free from ortho substituents is found to be a pre-requisite to strong binding. Within the group of molecules which satisfy the above critereon, size and shape are the dominant factors on which the relative sizes of K_{zeo} depend. The smaller and more symmetrical the molecule, the stronger the binding coefficient.

A favourable binding interaction therefore demands a hydrogen bonding type interaction coupled with a strong dispersive interaction between the molecule and the framework of the sieve. Any loss in symmetry of the molecule, reduces the dispersive interactions which occur. Furthermore, the less symmetric molecules tend to be larger, and unfavourable interactions can occur as they approach the limiting pore size of the sieve.

The origin of the polar interaction within the lattice of silicalite-1 is not immediately obvious. It is clear that the framework does not adhere to the ideal unit cell composition of $96SiO_2$ which would render it non-polar. The polar sites within the lattice are almost certainly as a result of broken siloxane bonds.

For the series of phenols studied, the coefficients for uptake from aqueous solution, K_L, are controlled by the relative strength of solvation of the sorbate molecule, since values of K_{solv} vary to a greater extent than those of K_{zeo}. The weakly solvated dimethylphenols are more readily sorbed from water than cresols, with the exception of 2,4-dimethylphenol, which has a molecular diameter which is too close to the limiting pore size of silicalite, to fit the observed pattern.

The main conclusion to be drawn from these experiments is that in a simple two component system, where the solvent is not significantly sorbed by the molecular sieve, the sorption behaviour of silicalite-1 can be explained in terms of the size and shape of the sorbate and the strength of its solvation shell. It is not unreasonable to suggest that if the gas phase sorption coefficient K_{zeo} was known for a sorbate, the Langmuir coefficient for sorption from aqueous solution K_L could be predicted, provided the vapour pressure and water solubility of that substance was known. Conversely, aqueous phase sorption provides a route by which to determine the gas phase sorption coefficient of molecules which have low vapour pressures.

Aqueous phase sorption experiments carried out in lithium chloride solution show that the value of K_{solv} decreases by a factor of 5 between pure aqueous solution and 5M LiCl solution, with a corresponding factor of 5 increase in K_L. This suggests that it may be possible to predict K_L values for the same sorbate

from different non sorbing solutions, if the solubility of the sorbate in that solution is known. Of course, there is a need for more experimental work, on a wider range of systems, before such a statement could be properly validated. However, the basis for such a study has been provided in this work.

It was found that the simple relationshp between K_L, K_{solv} and K_{zeo} did not hold for three component systems such as p-cresol, methanol and water. The reason for the breakdown in the theoretical treatment can be linked to the vast increase in the solubility of p-cresol in the mixed solvent. It is probable that the use of solubility of p-cresol is no longer applicable in the calculation of K_{solv}, at such high concentrations. The activity of p-cresol in solution would have to be determined and used in the calculation.

A study of the effect of the nature of the molecular sieve on the binding coefficient for each sorbate revealed that an increase in the relative number of hydrophilic centres in the sieve led to an increase in the binding coefficient of the phenol, but a reduction in sorption capacity. This observation suggests that in order to obtain optimum properties in terms of selectivity and capacity for a sorbate such as phenol, the presence of polar groups inside the sieve which were selective towards polar organic molecules rather than water, would be essential. An increase in water uptake by the sieve would be undesireable if the material was to be used in an aqueous phase separation process.

The introduction of aluminium into the framework does not provide such a site. The coefficient for the sorption of phenol by samples of ZSM-5 with increasing amounts of aluminium in the framework was not found to increase substantially, as opposed to water uptake, which showed a measureable increase.

It is likely that a radical change in the nature of the molecular sieve would

be required to obtain the optimum degree of selectivity and degree of uptake of polar organic molecules from aqueous solution. A recently discovered family of molecular sieves known as AlPO's (35), which are framework aluminophosphates, may provide an answer to this selectivity problem.

Silica molecular sieves however, are excellent candidates for the separation of less polar organics from water. It would be worthwhile to study the uptake of a molecule such as toluene by samples of silicalite-1 with different degrees of hydrophilicity. The effect of a change in the number of polar sites within the lattice on the sorption coefficient of such a molecule would be of interest.

External surface adsorption was shown to be negligible in comparison with zeolitic sorption for silicalite samples with crystal sizes greater than 6 μm. However a sample of silicalite-1 made up of 2 μm crystals showed substantial external surface adsorption. In terms of theoretical modelling this is an undesireable effect since ill-defined, multi-layer adsorption can take place. In a multi-component system, such as would be present in a commercial separation process, external surface adsorption would reduce the selectivity of the sieve. Larger molecules, not normally taken up, would adsorb on the external surface to an appreciable extent. It would therefore be important, for such an application, to ensure that the silicalite sample used consisted of large crystals with a smooth surface.

Framework topology is an important factor in determining the sorption properties of a molecular sieve. Silicalite-2, with a similar structure to silicalite-1 but with half its channel intersections larger by *ca* 30%, gave larger sorption capacities than silicalite-1 for certain sorbates. Therefore, small changes in framework topology can affect sorption behaviour, which is important when considering both practical application and theoretical

modelling.

Silicalite-1 and silicalite-2 both have a limiting pore size of 0.6 nm. This is a key point in terms of selectivity since molecules of larger dimensions are excluded. These molecular sieves therefore have an advantage over other sorbents such as activated charcoal, which contain macropores. In a biochemical separation process, uptake of protein and carbohydrates from the fermentation broth by material with macropores would lead to a substantial reduction in the sorption capacity for the desired product.

In this work, the presence of low molecular weight protein in aqueous solution was shown to have no effect on the uptake of p-nitrophenol by silicalite. This is an important point in terms of the applicability of silicalite to the downstream processing of fermentation broths where the presence of proteins and other surface active large molecules is highly likely.

The only disadvantage of the 0.6 nm pore size is that it limits the use of silicalite to the separation of products within the 0 to 0.6 nm size range. It would be useful, in order to provide greater scope, to make a silica molecular sieve with a larger limiting pore size. The discovery of such a material would be a positive step towards the commercialisation of silica molecular sieves in this field, as many molecules of potential interest, e.g. sugars, have diameters > 0.6 nm.

The ease of removal of sorbed material from the molecular sieve is an important consideration. The relative efficiency of the low molecular weight alcohols, propanol, ethanol and methanol for the removal of p-cresol from silicalite-1 is clearly established by the present work. Competitive sorption of the solvent by the molecular sieve greatly reduces the uptake of p-cresol. Propanol had a strong "displacer" action and was therefore found to be the

most efficient desorbent. For a 0.2M p-cresol solution in propanol, an uptake by silicalite-1 of only 2-3% (w/w) p-cresol was achieved. However, in a commercial separation process, it would not necessarily be advantageous to use a desorbent with a strong "displacer" action. The cost of the regeneration of the sieve would have to be taken into account.

The use of silicalite-1 in a column mode demonstrated the ease of regeneration of the sieve, as well as behaviour on continuous recycling. It is clear that in terms of the kinetics of sorption, the uptake and diffusion of p-cresol within silicalite-1 was fast enough to give sharp breakthrough curves. Desorption with methanol provides an efficient method for the removal of a certain amount of the sorbed cresol. A problem was encountered with residual cresol left in the sorbed phase after the desorption stage. This was eleviated, but not erradicated by an increase in the temperature of the desorbing solvent. The sorption of a fraction of p-cresol on especially favourable sites within the sieve is a possible explanation for this. The deactivation of these sites by a chemical or thermal method before use, may provide an answer to this problem. In a commercial process, it would perhaps be sensible to run such a column at a reduced capacity to avoid the cost of the removal of the last traces of sorbed material.

Continuous cycling revealed that the sieve lost efficiency, presumably due to the packing down of the crystals under pressure. The use of silicalite in a pelleted form or coated onto a non porous support material would solve this.

It appears from the present work that silicalite-1 would be an excellent sorbent for the downstream separation of bioproducts. It is unlikely that any major problems would be encountered in the operation of an industrial scale process. However, the commercial application of silicalite-1 or a similar

molecular sieve, depends on the occurrence of a separation problem to which it is uniquely suited.

References

1. A.F. Cronstedt, *Akad. Handl. Stockholm*, 1756, 17, 120
2. D.W. Breck, *Zeolite Molecular Sieves*, Wiley-Interscience, 1974, p188
3. R.M. Barrer, *J. Soc. Chem. Ind.*, 1945, 64, 130
4. D.W. Breck, W.G. Eversole, R.M. Milton, T.B. Reed and T.L. Thomas, *J. Amer. Chem. Soc.*, 1956, 78, 5963
5. R.M. Milton, U.S. Patent 2,882,244 (1959)
6. W.M. Meier, *Molecular Sieves*, Society of Chemical Industry, London, 1968, p10
7. W.J. Mortier, *Compilation of Extra Framework Sites in Zeolites*, Butterworths, London, 1982
8. D.W. Breck and T.B. Reed, *J. Amer. Chem. Soc.*, 1956, 78, 5972
9. P.A. Jacobs, *Carbonionic Activity of Zeolites*, Elsevier, 1977
10. G.T. Kokotailo, S.L. Lawton, D.H. Olson and W.M. Meier, *Nature*, 1978, 272, 437
11. G.T. Kokotailo, G.T. Chu, S.L. Lawton and W.M. Meier, *Nature*, 1978, 275, 119
12. E.L. Wu, S.L. Lawton, D.H. Olson, A.C. Rohrman,Jr. and G.T. Kokotailo, *J. Chem. Phys.*, 1979, 83, 2777
13. J. Dwyer and A. Dyer, *Chem. Ind.*, 2 April, 1984, p237
14. R.M. Barrer, *Zeolites and Clay Minerals as Sorbents and Molecular Sieves*, Academic Press, 1978, p37
15. G.W. Morey and E. Ingerson, *Econ. Geol.*, 1937, 32, 607
16. D.W. Breck, W.G. Eversole and R.M. Milton, *J. Amer. Chem. Soc.*, 1956, 78, 2338
17. D.W. Breck and N.A. Acara, U.S. Patent 3,216,789 (1965)
18. E.M. Flanigen, *Adv. Chem. Ser.*, 1973, 121, 119
19. R.M. Barrer and P.J. Denny, *J. Chem. Soc*, 1961, 971
20. R.M. Barrer, P.J. Denny and E.M. Flanigen, U.S. Patent 3,306,922 (1962)

21. R.M. Barrer and H. Villiger, *J. Chem. Soc., D*, 1969, 659

22. R.J. Argauer and G.R. Landolt, U.S. Patent 3,702,886 (1972)

23. Anon, *Chem. Week*, Jan 2, 1980, p29

24. R.M. Milton, *Molecular Sieves*, Wiley-Interscience, New York, 1974

25. R.W. Neuzil and J. W. Priegnitz, U.S. Patent 4,349,668 (1982)

26. P.B. Venuto and E.T. Habib,Jr., *Catal. Rev.-Sci. Eng.*, 1978, 18, 1

27. D.P. Burke, *Chem. Week*, Mar 28, 1979, 42

28. J.A. Rabo, R.D. Bezman and M.L. Poutsma, *Acta. Phys. Chem.*, 1978, 24, 39

29. W.W. Pitt, Jr., G.L. Haag and D.D. Lee, *Biotech. and Bioeng.*, 1983, 25, 123

30. N.Y. Chen, *J. Phys. Chem*, 1976, 80, 60

31. D.H. Olson, W.O. Haag and R.M. Lago, *J. Catalysis*, 1980, 61, 390

32. R.W. Grose and E.M. Flanigen, U.S. Patent 4,061,724 (1977)

33. E.M. Flanigen, J.M. Bennett, R.W. Grose, J.P. Cohen, R.L. Patton and R.M. Kirchner, *Nature*, 1978, 271, 512

34. C.A. Fyfe and J.M. Thomas, *Nature*, 1982, 296, 530

35. E.M. Flanigen and R.L. Patton, U.S. Patent 4,073,865 (1978)

36. D.M. Bibby, N.B. Milestone and L.P. Aldridge, *Nature*, 1979, 280, 664

37. A. Araya and B.M. Lowe, *J. Catalysis* 1984, 85, 135

38. J.L. Schlenker, W.J. Rohrbaugh, P. Chu, E.W. Valyocsik and G.T. Kokotailo, *Zeolites*, 1985, 5, 355

39. R.W. Grose and E.M. Flanigen, U.S.Patent 4,104,294 (1978)

40. R.B. LaPierre, A.C. Rohrmann, Jr., J.L Schlenker, J.P. Wood, M.K. Rubin and W.J. Rohrbaugh, *Zeolites*, 1985, 5, 346

41. D.M. Bibby and L.M. Parker, *Zeolites*, 1983, 3, 11

42. J.L. Schlenker, F.G. Dwyer, E.E. Jenkins, W.J. Rohrbaugh and G.T. Kokotailo, *Nature*, 1981, 294, 340

43. L.M. Parker and D.M. Bibby, *Zeolites*, 1983, 3, 8

44. A.C. Rohrman, Jr., R.B. LaPierre, J.L. Schlenker, J.D. Wood, E.W. Valyocsik,

M.K. Rubin, J.B. Higgins and W.J. Rohr, *Zeolites*, 1985, 5, 352

45. G.T. Kokotailo, J.L. Schlenker, F.G. Dwyer and E.W. Valyocsik, *Zeolites*, 1985, 5, 349

46. J.L. Casci, B.M. Lowe and T.V. Whittam, Eur. Pat. Appl. 63,436 (1982)

47. D.M. Bibby and M.P. Dale *Nature*, 1985, 317, 157

48. R.M. Barrer and J.F. Cole, *J. Chem. Soc.*, A, 1970, 1516

49. R.M. Barrer, *Adv. Chem. Ser.*, 1973, 121, 1

50. M.G. Howden, *CSIR Report CENG*, 1982, 413

51. S.G. Fegan and B.M. Lowe, *J. Chem. Soc. Faraday Trans. 1*, 1986, 82, 785

52. F.G. Dwyer and E.E. Jenkins, U.S. Patent 3,941,871 (1976)

53. L. Falth and U. Hakanson, *Recent Progress Reports, 5th Int. Conf. Zeolites*, (Ed. R. Sersale, C. Collela and R. Aiello), 1980, 41

54. M. Ghamami and L.B. Sand, *Zeolites*, 1983, 3, 155

55. K.J. Chao, T.C. Tasai, M-S. Chen and I. Wang, *J. Chem. Soc., Faraday Trans.* 1, 1981, 77, 547

56. R. Von Ballmoos, *The ^{18}O-Exchange Method in Zeolite Chemistry*, (Salle and Sauerlander, Frankfurt and Main), 1981, p74

57. G.H. Kuehl, Eur. Pat. Appl. 93,519 (1983)

58. D.M. Bibby, N.B. Milestone and L.P. Aldridge, *Nature*, 1980, 285, 30

59. M. Ghamami and L.B. Sand, *Zeolites*, 1983, 3, 89

60. S.G. Fegan and B.M. Lowe, *J. Chem. Soc., Faraday Trans. 1*, 1986, 82, 801

61. K.R. Franklin, University of Edinburgh, unpublished results

62. G.D. Price, J.J. Pluth, J.V. Smith, J.M. Bennet and R.L. Patton, *J. Am. Chem. Soc.*, 1982, 104, 5971

63. P. Chu and N.J. Woodbury, U.S. Patent 3,709,979 (1973)

64. L.D. Rollman and E.W. Valyocsik, U.S. Patent 4,108,881 (1978)

65. M.K. Rubin, C.J. Plank, E.J. Rosinsky and F.G. Dwyer, Eur. Pat. Appl. 14,059 (1980)

66. K.R. Franklin, University of Edinburgh, unpublished results

67. B.M. Lowe, *Zeolites*, 1983, 3, 300

68. S.G. Fegan, PhD Thesis, 1985, University of Edinburgh

69. D.H. Olson, G.T. Kokotailo and S.L. Lawton, *J. Phys. Chem.*, 1981, 85, 2238

70. P. Wu, A. Debebe and Y.H. Ma, *Zeolites*, 1983, 3, 118

71. C.G. Pope, *J. Phys. Chem.*, 1986, 90, 835

72. J.R. Anderson, K. Foger, T. Mole, R.A. Rajadhyaksha and J.V. Sanders, *J. Catalysis*, 1979, 58, 114

73. C.G. Pope, *J. Phys. Chem.*, 1984, 88, 6312

74. U. Lohse and B. Fahlke, *Chem. Tech.*, 1983, 35, 350

75. Von. R. Wendt, H. Thamm, K. Fiedler and H. Stach, *Z. Phys. Chemie*, Leipzig, 1985, 266, 289

76. H. Thamm and N.I. Regent, *Z. Chem.*, 1982, 22, 232

77. C.D. Chriswell and D.T. Gjerde, *Anal. Chem.*, 1982, 54, 1911

78. G.M.W. Shultz-Sibbel, D.T. Gjerde, C.D. Chriswell and J.S. Fritz, *Talanta*, 1982, 29, 452

79. T.P.J. Izod and J.A. Duisman, U.S. Patent 4,375,568 (1983)

80. D.J. Campbell, B.M. Lowe, A.G. Rowley and R.M. Williams, *Analytica Chimica Acta*, 1985, 172, 347

81. D.B. Broughton and C.G. Gerhold, U.S. Patent 2,985,589 (1961)

82. Anon, *Chem. & Eng. News*, Oct 6th 1975, p18

83. D.W. Sundstorm and F.G. Krautz, *J. Chem. Eng. Data*, 13, 1968

84. R.W. Neuzil, U.S. Patent 3,686,342 (1972)

85. R.W. Neuzil, U.S. Patent 4,326,092 (1982)

86. A.J. deRosset, U.S. Patent 3,917,734 (1975)

87. R.W. Neuzil, D.H. Rosback, R.H. Jensen, J.R. Teague and A.J. deRosset, *Chemtech*, 1980, 498

88. R.W. Neuzil, U.S. Patent 3,969,422 (1976)

89. R.W. Neuzil, U.S. Patent 4,386,225 (1983)

90. R.M. Dessau, *Adsorption and Ion Exchange with Synthetic Zeolites*, ACS Symp. Ser. No. 135, ed. W.H. Flank, 1980, 123

91. R.M. Dessau, Eur. Pat. Appl. 31,676 (1980)

92. R.M. Dessau, U.S. Patent 4,487,688 (1984)

93. R.M. Dessau, U.S. Patent 4,517,402 (1985)

94. M. Morbidelli, G. Storti and S. Carra, *Ind. Eng. Chem. Fundam.*, 1986, 25, 89

95. H. Odawara, Y. Noguchi and M. Ohno, U.S. Patent 4,014,711 (1977)

96. R.W. Neuzil and J.W. Priegnitz, U.S. Patent 4,340,724 (1982)

97. R.W. Neuzil and J.W. Priegnitz, U.S. Patent 4,349,668 (1982)

98. R.W. Neuzil and J.W. Priegnitz, U.S. Patent 4,373,025 (1983)

99. S. Kulprathipanja and R.W. Neuzil, U.S. Patent 4,372,876 (1983)

100. H. Tu and J.E. Rojo, U.S. Patent 4,345,946 (1982)

101. J.D. Sherman and C.C. Chao, Eur. Pat. Appl. 115,631, (1984)

102. J.D. Sherman, U.S. Patent, 4,456,774 (1984)

103. T.P.J. Izod, Eur. Pat. Appl. 13,451, (1982)

104. D.E. Earls, U.S. Patent Appl. 880,561 (1978)

105. R.M. Dessau, U.S. Patent, 4,272,288 (1981)

106. G.W. Young, J.R. Kiovsky and P.B. Koradia, *Liquid Phase Drying Applications of Zeolites*, ACS Symp. Ser. No. 135, ed. W.H. Flank, 1980, 201

107. V.T. Stannet, T.A. DuPlessis and A.M. Goineau, *J. Appl. Polymer Sci.*, 1972, 16, 2847

108. V.D. Mundale, A.L. Ravimohan and S.R. Lohokare, *CEW, Chem. Eng. World*, 1979, 14, 103

109. M.T. Cleary and R.W. Neuzil, U.S. Patent 4,329,280 (1982)

110. S. Kulprathipanja and R.W. Neuzil, U.S. Patent 4,367,364 (1983)

111. S. Kulprathipanja, U.S. Patent 4,433,195 (1984)

112. Y. Ma and Y.S. Lin, *AIChE Symp. Ser.*, 1985, 81, 39

113. F.F. Hartline, *Science*, 1979, 206, 41

114. T.K. Murphy, H.W. Blanch and C.R. Wilke, *Process Biochemistry*, Nov/Dec 1982, p6

115. W. A. Shumacher and V.W.S. Hwa, *Report Oak Ridge, Tenn: ORNL/MIT-298*, 1980, Part 1

116. W.A. Schumacher and V.W.S. Hwa, *Report Oak Ridge, Tenn: ORNL/MIT-304*, 1981, Part 2

117. C.D. Chriswell, H.R. Burkholder and D.J. Gjerde, *Ethanol Purification by Adsorption*, Technical Quarterly Progress Report, April-June 1981, Ames Laboratory, Iowa State University, U.S. Dept. of Energy Contract No. W-7405-Eng-82 Iowa State University, Ames, Iowa, USA, Rep. 154783 (1981)

118. C.S. Oulman and C.D. Chriswell, U.S. Patent 4,277,635 (1981)

119. N.Y. Chen and J.N. Miale, U.S. Patent 4,420,561 (1983)

120. R.M. Dessau and W.O. Haag, U.S. Patent 4,442,210 (1984)

121. N.Y. Chen, *J. Phys. Chem.*, 1976, 80, 60

122. A.J. Groszek, Eur. Pat. Appl., 101,254 (1984)

123. D.R. Garg and J.P. Ausikaitis, Canadian Patent CA. 1,195,258 (1985)

124. S.M. Klein and W.H. Abraham, *AIChE Symp. Ser.*, 1983, 79, 53

125. S.M. Klein, *Adsorption of Ethanol and Water Vapour by Silicalite, a Hydrophobic Molecular Sieve*, MS Thesis, Iowa State University, 1982

126. F.A. Farhadpour, A. Bono and U. Tuzin, *EBC - Symposium on Biotechnology*, 1983, Monograph IX

127. W.W. Pitt,Jr., G.L. Haag and D.D. Lee, *Biotech. Bioeng.*, 1983, 25, 123

128. E.K. Pye and A.E. Humphrey, *Production of Liquid Fuel from Cellulosic Biomass*, 1977, University of Pensilvania, Contract EY-76-5-02-4070

129. M. Larsson and B. Mattiason, *Chem. Ind.*, 1984, 428

130. R.W. Lencki, C.W. Robinson and M. Moo-Young, *Biotech. and Bioeng. Symp.*, 1983, 617, 608

131. S. Bui, X. Verykios and R. Mutharason, *Ind. Eng. Chem. Process Des. Dev.*, 1985, 24, 1209

132. J.C. Chao and C-Y Jenq, U.K. Pat. Appl., GB 2096125A (1982)

133. S. Kulprathipanja and R.W. Neuzil, U.S. Patent 4,343,623 (1982)

134. J.M. Curling, D. Low and J.M. Cooney, *Int. Biotech. Lab.*, Sept/Oct 1984, p8

135. Anon, *Chem. in Britain*, Oct. 1983, 808

136. H. Fukuda, T. Ogawa and T. Fujii, Eur. Pat. Appl. EP 178,153 (1984)

137. R.M. Busche, *Biot. Bioeng. Symp.*, 1983, 13, 597

138. I.S. Maddox, *Biotech. Letters*, 1982, 4, 759

139. N.B. Milestone and D.M. Bibby, *J. Chem. Tech. Biotechnol*, 1981, 31, 732

140. L.V. Denisova and A.T. Tolmacheu, *Russ. J. Phys. Chem.*, 1975, 49, 1050

141. N.B. Milestone and D.M. Bibby, *J. Chem. Technol. Biotechnol.*, 1983, 34A, 73

142. G.S. Haegh, *Stud. Surf. Sci. Catal.*, 1985, 24, 605

143. S.T. Wilson, B.M. Lok, C.A. Messina, T.R. Cannan and E.M. Flanigen, *J. Am. Chem. Soc.*, 1982, 104, 1146

144. C.D. Chriswell, D.J. Gjerde, G. Shultz-Sibel, J.S. Fritz and I. Ogawa, *An evaluation of the adsorption properties of silicalite for potential application in the isolation of low molecular weight organics from drinking water*, January 1983, EPA-600/1-83-001, Ames Laboratory, USDOE, Iowa State University

145. E. Narita, N. Horiguchi and T. Okabe, *Chemistry Letters*, 1985, 787

146. A.W. Adamson, *Physical Chemistry of Surfaces*, 2nd Adition, Interscience, (1967), p565

147. I. Langmuir, *J. Am. Chem. Soc.*, 1918, 40, 1361

148. G. Halsey and H.S. Taylor, *J. Chem. Phys.*, 1947, 15, 624

149. S.P. Zhdanov, A.V. Kiselev and L.F. Pavlova, *Kinetics and Catalysis (U.S.S.R.)*, 1962, 3, 391

150. E.W. Volyocsik and L.D. Rollman, U.S. Patent 4,205,053 (1980)

151. M.K. Rubin, E.J. Rosinsky and C.J. Plank, U.S. Patent 4,151,189 (1979)

152. R. Von Ballmoos and W.M. Meier, *Nature*, 1981, 289, 782

153. Z. Gabelica, B. Nagy, E.G.Derouane and J.P. Gilson, *Clay Minerals* 1984, 19, 803

154. M.K. Rubin, C.J. Plank, E.J. Rosinsky and F.G. Dwyer, Eur. Pat. Appl. 14059 (1980)

155. A. Seidell, *Solubilities of Organic Compounds, Vol 2, 2nd Ed.* D. Van Nostrand, 1941

156. D.R. Stull, *Ind. Eng. Chem.*, 1947, 39, 517

157. G. Kortüm, W. Vogel and K. Andrussow, *Dissociation Constants of Organic Acids in Aqueous Solution*, Butterworths, 1961, p 430-432

Appendices

Appendix 1

Calculation of Vapour Pressures at 25°C.

Sample calculation for phenol;

Information given;

Temperature /°C	Vapour pressure / mmHg
62.5	5
73.5	10

The following calculation was made to obtain a value for the vapour pressure at 25°C in atmospheres.

$$\Delta H = -R \ln(P_1/P_2) \{T_1T_2/(T_2 - T_1)\}$$

where P_1 and P_2 are values of vapour pressure for given temperatures T_1 and T_2 respectively.

therefore for phenol, $\Delta H = 59.337$ kJ mol^{-1}.

Substitution of this value into the following equation

$$P_3 = P_2 e^{(-\Delta H/R) \{1/T_3 - 1/T_2\}}$$

where P_3 is the value of vapour pressure at T_3,
gives for T_3 = 297K (25°C), P_3 = 0.344 mmHg or 4.526×10^{-4} atm.

Appendix 2

Results for the Uptake of Mono- and Di- Substituted Phenols from Aqueous Solution by Silicalite-1 (GS18) at 25°C.

Table (i) o-Cresol

Sample	Weight/g	Equilibrium Concentration 1000c/M	Error in concentration 1000c/M	100U/ (gg-1)	Error in 100U/ (gg-1)
A	0.1013	0.040	0.005	0.540	0.006
B	0.1062	0.075	0.005	1.033	0.008
C	0.1037	0.234	0.006	2.59	0.01
D	0.0995	0.309	0.006	3.06	0.03
E	0.1008	1.25	0.03	5.65	0.05
F	0.1066	1.95	0.04	6.27	0.06
G	0.1076	2.64	0.05	7.09	0.06
H	0.1042	3.88	0.06	7.22	0.08

Table (ii) m-Cresol

Sample	Weight/g	Equilibrium Concentration 1000c/M	Error in concentration 1000c/M	100U/ (gg-1)	Error in 100U/ (gg-1)
A	0.0928	0.221	0.008	3.55	0.03
B	0.0973	0.374	0.009	5.00	0.04
C	0.0975	0.91	0.01	6.72	0.06
D	0.1008	0.96	0.04	7.15	0.07
E	0.0987	1.99	0.05	8.14	0.09
F	0.1068	2.48	0.05	8.5	0.1
G	0.0930	5.1	0.1	8.4	0.2
H	0.0919	6.6	0.1	8.5	0.2

Table (iii) p-cresol

Sample	Weight/g	Equilibrium concentration /1000c/M	Error in concentration /1000c/M	100U/ (gg^{-1})	Error in 100U/ (gg^{-1})
A	0.1020	0.091	0.002	1.77	0.02
B	0.1030	0.160	0.002	2.68	0.04
C	0.1005	0.219	0.002	3.66	0.04
D	0.1011	0.302	0.002	4.58	0.06
E	0.1025	0.433	0.005	5.25	0.07
F	0.0955	0.750	0.006	6.01	0.09
G	0.0996	1.170	0.007	6.5	0.1
H	0.1090	1.27	0.02	6.7	0.1
I	0.1098	2.00	0.02	6.8	0.1

Table (iv) 2,4-Dimethylphenol

Sample	Weight/g	Equilibrium concentration /1000c/M	Error in concentration /1000c/M	100U/ (gg)	Error in 100U/ (gg)
A	0.0877	0.056	0.004	0.176	0.004
B	0.0943	0.306	0.004	0.263	0.006
C	0.0939	0.376	0.004	0.827	0.008
D	0.0922	2.12	0.03	1.21	0.04
E	0.0730	3.51	0.05	2.06	0.07
F	0.0782	5.11	0.06	2.54	0.09
G	0.0720	6.1	0.2	2.7	0.2
H	0.0951	8.3	0.2	2.5	0.3

Table (v) 2,5-Dimethylphenol

Sample	Weight/g	Equilibrium Concentration 1000c/M	Error in concentration 1000c/M	100U/ (gg-l)	Error in 100U/ (gg-l)
A	0.1011	0.017	0.004	0.945	0.007
B	0.1088	0.026	0.004	1.78	0.01
C	0.1041	0.037	0.004	2.79	0.01
D	0.1093	0.045	0.004	3.49	0.02
E	0.1089	0.053	0.004	4.43	0.02
F	0.1083	0.064	0.004	6.20	0.03
G	0.1070	0.104	0.004	7.10	0.04
H	0.1044	0.212	0.004	7.97	0.04
I	0.0989	0.316	0.005	8.47	0.04
J	0.1050	0.577	0.006	8.63	0.05

Table (vi) 3,4-Dimethylphenol

Sample	Weight/g	Equilibrium Concentration 1000c/M	Error in concentration 1000c/M	100U/ (gg-l)	Error in 100U/ (gg-l)
A	0.0957	0.045	0.003	1.323	0.008
B	0.1046	0.118	0.003	3.68	0.02
C	0.0992	0.395	0.004	4.85	0.03
D	0.1017	0.188	0.003	6.27	0.03
E	0.0998	0.700	0.004	7.17	0.04
F	0.1066	0.94	0.02	7.60	0.05
G	0.1011	1.56	0.02	8.54	0.06

Appendix 3

Results for the Uptake of p-Nitrophenol from Aqueous Solution by Silicalite-1 at 25°C.

Table (i) GS11

Sample	Weight/g	Equilibrium concentration 1000c/M	Error in concentration 1000c/M	100U/ (gg-1)	Error in 100U/ (gg-1)
A	0.0551	0.0111	0.0004	0.596	0.004
B	0.0547	0.0195	0.0004	3.24	0.02
C	0.0547	0.0201	0.0005	6.62	0.02
D	0.0553	0.303	0.005	8.0	0.1
E	0.0564	0.62	0.02	8.0	0.1
F	0.0558	1.47	0.04	10.1	0.3
G	0.0546	2.34	0.05	11.2	0.3
H	0.0558	3.20	0.05	11.9	0.4
I	0.0544	4.24	0.06	11.9	0.4
J	0.0545	5.09	0.07	12.6	0.5

Table (ii) GS12

Sample	Weight/g	Equilibrium concentration /1000c/M	Error in concentration /1000c/M	100U/ (gg)	Error in 100U/ (gg)
A	0.0546	0.0119	0.0005	0.590	0.007
B	0.0554	0.0094	0.0005	3.22	0.01
C	0.0550	0.0418	0.0007	6.38	0.06
D	0.0544	0.131	0.0006	9.1	0.1
E	0.0561	0.511	0.008	9.72	0.06
F	0.0543	1.68	0.02	9.0	0.1
G	0.0550	2.67	0.06	8.9	0.4
H	0.0551	3.58	0.07	9.4	0.5
I	0.0556	4.58	0.08	9.3	0.5

Table (iii) GS11(as)

Sample	Weight/g	Equilibrium Concentration 1000c/M	Error in concentration 1000c/M	100U/ (gg-1)	Error in 100U/ (gg-1)
A	0.0574	0.0733	0.0009	0.194	0.0007
B	0.0572	0.486	0.006	0.118	0.005
C	0.0591	0.34	0.01	1.16	0.09
D	0.0584	1.23	0.02	2.0	0.1
E	0.0584	1.69	0.02	2.2	0.2
F	0.0593	2.62	0.05	2.7	0.3
G	0.0586	3.51	0.06	3.6	0.4
H	0.0579	4.51	0.07	3.5	0.5
I	0.0591	5.48	0.08	3.7	0.5
J	0.0585	6.40	0.09	3.9	0.6

Table (iv) GS12(as)

Sample	Weight/g	Equilibrium concentration 1000c/M	Error in concentration 1000c/M	100U/ (gg-1)	Error in 100U/ (gg-1)
A	0.0583	0.101	0.001	-0.002	0.011
B	0.0576	0.505	0.008	-0.04	0.05
C	0.0576	1.01	0.01	-0.01	0.11
D	0.0581	1.48	0.02	0.12	0.13
E	0.0585	1.99	0.02	0.06	0.18
F	0.0580	3.11	0.06	0.73	0.42
G	0.0588	3.95	0.07	0.37	0.48
H	0.0577	5.09	0.08	-0.65	0.55
I	0.0585	6.09	0.09	-0.62	0.61
J	0.0570	7.01	0.10	0.24	0.70

Appendix 4

Results for the Uptake of Mono- and Di-Substituted Methyl Phenols from Aqueous Solution by Silicalite-1 (GS14) at 25°C.

Table (i) o-Cresol

Sample	Weight/g	Equilibrium Concentration 1000c/M	Error in concentration 1000c/M	100U/ (gg-1)	Error in 100U/ (gg-1)
A	0.1006	0.149	0.005	2.21	0.02
B	0.1087	0.254	0.006	3.36	0.03
C	0.1045	0.463	0.007	4.05	0.04
D	0.1012	0.833	0.009	4.94	0.04
E	0.0987	1.35	0.04	5.68	0.06
F	0.0983	2.01	0.04	6.11	0.07
G	0.1034	2.59	0.07	6.35	0.09
H	0.0958	3.83	0.07	6.9	0.1
I	0.1009	4.36	0.08	6.8	0.1

Table (ii) m-Cresol

Sample	Weight/g	Equilibrium Concentration 1000c/M	Error in concentration 1000c/M	100U/ (gg-1)	Error in 100U/ (gg-1)
A	0.1014	0.030	0.008	1.83	0.02
B	0.0977	0.176	0.008	3.39	0.03
C	0.0990	0.322	0.009	4.87	0.04
D	0.1011	0.68	0.01	6.04	0.05
E	0 .0993	1.52	0.05	6.95	0.08
F	0.1089	2.33	0.06	7.89	0.09
G	0.1022	3.37	0.07	8.1	0.1
H	0.1058	4.5	0.1	8.8	0.2
I	0.0981	6.5	0.1	8.3	0.2
J	0.1070	7.8	0.1	8.8	0.2

Table (iii) p-Cresol

Sample	Weight/g	Equilibrium Concentration 1000c/M	Error in concentration 1000c/M	100U/ (gg-l)	Error in 100U (gg-l)
A	0.0963	0.021	0.004	0.973	0.009
B	0.0982	0.055	0.004	1.92	0.02
C	0.0951	0.111	0.004	2.92	0.02
D	0.1003	0.179	0.004	3.61	0.02
E	0.0998	0.279	0.004	4.43	0.04
F	0.0977	0.462	0.006	5.36	0.04
G	0.1093	0.746	0.012	5.40	0.05
H	0.0964	1.30	0.02	6.35	0.06
I	0.1003	2.71	0.04	6.55	0.07

Table (iv) 2,4-Dimethylphenol

Sample	Weight/g	Equilibrium Concentration 1000c/M	Error in concentration 1000c/M	100U/ (gg-l)	Error in 100U/ (gg-l)
A	0.0552	0.025	0.002	0.24	0.02
B	0.0573	0.050	0.003	0.29	0.02
C	0.0573	0.434	0.006	1.37	0.07
D	0.0542	0.69	0.03	2.0	0.2
E	0.0543	2.47	0.05	3.6	0.4
F	0.0553	3.27	0.06	4.8	0.5
G	0.0555	4.58	0.08	5.0	0.7

Table (v) 2,5-Dimethylphenol

Sample	Weight/g	Equilibrium concentration /1000c/M	Error in concentration /1000c/M	100U/ (gg^{-1})	Error in 100U/ (gg^{-1})
A	0.0562	0.0124	0.0007	0.36	0.02
B	0.0568	0.0240	0.0008	1.97	0.07
C	0.0554	0.0744	0.0008	3.9	0.2
D	0.0580	0.0561	0.0009	5.0	0.1
E	0.0587	0.0510	0.008	5.4	0.1
F	0.0580	0.71	0.01	8.6	0.4
G	0.0587	1.47	0.02	8.9	0.3
H	0.0564	2.34	0.04	8.1	0.6

Table (vi) 3,4-Dimethylphenol

Sample	Weight/g	Equilibrium concentration /1000c/M	Error in concentration /1000c/M	100U/ (gg-1)	Error in 100U/ (gg-1)
A	0.0565	0.039	0.001	0.36	0.002
B	0.0596	0.073	0.001	2.45	0.008
C	0.0565	0.108	0.001	3.6	0.1
D	0.0567	0.35	0.01	5.0	0.2
E	0.0583	1.22	0.04	7.2	0.4
F	0.0559	3.79	0.07	7.3	0.6
G	0.0562	3.94	0.07	6.9	0.4
H	0.0577	9.2	0.1	6.0	1.7
I	0.0571	10.3	1.7	9.0	1.9

Appendix 5

Results for the Uptake of Phenol from Aqueous Solution by Molecular Sieves at 25°C.

Table (i) Silicalite-1 (GS18)

Sample	Weight/g	Equilibrium Concentration 1000c/M	Error in cncentration 1000c/M	100U/ (gg^{-1})	Error in 100U/ (gg^{-1})
A	0.1076	0.223	0.008	0.842	0.009
B	0.0965	0.63	0.04	1.68	0.04
C	0.098	1.56	0.05	3.00	0.05
D	0.1068	2.5	0.1	3.72	0.08
E	0.1027	4.3	0.1	4.6	0.1
F	0.0987	6.6	0.4	5.0	0.4
G	0.1012	8.3	0.4	5.5	0.4
H	0.0934	12.9	0.4	5.9	0.4
I	0.1008	16.7	0.5	6.2	0.5

Table (ii) ZSM-5 (GZ1)

Sample	Weight/g	Equilibrium concentration 1000c/M	Error in concentration 1000c/M	100U/ (gg-i)	Error in 100U/ (gg-i)
A	0.1059	0.375	0.009	1.45	0.01
B	0.0714	1.72	0.05	2.98	0.07
C	0.0704	3.04	0.09	3.9	0.1
D	0.0776	4.7	0.2	4.2	0.2
E	0.0824	5.9	0.2	4.5	0.2
F	0.0774	10.1	0.4	4.4	0.5
G	0.0799	13.6	0.4	4.7	0.5
H	0.0844	15.2	0.5	4.9	0.5

Table (iii) ZSM-5 (GZ2)

Sample	Weight/g	Equilibrium concentration 1000c/M	Error in concentration 1000c/M	100U/ (gg-i)	Error in 100U/ (gg-i)
A	0.1063	0.434	0.009	1.45	0.01
B	0.0813	1.81	0.05	2.67	0.06
C	0.0892	3.5	0.1	3.2	0.1
D	0.0903	5.1	0.2	3.4	0.2
E	0.0953	6.9	0.2	3.5	0.2
F	0.0947	10.9	0.4	3.5	0.4
G	0.0920	14.7	0.4	3.9	0.5
H	0.1178	15.7	0.5	3.9	0.4

Table (iv) ZSM-5 (GZ3)

Sample	Weight/g	Equilibrium concentration 1000c/M	Error in concentration 1000c/M	100U/ (gg-i)	Error in 100U/ (gg-i)
A	0.0842	0.53	0.01	1.76	0.02
B	0.0901	1.52	0.07	2.78	0.08
C	0.0873	3.7	0.1	3.7	0.1
D	0.0911	4.5	0.2	3.9	0.2
E	0.0881	6.6	0.2	4.2	0.2
F	0.0873	10.4	0.4	4.4	0.5
G	0.1003	13.8	0.4	4.4	0.4
H	0.1069	15.3	0.5	4.6	0.4

Appendix 6

Results for the Uptake of Phenols from Aqueous Solution by Silicalite-2 at 25°C.

Table (i) o-Cresol (KF1)

Sample	Weight/g	Equilibrium concentration /1000c/M	Error in concentration /1000c/M	100U/(gg-1)	Error in 100U/(gg-1)
A	0.0916	0.021	0.005	0.280	0.006
B	0.1032	0.039	0.005	0.627	0.006
C	0.0892	0.100	0.005	1.34	0.01
D	0.0947	0.578	0.007	3.73	0.02
E	0.1037	1.10	0.03	5.51	0.04
F	0.0911	3.02	0.06	7.04	0.09
G	0.0887	5.8	0.3	6.9	0.3
H	0.0917	6.6	0.4	7.2	0.3

Table (ii) m-Cresol (KF1)

Sample	Weight/g	Equilibrium concentration /1000c/M	Error in concentration /1000c/M	100U/(gg-1)	Error in 100U/(gg-1)
A	0.0563	0.043	0.005	0.96	0.01
B	0.0536	0.107	0.005	1.99	0.02
C	0.0515	0.366	0.006	3.79	0.03
D	0.0522	0.730	0.007	6.17	0.05
E	0.0493	1.55	0.03	8.02	0.09
F	0.0499	3.36	0.06	8.9	0.2
G	0.0497	3.85	0.07	10.1	0.2
H	0.0522	5.97	0.12	9.7	0.3

Table (iii) p-Cresol (KF1)

Sample	Weight/g	Equilibrium concentration /1000c/M	Error in concentration /1000c/M	100U/(gg-1)	Error in 100U/(gg-1)
A	0.0577	0.008	0.007	0.186	0.009
B	0.0513	0.015	0.007	0.413	0.009
C	0.0523	0.057	0.007	0.98	0.01
D	0.0555	0.15	0.01	1.81	0.02
E	0.0520	0.35	0.02	3.80	0.04
F	0.0552	0.56	0.02	5.35	0.04
G	0.0511	1.70	0.03	6.43	0.06
H	0.0532	4.47	0.07	6.9	0.1
I	0.0965	6.62	0.08	6.8	0.2

Table (iv) Phenol (KF2)

Sample	Weight/g	Equilibrium concentration /1000c/M	Error in concentration /1000c/M	100U/(gg-1)	Error in 100U/(gg-1)
A	0.0553	0.084	0.007	0.314	0.006
B	0.0551	0.17	0.03	0.66	0.03
C	0.0568	0.57	0.04	1.48	0.03
D	0.0546	1.35	0.04	2.62	0.05
E	0.0585	4.9	0.1	5.0	0.1
F	0.0555	7.0	0.4	6.4	0.4
G	0.0547	10.3	0.4	7.4	0.4
H	0.0559	15.5	0.5	7.9	0.4

Table (v) 2,4-Dimethylphenol (KF2)

Sample	Weight/g	Equilibrium concentration /1000c/M	Error in concentration /1000c/M	100U/(gg-1)	Error in 100U/(gg-1)
A	0.1050	0.123	0.004	0.113	0.005
B	0.0939	0.313	0.004	0.253	0.006
C	0.0948	0.771	0.005	0.315	0.008
D	0.0953	2.33	0.04	0.922	0.06
E	0.0926	4.01	0.05	1.75	0.09
F	0.0960	5.69	0.07	2.0	0.1
G	0.0917	6.7	0.2	2.3	0.3
H	0.0916	8.0	0.2	2.7	0.3

Appendix 7

Results for the Uptake of Phenol from Aqueous Salt Solutions by Silicalite-1 (GS18) at 25°C.

Table (i) 2.5M LiCl

Sample	Weight/g	Equilibrium concentration /1000c/M	Error in concentration /1000c/M	100U/ (gg-1)	Error in 100U/ (gg-1)
A	0.1066	0.113	0.007	0.824	0.007
B	0.0911	0.39	0.01	1.72	0.01
C	0.0925	1.19	0.07	2.99	0.08
D	0.0975	2.20	0.08	3.86	0.08
E	0.0956	3.28	0.09	5.24	0.09
F	0.0932	5.9	0.4	5.71	0.4
G	0.1034	7.6	0.4	6.0	0.4
H	0.0981	10.5	0.4	6.6	0.4

Table (ii) 5M LiCl

Sample	Weight/g	Equilibrium concentration /1000c/M	Error in concentration /1000c/M	100U/ (gg-1)	Error in 100U/ (gg-1)
A	0.0983	0.030	0.007	0.980	0.008
B	0.1056	0.098	0.007	1.78	0.01
C	0.0987	0.45	0.01	3.54	0.02
D	0.0969	1.12	0.04	5.00	0.05
E	0.0934	2.25	0.08	6.12	0.09
F	0.1018	3.6	0.2	6.3	0.2
G	0.1086	5.6	0.4	6.8	0.4
H	0.0957	10.0	0.4	7.0	0.4

Appendix 8

Results for the Uptake of p-Cresol from Solutions of Methanol in Water by Silicalite-1 (GS19) at 25°C.

Table (i) 10 MeOH : 90 H_2O (v/v)

Sample	Weight/g	Equilibrium concentration /1000c/M	Error in concentration /1000c/M	100U/(gg-1)	Error in 100U/(gg-1)
A	0.0977	0.099	0.004	0.992	0.007
B	0.1014	0.220	0.004	2.33	0.03
C	0.1042	0.602	0.007	4.05	0.02
D	0.0956	3.5	0.1	6.9	0.1
E	0.0943	7.7	0.1	7.7	0.2
F	0.0972	11.7	0.2	8.2	0.3
G	0.0997	20.9	0.3	8.7	0.4
H	0.0704	28.9	0.4	8.2	0.7

Table (ii) 20 MeOH : 80 H_2O (v/v)

Sample	Weight/g	Equilibrium concentration /1000c/M	Error in concentration /1000c/M	100U/(gg-1)	Error in 100U/(gg-1)
A	0.0903	0.32	0.01	0.842	0.002
B	0.0947	0.90	0.02	1.879	0.003
C	0.1000	2.12	0.03	3.11	0.04
D	0.1034	5.71	0.08	5.12	0.1
E	0.0907	10.6	0.2	5.42	0.2
F	0.1077	19.3	0.3	5.7	0.3
G	0.1045	29.0	0.5	6.4	0.6
H	0.0957	34.5	0.6	6.4	0.7

Table (iii) 30 MeOH : 70 H_2O (v/v)

Sample	Weight/g	Equilibrium concentration /1000c/M	Error in concentration /1000c/M	100U/(gg-1)	Error in 100U/(gg-1)
A	0.0994	0.62	0.02	0.43	0.02
B	0.0952	1.58	0.03	1.10	0.03
C	0.1029	3.21	0.06	2.00	0.06
D	0.0947	7.5	0.1	3.3	0.1
E	0.0996	11.0	0.2	4.5	0.3
F	0.1030	15.3	0.4	5.4	0.4
G	0.1080	24.4	0.5	6.1	0.5
H	0.1046	30.0	0.5	6.1	0.6

Appendix 9

Results for the Uptake of Phenol from Aqueous Solution by Silicalite-1 (GS20)

Table (i) 15°C

Sample	Weight/g	Equilibrium concentration 1000c/M	Error in concentration 1000c/M	100U/ (gg-1)	Error in 100u/ (gg-1)
A	0.0941	0.034	0.007	0.289	0.007
B	0.0848	0.113	0.007	0.588	0.009
C	0.0965	0.233	0.008	1.32	0.01
D	0.0933	0.47	0.04	2.08	0.04
E	0.0768	2.47	0.06	4.71	0.08
F	0.0857	6.2	0.2	7.0	0.2
G	0.1040	13.1	0.4	8.0	0.4
H	0.1051	14.6	0.5	7.9	0.4

Table (ii) 40°C

Sample	Weight/g	Equilibrium concentration 1000c/M	Error in concentration 1000c/M	100U/ (gg-1)	Error in 100U/ (gg-1)
A	0.0713	0.0128	0.007	0.391	0.006
B	0.0741	0.0394	0.009	1.06	0.01
C	0.0690	0.51	0.01	1.46	0.02
D	0.1038	1.27	0.07	2.50	0.09
E	0.0839	5.1	0.4	4.7	0.4
F	0.0952	6.8	0.4	5.8	0.4
G	0.0809	10.3	0.4	6.4	0.5
H	0.1413	18.2	0.8	6.7	0.5

Appendix 10

Lecture Series and Courses

The following lecture series and courses were attended during the three year research period:

Fortran 77 computing course
Edinburgh Regional Computing Centre

Computer Graphics
Edinburgh Regional Computing Centre

SERC/CRAC Graduate School
University of Stirling

LECTURE SERIES:

Techniques in Surface Analysis
Dr. H.F. Leach, University of Edinburgh

Biotechnology
Dr. R. Baxter, University of Edinburgh

X-Ray Crystallography
Dr. R.O. Gould, University of Edinburgh

Microcomputers
Dr. A.G. Rowley and A. King, University of Edinburgh

Medicinal Chemistry
Speakers from I.C.I Pharmaceutical Division

SEMINARS:

Research group seminars and departmental seminars were also attended.